THE UNIVERSITY *of* EDINBURGH

CANDIDATE GENE STUDIES IN PSYCHIATRIC ILLNESS

Helen Miranda Knight

Doctor of Philosophy

University of Edinburgh

2009

DECLARATION

I hereby declare this thesis has been composed by myself, and the work presented within is my own and has not been accepted for any previous application for a degree. Information obtained from sources other than this study is acknowledged in the text or included in the references.

Helen Miranda Knight

January 2009

GENERAL ACKNOWLEDGEMENTS

I would like to thank all individuals and family members who have consented to the donation of blood and tissue samples for research purposes. My thanks also extend to the clinicians and research nurses who tirelessly work to acquire these precious samples. Without the involvement of subjects, clinicians and research nurses, such genetic and biological studies could simply not be performed.

I would also like to acknowledge the enormous support I have received from my three supervisors, Douglas Blackwood, Walter Muir and Ben Pickard. My supervisors have not only guided me through my studies and been fierce opponents in heated debates about research findings but also have become close friends. My warm thanks also go to Alan Maclean and Pat Malloy for their dedication to the research, words of encouragement and laughter during the last four years. Without the advice and support provided by Pat and Alan the cytogenetic and sequencing data would not have been completed.

I would also like to thank Professors John Knight and David Attwell for proofreading and advice during the writing of this thesis. In addition, I am grateful to the head of the Medical Genetics Section, David Porteous, many members of the section, past and present, and individuals at Edinburgh University and other institutions for discussing research, kindly sharing materials, and providing advice on molecular techniques and computational programs.

Finally, I would like express my gratitude to Edinburgh University College of Medicine and Veterinary Medicine for giving me the opportunity to undertake this research by awarding me a Ph.D. scholarship.

ABSTRACT

Schizophrenia, bipolar disorder and major depression are common, heritable neuropsychiatric conditions and yet the source of the inherited risk remains largely unknown. This thesis focuses on two complementary strategies for identifying and characterising the genetic component of these illnesses: homozygosity mapping in consanguineous pedigrees, and genetic and neurobiological investigations of candidate genes identified by the analysis of structural chromosomal abnormalities carried by patients with psychiatric diagnoses.

In a family of a cousin marriage, five of six offspring presented with a rare combination of schizophrenia, sensori-neural hearing impairment and epilepsy. Two loci were located on chromosomes 22q13 and 2p24-25 where a series of markers were homozygous by descent (HBD). Five further HBD loci were identified in a second, related family where four of five offspring had hearing loss. However, there was no overlap of the HBD intervals in the two families, and sequencing coding regions of candidate genes failed to identify causative mutations.

A second study investigated the candidate gene *ABCA13* identified at a breakpoint region on chromosome 7 in a patient with schizophrenia who carried a complex chromosomal rearrangement. Re-sequencing exons encoding the highly conserved functional domains identified eight potentially pathogenic, rare coding variants. Case control association studies involving cohorts of schizophrenia, bipolar disorder and major depression revealed significant associations of these variants with all three clinical phenotypes, and follow-up in relatives displayed familial inheritance patterns. Disruption of ABCA13, expressed in human hippocampus and frontal cortex, implicates aberrant lipid biology as a pathological pathway in mental illness.

A third study focused on *GRIK4,* a candidate gene previously reported disrupted in a patient with schizophrenia who carried a chromosome abnormality. A deletion in the

3'UTR of *GRIK4*, encoding the kainate receptor subunit KA1, was identified as a protective factor for bipolar disorder. Using post mortem human brain tissue from control subjects, KA1 protein expression patterns were characterized in the hippocampal formation, amygdala, frontal cortex and cerebellum. KA1 expression was found significantly increased in subjects with the protective allele, supporting the hypothesis that reduced glutamatergic neurotransmission is a risk factor in major psychiatric illnesses.

Together, these novel discoveries define aspects of the genetic contribution to mental illness, implicate specific dysfunctional processes and suggest new directions for research in the quest to find rationally based treatments and preventative strategies for some of the most common and disabling psychiatric disorders.

PUBLICATIONS FROM THESIS

Knight HM, Maclean A, Irfan M, Naeem F, Cass S, Pickard BS, Muir WJ, Blackwood DH, Ayub M (2008) Homozygosity mapping in a family presenting with schizophrenia, epilepsy and hearing impairment. Eur J Hum Genet 16:750-758.

Pickard BS, Knight HM, Hamilton RS, Soares DC, Walker R, Boyd JK, Machell J, Maclean A, McGhee KA, Condie A, Porteous DJ, St Clair D, Davis I, Blackwood DH, Muir WJ (2008) A common variant in the 3'UTR of the GRIK4 glutamate receptor gene affects transcript abundance and protects against bipolar disorder. Proc Natl Acad Sci U S A 105:14940-14945.

The PDFs of these papers are attached in appendix 2. No explicit permission to include these papers is required as The European Journal of Human Genetics and Proceedings of the National Academy of Sciences (PNAS) both grant the noncommercial use of papers by authors.

POSTERS

Knight HM, Ayub M, Maclean A, Pickard BS, Muir WJ, Blackwood DH (2006) Homozygosity mapping in a consanguineous family with schizophrenia co-morbid with epilepsy and hearing impairment. XIVth World Congress on Psychiatric Genetics (ISPG).

Knight HM, Walker R, Porteous DJ, Muir WJ, Blackwood DHR, Pickard BS. (2008) GRIK4/KA1 protein expression in human brain tissue and correlation with a genetic variant associated with bipolar disorder. The Federation of European Neuroscience Societies (FENS).

CONTENTS

Declaration…..i
General acknowledgements.....ii
Abstract……..iii
Publications from thesis……..v
Contents……vi
List of figures……..…xiii
List of tables…….……...xvii
List of graphs…….....xviii
Abbreviations…….…….....xix

1 INTRODUCTION 1

ACKNOWLEDGEMENTS FOR CHAPTER 1..... 2
1.1 PSYCHIATRIC ILLNESS..... 3
1.1.1 Schizophrenia 3
1.1.2 Affective disorders..... 4
1.1.3 Epidemiological analysis of psychiatric disorders 5
1.1.4 Genetic models of psychiatric illnesses..... 6
1.1.5 What do we mean by genetic factor? 9
1.2 MOLECULAR APPROACHES TO THE STUDY OF PSYCHIATRIC DISORDERS…....10
1.2.1 Linkage analysis..... 10
1.2.2 Case-control association studies 11
1.2.3 The study of chromosomal abnormalities..... 14
1.3 AETIOLOGICAL THEORIES OF PSYCHIATRIC ILLNESS……..17
1.3.1 Aberrant function of neurotransmitter systems..... 17
1.3.2 Fatty acid hypothesis of schizophrenia..... 21
1.4 INTRODUCTION TO PROJECTS ……..……..23
1.4.1 Project 1: Homozygosity mapping in a consanguineous family..... 23
1.4.1.1 Homozygosity mapping in consanguineous populations …….. 23
1.4.1.2 The Pedigree …… 24
1.4.1.3 Hereditary hearing impairment, epilepsy and schizophrenia ……..… 25

1.4.1.4 Results of a genome-wide scan using microsatellite markers 25
1.4.1.5 A second related family 26
1.4.2 Project 2: Investigation of a complex chromosomal abnormality and the disrupted break point gene *ABCA13* 28
1.4.2.1 The mapping of breakpoints regions 28
1.4.2.2 ABC proteins and disease 31
1.4.3 Project 3: *GRIK4*- a candidate breakpoint gene for psychiatric illness 34
1.4.3.1 GRIK4 disrupted in a chromosomal re-arrangement 34
1.4.3.2 Case-control SNP-tag association & identification of a 3'UTR variant .. 34
1.4.3.3 The role of kainate receptors in glutamatergic neurotransmission 36
1.4.3.4 Alterations of kainate receptor subunit expression 37
1.4.3.5 KA1 Expression 39
1.5 AIMS..... ..41

2 MATERIALS AND METHODS.....43

2.1 CLINICAL SAMPLES.....44
2.1.1 Case samples.....44
2.1.2 Control cohort 45
2.1.3 1936 Lothian birth cohort 45
2.1.4 Pakistan families 46
2.1.5 Brain tissue samples 46
2.2 MATERIALS.....46
2.2.1 Chemicals and biological products 46
2.2.2 Kits 47
2.2.3 Solutions, buffers and loading dyes 48
2.2.4 Antibodies 53
2.2.5 Primers and microsatellite markers 54
2.2.6 BAC and fosmid clones 58
2.2.7 DNA 59
2.2.8 Cell lines, lymphocytes and RNA blood 60
2.2.9 Human brain tissue 60
2.3 GENERAL METHODS.....60
2.3.1 FISH techniques 60

2.3.1.1 Mini preparation of bacterial clone DNA 60
2.3.1.2 Nick translation 61
2.3.1.3 Preparation of metaphase arrested chromosomes 61
2.3.1.4 Hybridization 62
2.3.2 Sequencing 63
2.3.2.1 Polymerase chain reaction 63
2.3.2.2 Agrose gel electrophoresis 64
2.3.2.3 Exosapit clean up 64
2.3.2.4 Sequencing PCR 64
2.3.2.5 Ethanol/EDTA precipitation and sequence analysis 64
2.3.2.6 Sequence analysis 65
2.3.3 Confirmation of novel variants 65
2.3.3.1 Restriction enzyme assay 66
2.3.3.2 Cloning of PCR products 66
2.3.4 TaqMan assays 67
2.3.5 Genotyping 67
2.3.5.1 GRIK4 3'UTR variant 69
2.3.5.2 Chromosome 7 microsatellites 69
2.3.5.3 Whole genome SNP genotyping 69
2.3.6 RT-PCR 70
2.3.6.1 RNA preparation 70
2.3.6.2 cDNA synthesis 70
2.3.6.3 RT PCR 71
2.3.7 Immunohistochemistry 72
2.3.7.1 Immunoperoxidase staining 72
2.3.6 Antibody specicifity assays 73
2.3.6.1 Immunoblotting 73
2.3.6.2 Pre-immune antisera assay 74
2.3.6.3 Peptide pre-absorption blocking assay 75
2.4 IMAGE ANALYSIS 75
2.4.1 Image analysis 75
2.4.2 Image capture settings 75
2.5 DATA ANALYSIS 76

2.5.1 Chapter 3 76
2.5.1.1 Genome-wide analysis of autozygosity 76
2.5.1.2 Inbreeding coefficients 76
2.5.2 Chapter 4 77
2.5.2.1 Haplotype analysis 77
2.5.2.2 Amino acid conservation and splice site mutation prediction 77
2.5.2.3 Linkage analysis 78
2.5.3 Chapter 6 79
2.5.3.1 Testing for deviations from HWE 79
2.5.4 Chapter 7 79
2.5.4.1 GRIK4 protein expression correlation analysis 79
2.6 GENE/PROTEIN NOTATION 80
2.7 PEDIGREE DRAWING 82
2.8 STATISTICAL ANALYSIS 82
2.9 BIOINFORMATICS 83

3 HOMOZYGOSITY MAPPING IN A FAMILY PRESENTING WITH SCHIZOPHRENIA, EPILEPSY AND SENSORI-NEURAL HEARING LOSS 84

ACKNOWLEDGEMENTS FOR CHAPTER 3 85
3.1 PREFACE 86
3.2 RESULTS 86
3.2.1 A high density genome-wide SNP scan for linkage 86
3.2.2 Inbreeding coefficients and runs of homozygosity 90
3.2.3 A genome-wide linkage scan performed on a second related sibship 92
3.3 DISCUSSION 96

4 INVESTIGATION OF A COMPLEX CHROMOSOMAL ABNORMALITY AND THE DISRUPTED BREAK POINT GENE *ABCA13* 103

ACKNOWLEDGEMENTS FOR CHAPTER 4 104
4.1 PREFACE 105
4.2 RESULTS 105
4.2.1 Fine mapping of breakpoint regions on chromosomes 8p and 7p 105

4.2.2 Re-sequencing exons of the *ABCA13* gene encoding functional domains in cases of schizophrenia and controls……..……...……..109
4.2.2.1 Analysis of known SNPS …… 112
4.2.2.2 Novel intronic and synonymous variants…… 112
4.2.2.3 Novel non synonymous variants discounted as pathogenic …… 113
4.2.2.4 The detection of potentially pathogenic variants…… 113
4.2.2.5 Further assessment of the pathogenic nature of identified variants. 137
4.2.2.6 Cases carrying multiple rare risk variants…… 137
4.2.2.7 Association and Linkage analysis 139
4.2.2.8 Exploring potential gender effects. 140
4.2.3 The identification of a CNV within *ABCA13* 140
4.2.4 An affected individual homozygous for rare alleles 143
4.3 DISCUSSION 145
4.3.1 Cytogenetics and the chromosome 7 region in disease 145
4.3.2 Linking cytogenetics and rare variants: lessons from ASD 147
4.3.3 Rare variants in psychiatric illness 148
4.3.4 The nature of the *ABCA13* rare varants discovered: penetrance issues, variable expressivity, and mutation effects 151
4.3.5 Interacting variants in psychiatric illness 155
4.3.6 Odds ratio estimates for common and rare variants 156
4.3.7 How do the findings fit in with current models of complex genetic disease?..... 157
4.3.8 The function of ABCA13 and its potential involvement in biological processes……159
5 ANALYSIS OF ABCA13 EXPRESSION……..….....164
ACKNOWLEDGEMENTS FOR CHAPTER 5..... 165
5.1 PREFACE 166
5.2 RESULTS……..……166
5.2.1 RT- PCR of human *ABCA13* in cell lines and brain tissue……...166
5.2.2 IHC analysis of ABCA13 in human post mortem brain tissue…….168
5.3 DISCUSSION 173
5.3.1 ABCA13 expression in human and mouse tissues……..……..174

5.3.2 Expression profile and function of other ABCA sub-family members…….176

6 A CASE-CONTROL ASSOCIATION STUDY OF A VARIANT WITHIN THE 3'UTR OF GRIK4 AND BIPOLAR DISORDER…….....180

ACKNOWLEDGEMENTS FOR CHAPTER 6.....181

6.1 PREFACE.....182

6.2 RESULTS……...……... ……..……..182

6.3 DISCUSSION.....185

7 THE CHARACTERISATION OF KA1 EXPRESSION IN HUMAN BRAIN...193

ACKNOWLEDGEMENTS FOR CHAPTER 7.....194

7.1 PREFACE.....195

7.2 RESULTS……...……... ……..……..195

7.2.1 Antiserun specicity.....195

7.2.2 Frontal cortex.....197

7.2.3 Cerebellum.....199

7.2.4 Amygdala.....203

7.2.5 The hippocampal formation.....203

7.2.5.1 Hippocampus……. 203

7.2.5.2 Parahippocampal regions. 213

7.3 DISCUSSION.....217

7.3.1 Previous reports of KA1 expression in murine and human brain.....217

7.3.1.1 Frontal cortex…… 219

7.3.1.2 Cerebellum. 220

7.3.1.3 Amygdala…… 222

7.3.1.4 Hippocampus. 222

7.3.1.5 Parahippocampal regions…… 226

7.3.2 Descrepancies between studies: advantages and disadvantages of IHC 226

7.3.3 Expression patterns of kainate receptor subunits in the brain 227

7.3.4 The function of KARs and KA1 228

8 A GENOTYPE EXPRESSION CORRELATION STUDY OF KA1 IN HUMAN BRAIN……...…….....232

ACKNOWLEDGEMENTS FOR CHAPTER 8.....233

8.1 PREFACE.....234

8.2 RESULTS……..…….... ……..... 234

8.2.1 Quantification of KA1 expression.....234

8.2.2 Genotype/protein correlation in the hippocampus.....236

8.2.3 Genotype/protein correlation in the frontal cortex.....243

8.3 DISCUSSION.....246

8.3.1 Abnormalities in KAR subunit expression in individuals with psychiatric illness ……...249

8.3.2 Genotype specific KA1 increases in neuronal cells, dendrites and neuropil……...251

8.3.3 Genotype/KA1 expression in DG and link to neurogenesis.....253

8.3.4 Stress, psychiatric illness and a role for KA1.....254

8.3.5 Differential KA1 expression and neural circuits.....255

9 GENERAL DISCUSSION.....259

9.1 REVIEW OF PROJECTS.....260

9.2 WHAT DO THE FINDINGS TELL US ABOUT THE GENETIC ARCHITECTURE OF PSYCHIATRIC ILLNESS?.....262

9.3 FUTURE RESEARCH.....266

9.4 CONCLUDING REMARKS.....268

BIBLIOGRAPHY.....269

APPENDICES.....295

APPENDIX 1: CLINICAL DESCRIPTION OF THE CONSANGUINEOUS FAMILY....295

APPENDIX 2: TABLE S1.....297

APPENDIX 3: FIGURE S1.....298

APPENDIX 4: PUBLISHED PAPERS.....299

LIST OF FIGURES

Number		*Page*
FIGURE 1.1	Diagram of consanguineous pedigree	24
FIGURE 1.2	Constructed haplotypes of microsatellite markers on chromosome 22q13	27
FIGURE 1.3	Pedigree of second family of the same kindred	27
FIGURE 1.4	Schematic illustration of the complex chromosomal re-arrangement inv(7)(p12.3;q21.11), t(7;8)(p12.3;p23)	29
FIGURE 1.5	Schematic illustration of the breakpoint regions on chromosomes 7p12.3, 7q21.11 and 8p	29
FIGURE 1.6	Schematic illustration of the identified breakpoint region on chromosomes 7q21.11	30
FIGURE 1.7	Diagrammatic representation of ABCA13 protein structure	30
FIGURE 1.8	ABCA sub-family members	33
FIGURE 1.9	Diagrammatic illustration of a complex chromosomal re-arrangement identified as disrupting *GRIK4*	35
FIGURE 1.10	Diagrammatic representation of *GRIK4:* showing the cytogenetic and association findings	35
FIGURE 2.1	Illustration of IHC image analyzed by a colour deconvolution technique in Image J	81
FIGURE 3.1	SNP and microsatellite data identifying locus on chromosome 22q12.3-q13.3	87
FIGURE 3.2	SNP markers identifying HBD locus on chromosome 2p24.1-p25.3	89
FIGURE 3.3	SNP markers identifying HBD loci on chromosome 7q21.11-q31.1	94
FIGURE 3.4	SNP markers identifying HBD loci on chromosome 1p22.2-1q23.1	95
FIGURE 4.1	The breakpoint fosmid G248P87290G10 on chromosome 8	106
FIGURE 4.2	BACs and fosmids used to define the breakpoint on chromosome 8p23.1	106
FIGURE 4.3	Breakpoint fosmid 188G7 on chromosome 7	107
FIGURE 4.4	BACs and fosmids used to define the breakpoint on chromosome 7p12.3	108
FIGURE 4.5	Flow chart of findings initiated from the screening of exons encoding the functional domains of *ABCA13*	111

FIGURE 4.6	Family pedigree carrying R4454C	114
FIGURE 4.7	Sequence traces, amino acid position and conservation and family pedigree of the T4031A variant	117
FIGURE 4.8	The location of T4031 and ATP-binding site in a 3D-model	118
FIGURE 4.9	Sequence trace, restriction digest, position and conservation of R4728X	120
FIGURE 4.10	Co-segregation of R4728X with illness in four pedigrees	122
FIGURE 4.11	Conserved background haplotypes carrying the R4728X or T4031A mutations	123
FIGURE 4.12	Sequence trace, amino acid position and conservation of R4843C	125
FIGURE 4.13	Small families carrying the R4843C variant	125
FIGURE 4.14	Sequence chromatogram, splice variant sequence, amino acid position, and conservation, and segregation, of S3704R with illness in a large pedigree	127
FIGURE 4.15	Sequence chromatogram, amino acid position and conservation of H3609P and R3604Q	128
FIGURE 4.16	Family pedigrees carrying H3609P	130
FIGURE 4.17	Family pedigree carrying R3604Q	132
FIGURE 4.18	Sequence chromatogram, amino acid position, AA conservation and segregation of T4550A	133
FIGURE 4.19	Sequence chromatogram, amino acid position and conservation of R4590W	135
FIGURE 4.20	Sequence chromatogram, amino acid position and pedigree with H4262R	135
FIGURE 4.21	Schematic representation of the functional domains within ABCA13 and the locations of the identified putative mutations	136
FIGURE 4.22	Pedigree of family carrying the 11 kb intronic CNV deletion	142
FIGURE 4.23	Schematic illustration of fosmid clones used to investigate a possible deletion in an individual with schizophrenia	142
FIGURE 4.24	Interphase nuclei hybridized with fosmid and BAC DNA in an individual with schizophrenia and a potential deletion	144
FIGURE 4.25	Microsatellite marker genotyping on chromosome 7 in an individual with schizophrenia	144
FIGURE 5.1	Human *ABCA13* expression in cell lines and human tissue	167
FIGURE 5.2	ABCA13 870 antibody and corresponding pre-immune antiserum immunoreactivity in the medulla oblongata	170

FIGURE 5.3	High magnification images of ABCA13 870 antibody reactivity in layers 2 and 6 and the underlying white matter of the frontal cortex	171
FIGURE 5.4	High magnification images of ABCA13 870 antibody and corresponding pre-immune antiserum immunoreactivity in layer 3 of the frontal cortex	171
FIGURE 5.5	ABCA13 870 antibody and corresponding pre-immune antiserum immunoreactivity in the dentate gyrus and hilus of the hippocampus	172
FIGURE 6.1	Alignment of 3'UTR deletion/insertion in human, chimp, macaque and mouse	186
FIGURE 6.2	Relative expression levels of the deletion and insertion *GRIK4* alleles as determined by a fluorescently labelled PCR reaction	186
FIGURE 6.3	Schematic representations of multiple positive associations of *GRIK4* with antidepressant treatment and with schizophrenia and bipolar disorder	190
FIGURE 7.1	KA1 detection in cell lines and mouse	196
FIGURE 7.2	KA1 protein expression in layer 1 of the frontal cortex	196
FIGURE 7.3	KA1 protein immunoreactivity in layers 2 and 4 of the frontal cortex	198
FIGURE 7.4	KA1 protein immunoreactivity in layers 3 and 5 of the frontal cortex	198
FIGURE 7.5	KA1 protein immunoreactivity in layer 6 of the frontal cortex	200
FIGURE 7.6	Protein immunoreactivity for KA1 and GFAP in the white matter underlying the neocortex	200
FIGURE 7.7	Protein immunoreactivity for KA1 in the cerebellar cortex	201
FIGURE 7.8	High magnification images of KA1 protein immuno-reactivity in the cerebellum	202
FIGURE 7.9	Protein immunoreactivity for GFAP in the cerebellar cortex	204
FIGURE 7.10	Protein KA1 immunoreactivity in cortical layers surrounding deeper nuclei of the amygdala	204
FIGURE 7.11	Schematic illustration of the hippocampal formation and major pathway circuitry	206
FIGURE 7.12	KA1 and GFAP protein immuno-reactivity in the molecular layer and GCL of the dentate gyrus	207
FIGURE 7.13	KA1 expression in the granular cell layer of the dentate gyrus	208
FIGURE 7.14	KA1 expression in the DG hilus and CA4 region	210
FIGURE 7.15	KA1 expression in the CA3 and CA2 fields	211
FIGURE 7.16	KA1 immunoreactivity in the CA1 field	212

FIGURE 7.17 KA1 immunoreactivity in the alveus of the hippocampus and subiculum. 214

FIGURE 7.18 KA1 immunoreactivity in layers 1 and 2 of the entorhinal cortex 214

FIGURE 7.19 KA1 immunoreactivity in layers 3 and 5 and 6 of the entorhinal cortex 216

FIGURE 7.20 KA1 immunoreactivity in layers 1 and 2 of the perirhinal cortex 216

FIGURE 7.21 KA1 immunoreactivity in layers 3, 4, 5 and 6 of the perirhinal cortex 218

FIGURE 7.22 Schematic representation summarizing KAR subunit expression in the hippocampus and dentate gyrus 229

FIGURE S1 Comparison of KA1 expression in the CA3 field of the hippocampus in a heterozygous indel individual (a) and homozygous insertion individual (b). 298

LIST OF TABLES

Number		*Page*
TABLE 1.1	KA1 expression in brain	40
TABLE 2.1	Chemical and biological products used for molecular biological techniques	47
TABLE 2.2	Kits used for molecular biological techniques	48
TABLE 2.3	Antibodies and pre-immune serum	53
TABLE 2.4	Primers used for DNA PCR amplification and sequencing	54
TABLE 2.5	BAC and Fosmid clones used for cytogenetic analysis	58
TABLE 2.6	Primers used for TaqMan assays	68
TABLE 2.7	RT-PCR primers designed across exons encoding different parts of ABCA13	71
TABLE 3.1	Analysis of homozygosity tract lengths and inbreeding coefficients per individual	91
TABLE 3.2	HBD regions identified in the second related family	93
TABLE 4.1	Summary of identified breakpoint BAC and fosmid clones	108
TABLE 4.2	Novel variants identified from re-sequencing cases with schizophrenia and comparative controls	110
TABLE 4.3	The frequency of novel variants initially identified in cases, controls or both populations	111
TABLE 4.4	Known SNPs detected from the sequencing of case and control populations	114
TABLE 4.5	Putative pathogenic variants identified from initially screening of the *ABCA13* gene subsequent genotyped in larger cohorts of cases and controls	116
TABLE 4.6	In silico prediction of the functional/pathological consequences of all 13 newly identified non-synonymous variants	138
TABLE 4.7	Affected individuals identified as being biallelic for risk variants	138
TABLE 4.8	Comparison of percentage of males and females carrying risk variants	141
TABLE 6.1	Insertion/deletion genotyping results from individuals diagnosed with bipolar disorder and controls in the original and replication studies	184
TABLE 6.2	The combined data set from the original and replication indel study	184

TABLE 8.1	Details of individual samples used for the genotype correlation study	235
TABLE 8.2	Genotype Group Demographics	235
TABLE 8.3	Hippocampal cell counts and neuropil percentage means per individual sample	237
TABLE 8.4	Hippocampal cell count and neuropil percentage means per genotype group	238
TABLE 8.5	P and *F* values associated with hippocampal cell counts and neuropil immunoreactivity percentages	238
TABLE 8.6	Percentage increase in KA1 expression calculated for the deletion groups relative to the insertion group per hippocampal region.	241
TABLE 8.7	Analysis of genotype, gender, age, PMI, pH and hippocampal counts	242
TABLE 8.8	Frontal cortex cell count means per individual sample	244
TABLE 8.9	Frontal cortex cell count means per genotype group	244
TABLE 8.10	P and *F* values associated calculated for frontal cortex cell counts	245
TABLE 8.11	Mean percentage increase in frontal cortex KA1 expression estimated for the deletion allele groups relative to the insertion group	247
TABLE 8.12	Analysis of genotype, gender, age, PMI, pH and frontal cortex cell counts	248
TABLE S1	Re-calculated P-values for collective significance of the associated *ABCA13* variants	297

LIST OF GRAPHS

Number		*Page*
GRAPH 3.1	Graph of homozygous tract lengths (ROHs) for each pedigree member	91
GRAPH 8.1	Genotype effect on mean cell counts and neuropil abundance in the hippocampus	239
GRAPH 8.2	The deletion allele increases KA1 immunoreactivity in neuronal cells in the hippocampus	241
GRAPH 8.3	Genotype effect on mean cell counts in the frontal cortex	245
GRAPH 8.4	The deletion allele increases KA1 immunoreactivity in neuronal cells in the frontal cortex	247

ABBREVIATIONS

α	Alpha
aa	Amino acid
AA	Arachidonic acid
ABC	ATP binding cassette transporters
ABCA	ATP binding cassette transporter, subfamily A
ABCA1	ATP binding cassette transporter A1
ABCA4	ATP binding cassette transporter A4
ABCA12	ATP binding cassette transporter A12
ABCA13	ATP binding cassette transporter A13
AMD	Age-related macular degeneration
AD	Altheimer's disease
ADSL	Adenylosuccinate lyase
AMPA	α-amino-3-hydroxy-5-methyl-4-isoxazolepropionic acid
AREs	AU-Rich elements
ASD	Autism Spectrum Disorder
ATF4	Activating transcription factor 4
ATP	Adenosine triphosphate
ATP2A2	ATPase, Ca++ transporting, cardiac muscle, slow twitch 2.
BAC	Bacterial artificial chromosome
BBS	Bardet-Biedl syndrome
BDNF	Brain derived neurotrophic factor
BLAST	Basic local alignment search tool
BLAT	Basic local alignment tool
bp	Base pair
BP	Bipolar disorder
BRCA1	Breast cancer 1
BRCA2	Breast cancer 2
BSA	Bovine serum albumin
°C	Degrees centigrade
CDCV	Common disease – common variant hypothesis
CDFE	Cortical Dysplasia–Focal Epilepsy syndrome
CDRV	Common disease – rare variant hypothesis
cDNA	Complementary DNA
CA	Cornu ammonis
CACNA1C	Calcium channel, voltage-dependent, L type
CACNG2	Voltage-dependent calcium channel gamma-2
CAD	Coronary artery disease
cAMP	Cyclic adenosine monophosphate
CFTR	Cystic fibrosis transmembrane conductance regulator
CHB	Chinese population
CI	Confidence interval

cM	centiMorgans
CNS	Central Nervous System
CNTNAP2	Contactin-associated protein-like 2 precursor
CNTF	Ciliary neurotrophic factor
CNV	Copy Number Variant
CRC	Colorectal cancer
CRD3	Cone-rod dystrophy type 3
CSF2RA	Colony stimulating factor 2 receptor, alpha
CT	Computed tomography
DAB	Diaminobenzidine
DAPI	4',6-diamidino-2-phenylindole
DA	Dopamine
DAAO	D-amino acid oxidase
DAG	Diacylglycerol
D_2	Dopamine type-2 receptors
δ	Delta
DD	Darier disease
del	Deletion
DFNB	Deafness, Neurosensory, Autosomal Recessive
DFNB31	Autosomal recessive deafness type 31 protein
DG	Dentate gyrus
DGKH	Diacyl glycerol kinase
dH_2O	Distilled water
DISC1	Disrupted-In-Schizophrenia-1
DMD	Duchenne Muscular Dystrophy
DZ	Dizygotic
DNA	Deoxyribonucleic acid
DNase	A deoxyribonuclease
dNTP	Deoxyribonucleotide triphosphate
DSM	Diagnostic and Statistical Manual of Mental Disorders
DTNBP1	Dysbindin
DYNC1I1	Dynein, cytoplasmic 1, intermediate chain 1
EC	Entorhinal cortex
E-Coli	Escherichia coli
EDTA	Ethylenediaminetetraacetic acid
EEG	Electroencephalographic
EFAs	Essential fatty acids
EGFR	Epidermal growth factor receptor isoform b
EM	Electron microscopy
EM	Expectation Maximisation
EPSCs	Excitatory postsynaptic currents
$EPSC_{KA}$	Excitatory postsynaptic currents kainate receptor
ER	Endoplasmic Reticulum

F	Inbreeding coefficient
FISH	Fluorescence *in situ* hybridization
fMRI	Functional Magnetic Resonance Imaging
FPEVL	Familial Partial Epilepsy syndrome with Variable Loci
g	Grams
GABA	Gamma-aminobutyric acid
GAD	Generalized anxiety disorder
GAD_{67}	Glutamate decarboxylase
GAPDH	Glyceraldehyde 3-phosphate dehydrogenase
GC	Glucocorticoids
GCL	Granular cell layer
gDNA	Genomic DNA
GFAP	Glial fibrillary acidic protein
GFP	Green fluorescent protein
G6PD	Glucose-6-phosphate dehydrogenase
GPR24	G protein-coupled receptor 24
GRIA1	Glutamate ionotrophic receptor, AMPA 1
GRIA3	Glutamate ionotrophic receptor, AMPA 3
GRID2	Ionotropic glutamate receptor, delta subunit 2
GRIK1	Ionotropic glutamate receptor, kainate 1 (protein GLUR5)
GRIK2	Ionotropic glutamate receptor, kainate 2 (protein GLUR6)
GRIK3	Ionotropic glutamate receptor, kainate 3 (protein GLUR7)
GRIK4	Ionotropic glutamate receptor, kainate 4 (protein KA1)
GRIK4	Ionotropic glutamate receptor, kainate 5 (protein KA2)
GRIM3	Metobotropic glutamate receptor 3
GRIM4	Metobotropic glutamate receptor 4
GRIN1	NMDA receptor 1
GRIN2B	NMDA receptor subunit 2B
GWAS	Genome-Wide Association Study
h	Hilus
HBD	Homozygous-by-descent
HD	Huntington's disease
H DAB	Haematoxylin and DAB
HDL	High Density Lipoprotein
HDR	ATP binding cassette transporters
HGU	Human Genetics Unit
HPA	Hypothalamic-pituitary-adrenal axis
HRP	Hydrophobic dipping region
5-HT	5-hydroxytryptamine /serotonin
$5\text{-}HT_1$	Serotonin type 1 receptor
$5\text{-}HT_2$	Serotonin type 2 receptor
HTR2A	5-hydroxytryptamine (serotonin) receptor 2A
HTT	Huntingtin protein
HWE	Hardy–Weinberg equilibrium

IBD	Identity By Descent
ICD	The International Statistical Classification of Diseases and Related Health Problems
Id	Identity
IHC	Immunohistochemistry
indel	Insertion/deletion
ins	Insertion
iml	Inner molecular layer
IP3	Inositol-1, 4,5-triphosphate
IPSC	Inhibitory post synaptic currents
IPTG	Isopropyl β-D-thiogalactopyranoside
IREs	Iron-responsive elements
IRPs	Iron regulatory proteins
JAM3	Junctional adhesion molecule 3 precursor
JPT	Japanese population
KAR	Kainate receptor
kb	Kilobase
KCNB1	Potassium voltage-gated channel, subfamily G
KCND3	Potassium voltage-gated channel, Shal-related
KCNF1	Potassium voltage-gated channel, subfamily F
kDA	Kilo Daltons
Kir	Inward rectifying potassium channel
KO	Knock out
KRIT1	Krev interaction trapped protein 1
l	Stratum lucidum
LB	Luria-Bertani
LD	Linkage disequilibrium
LOD	Logarithm of odds
LSD	Lysergic acid diethylamide
LTP	Long term potentiation
LDP	Long term depression
µg	Micrograms
µl	Microlitre
µM	Microns
m	Stratum lucunosum moleculare
M	Molar
MAF	Minor allele frequency
Mb	Megabase
MCHR1	Melanin-concentrating hormone receptor 1
MDD	Major Depressive Disorder
MELAS	Mitochondrial Encephalopathy, Lactic Acidosis, and Stroke-like episodes
MeOH	Methanol
MERRF	Myoclonic Epilepsy with Ragged Red Fibers

MF-CA3	Mossy fibre-CA3
mg	Milligrams
$MgCl_2$	Magnesium chloride
mGluR	Metobotropic glutamate receptor
mHom	Mouse homogenate
min	Minutes
ml	Millilitres
mM	Millimolar
MR	Mental retardation
MRC	Medical Research Council
mRNA	Messenger RNA
MYLC2PL	Myosin light chain 2
MYO5B	Myosin VB
MZ	Monozygotic
nACh	Nicotinic acetylcholine
NaCl	Sodium chloride
NAD	Non affected with psychiatric illness
NaOH	Sodium hydroxide
NBD	Nucleotide binding domain
NCBI	National Center for Biotechnology Information
NLGN3	Neuroligin 3
NLGN4	X-linked neuroligin 4
ng	Nanograms
NMDA	N-methyl-D-aspartic acid
NMR	Nuclear magnetic resonance
NPL	Non parametric linkage analysis
NPAS3	Neuronal PAS domain-containing protein 3
NRG1	Neuregulin
NXN	Nucleoredoxin
o	Stratum oriens
OD	Optical density
oml	Outer molecular layer
OR	Odds ratio
p	stratum pyramidal
PAR	Population Attributable Risk
PBS	Phosphate buffered saline
PCM1	Pericentriolar material 1 protein
PCP	Phencyclidine
PCR	Polymerase chain reaction
PDE4D	Phosphodiesterase 4d
PDE4	Phosphodiesterase 4
PET	Positron emission tomography
pH	Power of Hydrogen
PI	Phosphoinositide
PIP_2	Phosphatidylinositol 4,5-bisphosphate

PKC	Protein kinase C
PLA2	Phospholipase A2
PLA2G6	Phospholipase A2, group VI
PPF	Paired pulse facilitation
PMI	Post mortem interval
PPP1R9A	Protein phosphatase 1, regulatory (inhibitor) subunit
PPP1R3B	Protein phosphatase 1, regulatory (inhibitor)subunit
PrS	Presubiculum
PTSD	Post traumatic stress disorder
qs	*quantum sufficiat* /quantity sufficient
QTL	Quantitative trait loci
r	Stratum radiatum
RGS4	Regulator of G-protein signaling 4
RIN	RNA Integrity Number
RNA	Ribonucleic acid
RNaseA	Ribonuclease A
RNS	Reactive nitrogen species
ROHs	Runs of Homozygosity
ROS	Reactive oxygen species
RP19	Retinitis pigmentosa type 19
rpm	Revolutions per minute of rotor
RTA	Road traffic accident
RT-PCR	Reverse transcription - PCR
s	Subiculum
SADS-L	Schedule for Affective Disorders and Schizophrenia-Lifetime
SCZ	Schizophrenia
SDS	Sodium dodecyl sulphate
SDSC	San Diego Super Computer
SDS-PAGE	SDS-polyacrylamide gel electrophoresis
SEM	Standard error of the mean
SEMA3A	Semaphorin 3E
SGZ	Subgranular zone
SHANK3	Proline-rich synapse-associated protein 2
SLC26A4	Pendrin
SLC26A5	Prestin isoform d
SLC6A4	Solute carrier family 6 member 4 / serotonin transporter gene
SORCS2	Sortilin-related VPS10 domain containing receptor 2
SNHL	Sensori-neural hearing loss
SNP	Single nucleotide polymorphism
SOX2	Sry-related HMG box transcription factor
SSC	Standard saline citrate
SSRI	Specific serotonin re-uptake inhibitor
STAR*D	Sequenced Treatment Alternatives to Relieve Depression
STGD	Stargardt disease
TAC1	Tachykinin 1 isoform

Taq	*thermus aquaticus*
TBE	Tris-Borate-EDTA
TBlast	Translated sequence database
TD	Tangier disease
TE	Tris-EDTA
THEX1	Three prime histone mRNA exonuclease 1
TMDs	Transmembrane cluster domains
TPH_2	Tryptophan hydroxylase 2
TRIOBP	TRIO and F-actin binding protein
TSPAN8	Transmembrane 4 superfamily member 3
Tween 20	Poly(oxyethylene) sorbitan monolaurate
TX-100	Triton-X-100
U	units
UCSC	University of California Santa Cruz
UPD	Uniparental disomy
USS	Upstream sequence
dUTP	2'-Deoxyuridine 5'-Triphosphate
UTR	Untranslated region
3'UTR	3 prime untranslated region
5'UTR	5 prime untranslated region
UV	Ultraviolet
VGCNL1	Voltage gated channel like 1
VEGF	Vascular endothelial growth factor
WFS1	Wolfram syndrome
WGH	Western General Hospital, Edinburgh
WHO	World Health Organization
WS	Wolfram syndrome
WTCCC	Welcome Trust Case Control Consortium
WT-CRF	Welcome Trust Clinical Research Facility
xg	Measure of relative centrifugal force
YAC	Yeast artificial chromosome
ZIP3	Solute carrier family 39

CHAPTER 1

INTRODUCTION

ACKNOWLEDGEMENTS FOR CHAPTER 1

The clinical data relating to the consanguineous families were collected by Dr M. Ayub, Dr M. Irfan and Dr F. Naeem. The clinical description of the family members was written jointly by Dr Mohammed Ayub and Professor Douglas Blackwood. Microsatellite genotyping was initially performed by me assisted by Alan Maclean.

The initial mapping of chromosomal breakpoints disrupted in the complex chromosomal re-arrangement inv(7)(p12.3;q21.11), t(7;8)(p12.3;p23) was performed by Pat Malloy, Ben Pickard and James Birtley.

1. INTRODUCTION

1.1 Psychiatric Illness

1.1.1 Schizophrenia

Schizophrenia is a leading cause of morbidity, incurs high public health costs and has a devastating impact on the lives of patients, their families, and on societies as a whole in populations world-wide. It is a debilitating, progressive neuropsychiatric disease characterized by alterations in mood, beliefs, perceptions and psychomotor behaviour - frequently accompanied by cognitive impairment. The lifetime morbid risk to the general population, as surveyed in developed countries, is close to 1%. The incidence of schizophrenia shows relatively little variation across a variety of different populations, suggesting culture and ethnicity are not important biological factors (Owen et al., 2002). Age of onset is usually in adolescence or early adult life with the mean age of onset later in women than for men (American Psychiatric Association, 2004). The illness typically follows a course of acute episodes which may then develop into a chronic form of the disease. Life expectancy is generally reduced and self-harming and suicide are relatively frequent and tragic consequences of the disease.

Traditionally the characteristic features of schizophrenia have been divided into two clusters of symptoms; positive symptoms (delusions, hallucinations and formal thought disorder), and negative symptoms (affective flattening, apathy, poverty of speech and psychological deficits in executive function and episodic memory). In turn, studies of symptomatology have shown that these positive and negative symptoms segregate into three distinguishable subgroups termed psychomotor poverty (primarily negative symptoms) disorganization (disorder of the form of thought and inappropriate effect) and reality distortion (delusions and hallucinations) (Liddle, 1987). Clinical diagnosis is based upon international definitions published in The International Classification of Disease ICD-10 (WHO 2003) and Diagnostic and Statistical Manual of Mental

Disorders DSM-IV (American Psychiatric Association, 2004). Both nosological manuals recognize sub-varieties or sub-categories of schizophrenia. For example, DSM-IV defines five sub-types, i.e. hebephrenic, catatonic, paranoid, simple and residual; and the ICD-10 a further two (post-schizophrenic depression and undifferentiated schizophrenia). However, there is no consistent evidence of differential prognosis or response to treatment between these types, and the manifestation of the characteristic symptoms of these sub-varieties may change with the course of a patient's illness. Likewise, family studies do not provide convincing evidence supporting these subdivisions. Indeed, psychiatric conditions such as schizotypal personality disorder categorized as "part of the genetic spectrum" of schizophrenia (Kendler et al., 1991) and schizoaffective and bipolar disorder, both classified separately, are relatively common in close relatives of schizophrenics (Craddock et al., 2005). This raises interesting questions about the aetiological relationship between schizophrenia and other psychiatric illnesses which, as yet, cannot be answered. It is clear that the standard definitions of psychiatric disease will inevitably evolve as neurobiological findings are reported and in a reciprocal manner, the interpretation and the direction of research will change with new models of psychiatric disease.

1.1.2 Affective disorders

'Affective disorders' include a wide variety of complex conditions that have as a core feature a pathological disturbance of mood. A fundamental clinical distinction in classification of these disorders is between mania and depression. Bipolar disorder (formerly known as manic depressive psychosis) is characterized by two or more manic episodes lasting at least one week and usually accompanied, at other times in a patient's history, by major depressive episodes. Symptoms of mania, as outlined in DSM-IV, include: inflated self-esteem, decreased need for sleep, elevated and irritable mood, distractibility, increased goal-directed activity and psychomotor agitation. Symptoms for depressive episodes include depressed mood, reduced energy and decreased activity, ideas of self-harming, reduced self-esteem and confidence, and pessimistic thoughts

(WHO, 2003). It is not uncommon for mania and depressive symptoms to occur simultaneously and to be accompanied by psychotic features and/or cognitive impairment. Furthermore, bipolar disorder itself is highly co-morbid with other conditions such as anxiety and substance abuse (Gelder et al., 2006). Lifetime prevalence is estimated between 0.5-1.5 per cent with similar rates in males and females. Mean age of onset is around 17 to 21, but symptoms may first appear at any stage in life (Smith and Weissman, 1992) (Kessler et al., 1997).

Major depressive disorder (MDD), formerly called endogenous depression or melancholia is now often termed unipolar disorder or recurrent depressive disorder. It is characterized by one or more depressive episodes lasting at least two weeks without other episodes of mania or hypomania. Lifetime population risk is higher than bipolar disorder although reported estimates differ between studies, ranging from 4 to 17% (Kessler et al., 1994; Weissman et al., 1998). Moreover, lifetime prevalence is twice as great in women as men in developed countries (Kessler et al., 1994; Weissman et al., 1998; Alonso et al., 2004) Age of onset varies widely, however, with the mean age generally reported to be mid-20s and to be similar for both males and females. Like schizophrenia, the pathogenesis of these affective disorders is not well understood and there are no biological diagnostic markers. Yet these disorders are associated with high mortality, high levels of heath service utilization, and they are estimated to be second only to ischaemic heart disease as a cause of global health burden in 2020 (Murray and Lopez, 1996).

1.1.3 Epidemiological analysis of psychiatric disorders

Epidemiological analysis of psychiatric illness involving family, twin and adoption studies provides strong evidence for the vertical transmission of genetic factors contributing to the expression of schizophrenia, bipolar and major depressive disorder. Extensive family studies, reviewed by Gottesman (1991), indicate the lifetime risk for first degree relatives of schizophrenics is approximately ten times greater (10%) than for

the general population (1%) (Gottesman, 1991). The risk increases to between 40 and 50% when both parents are affected and declines to about 3% for second degree relatives (Kendler, 2000). The lifetime risk for first degree relatives of bipolar individuals is similar to that of schizophrenia (5-10 %) but relative risk is estimated to be lower (2%) for MDD (Craddock and Jones, 2001). Furthermore, relatives of bipolar probands are also at increased risk of other affective disorders including major depressive disorder.

Adoption studies have consistently shown increased incidence of schizophrenia in biological relatives of schizophrenic adoptees but not in control adoptees or adoptive relatives. This implicates shared genetic rather than environmental influences (McGuffin et al., 1995). Moreover, based upon data from five recent twin studies, proband-wise concordance rates for MZ twins are between 41 and 65% as compared with 0-28% for DZ twin pairs. Consequently, heritability has been estimated at approximately 80-85% (Cardno and Gottesman, 2000). Likewise, concordance rates for bipolar MZ twins (50-60%) and major depressive disorder monozygotic (MZ) twins (46%) are higher than for dizygotic (DZ) twin pairs (20%) - with heritability rates for bipolar disorder calculated to be similar to schizophrenia (>80%) and lower for MDD (70%) (Kendler et al., 1993; McGuffin et al., 1996). From these findings it is clear that both the environment and genetics are aetiological factors and that genotype confers a predisposition or liability to develop the disease.

1.1.4 Genetic models of psychiatric illnesses

The study of psychiatric genetics is complicated by a number of issues, for example, phenotypic heterogeneity, incomplete disease penetrance and uncertainties concerning mode of inheritance. Nevertheless, three models hypothesized to explain the underlying genetics of complex traits have influenced how investigators approach and interpret genetic research. The first model, the quantitative trait loci (QTL) hypothesis, assumes that the genetic contribution to a disorder involves the additive and/or epistatic

interaction of several (oligogenic inheritance) or many (polygenic inheritance) genes of small effect. Under this model, also termed the 'common disease – common variant hypothesis' (CDCV), disease is postulated to stem from multiple common factors each with a small impact on disease risk (Chakravarti, 1999). In contrast, the single gene defect model, the 'common disease – rare variant' hypothesis (CDRV), proposes that a single gene can have a major effect on risk of disease and that these rare mutations are highly penetrant (i.e. most carriers express the disease phenotype). However, the term 'rare variant' has been used to describe two types of risk factor. Firstly, it is applied to severely deleterious mutations (of the type causing monogenic diseases) which are highly penetrant and individually rare, even specific to single patients or families hence showing familial segregation with a minor allele frequency (MAF) of <0.1%. Secondly, there are risk variants that are more common than deleterious mutations but rarer than polymorphisms (>1% in population) and are of moderate risk (i.e. have moderate odds ratios OR) and penetrance so that familial concentration may not appear to follow standard Mendelian segregation. Moreover, in the CDRV model different affected individuals may harbour both types of rare variant in the same or different 'high risk' gene, but each individual carries only one or two mutations (McClellan et al., 2007; Bodmer and Bonilla, 2008).

The third model, the mixed model of inheritance, suggests that a gene of major effect might act in combination with a background of polygenes. However, the testing of this model has yielded inconclusive results (McGuffin et al., 1995). Nevertheless, population genetics equilibrium models and empirical studies support a role for both rare and common variants. The genetic architecture of other common genetically complex chronic diseases such as colorectal cancer (CRC), breast cancer and Alzheimer's disease provide evidence that a significant proportion of the inherited susceptibility may be due to moderate to high penetrant rare mutations and common mulitfactorial variants (Di Rienzo, 2006; Bodmer and Bonilla, 2008).

1.1.5 What do we mean by a genetic factor?

From the preceding discussions it is clear that genetic factors predispose individuals to psychiatric illness and that multiple models exist to explain the underlying genetics of common complex disease. This leads to the next pertinent question: what exactly is meant by a genetic factor or variant? Traditionally, chromosomal abnormalities resulting in a loss, gain, inversion or disruption of genomic material, together with large-scale deletions or duplications of genomic sequence, are known to give rise to clinical disorders and syndromes. These lesions may result in the disruption of transcription of one or more genes and consequently may affect gene product dosage.

Similarly, small-scale deletions, insertions and duplications as well as point mutations within a gene are known to cause simple Mendelian diseases. Point mutations, the substitution of one nucleotide base for another, can be further classified into the subgroups, null mutations, missense mutations and silent mutations. Nonsense mutations, frameshift and cryptic splice variants (generally termed loss-of-function or null mutations) commonly result in a premature stop codon, truncated transcription products and reduced or no protein product as a consequence of mRNA products being broken down by nonsense mediated decay processes. Missense or non-synonymous mutations are the exchange of one nucleotide for another, causing substitution of a different amino acid in the peptide sequence. This may alter protein structure and activity by either reducing the efficacy of normal protein function or causing new and abnormal gain of functions. Silent mutations which can occur within exons (synonymous variants) or non-coding regions are base changes that do not change the protein sequence but may affect splicing, or transcription control. It is this class of mutation which is more likely to be neutral, i.e. it confers no change to protein function, and constitutes the majority of common single nucleotide polymorphisms (SNPs) in the human genome.

For simple Mendelian diseases, hundreds of different null mutations and missense mutations have been identified and consequently shown to have a significant effect on the function of a specific disease causing protein. For example, over 1600 mutations have been found in the CFTR gene which causes cystic fibrosis, with over 600 being missense and 500 nonsense, frameshift or splice mutations (Cystic Fibrosis Mutation Database 2008, http://www3.genet.sickkids.on.ca/cftr/). What is evident from the genetic research of simple Mendelian diseases, and more recently of common complex diseases such as breast cancer and colorectal cancer, is that these disorders are characterized by high alleleic heterogeneity (sets of multiple mutations in the same gene) particularly for rare causal mutations (McClellan et al., 2007). Disease causing sets of rare point mutations have already been identified in different genes known to underlie Autistic Spectrum Disorders (ASD) (Jamain et al., 2003; Laumonnier et al., 2004; Durand et al., 2007; Bakkaloglu et al., 2008). Moreover, putatively pathological ultra-rare variants have been reported in DISC1 (a schizophrenia candidate gene discussed in section 1.2.3); and in genes known to cause Wolfram syndrome (WS) and Darier disease (DD), two diseases frequently co-morbid with mood disorders (Kato, 2001; Song et al., 2008).

Common disease variants are candidates for susceptibility if there is a significant difference in the frequency of alleles between diseased and control groups. A group of susceptibility variants may be in the same gene or indeed a set of different genes with related functions indicating disruption of a biological pathway. Variants are assessed for their potential effect on protein function by a number of criteria including: occurrence in conserved functional regions of the protein; species and protein family amino acid conservation; charge and amino acid structural changes likely to affect protein folding and structure; variant segregation in affected members of families; and biochemical and functional assays. Furthermore, altered expression of the gene product assessed by genotype specific postmortem expression studies can lend further support for a variant's candidacy.

Owing to advancements in chip array technologies, another type of structural variant, copy number variants (CNVs), have grown in prominence in recent years. Copy number variants are submicroscopic DNA segments ranging from kilobases to megabases, variable in copy number compared to a reference genome. CNVs are classified into types according to their complexity and include deletions, duplications, multi allelic loci, and more complex loci (e.g. inversions) (Redon et al., 2006). In a seminal paper, Redon and colleagues estimate that over 360 megabases of DNA are covered with CNVs, which is approximate to 12% of the human genome. This is more nucleotide content per genome than [as yet known] single nucleotide polymorphisms (SNPs). Thus CNVs are likely to have a major effect on genetic diversity and evolution. Although many CNVs are postulated to be neutral polymorphisms there is emerging evidence that rare, inheritied and *de novo*, CNVs give rise to psychiatric disorders and other diseases (ISC, 2008; Stefansson et al., 2008; Walsh et al., 2008).

1.2 Molecular approaches to the study of psychiatric disorders

Molecular genetic research currently employs three main strategies to detect candidate genes: linkage analysis, case-control association studies, and investigation of cytogenetic abnormalities.

1.2.1. Linkage analysis

In families with multiple affected members, linkage techniques assess the co-inheritance of DNA marker alleles (microsatellite or single nucleotide polymorphisms SNPs) with a disease state. This approach has been highly successful in identifying susceptibility regions and genes for other complex disorders such as early-onset Alzheimer's disease. However, the genomic regions so mapped tend to be large, the technique has limited power to detect susceptibility genes of small effect and diagnosis of family members may change with time. Linkage studies of schizophrenia pedigrees have found evidence for linkage at genome-wide significance levels, although many positive findings have

failed to be subsequently confirmed. Two meta-analyses of schizophrenia linkage studies have been reported with some overlap in results. Badner and Gershon found support for the existence of susceptibility genes on chromosome 8p, 13q and 22q whilst Lewis and colleagues for chromosome 1q, 3p, 5q, 6p, 8p, 11q, 14p, 20q and 22q (Badner and Gershon, 2002; Lewis et al., 2003). Thus two regions, 8p and 22q were supported by both meta-analyses, but these loci are large and harbour hundreds of genes.

Genome-wide linkage scans have also provided some support for loci of large/moderate effect in multiplex pedigrees affected by bipolar and major depressive disorder. Again, there has been a lack of replicable findings and identification of causal factors or variants. The most consistent and replicated findings for bipolar disorder have been chromosome 4p16, 6q16-25, 11p15, 12q23-24, 18p11, 21q22 and 22q12 and for MDD 2q33, 3p12, 8p22, 12q22-23, 15q13, 18q21 (Camp et al., 2005; Levinson, 2006; Serretti and Mandelli, 2008). However, two meta-analyses have been performed using bipolar linkage data sets which showed no overlap in results. Badner and Gershon found strongest evidence for susceptibility loci on chromosome 13q and 22q whilst Bennett and colleagues for chromosomes 9p21-22, 10q11.2, 14q24-32 and 18p-q (Badner and Gershon, 2002; Bennett et al., 2002). What is evident from linkage studies is that there is some of overlap in candidate susceptibility loci between bipolar disorder and MDD (for example 12q23 a regions which houses the gene *ATP2A2* associated with Darier disease mentioned above) and bipolar and schizophrenia chromosome regions 18p11, 13q32, 10p14 and 22q11-13 (Berrettini, 2000).

1.2.2 Case-control association studies

Population-based case-control association studies involve comparing the frequency of polymorphic alleles in a sample of patients with ethnically matched non-symptomatic controls. These may be performed as genome-wide scans (Genome–Wide Association Study or GWAS) where the positions of the susceptibility loci or causal variants are unknown; as candidate gene studies over small genomic regions; or as a comparison of

frequencies of a putative disease variant itself. SNP-tag association studies utilise markers, predominately SNPs, as 'proxies' for susceptibility variants with the underlying assumption that the markers will be in linkage disequilibrium with the nearby disease susceptibility alleles. Typically, the minor allele frequencies of chosen marker SNPs are above 5%, and hence this approach is not designed to detect susceptibility alleles that are rare in the general population. As linkage disequilibrium blocks extend over relatively short genomic distances, SNP-tag association studies give higher resolution for mapping than linkage mapping but, for sufficient power to detect and confirm the presence of alleles of small effect, large sample sets screened with high-density markers are needed (Owen et al., 2002; Blackwood and Muir, 2004).

High powered multi-centre SNP-tag GWAS studies of non-psychiatric common complex diseases and traits have proved to be highly successful in identifying common risk loci (WTCCC, 2007; Kathiresan et al., 2008; Willer et al., 2008). Large collaborative studies of schizophrenia and MDD are currently underway although the results are still unpublished. Nonetheless, one small-scale and therefore less powered GWAS study of schizophrenia conducted by Lencz and colleagues found significant association at loci on the X and Y chromosomes (Xp22.32 and Yp11.3) neighbouring the *CSF2RA* gene at the level of genome-wide significance (Lencz et al., 2007). Furthermore, four GWAS studies provide suggestive or moderate evidence for susceptibility loci on chromosomes 1q32, 7q22.1, 2q32.1 and 12q24.23, although there is a lack of apparent correspondence between results (Mah et al., 2006; Kirov et al., 2008; O'Donovan et al., 2008; Shifman et al., 2008a). Similarly, while there are no reports of small scale GWA studies for major depressive disorder per se, a GWAS performed for neuroticism (a personality trait that shares genetic determinants with major depression and anxiety disorders) indicated suggestive evidence within the *PDE4D* gene on chromosome 5q11.2 (Shifman et al., 2008b).

In contrast, three collaborative SNP-tag GWAS studies have been performed for bipolar disorder. The Wellcome Trust Case Consortium (WTCCC, 2007) reported one SNP

rs420259, located on 16p12, which reached a level of genome-wide significance (WTCCC, 2007). This region, however, does not appear to be a BP linkage hotspot as analysed by two major meta-analyses of BP linkage (Badner and Gershon, 2002; Segurado et al., 2003). A second GWAS study, conducted by Baum and colleagues, obtained a nominal P-value for a marker within *DGKH*. In addition, several other loci showed replicated suggestive association, located within the genes *DFNB31*, *SORCS2*, *NXN*, and *VGCNL1* (Baum et al., 2008). A meta-analysis of these two studies indicated some overlap in the top association signals, the most consistent associations being for SNPs in or near to the genes *ZIP3*, *JAM3* and *DFNB31* (Baum et al., 2008). A third multi-centre study reported genome-wide significant association for SNPs in *MYO5B*, *TSPAN8* and *EGFR* (Sklar et al., 2008). Interestingly, the most consistent association found between this study and that of the WTCCC was for a SNP in a voltage-gated calcium channel, *CACNA1C*. The lack of consistent findings from GWA studies of schizophrenia and BP in relation to previously reported candidate loci and genes suggests either that common susceptibility loci are of modest effect with modest to low risk ratios, that genetic heterogeneity may be high, or that rare genetic factors other than common variants may play a larger part in the aetiology of these disorders.

Genome-wide association studies have also been reported with newly identified rare copy number variants in populations of cases and controls. Three recent studies of schizophrenia, using high resolution SNP chip arrays, show intriguing results. First, Walsh and colleagues reported a three-fold increase in rare (frequency less than 1%) structural variants in cases versus controls. This difference increased to four-fold when an independent set of cases of childhood onset schizophrenia were analysed. Moreover, there was an excess of CNVs disrupting genes from signalling networks, neurodevelopmental pathways including synaptic long-term potentiation, axon guidance signalling and glutamate receptor signalling (Walsh et al., 2008). A second multi-centre study also reported a 1.15-fold increase in large rare CNVs in patients with schizophrenia compared to controls. In addition they found significant association for 2 novel regions, 1q21.1, 15q13.3 as well as 22q11 - a region previously known to be

deleted in individuals with velo-cardio-facial syndrome a condition which is commonly associated with schizophrenia (ISC, 2008). These loci were also shown to be nominally associated with schizophrenia in a third study (Stefansson et al., 2008). Taken together, these findings strongly support a role for rare high risk structural variants contributing to the genetic burden of schizophrenia.

Case-control candidate gene association studies aim to identify risk alleles in or around a specific candidate gene. Hundreds of candidate gene studies have been performed for schizophrenia, bipolar disorder and MDD, with many findings being reported positive. However, confirmation of an association by independent replication is often not forthcoming and further evidence, whether genetic, functional or behavioural, is needed to confirm candidacy.

1.2.3. Chromosomal abnormalities

Distinct chromosomal rearrangements have been the starting point for identifying causal genes in common genetic disorders such as Duchenne Muscular Dystrophy (DMD), Wilms tumour, fragile-X syndrome and retinoblastoma (Pickard et al., 2005b). Individual inversions and translocations which result in breakpoints that directly disrupt gene transcripts enable both a candidate gene and the potential functional mutation sites to be rapidly identified and hence have the potential to identify individual gene components of pathological pathways or processes underlying disease. Although bypassing many of the problems associated with linkage and association studies, a number of issues inherent to this approach should be highlighted. Firstly, disruption of a gene in only one case does not prove causality and additional validation is needed. This can be provided by, for instance: the co-segregation of the mutation event with disease within a family; positive linkage or association findings for the breakpoint region; mutations detected in other unrelated cases; or neurobiological findings implicating a role for the gene in the pathogenesis of the disorder. Secondly, genes lying close to a breakpoint may also contribute to the clinical phenotype if their regulatory elements,

which control expression, are disrupted (Kleinjan and van Heyningen, 1998). Thirdly, novel, and putatively pathogenic, transcripts may be produced from the fusion sequence contributed by both chromosomes apposing the breakpoint.

These issues aside, the study of cytogenetic abnormalities has been, and continues to be, a highly effective strategy for discovering genes of major effect in neuropsychiatric illness. For instance, cytogenetic abnormalities identified in patients with autism spectrum disorders (ASD) (estimated to be approximately 3% of cases) have revealed new susceptibility genes in which rare causal and risk point-mutations have subsequently been detected, e.g. *NLGN3*, *NLGN4*, *SHANK3, CNTNAP2*. These lesions consequently implicate pathogenic disturbance of specific biological processes such as glutamatergic synapse function (Jamain et al., 2003; Vorstman et al., 2006; Durand et al., 2007; Bakkaloglu et al., 2008).

Cytogenetic research in schizophrenia, bipolar and MDD lags behind autism in that far fewer discrete chromosomal rearrangements have been identified in cases. Nevertheless, a number of disrupted breakpoint genes, e.g. *DISC1*, *PDE4B*, *NPAS3*, *GRIA3* and *GRIK4*, have gained strong support for their candidacy and provide some insight into putative pathological molecular and biological mechanisms.

Disrupted-in-schizophrenia 1 (*DISC1*) was originally mapped as a gene disrupted by a balanced translocation on chromosome 1q42 (1;11) (q42,1;q14.3) that segregated in a large Scottish pedigree with schizophrenia, bipolar disorder and MDD (St Clair et al., 1990; Millar et al., 2000; Blackwood et al., 2001). Linkage and association findings support a role of *DISC1* as a common susceptibility gene, and recently high risk ultra-rare coding variants in *DISC1* were associated with schizophrenia with an estimated attributable risk of approximately 2% (Porteous et al., 2006; Song et al., 2008). *DISC1* encodes a protein predicted to act as a 'hub' protein that connects multiple proteins involved in a number of biological processes such as neurodevelopment, cytoskeletal function and cAMP signaling. Of interest, the down-regulation of Disc1 leads to

accelerated neural integration resulting in aberrant positioning of dentate granule cells during the process of adult neurogenesis (Duan et al., 2007). Furthermore, Disc1 missense mouse mutants exhibit behaviour that is consistent with depression-like and schizophrenia-like phenotypes, and show macroscopic brain abnormalities similar to those reported for patients with schizophrenia and to lesser extent bipolar disorder (Clapcote et al., 2007).

Phosphodiesterase 4B (*PDE4B*) was identified as a breakpoint gene in two related individuals with psychiatric illness carrying a balanced t(1;16)(p31.2;q21) translocation (Millar et al., 2005). Subsequent to this finding, two studies have reported association of *PDE4B* with schizophrenia providing additional genetic support for its involvement in psychiatric illness (Pickard et al., 2007; Fatemi et al., 2008). PDE4B is a member of the PDE4 family which possesses cAMP hydrolysis activity that is specifically inhibited by the antidepressant drug rolipram. Moreover, members of this family are orthologous to the *Drosophila* learning and memory gene *dunce*, so named because mutations in the ortholog cause learning and memory deficits. Intriguingly, PDE4B and DISC1 were found to be protein-binding partners that modulate cAMP signaling in subcellular compartments (Millar et al., 2005). Hence, functional evidence strongly points to a cellular signaling mechanism which when disrupted underlies psychiatric illness.

Neuronal PAS domain protein 3 (*NPAS3*) was identified as a breakpoint gene disrupted in a reciprocal balanced translocation between chromosomes 9 and 14, in a Scottish family presenting with schizophrenia and unspecified functional psychosis co-morbid with learning disability (Kamnasaran et al., 2003; Pickard et al., 2005a). Single SNP and SNP haplotypes within *NPAS3* have subsequently been associated with schizophrenia and bipolar disorder, and (in a second independent study) with the efficacy of the antipsychotic drug iloperidone (Lavedan et al., 2008; Pickard et al., 2008a). Npas3 knockout mice manifest behavioural and neuroanatomical abnormalities reminiscent of schizophrenia, including a reduction of *reelin* expression in the adult brain and hippocampal neurogenesis defects (Erbel-Sieler et al., 2004; Pieper et al., 2005).

Glutamate receptor subunit 3 gene (*GRIA3*) was first identified as disrupted in a female with bipolar disorder and learning disability carrying a balanced translocation t(X;12)(q24;q15) (Gecz et al., 1999). A second structural variation, a partial tandem duplication of *GRIA3* was identified in an individual with autistic behaviour, learning disability, and severe psychomotor retardation (Chiyonobu et al., 2007). More recently, a single SNP and SNP haplotype within *GRIA3* was found to be associated with schizophrenia in females (Magri et al., 2008). Furthermore, rhesus monkeys chronically treated with the antipsychotic drug clozapine showed a significant increase in GRIA3 mRNA expression in the dorsolateral prefrontal cortex (O'Connor et al., 2007). *GRIA3* encodes an ionotropic glutamate AMPA subtype receptor involved in mediation of fast excitatory neurotransmission in the central nervous system. A gene encoding a second type of ionotropic glutamate receptor (*GRIK4*) has also been found to be broken in a chromosomal rearrangement carried in a patient with psychiatric illness, the details of which are discussed in section 1.4.3. These findings suggest that glutamatergic synapse function, strongly implicated as a pathogenic biological process of ASD, may also, through dysfunction of excitatory neurotransmission, play a role in the aetiology of schizophrenia and bipolar disorder.

1.3 Aetiological theories of psychiatric illness

1.3.1. Aberrant function of neurotransmitter systems

In the last twenty years standard and atypical antipsychotic drugs have become conventional treatments of schizophrenia. However, not all patients respond to acute or prolonged treatment and only limited effects are seen in some cases, whilst adverse side effects are common with most antipsychotic drugs. Given the need for more effective psychotropic agents, along with the observations that neurochemical agonists and antagonists particular to a neurotransmitter system produce, exacerbate or reduce disease symptoms, much psychopharmacological research has focused on theories of dysfunction in neurotransmitter systems (Cunningham Owens, 2004).

The most established neurotransmitter theory, 'the dopamine hypothesis', is based upon two early observations. First, schizophrenia-like symptoms occur in amphetamine abusers due to excessive dopamine release, and second, dopamine type-2 receptors (D_2) antagonists are effective in the treatment of schizophrenia (Snyder, 1973). Hence the theory proposes that pathological over-activity of the dopamine neurotransmitter system underlies psychotic symptoms. Reports of increased D_2 receptor densities and abnormal presynaptic DA metabolism, as shown in PET studies, lend support for the hypothesis (Harrison, 1999). However, it is unclear whether dopamine hyperactivity is a cause or consequence of disease. As the dopaminergic system reciprocally modulates activity in other neurotransmitter systems, in particular glutamate transmission, current views now emphasise that dopamine dysregulation may be secondary to glutamatergic abnormalities.

Dysfunction within the serotonergic neurotransmission system is also postulated to underlie the clinical manifestations of both schizophrenia and depressive disorders. This theory is based upon, and consequently supported by, several lines of evidence. First, epidemiological and behavioural studies strongly suggest that early life stress (acting concurrently with genetic factors) is an environmental precipitating factor to the development of psychiatric disorders (Blackwood and Knight, 2007). As serotonin (5-HT) is a neurochemical known to mediate adaptive and maladaptive responses to stressful events, alterations of its function could underlie pathological processes. Second, the hallucinogen, lysergic acid diethylamide (LSD) produces psychotomimetic effects similar to psychotic states and is an agonist of 5-HT_2 receptors (Geyer and Vollenweider, 2008). Third, HT_{2A}-receptor antagonism is known to contribute to the profile of 'atypical' antipsychotic action, and serotonin re-uptake inhibitors (SSRIs) are a major class of antidepressants. Finally, decreases in 5-HT_{1A} receptor binding and brain 5-HT_{2A} re-uptake sites are reported in depressed patients (Fujita et al., 2000).

Genetic studies have produced some evidence that variants in genes encoding proteins involved in serotonin-related neurotransmission are associated with bipolar disorder and

depression. For example, *SLC6A4* a serotonin transporter gene, TPH_2 a gene encoding for a rate-limiting enzyme for serotonin synthesis, and $5HTR_{1A}$ and $5HTR_{2A}$ genes encoding serotonin receptor subunits have shown consistent association. Furthermore, a functional polymorphism in the promoter region of the serotonin transporter gene *SLC6A4* was found to moderate the influence of stressful life events on depression (Caspi et al., 2003). However, although association of these genetic variants implies that a disturbance of serotonergic neurotransmission is a primary causal deficit, serotonin (like dopamine) can also modulate other neurotransmitter systems. Indeed, one mechanistic theory of depression is that decreased serotonin activity may '*allow*' these systems to act in abnormal and erratic manner and hence "facets of depression may be emergent properties of this dysregulation" (Mandell and Knapp, 1979).

The 'glutamate hypothesis' postulating hypoactive excitatory glutamatergic neurotransmission has recently become popular based on evidence emerging from pharmacological, animal, imaging and genetic studies. Initial observations indicated that the NMDA (N-methyl-D-aspartic acid) glutamate receptor antagonists phencyclidine (PCP) and ketamine cause transient psychosis resembling symptoms of schizophrenia in animals and healthy human volunteers. PCP has since been shown to exacerbate pre-existing symptoms in schizophrenic patients (Javitt and Zukin, 1991; Olney and Farber, 1995). More recently a drug, LY2140023, which is a selective agonist for metabotropic glutamate receptors, is reported to have effective antipsychotic properties (Patil et al., 2007). Furthermore, post mortem studies show decreased mRNA encoding for non-NMDA glutamate receptor subunits, alterations in glutamate synapse-related proteins and abnormalities in the cytoarchitecture of glutamatergic neurons in the prefrontal cortex and hippocampus of individuals with schizophrenia (Konradi and Heckers, 2003; Harrison and Weinberger, 2005). Likewise, abnormalities in glutamine and glutamate metabolism in the frontal lobe and anterior cingulate of schizophrenic patients as compared to controls have been indicated in several studies using imaging analysis (Theberge et al., 2002; Ohrmann et al., 2007).

In addition, linkage and association studies implicate genes which encode for proteins which can influence activity at glutamatergic synapses for both schizophrenia and bipolar disorder. Examples include, neuregulin 1 (NRG1) which has been shown to regulate expression of glutamate receptors, regulator of G-protein signalling 4 (RGS4) which inhibits signalling by the mGlu5 receptor, dysbindin (DTNBP1) located at pre- and post-synaptic glutamatergic sites, and G72 a protein that interacts with D-amino acid oxidase (DAAO) which is involved in the metabolism of D-serine, an agonist of glycine modulatory sites on NMDA subunits (Harrison and Weinberger, 2005).

Moreover, subunits of all four major classes of ionotropic glutamate receptor (NMDA, AMPA, kainate and delta) as well as the metabotropic G protein-coupled glutamate receptors have been implicated in the genetics of schizophrenia and other psychiatric conditions. For example, candidate gene association studies of the NMDA receptor subunits GRIN1 and GRIN2B, AMPA receptor subunit GRIA1, kainate receptor subunits GRIK2, GRIK3, and glutamate metabotropic receptor subunits GRIM3 and GRIM4 report significant association of polymorphisms or haplotypes within these genes with psychiatric disorders (Fallin et al., 2005; Shibata et al., 2006; Lang et al., 2007; Schiffer and Heinemann, 2007). Moreover, in addition to the cytogenetic abnormalities disrupting *GRIA3* and *GRIK4* discussed in section 1.2.3, a translocation breakpoint close to GRID2 t(4:20)(q22.2; p12.2) encoding an ionotropic delta subunit has been identified in a patient with schizophrenia (Malloy and Pickard, unpublished). Similarly, copy number variants have been detected in one case of schizophrenia and one case of bipolar disorder over the genomic region housing the kainate receptor subunit *GRIK3* (Wilson et al., 2006). Such consistent genetic findings strongly implicate glutamate transmission malfunction as a causal pathological factor, the consequences of which would affect key development processes such as synaptic formation and neurogenesis; neuroplasticity mechanisms underlying cognitive processing and ultimately the establishment of appropriate synaptic connectivity and brain circuitry.

The ‘dopamine’, ‘serotonin’ and ‘glutamate’ theories of neurotransmitter system dysfunction, as emphasised above, are unlikely to be exclusive of one another. Disturbance in one system may well have a ‘downstream’ effect upon the receptor function, circuitry and neurotransmission in other connecting brain regions. An interesting and more direct link between the function of different neurotransmitter systems has recently been made by Gonzalez-Maeso and colleagues when investigating the interaction between the serotonin and metabotropic glutamate receptors (Gonzalez-Maeso et al., 2008). This group demonstrated that 5-HT_{2A} and mGluR2 interact physically and form functional complexes in brain cortex, and that a hallucinogenic drug influencing one receptor alters functional activity in the other. They conclude that their result are “consistent with the hypothesis that the 5-HT2A–mGluR2 complex integrates serotonin and glutamate signaling” and therefore is a functional site potentially involved in the altered cortical cognitive processes of schizophrenia. These findings may be the start of nascent research indicating that disturbances in physiological interactions between a variety of different transmitter receptors underlie the neuropathology of psychiatric phenotypes.

1.3.2 Fatty acid hypothesis of schizophrenia

An alternative and less ‘mainstream’ aetiological theory originated from clinical observations made in the 1970s of an association between fever and psychotic symptom remission, and of a lower rate of rheumatoid arthritis in patients with schizophrenia. This led to the formulation of the ‘phospholipid hypothesis of schizophrenia’ which, stated simply, proposes that deficits in uptake or excessive breakdown of membrane phospholipids are associated with, and putatively contribute to, the pathophysiology of schizophrenia (Feldberg, 1976; Horrobin, 1977).

Evidence supporting this theory has come from both clinical and basic studies and centres on abnormalities in, or effects of, essential fatty acids (EFAs). The most consistent findings reported are depletion of EFAs in tissues of schizophrenic patients

(Glen et al., 1994; Yao et al., 1994; Peet et al., 1995; Doris et al., 1998; McNamara et al., 2007; McNamara et al., 2008); elevated serum/platelet PLA_2 activity in drug-free schizophrenics, (Gattaz et al., 1987; Noponen et al., 1993); and reduced phospholipid metabolism in patients and young offspring at risk of developing schizophrenia as suggested by NMR spectroscopy data (Pettegrew et al., 1993; Stanley et al., 1994; Volz et al., 2000). Furthermore, all published studies of the effects of omega-3 fatty acid supplementation given to neuroleptic-treated schizophrenic patients have reported positive therapeutic effects, see (Fenton et al., 1999) and (Yao et al., 2000) for comprehensive reviews.

In recent years a growing body of evidence based on imaging studies, microarray analysis, and metabolic and transcriptome investigation of myelin biosynthesis has implicated oligodendroglia pathophysiology in psychiatric disorders (Segal et al., 2007; Sokolov, 2007; Tkachev et al., 2007). Consistent with these discoveries are the findings that membrane phospholipids and the expression of genes encoding enzymes important in sphingolipid metabolism are significantly altered in post mortem brain tissue from schizophrenic patients and upregulated in response to antidepressant drugs (Schmitt et al., 2004; Narayan et al., 2008). However, in addition to myelination, disruption of lipid membrane structures and lipid biosynthetic pathways has the potential to affect many important biological processes including intracellular signalling pathways and neurotransmitter function. These processes will be discussed in detail in chapter four in relation to evidence that a candidate gene *ABCA13* (encoding a putative lipid transporter) contributes to the genetic load of psychiatric illnesses.

1.4 Introduction to projects

1.4.1 Project 1: Homozygosity mapping in a nuclear consanguineous family

1.4.1.1 Homozygosity mapping in consanguineous populations

Populations that are genetically isolated or have a high frequency of inbreeding tend to show an increased prevalence of recessive disorders. Historically, the study of inbred populations has been highly successful in the fine mapping of recessive traits. The effect of consanguinity reduces allelic and non-allelic heterogeneity and potentially increases linkage disequilibrium and hence the power to detect associations between genetic markers and disease (Sheffield et al., 1998). Likewise, mapping homozygous regions in affected individuals in consanguineous families is a powerful method of localising autosomal recessive genes. This technique, known as homozygosity or autozygosity mapping, assumes that affected offspring co-inherit two copies of a disease-related chromosomal segment from a common ancestor. Such positional cloning of recessive genes in families with rare genetic variants can provide valuable insight into the localisation and identity of genetic susceptibility factors involved in common types of disease with similar clinical features (Lander and Botstein, 1987).

The more closely related the parents, the greater proportion of their offspring's genome is expected to be homozygous. For example, offspring of first cousin marriages are expected to have 1/16 (6.25%) of their genome homozygous, and for second cousins the fraction is 1/64 (1.56%) (Wright et al., 1997; Weir et al., 2006). Formally this figure representing the proportion of homozygous autosomal genome is known as the inbreeding coefficient (*F*). It can be used to estimate parental relationships and highlights additional ancestral inbreeding loops. However, the greater the expected homozygosity in offspring, the greater the likelihood of identifying shared homozygous-by-descent (HBD) intervals in affected siblings which are unrelated to the 'disease' causing locus.

1.4.1.2 Family description

The original family investigated comes from North Punjab, Pakistan - a region where consanguineous marriages are frequent. The parents are first cousins and there is additional (remote) consanguinity in the ancestral kindred. The parents themselves have no detectable clinical disorders. However, five out of their six children present with either schizophrenia, epilepsy or sensori-neural hearing impairment or a combination of all three (Figure 1.1). A full clinical description of the family is presented in appendix 1. The unusual phenotype in several offspring of a cousin marriage is strongly suggestive of a rare, Mendelian recessive disorder, although other forms of inheritance can not be dismissed. This family therefore presents with a unique opportunity to identify one or several autosomal recessive genes for these conditions.

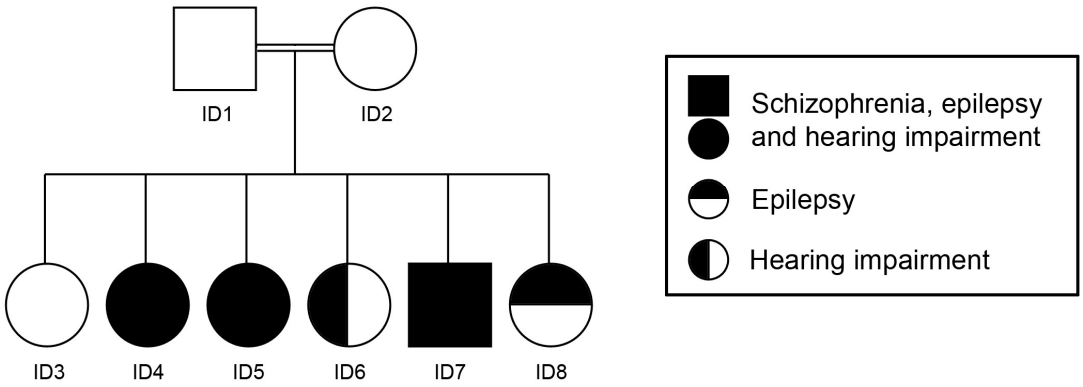

Figure 1.1 Diagram of consanguineous pedigree. Open shapes represent non-affected individuals. Filled shapes denote siblings with schizophrenia, epilepsy and hearing impairment. Half filled circles represent epilepsy or deafness.

1.4.1.3 Hereditary hearing impairment, epilepsy and schizophrenia

Hereditary hearing impairment is a highly genetic heterogenous condition subdivided into syndromic and non-syndromic forms. 77% of non-syndromic cases show autosomal recessive inheritance and commonly give rise to sensori-neural defects (Petit, 1996). Approximately 50 loci have been linked to recessive non-syndromic hearing impairment NSHI, the majority of which were mapped in large consanguineous pedigrees (Van Camp, 2005). Mutations in over twenty genes have subsequently been identified and typically cause disruption of the molecular mechanisms that underlie sensory processing in hair cells of the cochlea (Piatto et al., 2005; Brown et al., 2008).

Epilepsy can be characterized by partial or generalized seizures depending on the pattern and localization of ictal activity within the brain. Further sub-classification of forms into specific syndromes involves evaluation of age of onset, clinical and electroencephalographic (EEG) features. Both monogenic and polygenic inheritance patterns have been described, indicating variation in both genetic factors and mode of inheritance. Linkage mapping in pedigrees with monogenic Mendelian epilepsy has revealed several causative genes encoding ion channel subunits. Moreover, variants in two genes, a T-type calcium channel subunit and $GABA_A$ δ-receptor subunit have been implicated by electrophysiological studies for some forms of complex epilepsy [reviewed by (Mulley et al., 2005)].

Investigating genetic contributions to schizophrenia is complicated by the likely presence of variable phenotypic presentation, incomplete penetrance and both locus and allelic heterogeneity. Given the uncertainties concerning the mode of inheritance of schizophrenia discussed earlier, the study of rare, even singular families may provide important clues about the genetic aetiololgy of the illness.

1.4.1.4 Results of a genome-wide scan using microsatellite markers

The initial work with this family was completed as a twelve-week project contributing to my MSc by Research in neuroscience degree awarded 2004. A genome-wide scan using microsatellites revealed only one marker, D22S423, on chromosome 22q13 that was heterozygous in both parents and the unaffected offspring and homozygous for affected offspring in the first family. Fine mapping of the region by means of nineteen additional markers revealed two further microsatellites with the same pattern of homozygosity by descent (HBD) markers; D22S1178 and D22S1151, located 1.1 Mb and 3.1 Mb telomeric to D22S423. Construction of parental haplotypes, illustrated in Fig. 1.2, indicated that D22S530 and D22S276 were also homozygous for the 'disease' alleles in all affected siblings and, importantly, either heterozygous or homozygous with one normal derived allele in non-affected parents. Consequently, three candidate regions define the boundaries of a 3.3 Mb candidate disease locus (Fig. 1.2). Assuming a recessive mode of inheritance, a maximum LOD score of 1.8, at zero recombination fraction Θ was calculated for D22S423, D22S1178 and D22S1151.

1.4.1.5 A second and related nuclear family presenting with deafness

The second nuclear family of the same clan was identified with a high incidence of deafness (Figure 1.3). In this family, five of the siblings were affected with severe deafness. A more detailed clinical description of family members is as yet unavailable.

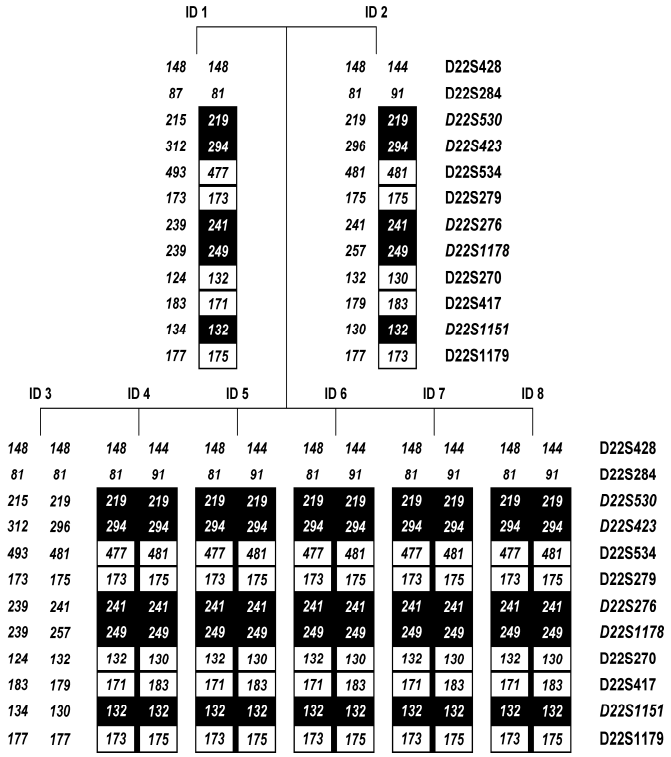

Figure 1.2 Constructed haplotypes of microsatellite markers on chromosome 22q13. The disease haplotype is boxed. Homozygous-by-descent conforming markers are shaded. Marker numbers denote microsatellite repeat genotype calls.

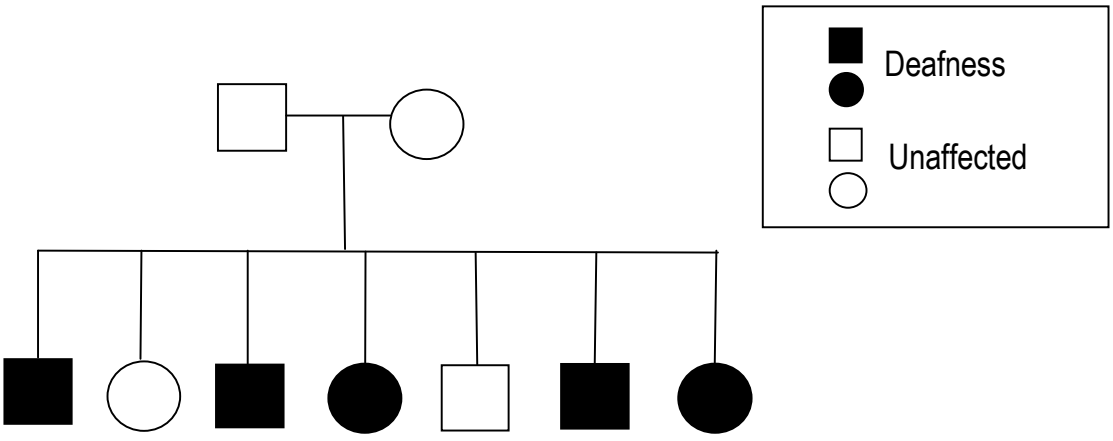

Figure 1.3 Pedigree of second family of the same kindred. Filled shapes denote siblings with deafness.

1.4.2 Project 2: Investigation of a complex chromosomal abnormality and identified breakpoint gene *ABCA13*

1.4.2.1 The mapping of breakpoint regions

A complex chromosomal rearrangement involving a pericentric inversion of chromosome 7 coupled with a translocation event between chromosome 7 and 8 was previously identified in a patient with severe and chronic schizophrenia, as illustrated in Figures 1.4 and 1.5. Family history or karyotypic information was not available and hence it is unknown whether this cytogenetic abnormality is *de novo* or inherited. BAC and YAC Fluorescence in situ Hybridization (FISH) analysis positioned the three breakpoints within the regions of 7q21.11, 7p12.3 and 8p23.2. The breakpoint on 8p23.2 is located within a 4 Mb interval which contains a *defensin* gene cluster. Copy number variants of this cluster exist in the normal population, varying between 2 and 12 copies. This may explain the multiple FISH signals on the normal and derived chromosome 8 that are evident in the patient and which complicate the fine mapping process. 7q21.11 houses no potential candidate genes, as schematically illustrated in Figure 1.6. In contrast, detailed characterization of the breakpoint region on 7p12.1 found BAC, RP11-12G8, to be broken. This BAC spans a genomic region of 180 kb and is situated in the middle of a large gene, *ABCA13* (NM_152701, NP_689914.2) and hence indicates that *ABCA13* is directly disrupted by the chromosomal rearrangement. Unfortunately, additional family data or samples are unavailable from the individual with the translocation.

Chromosome 7p12.1, the region where *ABCA13* is located, is an area as yet not linked to psychiatric illness. Thus, to confirm that disruption of *ABCA13* is causative of disease, further genetic evidence of an association is needed. One method is to perform a case-control SNP-tag association study. An alternative strategy is to screen highly conserved coding regions of *ABCA13* for mutations in a population of unrelated karyotypically normal schizophrenic cases. This approach has, as an advantage, the potential to identify directly both rare and common causative mutations, rather than markers merely in linkage disequilibrium with susceptibility factors or a disease-causing event.

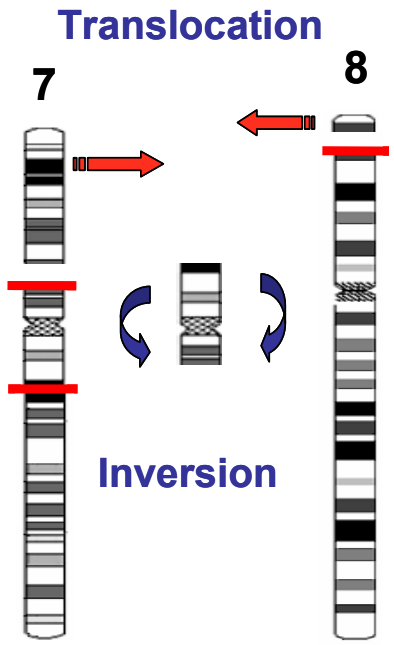

Figure 1.4 Schematic illustration of the complex chromosomal re-arrangement inv(7)(p12.3;q21.11), t(7;8)(p12.3;p23).

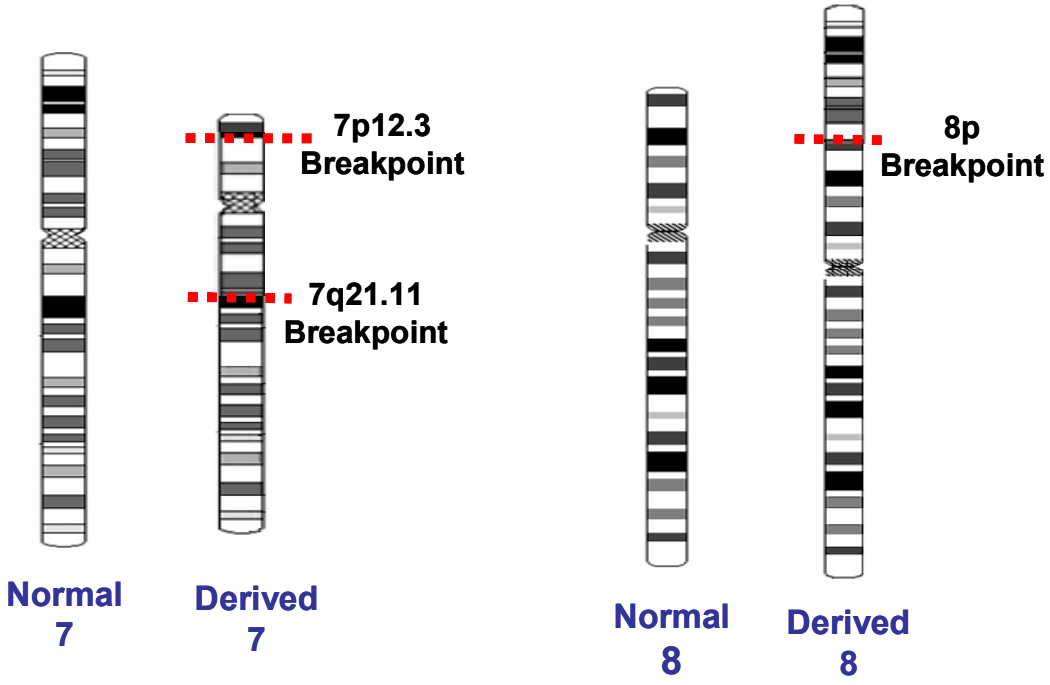

Figure 1.5 schematic illustrations of the breakpoint regions on chromosomes 7p12.3, 7q21.11 and 8p23.

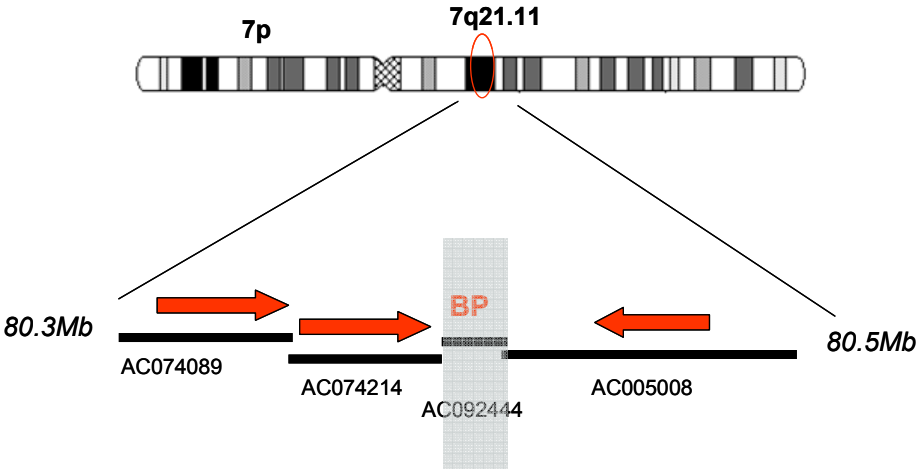

Figure 1.6 Schematic illustration of the identified breakpoint region on chromosomes 7q21.11. Arrows denote the breakpoint being either downstream or upstream of FISHED cloned BACs. The breakpoint is positioned within BAC AC092444.

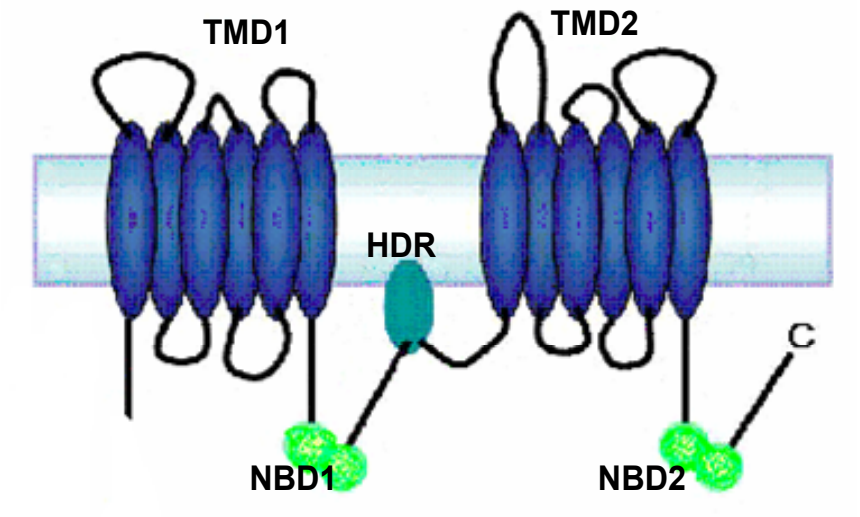

Figure 1.7 Diagrammatic representation of ABCA13 protein structure. The highly conserved function domains, nucleotide binding domains 1 and 2 (NBD's), transmembrane domain clusters (TMD's) and the hydrophopic dipping region (HDR) are indicated.

1.4.2.2 ABC proteins and disease

ABCA13 is a member of the ATP binding cassette transporter gene super-family (ABC) which encode ATP-hydrolysing transmembrane proteins that shuttle a variety of allocrites (transported molecules) across cellular membranes. ABC protein genes have been divided into 7 sub-families based on amino acid sequence phylogeny (designated A-G). Genetic variations in genes of the ABC super-family cause or contribute to a variety of human disorders with Mendelian and complex inheritance. Moreover, variations in gene mutations in several of ABC genes lead to multiple distinct clinical phenotypes (Dean et al., 2001; Uitto, 2005). In mammalian cells, ABC proteins typically exist either as full length transporters consisting of two transmembrane cluster domains (TMDs) paired in tandem to two nucleotide binding domains (NBDs) [diagrammatically illustrated in figure 1.7], or as half transporters that contain only one TMD and NBD which homo - or heterodimerize with other half transporters to function. Distinctive features of all ABC proteins are the highly conserved Walker A and B and signature motifs and stacking aromatic D, H and Q loops contained within the NBDs which are involved in NBD-ATP or intra-NBD protein-protein interaction required for ATP hydrolysis (Linton and Higgins, 2007).

The human ABCA subfamily is composed of 12 members, *ABCA1-10*, *ABCA12* and *ABCA13* subdivided into groups. One group, *ABCA5*, *A6*, *A8*, *A9*, *and A10,* forms a gene cluster on human chromosome 17q24 and shares structural similarities not evident in other ABC transporters. In addition to the 12 human ABCA proteins, four additional proteins (ABCA14 - A17) are expressed in rodents (Chen et al., 2004). Members of the human ABCA sub-family are also associated with a diverse range of clinical conditions For example: ABCA1 causes Tangier disease and familial hypoalphalipoproteinaemia; ABCA1 and 2 are both associated risk factors for Alzheimer's disease; ABCA3 causes respiratory distress syndrome and ABCA4 causes Stargardt disease, retinitis pigmentosa, cone rod dystrophy and age-related macular degeneration.

Furthermore, ABCA12, which shares the highest amino acid sequence similarity (47%) to ABCA13, causes two dermatological phenotypes; a severe form known as harlequin ichthyosis, and a milder form of the disease termed lamellar ichthyosis type 2 (Kaminski et al., 2006). ABCA members, so far functionally characterized, are all involved with lipid molecule transportation. Figure 1.8 summarizes the chromosomal, putative allocrite transported, function and associated disease for ABCA family members.

The functional role of ABCA13 is, as yet, undetermined. However, the presence of a conserved C-terminal motif known to be shared among the lipid transporting group and also present in ABCA13 suggests that it too is a lipid transporter. *ABCA13* is the largest ABC transporter gene described to date, approximately 450kb consisting 62 exons and encoding for a protein product composed of 5058 amino acids. One unique feature of ABCA13 is an extremely long N-terminal transmembrane and cytoplasmic tail spanning more than 3500 amino acids. Indeed, there is some debate whether the N-terminal component, relating to exons 1-30, is in fact a separate protein (Prades et al., 2002; Albrecht and Viturro, 2007). Moreoever, RT-PCR detected four alternatively spliced transcripts which would result in a loss of either the first N-terminal cytoplasmic-transmembrane domain, or in alternative C-termini that could potentially encode functional transporters (Prades et al., 2002).

Tissue profiling of the major *ABCA13* transcripts indicated highest expression in human trachea, testis and bone marrow, and cell line expression studies indicate that *ABCA13* is expressed in leukemia, prostate tumor, and CNS tumour cell lines including glioblastoma cells lines derived from human brain oligodendrocytes (Prades et al. 2002). In contrast, PCR analysis of mouse tissues detected highest expression of *Abca13* in submaxillary gland, epididymus, ovary and thymus and lower levels in the brain, eye, kidney, heart, skeletal muscle, testis and mouse embryo. Furthermore, analysis of the putative murine *Abca13* promoter region revealed potential transcription factor binding sites associated with myeloid- and lymphoid- derived cell types (Barros et al., 2003).

ABCA Subfamily	Allocrite	Function	[1]Disease
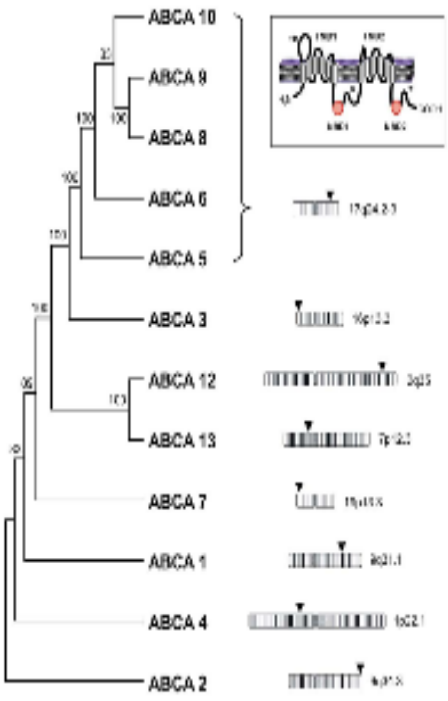 ABCA 10	Lipid	Lipid transport	None
ABCA 9	Lipid	Lipid homeostasis	None
ABCA 8	Lipid	Drug transport	None
ABCA 6	Lipid	Lipid homeostasis	None
ABCA 5	Lipid	Lysosomal trafficking	None
ABCA 3	Lipid	Surfactant secretion	Respiratory distress syndrome
ABCA 12	Lipid	Lipid transport	Harlequin ichthyosis, Lamellar ichthyosis type 2
ABCA 13	-	-	-
ABCA 7	Lipid	Lipid transport	Sjogren's syndrome
ABCA 1	Lipid	Lipid transport	Tangier disease, FHA, Alzheimer's
ABCA 4	Lipid	Lipid transport	ARMD,SD, ARRP,
ABCA 2	Lipid	Lipid transport	Alzheimer's disease

[1]FHA, familial hypoalphalipoproteinaemia; ARMD, age-related macular degeneration, SD, stargardt's disease; ARRP, age related retinitis pigmentosa.

Figure 1.8 ABCA subfamily members. Chromosomal location, putative function and associated diseases are listed. *ABCA5*, *A6*, *A8*, *A9*, *and A10,* forms a gene cluster on human chromosome 17q24. *ABCA3*, *A12*, *A7*, *A1*, *A4*, *and A2* all transport lipid species across cellular membranes. Figure adapted from Kaminski et al. *2006 Biochimica et Biophysica 1762: 510-52.*

1.4.3 Project 3: *GRIK4*- a candidate breakpoint gene for psychiatric illness

1.4.3.1 *GRIK4* disrupted in a chromosomal re-arrangement

A patient with chronic schizophrenia co-morbid with mild mental retardation was identified by cytogenetic analysis as having a karyotype abnormality (46, XX, ins(8;11)(q13;q23.3q24.2) inv(2)(p12q32.1) t(2;11)(q21.3;q24.2) der(2)(2qter->2q32.1::2p12>2q21.3::11q24.2>11qter)der(11)(11pter>11q23.3::2q21.3>2q32.1::2p12->2pter) der(8)(8pter->8q13::11q23.3->11q24.2::8q13->8qter). This chromosome re-arrangement involves a pericentric chromosome 2 inversion coupled with modified translocation events between chromosome 2 and 11, and 11q and 8q, illustrated in figure 1.9. Clear family history or karyotypic information was not available and hence it is unknown whether this cytogenetic abnormality is *de novo* or inherited. The breakpoint at 11q23.2 directly disrupts a high affinity kainate ionotropic glutamate receptor subunit gene, *GRIK4* (NM_014619, NP_055434.2) alternative protein nomenclature KA1). It is hypothesised that the breakpoint positioned between exon 2 and 3 results in the truncation of all putative transcripts on the derived chromosome 11, and hence haploinsufficiency of GRIK4 protein expression (Pickard et al., 2006).

1.4.3.2 Case-control SNP-tag association and identification of 3'UTR variant

A case-control association study on *GRIK4* was performed to assess its contribution to psychiatric illness in the karyotypically normal population. Two discrete regions within *GRIK4* were found to be strongly associated with schizophrenia and bipolar disorder (figure 1.10). A 3-SNP haplotype in the centre part of the gene was associated with susceptibility to schizophrenia (p=0.0430 s.e.0.0064; OR 1.453, 95% CI 1.182-1.787) and two single SNP markers positioned within the 3' UTR region were associated with a protective effect against bipolar disorder (p=0.0190 s.e.0.0043; OR 0.624, 95% CI 0.485-0.802). Subsequent screening of the 3'UTR region in bipolar protective haplotype homozygous carriers revealed a 14bp deletion (ss79314275) in linkage disequilibrium with the SNP haplotype (p=0.001) (Pickard et al., 2008b).

Figure 1.9 Diagrammatic illustration of a complex chromosomal re-arrangement identified as disrupting *GRIK4*. The red line denotes the approximate position of *GRIK4* (11q23.3) disrupted by one the breakpoints. Figure adapted from Figure 1, Pickard et al., 2006.

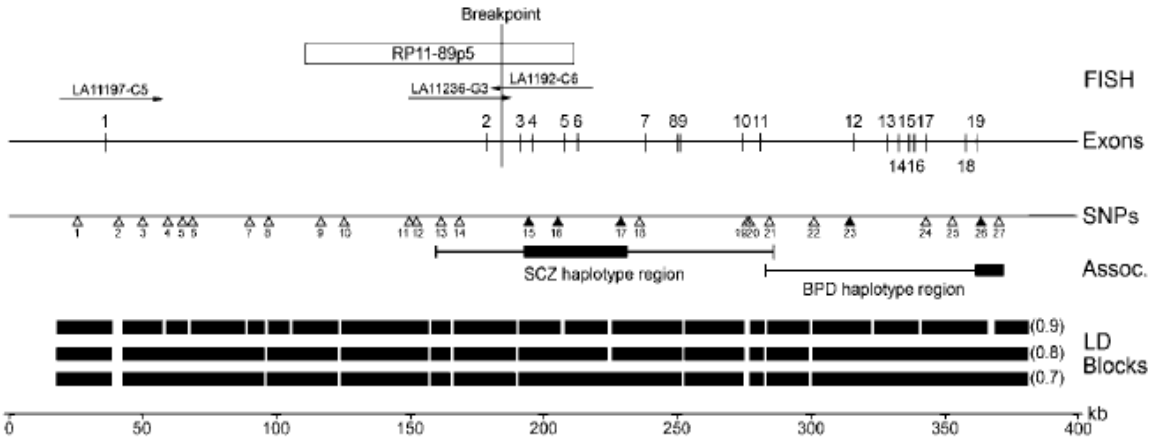

Figure 1.10 Diagrammatic representation of *GRIK4:* showing the cytogenetic and association findings. Figure from Pickard et al., 2006 (Figure 4).

This deletion, although not in a coding region of the gene, may affect mRNA distribution and regulation and thus have an effect upon the physiological properties of kainate receptors (KARs) by perturbing receptor subunit availability.

1.4.3.3 The role of kainate receptors in glutamatergic neurotransmission

Kainate ionotropic glutamate receptors (KARs) subunits are divided into two classes based on their structural homology and affinity for [^{3}H] kainate. GluR5, (*GRIK1*) GluR6, (*GRIK2*) GluR7, (*GRIK3*) are classified as 'low affinity' subunits while KA1 (*GRIK4*) and KA2 (*GRIK5*) show high-affinity kainate binding. These subunits form transmembrane tetrameric receptor assemblies activated by glutamate and kainate, and are present at pre- and post-synaptic locations. However, only GluR5, GluR6 and GluR7 can form functional homomeric and heteromeric receptors, whereas KA1 and KA2 participate in heteromeric receptors by partnering any of the GluR5-7 subunits (Pinheiro and Mulle, 2006).

The activity of kainate receptors and their precise subcellular localization in synaptic domains have been inferred mainly from electrophysiological studies. Kainate receptor complexes are thought to function through two forms of signalling, a canonical pathway involving ion influx and a noncanonical signalling pathway involving receptor coupling to G proteins. Post-synaptic KARs participate directly in excitatory post-synaptic currents (EPSCs) by mediating part of the synaptic current charge. Pre-synaptic KARs are implicated in regulating transmitter release through noncanonical signalling pathways at both excitatory (glutamatergic) and inhibitory (GABAergic) synapses (Lerma, 2006). Moreover, in several populations of neurons, e.g. CA1 pyramidal cells of the hippocampus, post-synaptic KARs are reported not to participate directly in excitatory neurotransmission, suggesting that they are localised to extrasynaptic domains in somato-dendritic compartments (Jaskolski et al., 2005).

KAR mediated synaptic transmission is reported to be particularly important for mossy fibre long term potentiation (LTP) in the hippocampus and long term depression (LTD) in the perirhinal cortex. In addition, KAR complexes have been implicated to play a role in axon navigation and synapse formation during development (Lerma, 2006; Park et al., 2006). Hence it has become clear that KARs are involved in short term synaptic plasticity mechanisms, synaptic integration and long-term modulation of neurotransmission, the disruption of which would have profound effects upon information processing by neural networks during development and in adulthood.

1.4.3.4 Alterations of kainate receptor subunit expression

Over the last two decades evidence has emerged suggesting down-regulation of kainate receptor function in severe psychiatric disorders. Post mortem studies of mRNA transcripts and protein immunoreactivity have consistently reported reduced expression of kainate receptor subunits in post mortem brain of patients with schizophrenia or bipolar disorder compared to matched controls. The key regions studied, and indeed implicated to be of functional relevance to psychiatric illness, are the medial temporal lobe, thalamus, anterior cingulate cortex and frontal cortex.

The medial temporal lobe includes a system of anatomically related structures that are essential for the integrative processing of cognitive and emotional information and the encoding and retrieval of declarative memory. This system consists of the hippocampal region (CA subfields, dentate gyrus (DG), and subicular complex) and adjacent, anatomically related parahippocampal cortex, which includes the entorhinal and perirhinal cortices (Squire and Zola-Morgan, 1991). Kerwin and colleagues, using the technique of quantitative autoradiography, first reported a reduction of kainate subtype binding in mossy fibre CA3/4 zone in the left hippocampus, and bilateral losses in dentate gyrus and parahippocampal regions in tissue from schizophrenic individuals (Kerwin et al., 1990). Subsequent findings suggest that specific subunits are decreased in subregions of the hippocampus and parahippocampus. For example, decreases in KA2

GluR5, GluR6 mRNA and Glur5, Glur6, and Glur7 protein immunoreactivity in the hippocampus were found in patients with schizophrenia (Porter et al., 1997; Benes et al., 2001; Scarr et al., 2005). Similarly, a reduction in GluR6 mRNA in the entorhinal cortex and Glur5 mRNA in the perirhinal cortex has been associated with schizophrenia and with schizophrenia, bipolar disorder and MDD respectively (Beneyto et al., 2007).

The thalamus is a structure involved in the modulation, integration and relaying of sensory information from the periphery to the cerebral hemispheres (Kandel et al., 2000). Two studies have investigated kainate receptor subunit levels in the thalamus from cases and controls, one reporting positive and the other negative results. Ibrahim and co-workers found significantly lower levels of KA2 mRNA within thalamic nuclei in schizophrenic patients than in comparison subjects. However, they also reported no significant differences in GluR5, GluR6, GluR7, and KA1 mRNA expression or in [^{3}H]kainate binding levels (Ibrahim et al., 2000). In contrast, Dracheva et al. report no evidence of altered KA2 and GluR5-6 mRNA levels in thalamic tissue from schizophrenic patients (Dracheva et al., 2008).

The anterior cingulate cortex specializes in the processing of emotional stimuli, expression of emotional behaviour, mood regulation, organization of higher cognitive functions and autonomic response to emotional states (Devinsky et al., 1995). Woo and colleagues examined kainate receptor subunits mRNA co-localizing with GAD_{67} mRNA, i.e. in GABAergic expressing interneurons, in anterior cingulate cortex tissue from control, schizophrenic and bipolar disorder individuals. They found reduced levels of GAD_{67} co-expressed GluR5 mRNA in layer 2 of the cortex for schizophrenia and bipolar disorder, but no difference between the groups for GluR6 mRNA (Woo et al., 2004).

Finally, the frontal cortex, important for higher executive functions, has been investigated by several groups all of whom report positive results. Meador-Woodruff et al. reported a shift in subunit stoichiometry, with increased expression of GluR7 mRNA

and decreased KA2 mRNA associated with schizophrenia (Meador-Woodruff et al., 2001). In contrast, decreases in GluR7 and KA1 mRNA in the left superior gyrus of neuroleptic-free schizophrenic individuals were found by Sokolov (Sokolov, 1998). A third study, by Garey and co-workers, found a significant reduction in numerical density of neurons immunopositive to GluR6 and GluR7 in the orbitofrontal cortex of chronic schizophrenics (Garey et al., 2006) These findings, taken collectively, strongly suggest that decreases in kainate receptor subunits in specific brain regions are associated with psychiatric phenotypes.

1.4.3.5 KA1 expression

Electrophysiological data indicates that kainate receptors are widely expressed throughout the mammalian nervous system. Although the KA2 subunit is reported to be ubiquitously expressed, animal studies suggest that KA1 expression is more specific to given brain regions and cell types (Porter et al., 1997). Table 1 summarizes the findings of expression studies of KA1 mRNA transcripts or protein immunoreactivity performed on brain tissue from rodent and human hippocampus, frontal cortex and cerebellum. Of note, KA1 protein subcellular localization in human brain has not, as yet, been characterized.

Table 1.1 KA1 expression in brain

Technique	Species	Hippocampus	Frontal cortex	Cerebellum	Reference
Quantitative a utoradiography [3H}KA binding so KA1 & KA2	Human	Kainate binding in mossy fibre terminal of CA3 and CA4 and dentate gyrus	No data	No data	Kerwin et al., 1990
35 S-labelled ISHH mRNA expression	Human	Dentate gyrus	Layers II – VI	No consistent signal	Porter et al., 1997 Meador-Woddruff et al., 2001 Scarr et al., 2005
Quantitative RT-PCR mRNA expression	Human	No data	Expressed in left superior frontal gyrus	No data	Sokolov, B.P. 1998
Quantitative autoradiography [3H}KA binding so KA1 & KA2	Rat	CA3/CA4 mossy fibre terminals	No data	No data	Represa et al.,1987
35 S-labelled ISHH mRNA expression	Rat	Dentate gyrus cells strong signal CA3, CA1	Superficial and deep laminae	White matter only Layers II & IV	Porter et al.,1997
35 S-labelled ISHH mRNA expression	Rat	CA3 pyramidal cells	No data	No data	Wisden and Seeburg1993
Immuno histochemistry KA1 protein expression	Rat	GCL in dentate gyrus, CA3, hilus polymorphic neurons Dendritic structures post synaptic to CA3 fibre; stratum radiatum CA1 pyramidial cells & apical dendrites	Layer V pyramidal neuron Layers II & III, VI Subpopulation of GABAergic interneurons	Purkinje cell somata & dentritic processes Molecular layer-fibres not somata stained Bergman glial processes	Fogarty et al.,2000 .
Immuno histochemistry KA1 & KA2_knockout mice KA1-Cre transgenic _mice	Mouse	Hilus polymorphic layer Dentate gyrus granule cells CA3 pyramidal cells & dendrites	Layers II & V	Purkinje cells	Kask et al., 2000; Darstein et al.,2003

1.5 Aims

This thesis outlines the genetic and biological investigation of candidate genomic regions and genes implicated in psychiatric illness and co-morbid conditions. The aims of the three independent studies presented in this thesis are described below.

Project 1 **Homozygosity mapping in two consanguineous families**

1. Chapter 3: To perform high density positional cloning in a consanguineous family with schizophrenia and co-morbid conditions and concurrently assess the extent of homozygosity in terms of degree of inbreeding.
2. Chapter 3: To screen candidate genes for potential causative mutations in HBD regions identified.
3. Chapter 3: To analyze homozyosity in a second (related) family presenting with deafness to establish if there is any overlap in HBD regions in all affected individuals from both families.

Project 2 **Investigation of a complex chromosomal abnormality and the identified break-point gene *ABCA13***

1. Chapter 4: To fine map the exact breakpoint positions of a complex chromosomal re-arrangement.
2. Chapter 4: Gather further evidence that disruption of *ABCA13* is putatively causative of psychiatric illness by screening highly conserved coding regions of *ABCA13* for rare risk variants.
3. Chapter 4: Analyze known SNPs and newly identified variants to assess potential differences in frequency between cases and controls.
4. Chapter 5: Determine *ABCA13* transcript expression in different cell lines, blood and lymphoblastoid cells and expression of ABCA13 protein in human brain.

Project 3 ***GRIK4*- a candidate breakpoint gene for psychiatric illness**

1. Chapter 6: Further investigate an association between a variant in the 3'UTR of GRIK4 and bipolar disorder.
2. Chapter 7: Characterise the expression of KA1 in human brain tissue.
3. Chapter 8: Investigate the potential consequence of the 3'UTR variant upon GRIK4 protein distribution and abundance in human brain by means of a genotype/protein correlation study.

CHAPTER 2

MATERIALS AND METHODS

2. Materials and Methods

2.1 Clinical samples

2.1.1 Case Samples

Subjects were Caucasian individuals contacted through inpatient or outpatient services of hospitals in southeast and central Scotland, and Grampian. Samples from southeast and central regions, Fife, Borders and Lanarkshire were collected by Douglas Blackwood, Walter Muir and Donald McIntyre and other clinical colleagues. Samples from Grampian and other parts of Scotland were obtained by David St Clair. Samples were collected over a period of more than 15 years. Diagnoses were made according to DSM-IV criteria of the American Psychiatric Association (Diagnostic and Statistical Manual of Mental Disorders, third edition. Washington DC, (American Psychiatric Association, 2004) Phenotyping methods for all patients was through personal interview using the 'Schedule for Affective Disorders and Schizophrenia-Lifetime' version (SADS-L) (Endicott and Spitzer, 1978), supplemented by hospital case notes and information provided by medical staff and relations of cases. Diagnosis was reached by consensus between two experienced psychiatrists. Patients gave written informed consent for the collection of DNA samples for use of genetic studies and studies were approved by the Multicentre Research Ethics Committee for Scotland and by local ethics committees.

Exclusion criteria for schizophrenia were history of severe head injury, epilepsy, drug or alcohol use considered the major cause of psychosis. There was no pre-selection of cases based on family history of other phenotypic variables. These patients are a representative sample of the total population of patients with a diagnosis of schizophrenia attending psychiatric services in south Scotland. For bipolars all the above also applied but the inclusion criteria were diagnosis of bipolar 1, bipolar 2 and schizoaffective disorder (manic). For MDD inclusion was diagnosis of recurrent major depression. Single cases

and minor depression were excluded. Also excluded were patients with depression and a first degree relative with Scz or BP. A large cohort was recruited from an affective disorders treatment service where most referrals are aged under 25 years so there is a bias in the cohort towards early onset recurrent depression. Recruitment was of consecutive referrals from primary care and there was no selection based on family history.

2.1.2 Controls

The control population was obtained from several sources. One group of controls were recruited through the South of Scotland Blood Transfusion Service and the Grampian Blood Transfusion service. Blood donor controls were not screened to exclude individuals with a personal or family history of a major psychiatric illness. However, blood donors are not accepted if they self reported that they are currently on medication or have a history of a chronic illness. A second group of controls were recruited at the Edinburgh University Student Health Service. These students were taking part in a study of glandular fever epidemiology and again were not screened for personal or family history of mental illness. A third group of controls were recruited from hospital staff and social networks of the research team.

2.1.3 Lothian Birth Cohort control samples

A fourth group of controls were from the 1936 Lothian Birth Cohort (LBC 1936). Subjects of the 1936 Lothian Birth Cohort were recruited for a recent study intended to examine influences on cognitive aging between childhood and old age (Deary et al., 2007). The participants comprised surviving members of the Scottish Mental Survey of 1947. They underwent medical, cognitive and physical assessment in addition to giving blood and filling in personality, quality of life and other psycho-social questionnaires, full details of which are reported by (Deary et al., 2007). These individuals were not screened for psychiatric illness and no information regarding family history of psychiatric illness was obtained. Ethics permission for the original study protocol, which

included the examination of candidate 'cognition' genes, was obtained from the Multi-centre Research Ethics Committee for Scotland.

2.1.4 Pakistan families

Recruitment and clinical information pertaining to the two consanguineous families from Pakistan was obtained by Muhammad Ayub, an experienced psychiatrist assisted by Muhammad Irfan and Farooq Naeem. Fully informed written consent was attained from each member of the families. The study was approved by the appropriate UK and Pakistani ethics of research committees.

2.1.5 Brain tissue samples

Brain tissue sections used for the genotype/expression correlation study were from individuals asymptomatic for psychiatric illness as ascertained by a psychiatrist, Dr Douglas Blackwood. 12 genotyped samples were matched for age, gender and cause of death by Dr Robert Walker of Edinburgh University MRC Sudden Death Brain and Tissue Bank. Paraffin embedded postmortem human coronal sections of the hippocampus and parietal frontal cortex were received coded and the study performed blinded. The MRC Sudden Death Brain Bank is fully described by (Millar et al., 2007).

2.2 Materials

2.2.1 Chemicals and biological products

All general use chemicals, reagents and biological products were from Sigma-Aldrich or Invitrogen unless otherwise stated below. Chemical and biological products, kits and solutions used are listed in tables 2.1 and 2.2 and section 2.2.3 respectively.

METHOD	CHEMICAL/PRODUCT	SOURCE
FISH detection	avidin Texas red® DCS	Vector laboratories
FISH detection	Anti-Digoxigenin fluorescein FAB fragments	Roche
FISH	Cot-1 Human DNA	Roche
FISH	Vectashield mounting medium	Vector laboratories
FISH	DNase1 recombinant	Roche
FISH	Digoxigenin-11-dUTP	Roche
FISH	Biotin-16-dUTP	Roche
FISH	Vulcanising solution	REMA TIP TOP
PCR sequencing preparation	exoSAP-IT	GE Healthcare
Restriction digest	TAQ$^{\alpha}$1	New England BioLabs
Section mounting	Pertex mounting medium	CellPath

Table 2.1 Chemical and biological products used for molecular biological techniques.

2.2.2 Kits

METHOD	KIT	SOURCE
cDNA preparation	First Strand cDNA Kit	Roche
DNA extraction	Qiagen plasmid mini preparation kit	Qiagen
FISH	Illustra™ Nick column kit	GE Healthcare
Immunoblocking	Avidin/biotin kit	Vector laboratories
Immunodetection (western)	Amersham ECL Plus™	GE Healthcare
Immunodetection (histology)	StreptABComplex/HRP Duet	DAKO

Immunodetection (histology)	DAB Substrate kit for peroxidase	Vector laboratories
Membrane transfer	X-cell sureLock™ Minicell?	Invitrogen
Protein electrophoresis	NuPAGE Novex Bis Tris gels	Invitrogen
Protein concentration	DC Protein concentration assay	BIORAD
PCR amplification	10x PCR Enhancer	Invitrogen
PCR amplification	Expand long-range PCR kit	Roche
PCR product purification	QIAquick PCR purification kit	Qiagen
PCR product cloning	Qiagen PCR cloning kit	Qiagen
Plasmid DNA isolation	GenElute™ Plasmid miniprep kit	Sigma-Aldrich
RNA extraction	RNeasy Mini kit	Qiagen

Table 2.2 Kits used for molecular biological techniques.

2.2.3 Solutions, buffers and gel loading dyes

Ampicillin stock solution (10mg/ml)
Ampicillin sodium salt
Qs (quantity sufficient) 50ml dsH_2O 5g
Filter-sterilize and store at -20°

Blocking buffer *(FISH)*
Marvel skimmed milk 0.5g
20x SSC 2ml
dsH_2O 8ml

Blocking buffer *(immunoblotting)*
Marvel 2.5g
PBS 50ml
TWEEN 100µl

Blocking *(immunohistology)*
20% Goat serum
PBS/1%TX100 100µl

0.01M Citric Acid pH 6.0

Citric Acid	1.92g
Qs1L dsH_2O	
pH 6.0	

Coomassie Brilliant Blue protein stain

Coomassie stain	0.25g
Methanol: Water (1:1 v/v)	90ml
Glacial acetic acid	10ml
filter	

Coomassie de-stain

Glacial acetic acid	100ml
Methanol	300ml
dsH_2O	600ml

Denaturing solution *(FISH)*

formamide (99%)	140ml
20x SSC	20ml
dsH_2O	40ml

make fresh and add a few drops of HCL to bring pH to 7.0, transfer to staining dish and heat in water bath set to 70°C

1M DDT

Dithiothreitol	0.7g
Qs 5ml dsH_2O	

EDTA solution 0.5M pH 8.0

Disodium ethylenediaminetetra acetate	1.86.1g
dsH_2O	800ml
pH to 8.0	

30% Ethanol

30ml ethanol (99.7-100% v/v) to every 100ml dsH_2O

70% Ethanol

70ml ethanol (99.7-100% v/v) to every 100ml dsH_2O

90% Ethanol

70ml ethanol (99.7-100% v/v) to every 100ml dsH_2O

50% Formamide Solution

formamide (99%)	500ml
2x SSC	100ml
dsH_2O	400ml

Hybridisation mix buffer *(FISH)*

Deionised formamide	50µl
Dextran Sulphate 50%	20µl
20X SSC.	10µl
Tween 20	1µl
dsH_2O, Store at -20°	19µl

3% Hydrogen Peroxide in Methanol

30% hydrogen peroxide	50ml
Methanol	450ml
Store at 4°	

IPTG stock solution (100mM)

Isopropyl β-D-thiogalactopyranoside	238.3mg
Qs 10ml dsH_2O	
Filter-sterilize and store at -20°	

Luria-Bertani broth (LB)

1% (w:v) Bacto-Tryptone (Difco)
0.5% (w:v) Bacto-Yeast extrct (Difco)
0.1% (w:v) NaCl
pH 7.0 autoclave

LB-agar

LB broth with 15g Bacto-Agar (Difco) per litre
autoclave

Lithium carbonate 0.07M

Lithium carbonate	5g
Qs 1L dsH_2O	

10xNick Translation buffer

Tris HCl pH7.5	500mM
$MgCl_2$	50mM
β-mercaptoethanol	14.4M
bovine serum albumin	50mg/ml

Mounting mix medium *(FISH)*

Vectashield	0.5ml
DAP1 (50 µg/ml)	20µl

Orange G loading buffer

Glycerol	30ml
dsH_2O	70ml
Orange G	1g

1xPBS

KH_2PO_4	
Na_2HPO_4	1.157g
NaCl	6.971g
Qs 500ml dsH_2O	43.83g

PBS/ 1% TX100

PBS	495ml
TX100	5ml

Ponceau stain

Ponceau S	0.5g
Acetic acid	2ml

Laemmli protein sample buffer (2x)

Tris (hydroxymethyl)-methylamine (0.5M, pH6.8)	
Glycerol	02ml (100mM)
SDS (20% solution)	2ml (20%)
Bromophenol Blue	2ml (4%)
Qs 10ml dsH_2O, store at RT. Add 100mM DTT before use	0.2g (0.02%)

Primer mix

Glycerol	6ml
TE	7ml
DMSO	1ml

RIPA buffer

Tris (hydroxymethyl)-methylamine (pH7.5)	0.61g
NaCl (150mM)	0.9g
dsH_2O	80ml
1% Trition	1ml
sodium deoxycholate (10% solution)	2.5ml
sodium deoxycholate (20% solution)	250µl
1mM EGTA (100mM solution)	1ml
Add 100µl protease inhibitors to 5ml RIPA lysis buffer before use	

Running Buffer (for Tris-acetate gels)

20x Nupage Tris-acetate SDS running buffer	20ml
dsH_2O	400ml

0.1% SSC solution

20x SSC	5ml
dsH_2O	995ml

2x SSC solution

20x SSC	80ml
dsH_2O	720ml

4x SSC solution plus Tween 20

20x SSC	200ml
dsH_2O	800ml
Tween 20	0.5ml

20x SSC solution

NaCl	175.3g
Sodium citrate	88.2g

Qs 1L dsH_2O, autoclave

20x TBE

Tris	242.0g
20mM EDTA	14.88g
boric acid	123.4g

Qs 1L dsH_2O autoclave

TE pH 8.0

10mM Tris Cl pH 7.4
1mM EDTA pH 8.0

Transfer Buffer

x20 NuPage Transfer buffer	25ml
methanol	100ml
dsH20	375ml

0.05 Tris-HCL pH 6.7

Trizma hydrochloride	7.88g

Qs 1L dsH_2O
pH 6.7

Wash Buffer *(immunoblotting)*

10x PBS	100ml
dsH2O	900ml
Tween	2ml

X-gal stock solution

5-bromo-4chloro-3-indolyl β-D-galactopyranoside	400mg
dimethylformamide	10ml

protect from light and store at -20°C

2.2.4 Antibodies and pre-immune serum

Non-commercial polyclonal antibodies and pre-immune serum were obtained from AFFINITI Research Products Limited and EUROGENTEC, and used at dilutions stated in table 2.3. Pre-immune serum was taken prior to immunization. Antibody ABCA13 870 was raised in rabbit against a peptide from the C-terminus of human ABCA13 (aa PQHIKNRFGDGYTVKC), and antibody GRIK4 272 was raised in rabbit against a peptide from the C-terminus of human (aa CRSEESLEWEKTTNSSEPE). All antibodies were immunoaffinity purified by coupling the immunizing peptide to the appropriate sepharose column. The peptide relating to the ABCA13 protein sequence that was used to raise the 870 antibody and subsequently used for a peptide blocking assay, was manufactured and purified by Invitrogen.

Antibody	Species	Dilution	Supplier
GRIK4 272	rabbit	1:10 IHC 1:500 Blotting	AFFINITI research products limited
ABCA13 870	rabbit	1:20	EUROGENTEC
Pre-immune serum *seq 1*	rabbit	1:2000	EUROGENTEC
GFAP	rabbit	1:500	ZYMED Laboratories
α-tubilin	rabbit	1:10000	Abcam plc.
biotinylated secondary antibody	Goat	1:200	Invitrogen
HRP secondary antibody	Goat	1:5000	Invitrogen

**Pre-immune serum seq 1 denotes from an animal subsequently injected with ABCA13* `PQHIKNRFGDGYTVKC`

Table 2.3 Antibodies and pre-immune serum. Suppliers and working dilutions shown.

2.2.5 Primers and Microsatellite markers

Genomic sequence information for the genes *ABCA13, KCNF1*, *ATF4*, *GPR24 CACNG2, GAPDH* and *G6PD* were obtained from the University College Santa Cruz (UCSC) [NCBI Build 35 and 36.1] genome browser. Oligonucleotide primers were designed using PRIMER3 [http://workbench.sdsc.edu] (Rozen and Skaletsky, 2000). Primers were designed from repeat and SNP-free regions of sequence. Due to a high number of repetitive sequences and/or pseudogenes, separate amplification primers and sequence primers were utilised when sequencing *ATF4* and *KCNF1*. Specificity of all primers was checked by Blast and BLAT analysis http://www.ncbi.nlm.nih.gov/Blast.cgi, http://genome.ucsc.edu/cgi-bin/hgBlat. Primer sequences and amplification conditions are listed in Table 2.4. PCR Primers were re-suspended at a concentration of µg/µl in primer mix and stored at -20° C.

Microsatellite markers used for chromosome 7 genotyping were a component of a linkage set, ABIPRISM® linkage mapping set, MD10 version 2 (PE Biosystems). These were: DS7517, D7S531, D7S493, D7S516, D7S484, D7S519, D7S669, D7S630, D7S657, D7S515, D7S846, D7S530, D7S640, D7S684, D7S661, D7S636, and D7S798.

Table 2.4 Primers used for DNA PCR amplification and sequencing

Gene /Exon	Primers 5'- 3'	Cycling conditions
ABCA13 Exon 32		95°C 120s
F	CTC CTT CAT GGG TTC CTT CA	95°C 30s, 55°C 30s, 68° 55s x35
R	TTC TTG CAA TCT CAT GTG GC	68°C 10min, 8° 20 min
ABCA13 Exon 33		95°C 120s
F	CTG AAT TTG CAA GCA AGC AG	95°C 30s, 55°C 30s, 68° 55s x35
R	AAG CAG ATA TCA GAA AGC CCA	68°C 10min, 8° 20 min
ABCA13 Exon 34		95°C 120s
F	TGA CAC TTC AAG CAT CTC GG	95°C 30s, 55°C 30s, 68° 55s x35
R	CCA GAC GTC AAG GGT GGT AT	68°C 10min, 8° 20 min
ABCA13 Exon 35		95°C 120s
F	TGG CCA GTG ATA TTG ACC TTC	95°C 30s, 55°C 30s, 68° 55s x35
R	CAC TTG GGA AAC AAA GGC AT	68°C 10min, 8° 20 min
		95°C 120s

ABCA13 Exon 37		
F	TTGATTTGTGTGCTTCACAGAG	94°C 30s, 54°C 30s,72°C 1min x32
R	GCCTTTCACCCGTGTCTCTA	72°C 10min
ABCA13 Exon 38		95°C 120s
F	AACCAGGTCAGCAGAAGGTG	94°C 30s, 54°C 30s,72°C 1min x32
R	AATTCAATGCCTTCCCACAG	72°C 10min
ABCA13 Exon 39		95°C 120s
F	TCACGTGTGTGTAGCATCCA	94°C 30s, 54°C 30s,72°C 1min x32
R	AAAGGTCAAACACAAAGTAAGCAA	72°C 10min
ABCA13 Exon 40		95°C 120s
F	CCAGGACGCATTTCAATTTT	94°C 30s, 54°C 30s,72°C 1min x32
R	ACAGAAGGCCTCCACTGAGA	72°C 10min
ABCA13 Exon 43		95°C 120s
F	TAA AGG GGA CAC TCA AGG GA	95°C 30s, 55°C 30s, 68° 55s x35
R	AGA CAG CCT GAG AGG AGC AA	68°C 10min, 8° 20 min
ABCA13 Exon 50		95°C 120s
F	TTG TGT TCT TCG TCA GGT GC	95°C 30s, 55°C 30s, 68° 55s x35
R	AGA TGA CCC CTT TTT GTG GA	68°C 10min, 8° 20 min
ABCA13 Exon 51		95°C 120s
F	TCC ACG GCT ACA GAA CTC CT	95°C 30s, 55°C 30s, 68° 55s x35
R	GTC CCT TGC AGA AGC AAC AT	68°C 10min, 8° 20 min
ABCA13 Exon 52		95°C 120s
F	TGC ATT TTC AGG GAT TCA CC	95°C 30s, 55°C 30s, 68° 55s x35
R	TCG TCA ATT GTT GCT AAG CC	68°C 10min, 8° 20 min
ABCA13 Exon 53		95°C 120s
F	GGG AAG ACC TGG AAC ACA GA	94°C 30s, 54°C 30s,72°C 1min x32
R	GGG TGA CTG ACA CCA ATC AA	72°C 10min
ABCA13 Exon 54		95°C 120s
F	AAAGCTGACTGCCCAGAAGT	94°C 30s, 54°C 30s,72°C 1min x32
R	TGAAGGCTATTTTTGGCTCTG	72°C 10min
ABCA13 Exon 55		95°C 120s
F	CAAACCAGCAAAGTCAACTCA	94°C 30s, 54°C 30s,72°C 1min x32
R	TTTTCCCCACATCAGAGGAG	72°C 10min
ABCA13 Exon 56		95°C 120s
F	AAACTGCAGTGGACTTGTTATTGA	94°C 30s, 54°C 30s,72°C 1min x32
R	CATATTAGAAAATCTCTTGCAGGTAA	72°C 10min
ABCA13 Exon 57		95°C 120s
F	CTCCAGCTGCAGAAAACTCC	94°C 30s, 54°C 30s,72°C 1min x32
R	ATGCTGGCTTATGGCAAAAC	72°C 10min
ABCA13 Exon 58		95°C 120s
F	TGGCTTTGTTGAGCAGAGTG	94°C 30s, 54°C 30s,72°C 1min x32
R	TCCCTCAGGAAGACCTGAAA	72°C 10min
ABCA13 Exon 59		95°C 120s
F	CTCCAGCTGCAGAAAACTCC	94°C 30s, 54°C 30s,72°C 1min x32
R	ATGCTGGCTTATGGCAAAAC	72°C 10min

ATF4 Amp 1		ELRK 95°C 120s
F	GCCCTGAGCCAATAAGAGC	94°C 60s, 56°C 30s,72°C 2min x32
R	GGGGCCAAGTGAGTCAGATA	72°C 15min
ATF4 Amp 2		ELRK 95°C 120s
F	TAGGGGCCTCCTACCTTTGT	94°C 60s, 56°C 30s,72°C 2min x32
R	GATCTTCAGCCTTGGACTGC	72°C 15min
ATF4 Seq 5'UTR		96°C 60s
F	ATCTAGGGCCCTGAGCCAAT	96°C 10s, 50°C 5s, 60°C 4min x25
R	AAAACTACATCTGTGGGCGG	4°C 10min
ATF4 Seq Exon1 (1)		96°C 60s
F	CGTCCCCATAGAGACGAAGT	96°C 10s, 50°C 5s, 60°C 4min x25
R	ATCTTGGTTCCTGCCACGTT	4°C 10min
ATF4 Seq Exon1 (2)		96°C 60s
F	CTTCCCCAGGAGCCCTAC	96°C 10s, 50°C 5s, 60°C 4min x25
R	TAGATCCCACCAGGACGATG	4°C 10min
ATF4 Seq Exon 2 1		96°C 60s
F	AGGGGCCTCCTACCTTTGTA	96°C 10s, 50°C 5s, 60°C 4min x25
R	GAGAACACCTGGAGATGGGA	4°C 10min
ATF4 Seq 3'UTR		96°C 60s
F	AAGGAGGAAGACACCCCTTC	96°C 10s, 50°C 5s, 60°C 4min x25
R	GTTAAGACCAGCTTGGGGTG	4°C 10min
CACNG2 5'		95°C 120s
F	AAGACCGAAGGTTGCATCTC	94°C 30s, 54°C 30s,72°C 1min x32
R	TCCCACAGCTATGGTCATCA	72°C 10min
CACNG2 Exon 1	TTCTGATCTCAAAAGGCAAGC	95°C 120s
F	GAGGATGTTTGAGGGGATGA	94°C 30s, 54°C 30s,72°C 1min x32
R		72°C 10min
CACNG2 Exon 2		95°C 120s
F	GAAGGCAGCGTTTTGAAGTC	94°C 30s, 54°C 30s,72°C 1min x32
R	GAGACCTGGAGGTCGACTGA	72°C 10min
CACNG2 Exon 3		95°C 120s
F	CTGACGGTGTGCTGGAGTT	94°C 30s, 54°C 30s,72°C 1min x32
R	GTTGCTACAGGACAGGAGCC	72°C 10min
CACNG2 Exon 4		95°C 120s
F	ATGTCCATCTACACCGCCC	94°C 30s, 54°C 30s,72°C 1min x32
R	TTTGCTTTTGGAAGGTCTCC	72°C 10min
CACNG2 3'		95°C 120s
F	ACCACCCCCGTATAAAGACC	94°C 30s, 54°C 30s,72°C 1min x32
R	GGGGGTTAAAGGGAACAGAA	72°C 10min
KCNF1 Amp 1		ELRK 95°C 120s
F	GTGCCTTGCAGAATTTCACC	94°C 30s, 54°C 30s,72°C 2 min x32
R	TACTCCAGGGTGAACCAGC	72°C 10min

KCNF1 Amp 2		ELRK 95°C 120s
F	GTGCTCTCCTTCCTGCTCAT	94°C 30s, 54°C 30s,72°C 2 min x32
R	GTGCCTGAGCTACTCTTGGG	72°C 10min
KCNF1 Seq 1		96°C 60s
F	GCCTTGCAGAATTTCACCAG	96°C 10s, 50°C 5s, 60°C 4min x25
R	CCCCACGTTGACGACTATCT	4°C 10min
KCNF1 Seq 2	AGATAGTCGTCAACGTGGGG	96°C 60s
F	AGGGTGAACCAGCCAATG	96°C 10s, 50°C 5s, 60°C 4min x25
R		4°C 10min
KCNF1 Seq 2		96°C 60s
F	CTTCCTGCTCATCCTCGTCT	96°C 10s, 50°C 5s, 60°C 4min x25
R	ACGCGCTGCTTGTTGTAGTA	4°C 10min
KCNF1 Seq 3		96°C 60s
F	TACTACAACAAGCAGCGCGT	96°C 10s, 50°C 5s, 60°C 4min x25
R	AACCTACAACACGGAGGGTG	4°C 10min
Cloning T7		96°C 60s
F	GTAATACGACTCACTATAG	96°C 10s, 50°C 5s, 60°C 4min x25
		4°C 10min
RT-PCR primer 1		ELRK 95°C 120s
F	TGGAGAAATACCTGGGAGGA	94°C 60s, 56°C 30s, 72°C 180s x32
R	ATGATGGGATTCCCTGATGA	72°C 15min
RT-PCR primer 2		ELRK 95°C 120s
F	AGCAAATGGCTTGCTCAACT	94°C 60s, 56°C 30s, 72°C 180s x32
R	TCTGGAAAAGGCTGGACATT	72°C 15min
RT-PCR primer3		ELRK 95°C 120s
F	GGATTCTCCATCCTGTCTGC	94°C 60s, 56°C 30s, 72°C 180s x32
R	GGAATCAATGCCGAAGTTGT	72°C 15min
RT-PCR primer 4		ELRK 95°C 120s
F	CTGGATGAGAACCTGCATCA	94°C 60s, 56°C 30s, 72°C 180s x32
R	TGGGTGAGAAAAGGGATCTG	72°C 15min
RT-PCR primer 5		ELRK 95°C 120s
F	GTCTCCATTTCCCTGGAGGT	94°C 60s, 56°C 30s, 72°C 180s x32
R	ACGAAGAGGACTGGCAGCA	72°C 15min
GAPDH		ELRK 95°C 120s
F	CAATGACCCCTTCATTGACC	94°C 60s, 56°C 30s, 72°C 180s x32
R	TGAGCTTGACAAAGTGGTCG	72°C 15min
G6PD		ELRK 95°C 120s
F	CAACCACATCTCCTCCGTG	94°C 60s, 56°C 30s, 72°C 180s x32
R	ATCTTGGTGTACAGGGCCTC	72°C 15min
GRIK4 3'UTR		ELRK 95°C 2 mins
F FAM	GTGGGAGAAAACCACCAACA	94°C 45s, 57°C 60s,72°C 45s x7
R	GGGGGAAATTCAACTGATGAT	94°C 45s, 56°C 60s,72°C 45s x7
		94°C 45s, 55°C 60s,72°C 45s x26
		72°C 15min

* *ELRK denotes Expand long-range kit was used (Roche)*

2.2.6 BAC and fosmid clones

Bacterial BAC and fosmid clones were obtained from Human TilePath BAC and fosmid set, Wellcome Trust Sanger Institute, Wellcome Trust Genome Campus, Hinxton, Cambridgeshire, CB10 1SA, UK. Clones used are listed in table 2.5

Table 2.5 BAC and Fosmid clones used for cytogenetic analysis

Cytogenetic Position	Genomic location	BAC & Fosmid Clones
7p12.3	48300227 - 48481716	RP11-12G8
7p12.2	50625897 -50785397	RP11-252B16
7p12.3	48399226- 48587664	RP11-479I17
7p12.3	48342399- 48384744	G248P8188G7
7p12.3	48318520 - 48361823	G248P82942G4
7p12.3	48367894 - 48412601	G248P87241B7
7p12.3	48581759 - 48622719	G248P87291H3
7p12.3	48556511 - 48596971	G248P87497D6
7p12.3	48578957 -48622314	G248P85917G11
7p12.3	48503748 - 48540697	G248P82255H9
7p12.3	48534410 - 48575724	G248P82734E6
7p12.3	48404090 - 48438107	G248P82093A10
7p12.3	48335120 - 48375794	G248P85542D8
7p12.3	48318520 - 48361823	G248P82942G4
7p12.3	48314130 - 48356539	G248P88933F11
8p23.1	9670916 - 9832224	RP11-56F16
8p23.1	6936560 - 7093758	RP11-158L15
8p23.1	8166168 - 8312811	RP11-213A20
8p23.1	7582055 - 7764571	RP11-499J9
8p23.1	8907289 - 9074592	RP11-429B7

8p23.1	9370526 - 9530265	RP11-179E13
8p23.1	9002003 - 9194364	RP11-116H16
8p23.1	8645798 - 8828200	RP11-18L2
8p23.1	8758387 - 8925126	RP11-151D16
8p23.1	8837122 - 9012651	RP11-90J21
8p23.1	8966327 - 9116035	RP11-179A8
8p23.1	8927012 - 8963589	G248P87609F9
8p23.1	8971187 - 9009657	G248P8175C4
8p23.1	9083226 - 9123378	G248P81016E4
8p23.1	9012116 - 9051241	G248P88001D3
8p23.1	9040227 - 9078421	G248P81557D1

2.2.7 DNA

Genomic DNA was extracted from venous blood using standard methods by either former members of the Medical Genetics Section, MMC, Western General Hospital (WGH) or more recently the genetics core, Wellcome Trust Clinical Research Facility (CRF), WGH. DNA concentration quantification and quality control checks were performed previous to my receiving the samples. Samples used for TaqMan assays and *GRIK4* genotyping were already plated at working stock concentrations of 10ng/ul, and stored at the CRF.

2.2.8 Cell lines, Lymphocytes, RNA Blood and mouse brain homogenate

In house cell lines LAN5, SH-SY5Y (human neuroblastoma derived), U373, MOG (human glioblastoma derived) and HEK293 (embryonic human kidney) were cultured using standard laboratory practice, and the pellets gifted to my studies by Ben Pickard and Lorna Maclaren. RNA from lymphocyte and total blood was provided by Pat Malloy. Mouse brain homogenate was donated by Shaun Mackie.

2.2.9 Human brain tissue

Hippocampus and frontal cortex human brain tissue and Paraffin embedded post-mortem Human brain sections were donated by the Edinburgh University MRC Sudden Death Brain Bank (http://www.edinburghbrainbanks.ed.ac.uk/). Histology was performed on coronal sections of the hippocampus, amygdala, cerebellum and transverse sections through the rostral medulla oblongata at the level of the inferior olivary nucleus. Coronal sections from the frontal cortex were taken in a parasagittal plane.

2.3 General Methods

Molecular biology techniques were developed from (Sambrook et al., 1989), unless otherwise stated.

2.3.1. Molecular cytogenetics: Fluorescence in situ hybridization (FISH)

Fluorescence in situ hybridization (FISH) is a technique that is used to detect chromosomal deletions, translocations and copy number variants by hybridizing fluorescently labeled DNA probes to metaphase arrested chromosomes (Trask, 1991). This method involves several steps; namely: a mini-prep to isolate bacterial DNA; nick translation to tag the DNA with chemically modified deoxynucleotide triphosphates (dNTPs); preparation of metaphase chromosomes from lymphocytes and dropping onto microscope slides; hybridization of the tagged probes to the chromosomal DNA on the slides; and probe detection through fluorescein-labeled conjugated antibodies or enzymes. Each step will be described below.

2.3.1.1. Miniprep preparation of Bacterial DNA

A single bacterial colony was used to inoculate 5ml of LB-Broth with the appropriate antibiotic added. The cultures was grown overnight at 37°C in a shaker incubator. 2ml of

bacterial culture was centrifuged for 5 minutes at 3000rpm. DNA was isolated from the pellets using the Qiagen plasmid mini kit. In brief, the pellet was resuspended in 0.3ml of P1 solution before adding 0.3ml P2 and incubated for 5 minutes at room temperature. Next, 0.3ml of P3 was added and the lysate incubated for 10 minutes on ice before centrifugation at 13000rpm for 10 minutes.

The supernatant was transferred to a new micro-tube, 0.8ml of isopropanol added and left on ice for 15 minutes followed by centrifugation at 13000rpm for 15 minutes. The supernatant was subsequently removed and 0.5ml of 70% alcohol added to wash the pellets before centrifugation at 13000rpm for 5 minutes. The supernatant was again removed and the pellets air dried at room temperature. Once the DNA pellets had become translucent they were re-suspended in 40µl TE (pH 8.0) and left to sit for one hour at room temperature before storage at -20°C. The quality of the DNA was determined by agarose gel electrophoresis (section 2.3.2.2).

2.3.1.2. Nick Translation

Nick translation is a procedure used to label bacterial DNA with chemical modified nucleotides before the 'tagged' probe is hybridized to metaphase chromosomes. The method used was as follows. To make a total volume of 20µl of reaction mix, 0.5mM of dCTP, dGTP & dATPs; 2.5µl of undiluted biotin-16-dUTP or digoxigenin-11-dUTP; 2µl nick translation buffer; 1µl DNA polymerase; 1µl DNase (working solution diluted 1:600) and 6µl bacterial DNA was added to an micro-tube and incubated for 1.5-2hrs at 16°C. To separate nick translated DNA from unincorporated nucleotides, 100µl of labeled DNA solution is run through nick columns and centrifuged for 4 minutes at 1800rpm.

2.3.1.3. Preparation of metaphase arrested chromosomes

Metaphase-arrested chromosomes and interphase nuclei for cytogenetic analysis were prepared by Pat Malloy. In order to generate metaphase-arrested chromosomes for

cytogenetic analysis, 0.8mls of patient blood were cultured for 71hrs in medium containing phytohaemagglutinin (Peripheral Blood Medium, Sigma). The short-term cultures were treated with colcemid for one hour, followed by a conventional fixing procedure. Fixed chromosomes were dropped onto microscope slides and stored for one week prior to use in FISH experiments.

2.3.1.4. Hybridization

Prior to hybridization, the labeled probes were precipitated and re-suspended to produce a more concentrated solution whilst simultaneously Cot-1 and salmon sperm (which act a competitive DNA by binding to repetitive sequences within the probes) are added to decrease background signal. Quantities used: 15µl Bac DNA or 20µl fosmid DNA; 0.5µl salmon sperm (10mg/ml); 8µl and 5µl cot1 for Bac or fosmids respectively; precipitated in 2 times total volume of absolute alcohol and dried under vacuum in a rotational-vacuum-concentrator RVC2-18 (Christ freeze Dryers) for 30 minutes. Pellets were then reconstituted by adding 10µl hybridization mix buffer and left at room temperature for an hour. The probes were subsequently denatured by being heated to 70°C in a water bath and then transferred to a second water bath set at 37°C for 15 minutes.

Simultaneously to this process, the metaphase-arrested chromosome slides were prepared for hybridization. This involved: RNaseA treatment in 200ml of 2xSSC & 2ml of 10mg/ml RNaseA at 37°C for 30 minutes, followed by a wash in 200ml 2xSSC and dehydration through 70% 90% and 100% ethanol (2 minutes each) and air dried. The slides were then pre-warmed by placing them in an oven set at 70°C for 5 minutes; denatured in 70°C denaturing solution for 2-3 minutes; quenched in ice cold 70% ethanol proceeded by dehydration in the ethanol series (2 minutes each), air dried and warmed on a metal tray in a water bath set at 37°C. 10µl of labeled probe was then dispensed onto each slide, the slides covered with a 22x32mm coverslips and left overnight at 37°C.

After incubation overnight, the slides were washed in 50% formamide at 45°C for 2x 7 minutes. This was proceeded by further washes in 0.1x SSC at 60°C (2 x7 minutes) before the slides were transferred into 4 x SSC, 0.0.5% Tween 20 and left at room temperature. Simultaneously, fluorochrome-labeled avidin Texas red® DSC (Vector) or anti-digoxigenin fluorescein FAB fragments were diluted in blocking buffer (1:500 avidin; 1:10 anti-DIG) and centrifuged for 7 minutes. 40µl of the avidin or FITC block mix was dispensed onto the slides using 22x22mm coverslips and incubated for 30 minutes at 37°C. Coverslips were then gently removed and slides washed in 4xSSC, 0.1% Tween 20 heated to 45°C (3 cycles of 3minutes). Lastly, 40µl of mountant mix (0.5ml vectorshield antifade and 10µl DAPI) was applied to 22x50mm coverslips and overlaid with slides, blotted, and sealed with Tip Top rubber solution. Slides were stored at 4°C when not analysed under the microscope.

2.3.2. Sequencing

2.3.2.1 Polymerase Chain Reaction

Standard PCR amplification reactions were performed using Invitrogen reagents. However, when amplifying long sequences, or if the sequence had a high GC content, the Expand long-range PCR kit (Roche) was used. Using Invitrogen reagents, PCR was performed with a final volume of 25µl comprised of: 25-50ng template DNA; 2.5µl of 2mM dNTPs; 5µmol primer; 2.5µl 10xPCR Invitrogen amplification Buffer; 7µl dsH_2O; 0.25U Invitrogen *Taq* DNA polymerase and either 10µl or 1x enhancer solution. Using the Expand long-range PCR kit, a total volume of 16µl comprised; 25ng template DNA; 25mM of each dNTP; 5µmol primer; 1.7µl expand long-range Buffers 2 &3; 13.3µl dsH_2O and, 0.25U Invitrogen *Taq* DNA polymerase. The amplification was carried out on a MJ Research Peltier Thermal Cycler, PTC-255 (MJ Research) using the primers listed and under cycling conditions presented in table 2.4.

2.3.2.2 Agarose gel electrophoresis

DNA/RNA integrity and PCR reaction efficacy were determined by Agarose gel electrophoresis. In general, agarose gels of 2% and 0.8% were used for resolution of small (~ 0.2kb-1kb) and large (>1kb) fragments respectively. Agarose gels were prepared by heating agarose in 1xTBE buffer. After dissolution of the agarose, SYBR Safe™ was added to the gel at a final concentration of 1µl/100ml. Sample and 1kb DNA ladder were loaded using orange G loading buffer. Electrophoresis was performed using Hybaid Electro-4 gel tanks. The gel was submerged in 1xTBE buffer and a current of 80-100V was passed through the buffer to allow migration of the DNA through the gel. Fragments were visualized using by UV transillumination (Thistle Scientific) and images captured using a digital imager, Uvidoc (Uvitec).

2.3.2.3 ExoSAP-IT treatment of PCR products

To remove excess primers and dNTPs, PCR products underwent ExoSAP-IT™ treatment. In general, 1-3µl PCR product, 2µl dsH_2O and 1µl ExoSAP-IT™ were incubated on a thermal cycler for 60 minutes at 37°C followed by 20 minutes at 80°C.

2.3.2.4 Sequencing PCR

PCR sequencing reactions were performed using BigDye® Terminator Ready Reaction Mix v3.1 with 1.2µl BDv3.1, 1µl primer 3.2µM, 1.8µl dsH_2O, added to the ExoSAP-IT treated PCR products giving a total reaction volume of 10µl. Sequencing reactions were performed on a MJ Research Peltier Thermal Cycler using following cycling conditions: 96°C -1min, 96°C -10s, 50°C -5s 60°C -4 min times 25 cycles; 4°C -10min.

2.3.2.5 Ethanol/EDTA Precipitation and sequence analysis

Following sequencing PCR, products were precipitated in an Ethanol/EDTA solution to stabilize extension products and to wash out unincorporated dyes. 2.5µl of 125mM

EDTA followed by 30µl 100% absolute ethanol was added to products, mixed and incubated for 10 minutes. Products were then centrifuged at 3,000rpm for 30 minutes, ethanol removed and a further 30µl 70% ethanol dispensed. The samples were again centrifuged for 15 minutes, ethanol removed and products air dried. Samples were run on an Applied Biosystems 3730 DNA analyser at the WT-CRF or sequencing department at the MRC HGU.

2.3.2.6 Sequence analysis

Sequence chromatograms were aligned using the PhredPhrap software and visualized with the Consed program (Gordon et al., 1998) (http://www.genome.washington.edu/consed/consed.html) or alternatively using Chromas (McCarthy 1998) and Finch TV (Geospiza, INC.) (http://www.geospiza.com). Variants were identified by visual inspection of forward and/or reverse sequence traces.

2.3.3 Confirmation of novel variants

Newly identified variants were confirmed by repeat re-sequencing, restriction enzyme assays and cloning of PCR product followed by sequencing of cloned DNA. For both restriction enzyme assays and cloning of PCR product, PCR products were first purified using the QIAquick PCR purification kit as instructed by the supplier. In brief, 150µl of buffer BP was added to 30µl PCR product and spun in a QIAquick column at 13,000 rpm for 30s. The flow-through was discarded and DNA washed using 0.75ml buffer PE before being spun again (13,000 rpm for 30s). Flow-through was removed and DNA in QIAquick column was centrifuged for an additional 1 minute (13,000 rpm). Finally, DNA was eluted by adding 30µl dsH_2O followed by centrifugation for one minute (13,000 rpm).

2.3.3.1 Restriction enzyme digest

A Taq$^{\alpha}$1 restriction enzyme (New England BioLabs) digest assay was used to confirm the variant R4728X. Following PCR product purification, 3µl of 1xNE buffer, 0.3µl BSA and 3µl of Taq$^{\alpha}$1 restriction enzyme and 8.7µl of dsH_2O was added to 15µl of PCR DNA, incubated at 65°C overnight. DNA fragments were visualized by Agarose gel electrophoresis (section 2.3.2.2).

2.3.3.2 Cloning PCR products

The cloning of PCR products was used to confirm the presence of variants giving rise to the amino acid substitutions H3609P, S3703R, T4031A and R3604Q. Following purification, PCR products were cloned using the Qiagen PCR cloning kit (Qiagen). In brief, 1µl of pDrive cloning vector and 5µl ligation master mix was added to 4µl of purified PCR DNA gently mixed and incubated at 16°C overnight. Transformation of PCR DNA was executed using a heat shock method as follows. 2µl of ligation reaction mix was added to 25µl of E-coli competent cells, incubated for 30 minutes, heat shocked at 42°C for 30 seconds and left on ice for one minute. Subsequently the ligation reaction/competent cell mix was added to 250µl of L-broth growth media already warmed to 37°C and left on a shaker to incubate for one hour.

The L-broth medium mix was plated on agar plates treated with chromogenic substrates IPTG and X/Gal to determine the efficacy of transformation, - a technique termed 'blue/white screening' (Joung et al., 2000). Agar plates were made by heating agar to 50°C, adding appropriate antibiotics (1µl/ml of ampicillin [100mg/ml stock]), poured into Petri dishes and dried in an oven. 40µl of IPTG (100mM) and X/Gal (40 mg/ml) was spread over each plate before the L-broth medium transformation mix was plated and left to incubate in an inverted position at 37°C overnight. As approximately half of the cloned PCR product colonies should contain the mutant allele, DNA from 10 colonies of each variant was purified. The white colonies which indicated no production of the enzyme β-galactosidase and hence successful incorporation of plasmid DNA were

subsequently cultured in L-broth, pelleted and DNA isolated using the GenElute™ Plasmid Purification kit (Sigma-Aldrich) according to manufacturer's instructions.

The cloned PCR product DNA was directly sequenced using the Qiagen PCR cloning kit T7 promoter primer. The sequencing reaction was performed using the BigDye® Terminator Ready Reaction Mix v3.1 with a final volume of 10ul comprising of 1µl BDv3.1, 1µl primer 3.2µM, 2µl cloned DNA and 6µl dsH_2O. Primer details are presented in table 2.2.5.1. Sequencing reactions were performed on a MJ Research Peltier Thermal Cycler using following cycling conditions: 96°C -1min, 96°C -10s, 50°C -5s 60°C -4 min times 25 cycles; 4°C -10min. Following the sequencing reaction, products were precipitated in an Ethanol/EDTA solution and run on an Applied Biosystems 3730 DNA analyser.

2.3.4 TaqMan assays

TaqMan Assays-by Design were used to determine the frequency of variants in control and case populations. Primers employed for the TaqMan assays were designed by ABI and listed in Table 2.6. Assays were performed and genotypes called by staff at the WT-CRF. All genotypes were confirmed through re-sequencing.

2.3.5 Genotyping

In-house genotyping was performed using the primers listed in table 2.4. It was performed under cycling conditions stated in table 2.4 or section 2.3.5.2 and using the reagents presented below. Amplification was carried out on a MJ Research Peltier Thermal Cycler, PTC-255 (MJ Research), and DNA fragments visualized by Agarose gel electrophoresis (section 2.3.2.2). PCR products were run on an Applied Biosystems 3730 DNA analyser at the WT-CRF or MRC HGU sequencing department. Genotypes were analysed with Genemapper v3 software (Applied Biosystems).

Variant	Primer	Reporter sequence
R4728X	GGACCAATGGAGACATTCTTGTGTT CCCAAACTAATATCTTGCACAGCAA	AAAGCGTCGATAATGT AAAGCGTCAATAATGT
T4031A	TGCTTGGACCCAGGTCGTA TCACTCAGCGCTTCAGCTT	TCATCTTCACAACCCACC ATCTTCACAGCCCACC
R3604Q	TGCTGTGGTAACCTTGGGTTTT CAGGCCAGGAAATGGATCACT	TCCCATCATCCGCATAT CTCCCATCATCTGCATAT
H3609P	TGTGGTAACCTTGGGTTTTTTCTCT GAACCAGGCCAGGAAATGGAT	CACTGGATGCACTCC ACTGGAGGCACTCC
S3704R	CAGCTTTCTGCCCTACATAGTTCT TGGGATTTTGTCTTGTTAGATAGATTGCA	TACATAACCAATTAAGTTTTGT CATAACCAATTAAGGTTTGT
T4550A	CAAGGTCTTAGAATGTATCTGCCATAGAT CGAACTGGAAAAGATTCTGGACATC	CAGATATGCAACTCTTCCA ATATGCAGCTCTTCCA
H4262R	CCCTCCCCTCAGACTCACA CGAAATCAAAGGAACAAAAACAACTTACCT	CCCGCTGGTAATGT CCCGCTGGTAACGT
P4648A	CCACAACTTCGGCATTGATTCCTA CGAAGATCCAGCCCAGAAAGTTC	ATCTCAAAGGGACTCACA TCTCAAAGGCACTCACA
R4590W	GGCCTTTGTACCATGCTCATAAC GTGATGCTACAAAGCTACTGACCTT	ATTATGCCCCGGTTGC CATTATGCCCTGGTTGC
P4648A	CCACAACTTCGGCATTGATTCCTA CGAAGATCCAGCCCAGAAAGTTC	ATCTCAAAGGGACTCACA TCTCAAAGGCACTCACA

Table 2.6 Primers used for TaqMan assays.

2.3.5.1 Genotyping GRIK4 3'UTR variant

Genotyping was performed using gDNA from a population of control and bipolar disorder samples details of which are given in sections 2.1.1, 2.1.2 and 2.1.3. In addition, gDNA extracted from Human brain tissue was genotyped by a second experimenter for indel status as part of the GRIK4 genotype/protein expression study. PCR amplification reactions were performed using the Expand long-range PCR kit (Roche) with a final volume of 16ųl was comprised of: 25ng template DNA; 25mM of each dNTP; 5µmol primer; 1.7µl expand long-range Buffer 1; 13.3µl dsH_2O and, 0.25U Sigma *Taq* DNA polymerase. Products were diluted 400-fold before separated on the DNA analyzer.

2.3.5.2 Chromosome 7 microsatellites

Amplification reactions were performed using sigma reagents with a final volume of 16.6ųl comprised of: 50ng template DNA; 1.6µl 2mM dNTP's; 5µmol primer; 1.6µl sigma buffer; 9µl dsH_2O and, 0.25µl sigma *Taq* DNA polymerase. Amplification cycling conditions were as follows: 93°C -1 minute; 93°C -20s, 65°C -30s, -1°C per cycle, 72°C -1 minute x 9 times; 93°C -20s, 55°C -30s, 72°C -1 minute x 29 times; 72°C -10 minutes. Products were diluted 20-fold before separated on the DNA analyser.

2.3.5.3 Whole genome SNP genotyping

The genome wide scan of two consanguineous Pakistan families employed 5858 biallelic SNPs typed at Illumina Inc., San Diego, USA using proprietorial bead-array technology (Linkage IV panel). Marker spacing was approximately 480Kb (0.6cM) and locus success rate 99.2%. SNP data was analysed and checked for potential genotyping errors both by visual examination and by *PLINK* v0.99 Mendel error test (Purcell et al., 2007) (http://pnug.mgh.harvard.edu/~purcell/plink).

2.3.6. Reverse-transcriptase PCR

2.3.6.1 RNA preparation

RNA was extracted using RNeasy Mini Kit (Qiagen) as per manufacturer's instructions. In brief, cell line and blood pellets were thawed before adding 600µl RLT buffer (containing guanidine-thiocyanate to inactivate RNases hence ensuring purification of intact RNA) and homogenized in a QIA shredder spin column (Qiagen) spun for 2 minutes at 13000 rpm. An equal amount of 70% ETOH was added to the lysate, mixed well and applied to an RNeasy mini spin column spun at 10000 rpm for 15 seconds. The sample was then washed in 350µl RW1 buffer, spun at 10000 rpm for 15 seconds before 80µl of DNase1 incubation mix was dispensed directly onto the spin column membrane and left at room temperature for 15 minutes. The column was then again washed in RW1 buffer and 500µl RPE buffer added, spun for two minutes at 10000 rpm. RNA was then eluted in 30µl RNase-free water and stored at -70°C.

RNA concentrations and RNA Integrity Number (RIN) values, the proprietary quality score for total RNA, and were obtained using the Agilent BioAnalyzer platform. All scores were above 9, indicating that the RNA was not degraded and of a high quality.

2.3.6.2 cDNA synthesis

RNA was reverse transcribed to cDNA with First Strand cDNA Kit (Roche) using primers oligo-p$(dT)_{15}$ primer method. This technique produces single stranded RNA using AMV reverse transcriptase. The synthesis reactions were performed with a final volume of 20µl master mix comprised of: 2µl x10 reaction buffer; 4µl 25mM $mgCl_2$; 2µl 10mM dNTPs; 2µl oligo-p$(dT)_{15}$ primer; 1µl RNase inhibitor; 0.8µl AMV reverse transcriptase and 8.2µl dsH_2O. The reactions were cycled on a thermal cycler (Pelter PTC-225) as follows: 25°C -10min, 42°C -10min, 99°C -5min, 4°C -5 min. cDNA was stored at -20°C .

2.3.6.3 RT-PCR

To investigate any potential differences in expression of various regions of ABCA13, i.e. the possibility *ABCA13* encodes for two half transporters, several pairs of primers were designed across exons as summarized in table 2.7 below. In addition to cell lines (LAN5, SH-SY5Y, U373, MOG, HEK293 and lymphoblastoid), human blood RNA and human hippocampus and frontal cortex tissue were tested. PCR amplification was conducted using reagents in the Expand Long-range PCR kit (Roche) as described in section 2.3.2.1. Primer details and cycling conditions are presented in table 2.4 (section 2.2.5.). PCR products were visualized by Agarose gel electrophoresis (section 2.3.2.2).

Primer	Exons	Position	Material Tested
Primer 1 - N terminal	18, 179, 20, 21, 22	Large Intracellular loop before functional domains	Cell lines, blood RNA
Primer 2 -1st half	25, 26, 27, 28	1st half of protein before TMD1	Cell lines, blood RNA
Primer 3 -2nd half	50, 51, 52, 53	2nd half of protein, TMD2	Cell lines, blood RNA
Primer 4 - middle short	41, 42, 43, 44, 45, 46,	Middle of protein between TMD/NBD1 and TMD/NBD2	Cell lines, blood RNA, hippocampus
Primer 4 - middle long	39, 40, 41, 42, 43	Middle of protein including exons encoding NBD1, HPR.	Hippocampus and cortex

Table 2.7 RT-PCR primers designed across exons encoding different parts of ABCA13. Exons, position within protein and biological material tested listed.

2.3.7. Immunohistochemistry

Immunohistochemistry was performed using an indirect immuno-peroxidase staining technique (Nakane and Pierce, 1967). This technique involves a number of steps, namely: dewaxing; pretreatments such as the blocking of endogenous activity and antigen retrieval to uncover hidden antigenic sites; the blocking of non-specific sites; incubation with unlabelled antibody, labeling with a secondary antibody which is coupled to the enzyme streptavidin-horseradish peroxidase; and detection through 3, 3'-Diaminobenzidine (DAB) reactivity. The protocol used, developed from (Harlow and Lane, 1998) is detailed in section 2.3.7.1 below.

2.3.7.1 Immunoperoxidase staining

10µm formalin-fixed paraffin embedded sections were placed in a slide rack and dewaxed in xylene, rehydrated through a graded alcohol series (70%, 100%) and incubated in picric acid for 15 minutes (Sigma-Aldrich). Endogenous peroxidase activity was blocked by placing the sections into 0.3% hydrogen peroxide/methanol for 30 minutes. Antigen retrieval was performed by incubating the sections in a citric acid buffer (0.01 M citric acid, pH6.0) and heated in a pressure cooker (BioGenix). Slides were then transferred to a shandon sequenza slide rack (Thermo Fisher Scientific). To prevent non-specific binding of the secondary antibody and extraneous binding of endogenous avidin-biotin sites, sections were first incubated in 100µl 20% goat serum diluted in PBS-Triton-X-100 (PBS with 1% T-X-100) followed by blocking using an avidin/biotin blocking kit (Vector Laboratories) according to the manufacture's instructions. 100µl of primary antibody was incubated overnight at 4°C. Following two washes in PBS with 1% T-X-100 slides were incubated in 100µl goat anti rabbit biotinylated secondary antibody and washed again.

Detection of the biotinylated secondary antibody was performed with the streptavidin-biotin peroxidase complex kit (DAKO StreptABComplex/HRP Duet) and according to

supplier's instructions. Slides were removed from the Sequenza slide rack and antibody signal was detected using DAB coupled to an enhancing solution performed using the DAB substrate kit for peroxidase (Vector Laboratories). Sections were counterstained in Harris hematoxylin for 20 seconds, dipped in lithium carbonate to turn the tissue blue, dehydrated, cleared and mounted using Pertex mounting medium. A negative control (no primary antibody or pre-immune serum) and a positive control (staining for GFAP expression) were performed every IHC experiment. No signal was seen without addition of primary antibody or when incubated with pre-immunised serum.

2.3.8. Antibody specificity assays

To determine the specificity of the antibodies raised against GRIK4 and ABCA13, a number of assays were conducted. These were: immunoblotting to demonstrate that the antibody binds to a protein of the appropriate size (section 2.3.8.1); the use of pre-immune antiserum to resolve whether primary antibody immunoreactivity is different from non-specific antisera staining (section 2.3.8.2); and, pre-absorption of antibody with peptide against which the antibody was raised (section 2.3.8.3).

2.3.8.1. Immuno-blotting

Pre-immune sera and an appropriate peptide with which to perform a pre-absorption assay were not available to investigate GRIK4 specificity. Therefore, immunoblotting was conducted to verify that the GRIK4 antibody binds to a protein of the same size (~107KDa) as GRIK4. The method used is as follows. 500µl of ice cold RIPA buffer was added to SH-SY5Y and U373 cell line pellets, sonicated in a water bath for 10 minutes (Wolf laboratories ltd), left on a rotator for 20 minutes and centrifuged at 13000rpm at 4°C for 20 minutes. The supernatant was removed and stored at -70°C until use.

Protein gel electrophoresis was performed using 7.5µl and 2.5µl of lysate and 8.4µg/µl mouse brain homogenate using NuPAGE Electrophoresis System, as per manufacturer's

instructions (3-8% Nupage Tris-Acetate gel) and stained with Coomassie Brillant Blue stain to determine appropriate protein loading concentrations. Gels were dried using DryEase Mini-Gel Drying System. Consequently, 9.0µl of SH-SY5Y and U373 lysate and 4.5µl of mouse brain homogenate were used for protein gel electrophoresis as described above and transferred with X-cell SureLock™ MiniCell (Invitrogen) as per manufacturer's instructions to a PVDF membrane (Hybond-P PVDF Membrane, Amersham Biosciences). Ponceau's stain was used to verify successful protein transfer onto PVDF membrane. Following five minutes' incubation in Ponceau S, membranes were destained in dsH_2O. The membrane was subsequently incubated in 40ml 10% Marvel PBS-Tween 20 at 4°C overnight.

Primary antibody GRIK4 272 was incubated at a concentration detailed in table 2.3 (section 2.2.4) for one hour, followed by three washes in wash buffer and incubation with HRP secondary antibody for 30 minutes. Detection was performed with ECL Plus Western Blotting detection system (GE Healthcare) following supplier's instructions, and visualized on X-ray film.

2.3.8.2 Pre-immune antisera assay

Pre-immune serum should bind to proteins within brain tissue in a non-specific manner and hence characterize non-specific immunoreactivity. Prior to use of pre-immune serum obtained from the same animal in which ABCA13 780 antibody was raised, antisera protein concentration was determined by using BIORAD DC protein Assay as outlined in the manufacturer's guidelines. Using EXCELL, a BSA standard curve was generated and a straight line equation was used to calculate protein concentrations. Based on an approximation of the primary antibody concentration (~0.2mg/ul), it was estimated that the pre-immune serum was circa 50 times more concentrated. The serum was titrated by using 1µl diluted in 250µl, 1ml, 2.5ml and 5ml of block (relating to dilution factors of 5 times, 25 times, 50 times and 100 times primary antibody concentration estimates) and incubated with the brain sections during the IHC protocol

instead of primary antibody. The 2.5ml dilution, predicted to be roughly equivalent to the estimated antibody concentration used in this technique, produced non-specific immunoreactivity which was most similar in concentration to primary antibody immunoreactivity.

2.3.8.3 Peptide preabsorption of antibodies

An alternative approach to determine specificity is to pre-absorb a primary antibody with the appropriate immunizing peptide which should consequently block any specific immunoreactivity. 5µg of peptide per 1µl of primary antibody diluted in 100µl block was left to incubate overnight on a rotator at 4°C. Before use, the antibody/peptide solution was centrifuged at 8000rpm for 30 minutes. Simultaneously, primary antibody with no peptide was taken through the same procedure.

2.4. Image Acquisition

Images were visualized on a Zeiss Axioskop 2 MOT epifluorescence microscope with a chroma number 81000 multi-spectral filter set, and 3 lenses of 16x, 40x and 100x magnification. The microscope was attached to an ORCA-ER digital camera (Hamamatsu Photonics) and images captured using SmartCapture 2 version 3 software (Digital Scientific Ltd). FISH prepared slides and immunohistochemistry DAB treated brain sections were analyzed following standard microscopy procedures and under fluorescence and bright field conditions respectively.

2.4.1. Image capture settings

Images capture settings and image saving formats were standardized across samples. However, image capture exposure times were set ‘automatic’, i.e. not manually set at a fixed value, which could potentially introduce a bias when assessing protein expression semi-quantitatively as pertinent to the aim of chapter 8. To investigate this possibility, images from a small subset of IHC samples assessed as having either high or low

expression values were recaptured with a set exposure time of 0.01s and re-analyzed for neuropil staining using the methodology described in section 2.5.4.1. The expression values taken under automatic and fixed conditions were found to be similar, suggesting that image capture using the automatic exposure setting would not be a confounding factor.

2.5 Data Analysis

The methods employed for data analysis are discussed by chapter below.

2.5.1. Chapter 3

2.5.1.1 Genome-wide analysis of autozygosity

Analysis of homozygous SNPs and tracts across 22 autosomes in each individual was performed using *PLINK* v0.99 (http://pnug.mgh.harvard.edu/~purcell/plink (Purcell et al., 2007) using 'Runs of homozygosity' analytical tool set. In addition to identifying SNP markers homozygous in each affected member but heterozygous in non-affected individuals, the length of autozygous runs and number of tracts were estimated for individuals belonging to the first consanguineous family. Inspection of homozygous tract lengths was limited to 5 or more consecutive SNPs and low SNP densities in centromeric regions were excluded. The length of homozygous regions was taken to be from the most proximal to the most distal homozygous SNP and the programme allows one heterozygous SNP within this run. Marker positions were based upon NCBI build 35 physical map and DeCode genetic map.

2.5.1.2 Inbreeding coefficients

Inbreeding coefficients (*F*) were estimated using FEstim (Leutenegger et al., 2003; Leutenegger et al., 2006). MAFs (Minor Allele frequencies) as determined for both the Caucasian CEPH (Utah residents with ancestry from Northern and Western Europe) and

Asian populations (Japanese and Chinese) were provided by Illumina (http://www.illumina.com/). MAF data were not available for the Punjabi population. To eliminate the possibility that a dense marker map of 5858 SNPs would lead to an overestimation of *F* due to linkage disequilibrium, three marker maps were evaluated: 5858 SNPs, intermarker distance ~ 0.6 cM; 1170 SNPs intermarker distance ~3cM; and 585 SNPs, intermarker distance ~6 cM. The formatting of low density marker files was performing by Steven Cass using a perl script programme. The lower marker density maps produced consistently higher inbreeding coefficients, suggesting that LD does not contribute to inflated *F* estimates. Inbreeding coefficients estimated using allele frequencies calculated for the Asian population were consistently higher at all marker densities than estimates calculated using CEPH population frequencies. Therefore inbreeding coefficients presented in table 3.1 (chapter 3.2.2) reflect more conservative estimates generated using CEPH allele frequencies.

2.5.2. Chapter 4

2.5.2.1 Haplotype analysis

As discussed in chapter 4, two newly identified rare variants, R4728X and T4031A, appear to be carried on a conserved haplotype. To investigate the frequency of these haplotypes in the general population, in phase data from five SNPs, rs1526093, rs17132289, rs17548783, rs1316349, rs7778411 all positioned within *ABCA13* were downloaded for 30 CEPH trios from HapMap Phase II build 125 (http://www.hapmap.org. The frequencies of 4 SNP and 2 SNP haplotypes were calculated using haploview version 3.2. program (Barrett et al., 2005) (http://www.broad.mit.edu/mpg/haploview/).

2.5.2.2 Amino acid conservation and splice site mutation detection

ABCA13 variants identified as mutated were assessed for species and ABCA sub family amino acid conservation. Species conservation data was obtained from the University

College Santa Cruz (UCSC) [NCBI Build 35 and 36.1] genome browser. Human ABCA13 orthologues were also determined using a blast search against the translated sequence database (tblast) via the NCBI website (http://ncbi,nlm.nih.gov/BLAST/). Protein sequences for ABCA subfamily members were retrieved directly from the swissProt database (Boeckmann et al., 2003) http://www.expasy.ch/sprot/, and multiple sequence alignments generated automatically using Clustal X (Thompson et al., 1997) http://www.clustal.org/. Potential splice site variants were assessed using Berkeley Drosophila Genome Project splice site predication tool (Reese et al., 1997) http://www.fruitfly.org/seq_tools/splice.html.

2.5.2.3 Linkage analysis

Non-parametric linkage analysis was conducted by Douglas Blackwood using Merlin (Abecasis et al., 2002) to calculate allele sharing between all pairs of affected relatives in 15 families. There was complete ascertainment of all families of probands with a mutation, i.e. every first and second degree relative obtainable was contacted. However, there is still the potential for case family bias in that probands where there was no family information available may indeed have no family history of psychiatric illness. Moreover, we were unable to follow up control individuals.

The analysis was performed under the following assumption; a broad phenotype model that included as cases schizophrenia, bipolar disorder, recurrent and single episode major depression, anxiety states and alcoholism. The 15 families carried 9 different variants with variable penetrance and allele frequencies. However, linkage analysis was conducted assuming a single rare variant with a frequency of 0.001 in all families and hence this is a conservative estimate as all variants were in fact rarer than this.

2.5.3. Chapter 6

2.5.3.1 Testing for deviations from Hardy-Weinberg Equilibrium

The standard χ^2 test of independence was used to examine if the observed genotype frequencies of the *GRIK4* insertion/deletion variant in control samples deviate from Hardy Weinberg Equilibrium (HWE). This was performed using the Hardy-Weinberg Equilibrium Calculator, http://www.changbioscience.com/genetics/hardy.html.

2.5.4. Chapter 7

2.5.4.1 GRIK4 protein expression correlation analysis

For each of the 12 samples (genotype status: 5 heterozygotes, 6 homozygote insertions and 1 homozygote deletion) immunohistochemistry was performed (blind to genotype) on three sections of the hippocampus and parietal frontal cortex. Immunopositive neuronal and glial cells were manually counted in the molecular layer and granular cell layer of the dentate gyrus, alveus, hilus, CA4, CA3 and CA1 of the hippocampus and layers 1-6 of the frontal cortex.

DAB immunopositive staining in the nucleus, cell body and processes of neuronal cells were all included as 'neuronal positive cell counts'. However, neuronal cells within a given quantified region which labelled positive for cytoplasmic, process or nuclear staining concurrently were scored only once. In regions where there was only evident dendritic/axonal labelling, i.e. the molecular layer of the hippocampus, each KA1 positive process was counted separately as it could not be ascertained from which neuronal cell each process projected. In the granular cell layer of the dentate gyrus, granular cell labelling was predominantly nuclear and hence each KA1 DG positive cell was counted separately. Likewise, glial counts were based upon clear cytoplasmic labelling and each immunopositive glial cell was counted individually.

Immunoreactive positive counts were quantified within circles of 50µm radii (x40 magnification) or 100µm radii (x16 magnification) using Image J image processing program (Rasband, 1997-2007) (Abramoff et al., 2004) http://rsb.info.nih.gov/ij/. Two circles were counted in 5-10 captured images randomly selected from each region of interest per slide and using a minimum of two slides per individual. Neuronal and glial cell positive counts were averaged per region before statistical analysis.

Neuropil immunoreactivity was assessed semi-quantitatively using a colour deconvolution technique in Image J (Ruifrok and Johnston, 2001) http://imagejdocu.tudor.lu/imagej-documentation-wiki/plugins/colour_deconvolution. Immunoreactivity was semi-quantified within two 100µm radius circles from 5-10 captured images randomly selected from each region of interest per slide using a minimum of two slides per individual The built-in stain vector setting used was Haematoxylin and DAB (H DAB) and background subtraction with colour correction was applied to the images before images processing. An appropriate pixel bin (window of pixel intensity) was manually chosen which represented genuine neuropil immunoreactivity (70-130 bin out of 255 pixels) and the number of pixels in this bin was percentaged over total pixel values. Figure 2.1 illustrates an IHC image analyzed by using this colour deconvolution technique. Percentages were averaged for each individual and statistics performed on the percentage means when comparing genotype groups.

2.6 Gene/protein notation

The notation and abbreviation of genes and proteins cited within this thesis follows standard scientific practice. Human transcripts are written in capitals whereas the first letter of a rodent transcript is capitalized and the remainder of the gene/protein written in lower case. Human and rodent genes and mRNA products are italicized to distinguish them from their protein products.

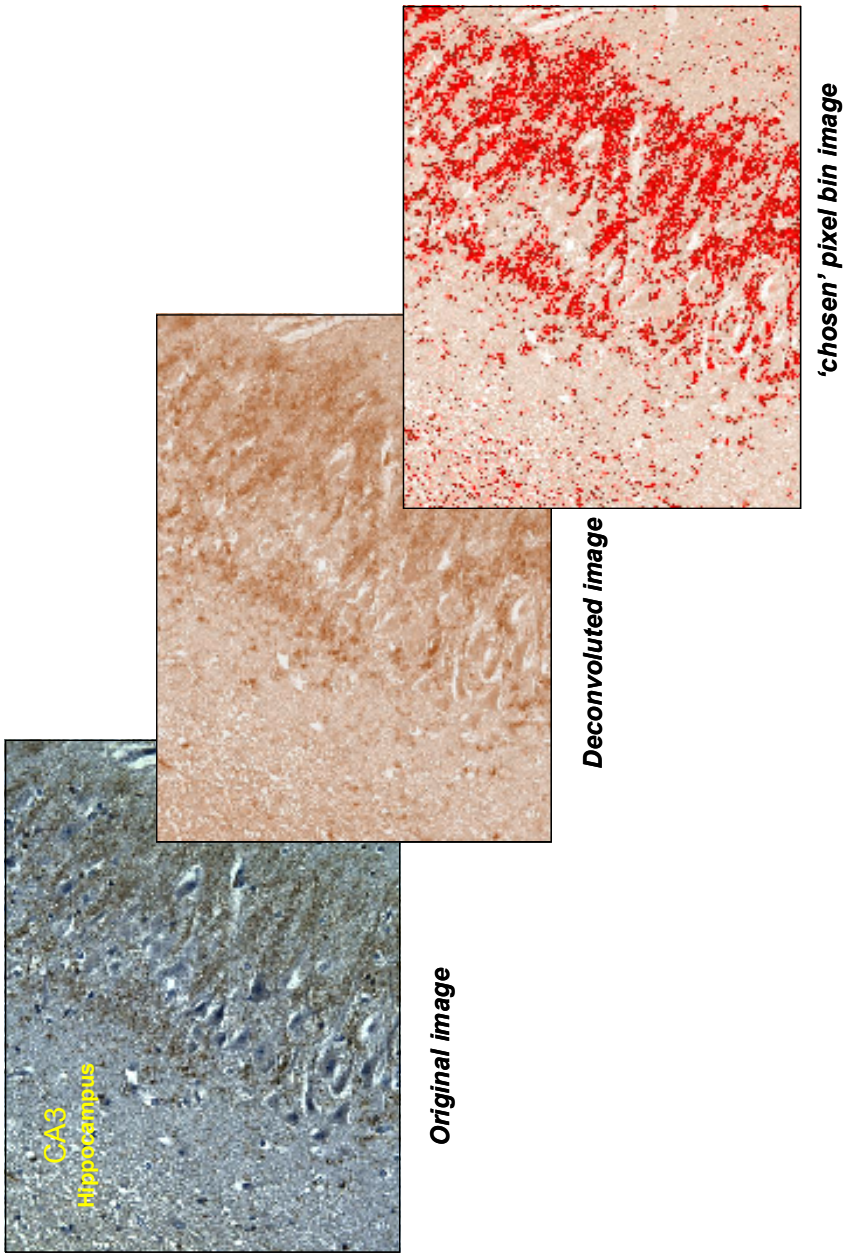

Figure 2.1 Illustration of IHC image analyzed by a colour deconvolution technique in Image J. The original image was captured on an epifluorescence microscope. The built-in stain vector setting and background subtraction with colour deconvolution correction was applied. A third stage involved choosing an appropriate pixel bin which represented genuine neuropil immunoreactivity.

2.7 Pedigree drawing

Pedigrees were drawn using Progeny Desktop Version 5 or Sarah Whittal, a graphics illustrator working in the Medical Genetics section, MMC. Standard pedigree symbols were used (Bennett et al., 1995). Squares and circles represent males and females respectively. Non-affected individuals are shapes not filled. Affected individuals are shaded and diagnosis is indicated by different colour shading. Black arrows depict the probands in each family and diamonds more than one unaffected individual.

2.8 Statistics

Standard statistics were calculated using Minitab 15 Statistical software or on line statistical calculators. For the GRIK4 genotype/expression study, correlations between gender, age, post mortem interval (PMI), tissue pH and genotype were investigated using the non-parametric Spearman's rank correlation test. The distribution of mean protein expression values (counts and neuropil staining percentages) for all samples were tested for normality using the Anderson-Darling test (Anderson and Darling, 1952). If the distribution were deemed normal, differences between genotype groups were tested using one-way ANOVA's – a parametric test.

However, if the mean population distribution was found not to be normal, the non-parametric Kruskal-Wallis test was employed. These tests were performed by dividing the genotype groups in two ways. First, the homozygote insertion group versus heterozygotes alone, and second the homozygote insertion group versus heterozygotes plus the one homozygote deletion sample.

To test the difference in frequency of a variant between cases and controls, Fisher's exact test (when cell values were less than 5) and Chi Square test ($\chi 2$) were used (GraphPad Software (http://www.graphpad.com/quickcalcs/contingency1.cfm). The Chi Square test ($\chi 2$) was also used to calculate the significance of the burden of all newly

identified nonsynonymous variants with a minor allele frequency of less than 0.01. This analysis included 32 mutated alleles out of 2646 control chromosomes and 101 mutated alleles in 3710 joint case chromosomes. Odds ratios (ORs), the measure of effect size, were calculated using the Odds Ratio calculator written by D.J.R. Hutchon, http://www.hutchon.net/ConfidOR.htm.

2.9 Bioinformatics

Blast: http://ncbi,nlm.nih.gov/BLAST/

BLAT: http://genome.ucsc.edu/cgi-bin/hgBlat

ClustalX: http://www.clustal.org/.

Decipher: https://decipher.sanger.ac.uk/

Ensemble: http://www.ensembl.org/index.html

FinchTV : (http://www.geospiza.com).

Gen Bank:http://www.ncbi.nlm.nih.gov

GraphPad: http://www.graphpad.com/quickcalcs/contingency

HapMap: http://www.hapmap.org.

Haploview: http://www.broad.mit.edu/mpg/haploview/

HWE calculator: http://www.changbioscience.com/genetics/hardy.html.

Image J: http://rsb.info.nih.gov/ij/

PubMed: http://www.ncbi.nlm.nih.gov/Literature/

Illumina: http://www.illumina.com/).

Plink: http://pnug.mgh.harvard.edu/~purcell/plink

Repeat Masker: http://repeatmasker.genome.washington.edu/

OR calculator: http://www.hutchon.net/ConfidOR.htm.

SDSC Biology workbench: http://workbench.sdsc.edu/

Splice Site Predication http://www.fruitfly.org/seq_tools/splice.html

SwissProt: http://www.expasy.ch/sprot/

UCSC: http://genome.ucsc.edu/

CHAPTER 3

HOMOZYGOSITY MAPPING IN A FAMILY PRESENTING WITH SCHIZOPHRENIA, EPILEPSY AND HEARING IMPAIRMENT

ACKNOWLEDGEMENTS FOR CHAPTER 3

I am grateful to the members of the family who have given their full consent to these studies. Clinical data was collected by Drs. M. Ayub, M. Irfan and F. Naeem. I was assisted by Steven Cass in the re-formatting of genotype data for the program FEstim. I thank Prof. Alan Wright and Dr. Caroline Hayward at the Medical Research Council Human Genetics Unit, Western General Hospital, Edinburgh for their advice and assistance with the analysis of homozygous tracts and to Dr. Anne-Louise Leutenegger for discussion and the program FEstim.

3. HOMOZYGOSITY MAPPING IN A FAMILY PRESENTING WITH SCHIZOPHRENIA, EPILEPSY AND HEARING IMPAIRMENT.

3.1 Preface

Homozygosity mapping was initially performed on family members by means of a low density microsatellite genome-wide scan. This led to the fine mapping of a region on chr22q13.3 which was found to be homozygous by descent (HBD). We observed the occurrence of heterozygosity between the closely spaced HBD regions which may be explained either by double recombination events or by mutation of the microsatellite markers. To determine which hypothesis was more accurate and to simultaneously fine map the genome at an even higher resolution, a second scan using SNP markers was conducted.

3.2 Results

3.2.1 A high density genome-wide SNP scan for linkage

The whole genome SNP data confirmed HBD on chromosome 22q13 with fifteen markers covering a region of approximately 12 Mb displaying the HBD pattern. As indicated in figure 3.1, the presence of intercalated non-HBD SNP markers gives rise to seven HBD candidate regions located between 35 Mb (q12.3) and 47 Mb (q13.3) on chromosome 22. Interestingly, the largest interval spanning 3 Mb almost completely overlaps with the microsatellite defined intervals, suggesting that mutations within the microsatellites have occurred.

This putative disease interval houses a large number of genes and thus the choice of which genes to screen for mutations was based on functional candidacy. *Activating Transcription Factor 4* (*ATF4*) located on 22q13.1 is a strong candidate gene for psychiatric illness.

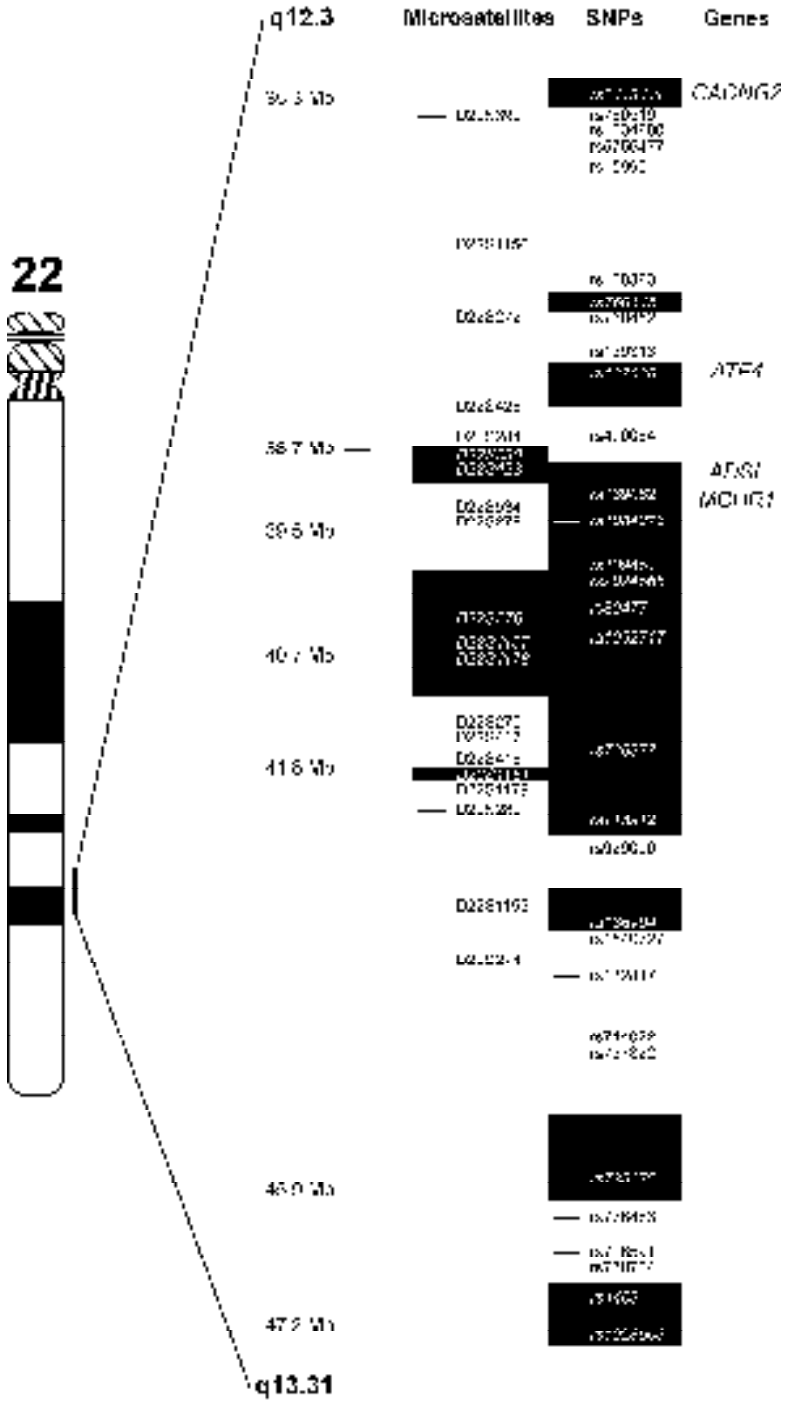

Figure 3.1 SNP and microsatellite data identifying the locus on chromosome 22q12.3-q13.3. HBD conforming markers are shaded, non-HBD intervals are not shaded. Physical distance along chromosome is indicated.

ATF4 interacts with DISC1, an established susceptibility factor for schizophrenia identified by multiple genetic and biological studies (Millar et al., 2000; Morris et al., 2003).

A second strong candidate, *CACNG2,* encodes the protein stargazin, an L-type calcium channel subunit which also functions as a regulator of post-synaptic membrane targeting for AMPA type glutamate receptors. Intronic mutations in *CACNG2* result in recessively inherited epilepsy and ataxia in *stargazer* mice. However, the introns are large and the exact position of some murine mutations is unknown. Furthermore, polymorphisms within human *CACNG2* are associated with schizophrenia, and response to the mood stablilizer lithium, and aberrations in DNA copy number in clones containing *CACNG2* have been found in individuals with bipolar disorder and schizophrenia (Wilson et al., 2006; Liu et al., 2008; Silberberg et al., 2008).

A third candidate, *GPR24* (alternative nomenclature *MCHR1)*, encodes for a G protein-coupled receptor which binds melanin-concentrating hormone at the plasma membrane. Single SNPs and several specific haplotypes within *GPR24* have been significantly associated with both SCZ and BP in Scottish and Faeroe Island disease populations (Severinsen, 2006; Severinsen et al., 2006a). Animal models of depression and anxiety also indicate that GPR24 antagonists produce a profile similar to clinically used antidepressants and anxiolytics (Borowsky et al., 2002; Chaki et al., 2005). All three candidate genes positioned on chromosome 22q12-3 within HBD intervals were screened by sequencing family members in order to identify mutations evident in the affected individuals only. No obvious potential functional variants were identified in any of the coding and promoter regions.

In addition to chromosome 22, the SNP data revealed a second interval on chromosome 2p24-25 that was homozygous in all affected family members and heterozygous in unaffected individuals.

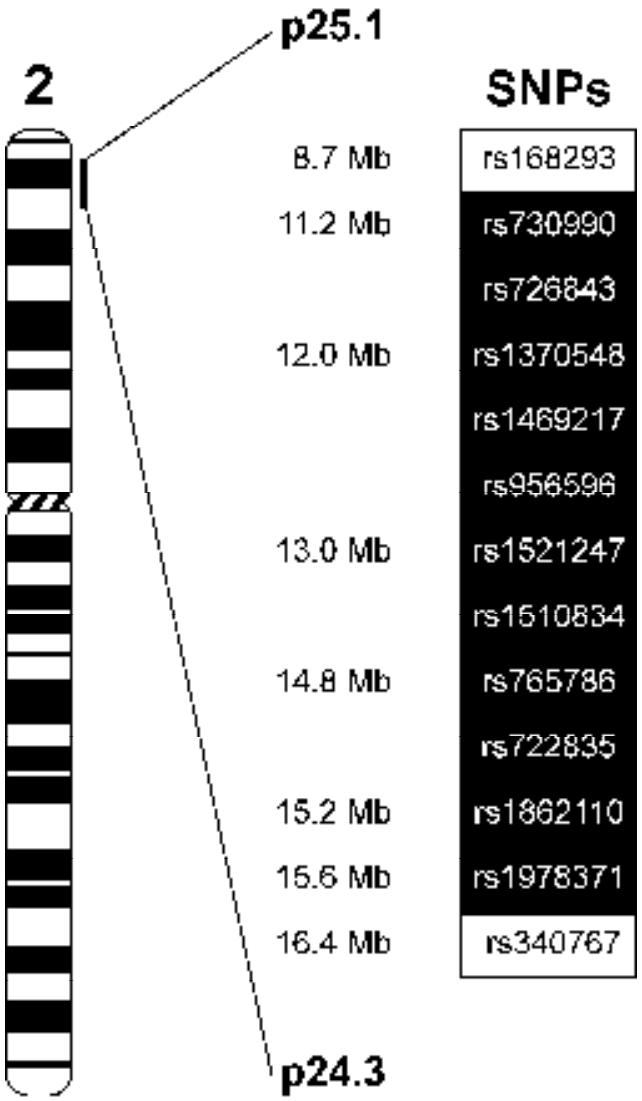

Figure 3.2 SNP markers identifying the HBD locus on chromosome 2p24.1-p25.3. SNP markers homozygous in all affected individuals are shaded black and non-HBD intervals white.

This region identified by markers rs730990 to rs1978371 spans a distance of ~5.4 Mb (figure 3.2), located 11 Mb proximal from the pter. HBD was undetected in the first scan because the microsatellite markers used are not positioned within this region. Candidate genes at 2p24.3-25.1 are relatively sparse. One gene of interest based on its function is *KCNF1*, a potassium voltage-gated channel of subfamily F.

Mutations in voltage-gated potassium channel subunits have been found to be responsible for both monogenic epilepsies and heritable autosomal recessive syndromes such as Jervell and Lange-Nielsen Syndrome in which hearing impairment is a clinical feature (Jervell and Lange-Nielsen, 1957; Schwartz et al., 2006). The promoter and coding regions of *KCNF1* was screened in all family members for mutations or functional variants. No such mutations were identified.

3.2.2 Inbreeding coefficients and runs of homozygosity (ROHs)

The inbreeding coefficients calculated using the 5858 SNP density map are presented in table 3.1. As expected, *F* values for the parents (Id 1: 0.136 ± 0.027, Id 2: 0.090 ± 0.021) are lower than all siblings (average 0.195 ± 0.025), range 0.16-0.22). In addition, runs of homozygosity (ROHs) across the 22 autosomes were analysed for each family member (graph 3.1). ROHs involving 5 or more contiguous SNPs approximately 2 Mb in length were evaluated and shorter tracts of homozygosity were excluded.

Table 3.1 presents the average, median and ROH range per individual. ROH length averages range from 5 Mb to 7 Mb and length median from 2.97 Mb to 4.08 Mb. The mother (Id 2) was found to have the shortest tracts, and a trend towards all offspring having longer average and median tract lengths than both the parents is apparent. The longest homozygous tract for each individual ranged between 40 and 74 Mb, with the most extensive being the 74 Mb found in individual 4.

Family Individual	Average (Mb)	Median (Mb)	Range (Mb)	# of tracts	Inbreeding coefficient (*F*)
Id 1	6.52 (SD 9.3)	3.30 (IQR 2.2-5.8)	0.7- 55.2	100	0.136 (SD 0.027)
Id 2	5.00 (SD 6.0)	2.97 (IQR 2.1-5.2)	0.5 - 46.6	92	0.090 (SD 0.021)
Id 3	6.00 (SD 7.4)	3.62 (IQR 2.4-5.6)	0.1 - 39.3	119	0.161 (SD 0.260)
Id 3	6.52 (SD 9.1)	4.08 (IQR 1.8-6.7)	0.3 - 73.7	112	0.205 (SD 0.027)
Id 4	6.89 (SD 9.2)	3.49 (IQR 2.4-6.7)	0.1 - 53.8	108	0.186 (SD 0.028)
Id 5	6.18 (SD 7.9)	3.98 (IQR 2.4-6.0)	0.3 - 60.2	114	0.175 (SD 0.025)
Id 6	6.72 (SD 8.5)	3.97 (IQR 2.7-6.4)	0.1 - 61.3	106	0.222 (SD 0.029)
Id 7	7.16 (SD 9.4)	3.76 (IQR 2.3-6.3)	0.1 - 55.0	106	0.222 (SD 0.031)

NOTE- Analysis of homozygous segments was limited to 5 or more contiguous SNP in a tract. Hence, the minimum value presented for range represents shortest tract length of 5 contiguous SNP.

Table 3.1 Analysis of homozygosity tract lengths and Inbreeding Coefficients (*F*) per Individual. ID 1 and 2 are parents, and siblings 4, 5, 6, 7, and 8 are all affected.

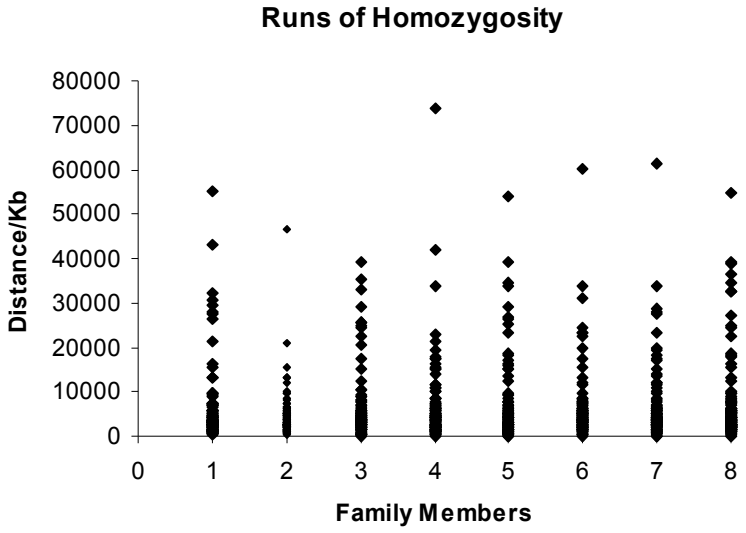

Graph 3.1 – Graph of homozygous tract lengths (ROHs) for each pedigree member. ID 1 and 2 are parents, and siblings 4, 5, 6, 7, and 8 are all affected. ROHs were limited to 5 or more contiguous SNP in a tract.

The total number of ROHs per individual (ROH count) ranged between 92 and 114, with the parents having lower counts than their children. These data are consistent with the estimated *F* values and indicate increased homozygosity in the offspring owing to inbreeding over many generations.

3.2.3 A genome-wide linkage scan performed on a second related sibship

A second nuclear family of the same inbred clan was identified with a high incidence of deafness. We hypothesised that a common disease factor(s) may be responsible for recessive hearing loss in both families. A high density genome-wide SNP scan performed on the second family revealed five HBD intervals situated on chromosomes 1p22-1q23, 7q21-q31, 8q12.1-12.3, 12p13.32-31, and 20q13. Table 3.2 lists HBD markers, the chromosomal and genomic location of SNPs defining each HBD locus, and strong candidate genes housed within HBD regions. These regions, however, do not overlap with the HBD loci detected in affected siblings from the first family.

The largest intervals, located on 1p22.2-1q23.1 and 7q21.11-q31.1, are not mass blocks of HBD but instead punctuated by intermittent non HBD-conforming markers, as illustrated in figures 3.3 and 3.4. Thus the region detected on chromosome 7q21.11-q31.1 has a total of 13 SNPs within 9 loci covering a region of approximately 25 Mb displaying the HBD pattern. A 'core' region with the most densely populated HBD markers is positioned from 105 Mb to 108 Mb and houses within the HBD loci two genes, *SLC26A4* and *SLC26A5*, causally associated with hereditary sensori-neural hearing loss (SNHL) (Li et al., 1998; Liu et al., 2003; Yoon et al., 2008).

Likewise, twelve HBD positive markers, located within 8 HBD loci, define the boundaries of a broad HBD interval spanning over 65 Mb on chromosome 1p22-1q23. Again, a core region would appear to be positioned between 117 Mb and 120 Mb although candidate genes are lacking in this region.

	SNPs		Localization (bp)		
Chromosome	**Start**	**End**	**Start**	**End**	**Genes**
1p22.2	rs954145	rs954145	89869842	90982574	
1p22.2	rs912794	rs912794	92087279	93467377	
1p13.2	rs1246194	rs1246194	112007914	112289357	*KCND3*
1p13.2	rs930548	rs930548	112289357	113049888	*KCND3*
1p13.1	rs998532	rs998532	117358754	118102273	
1p12	rs2064902	rs927208	119805842	120058236	
1q21.3	rs13320	rs13320	148559041	151269919	
1q23.1	rs857803	rs857819	156870624	157412932	
7q21.11	rs42002	rs42002	82484146	83568385	
7q21.11	rs764077	rs764077	83747016	86119134	
7q21.12-13	rs1468121	rs1468121	87451497	88629233	
7q21.2-3	rs9008	rs9008	90332855	92724748	
7q21.3	rs1859121	rs1053275	94569490	97269100	
7q22.1	rs11178	rs201492	100155234	103118180	*SLC26A5*
7q22.2	rs234	rs234	104617931	105622519	
7q22.2	rs1024761	rs1024761	105622519	106160139	
7q22.3-31.1	rs1476878	rs2028030	106160139	108677991	*SLC26A4*
8q12.1-12.3	rs1873104	rs997493	57984794	63031658	
12p13.32-31	rs617022	rs1558776	5081022	5618083	
20q13.13	rs911411	rs911411	47151838	47444415	
20q13.13	rs119416	rs119416	47469004	47511609	*KCNB1*

Table 3.2 HBD regions identified in the second related family. The chromosomal and genomic locations of SNPs defining each HBD locus are listed as are key candidate genes.

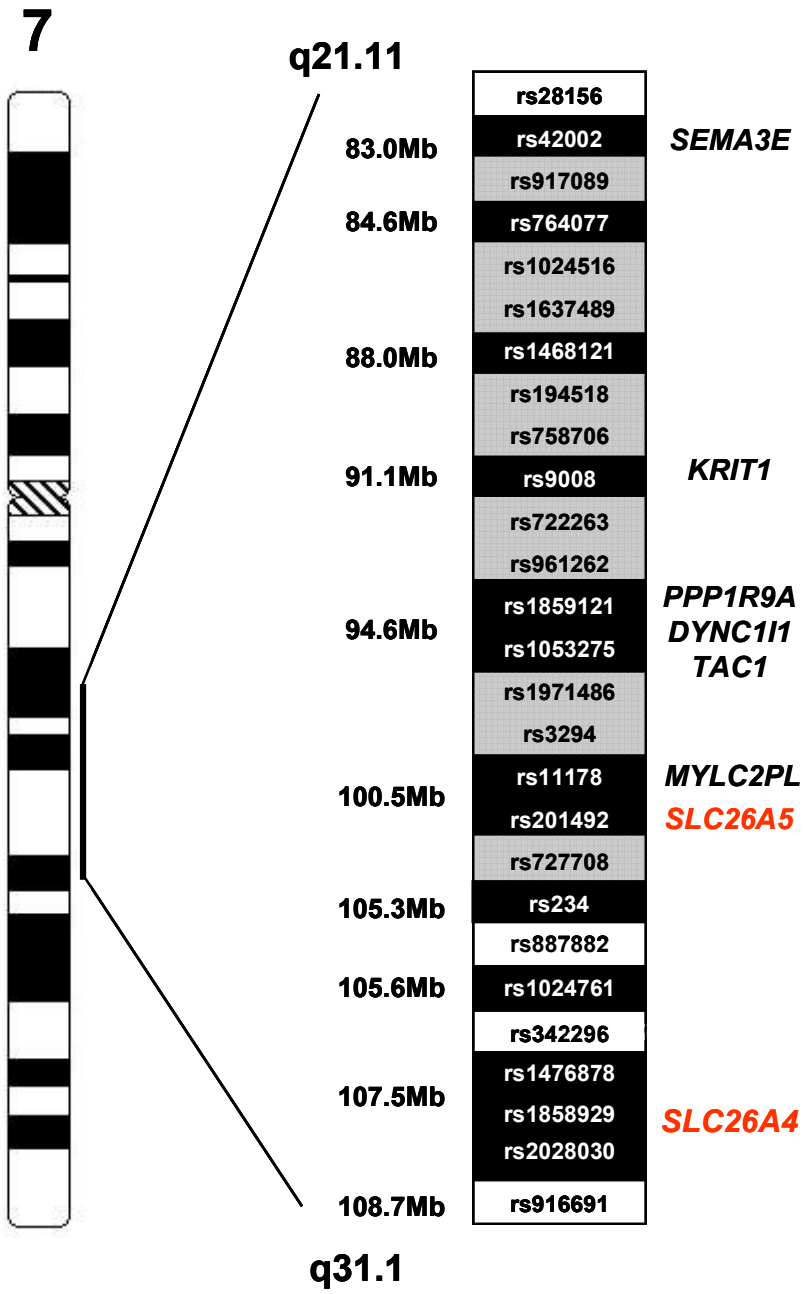

Figure 3.3 SNP markers identifying HBD loci on chromosome 7q21.11-q31.1. SNP markers homozygous in all affected deaf individuals are shaded black. Non-HBD markers shaded light grey denotes more than one SNP between HBD intervals. Non-HBD markers shaded white denotes only 1 SNP between HBD markers. Potential candidate genes are shown in black and genes previously identified to cause SNHL are in red.

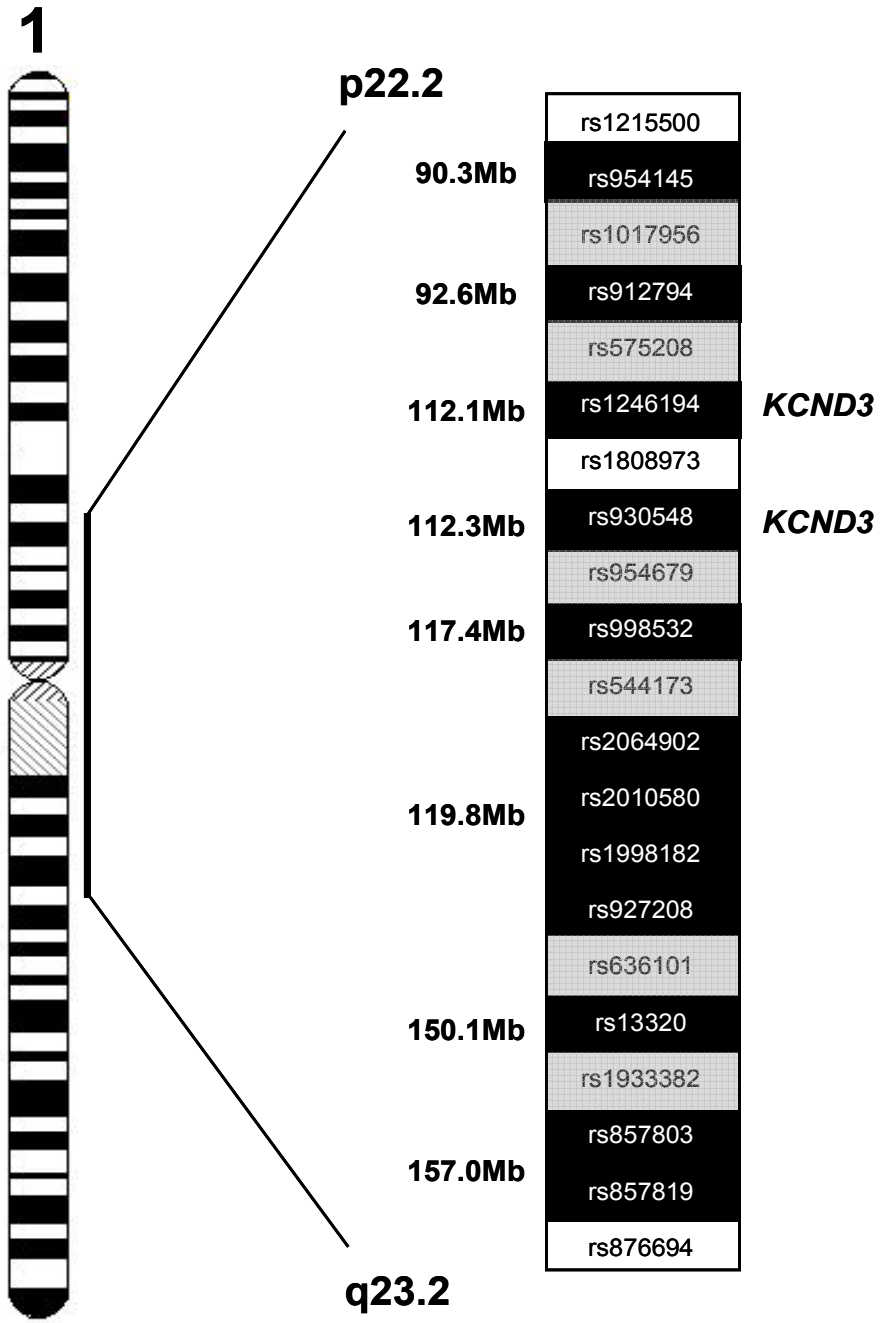

Figure 3.4 SNP markers identifying HBD loci on chromosome 1p22.2-q23.1. SNP markers homozygous in all affected deaf individuals are shaded black. Non-HBD markers shaded light grey denotes more than one SNP between HBD intervals. Non-HBD markers shaded white denotes only 1 SNP between HBD markers. The location of *KCND3*, a strong candidate gene, is indicated.

Conversely, HBD loci identified on chromosomes 8q12.1-12.3, 12p13.32-31, and 20q13 are more compact, each consisting of two HBD markers, and span smaller intervals of approximately 5-6Mb (8q12.and 12p13) and 800 kb (20q13).

3.3 Discussion

This chapter reports the mapping of two putative loci on chromosome 22q13 and 2p24-25 for a rare combination of schizophrenia, sensori-neural hearing impairment and epilepsy present in five out of six offspring of first cousin parents. A second genome-wide scan performed on a family belonging to the same kinship and in which five out of the seven offspring present with hearing loss, resulted in the mapping of HBD loci on chromosomes 1p22.2-1q23.1, 7q21-q31.1, 8q12, 12p13 and 20q13.

The consanguineous parents of the first family have estimated inbreeding coefficients higher than expected for offspring of first cousins (6%), while the average value for the offspring (19%) is greater than that predicted for double first cousins (12.5%). These values, although very high, are still within the range of estimates (5%-20%) reported for offspring of first cousin marriages of Pakistani and Arabian descent (Woods et al., 2006) and are in keeping with our knowledge that, historically, marriages within this family have been restricted to a small group of individuals from a small geographical region.

Detailed analysis of genome-wide ROHs revealed that the longest tracts in the present study range between 40 and 73 Mb. In contrast, the maximum ROH length as calculated in a high density SNP scan of outbred HapMap populations was found to range between 2.63 Mb (Chinese population [CHB]) and 17.91 (Japanese population [JPT]) (Gibson et al., 2006). Average ROH counts estimated by the authors varied between 4.4 and 8.4 depending on the outbred population (Gibson et al., 2006). A higher mean value of 35.9 counts per subject was estimated in a second high density SNP scan of individuals with European ancestry (Curtis et al., 2008). In the present study family counts were much higher ~100 runs, suggesting more tracts and longer runs of homozygosity consistent

with inbreeding effects. However, the measure of a 'ROH' differs between the studies with the criteria in both the outbred population SNP scans were stricter than in the present study (i.e a ROH being 10 or more contiguous SNPs as opposed to 5 contiguous SNPs used here). Therefore the counts estimated in the present study may be inflated due to the inclusion criteria.

In the aforementioned study of 48 affected individuals with diverse autosomal recessive diseases born of first cousin marriages and of Pakistani and Arabian descent, an average 20 homozygous segments exceeding 3 cM in size and an average tract size of 19.5 cM per affected person was estimated (Woods et al., 2004). The present data yields estimates of an average tract size for offspring of ~ 6.58 ± 0.44 Mb and an average tract count 111± 5(SEM). Assuming parity between cM and Mb, this would suggest a five-fold greater number of tracts that are, on average, a fifth of the size of that reported by Woods et al.- a difference which may reflect more remote ancestry through additional ancestral inbreeding loops in this family.

In this study we have carried out analysis based on a recessive model assuming this is to be a single rare phenotype that includes features of hearing loss, epilepsy and schizophrenia. A link between deafness and schizophrenia has been described in the literature, particularly in old age (Cooper, 1976). However, it is unlikely that the schizophrenia phenotype in the family is a direct result of deafness as the onset is early and the symptoms of psychosis are episodic with good recovery between episodes. Furthermore, we argue that mutations in one or more genes located in the identified HBD regions interact with environmental or other genetic factors, giving rise to the variable penetrance/expressivity of clinical features. Nevertheless, other modes of inheritance should be considered. For example, dominant inheritance with variable penetrance and mitochondrial inheritance which indeed can give rise to phenotypic manifestations similar to that of this family (e.g. MELAS and MERRF disorders) (Simon and Johns, 1999). However, the existence of inbreeding and the lack of cases

identified with the phenotype from the same region in Punjab do not support these alternative models.

Deletions and duplications can disturb the expected patterns of marker genotypes within pedigrees. A common deleted segment on one chromosome in both parents would result in missing genotype data in all siblings that inherit this deletion (i.e. null genotypes). Likewise, apparent SNP genotyping failures may indicate commonly inherited duplicated regions (Redon et al., 2006). SNP marker analysis did not reveal any single SNP or regions of missing data in affected siblings from either family, nor were there any Mendelian inconsistencies identified at the resolution of our marker density (~480 kb). Therefore, although the phenotype is consistent with a contiguous gene syndrome, no gross duplications or deletions are evident.

The lack of overlap of HBD regions in affected individuals from both sibships disproves our hypothesis that a common disease factor(s) may be responsible for recessive hearing loss in both families. However, a similar finding has been reported in the mapping of Bardet-Biedl syndrome (BBS) loci investigated in a large extended consanguineous Lebanese pedigree. In this family, two loci and subsequently identified disease-causing genes corresponding to the same clinical phenotype were found to segregate in different branches of the extended family. The authors concluded that owing to the high nonallelic heterogeneity and increased cumulative prevalence of BBS in inbred populations (similar to non-syndromic hearing loss), it was unsurprising that mutations in two different causal genes were segregating and should, by exemplar, emphasise a possible 'pitfall' of homozygosity mapping in extended kinships (Laurier et al., 2006).

Another limitation of homozygosity mapping, as for linkage studies of small families, is that it detects large disease intervals that may house hundreds of genes. Although fine mapping or previous linkage reported in other families may reduce the size of the putative interval, the overall aim of such studies, gene identification, is dependent on examining functional candidate genes in the region. With regard to hereditary sensori-

neural hearing loss (SNHL), the recently documented *DFNB47* locus is linked to autosomal recessive hearing impairment and maps to a 5.3 Mb sized region on 2p24.3-25.1 (Hassan et al., 2006). Of interest, the maximum LOD score of 4.7 is reported for markers D2S1400 and D2S262, both of which are located within our chromosome 2 HBD region. The two large pedigrees segregating this locus live in Pakistan but are geographically distant from the family described and there is no suggestion that the families will be related. As in the current study, the candidate gene, *KCNF1*, was screened in affected individuals in these two large kindreds and the results were also negative.

A second locus linked to autosomal recessive SNHL maps to 22q13.1. *DFNB28* was mapped in a large consanguineous Palestinian family, in addition to smaller consanguineous families from Pakistan, Indian and America (Walsh TD, 2000; Riazuddin et al., 2006; Shahin et al., 2006). Subsequently, causative mutant alleles have been identified in the gene *TRIOBP* encoding for a protein which has a role in actin cytoskeletal organization in cochlear sensory hair cells of the inner ear. The interval containing *TRIOBP* (36.5 Mb) is located between HBD loci identified in the present family in a region where SNPs were not typed. Hence, it is possible that this location is HBD and that mutant alleles within *TRIOBP* are carried in affected offspring.

The large regions on 7q21-q31 and 1p22.2-1q23.1 homozygous in affected siblings of the second related family presenting with hearing loss also house five autosomal recessive SNHL loci. *DFNB39* located on 7q11.22-q21.12 was found to segregate in a consanguineous family from Pakistan (Wajid et al., 2003). However, as yet no causative mutations have been identified. *DFNB4*, *DFNB14*, and *DFNB17* housed within 7q31.1 were mapped in consanguineous families from India, Israel and Lebanon (Baldwin et al., 1995; Greinwald et al., 1998; Li et al., 1998; Mustapha et al., 1998). Mutations in the gene *SLC26A4* encoding a sodium-independent transporter of chloride and iodide and known to cause Pendred syndrome (a congenital sensorineural hearing loss syndrome) were reported to segregate in one family but are absent in individuals from other hearing

loss pedigrees (Li et al., 1998; Yoon et al., 2008). However, a splice variant in a second and neighbouring gene, *SLC26A5,* which encodes a membrane motor protein of cochlear outer hair cells, was found to be responsible for recessive deafness in two unrelated families (Liu et al., 2003). As stated earlier these genes, both known to cause hearing loss, are positioned within smaller HBD loci on chromosome 7q22.

Likewise, *DFNB32* linked to autosomal recessive SNHL maps to 1p13.3-p22.1 and is located within the broader HBD region on chromosome chr1 p22.2-q23.1 (Masmoudi et al., 2003). Currently the *DFNB32* gene has not been identified. Nevertheless, a key candidate, *KCND3* (encoding a voltage-gated potassium channel) is positioned distal to the *DFNB32* locus but within two intermittent HBD loci detected in this present family. As the other HBD loci identified in this second sibship (8q12, 12p13 and 20q13) do not house SNHL-linked loci, chromosome 7q21.1-q31.1. and 1p22.2-q23.1 are the key candidate intervals on which to focus re-sequencing efforts with the aim of discovering causative mutations associated with recessive hearing loss within this family.

Findings from linkage studies provide strong evidence that a single major gene on chromosome 22q12 is responsible for an idiopathic epilepsy syndrome. Familial partial epilepsy syndrome with variable loci (FPEVL), an autosomal dominant and clinically heterogeneous condition, was initially mapped in two large French-Canadian pedigrees to a ~4 Mb interval on chr 22q11-q12 (Xiong et al., 1999). Two preceding studies confirmed linkage for FPEVL in Dutch, Spanish and French-Canadian pedigrees reporting a combined LOD score of 6.3 for the Spanish and three French-Canadian pedigrees (Callenbach et al., 2003) (Berkovic et al., 2004). Of note, members of these pedigrees are reported to have psychiatric problems including the diagnosis of paranoid schizophrenia. Although not overlapping with the present study's disease interval on 22q13, the most telomeric region of the FPEVL locus is just ~4 MB from our HBD region.

Epidemiological and clinical characteristics common to schizophrenia and bipolar disorder suggest the two disorders share genetic and non-genetic susceptibility factors (Berrettini, 2000). Over the last decade converging evidence from independent studies strongly implicates chromosome 22q as a candidate region for susceptibility genes for these disorders. Positive findings, as reported in 1999, cluster in a region of 4-5cM on 22q13.1, an interval mapping directly to our 'core' region between markers D22S284 and D22S270 (Schwab and Wildenauer, 1999). More recent linkage analysis of markers on 22q for schizophrenia and bipolar disorder fulfils the criteria of suggestive or significant linkage implicating a broad genomic region spanning 22q12.3-q13.3 that coincides with the findings of the present study. For example, linkage found at markers D22S1161 and D22S922 (P = 0.0081) 22q13.3 for bipolar disorder and D22S279 and D22S276 (P =0.0075) 22q13.2 for schizophrenia in pedigrees from the Faroe Islands (Jorgensen et al., 2002). DeLisi and coworkers also report a LOD score of 2.0 at marker D22S283 (22q12.3) in a genome-wide scan of 382 sib pairs with schizophrenia and schizoaffective disorder. Moreover, two studies have found linkage with markers in bipolar families in the region of 22q12.3: [D22S277 non parametric score 0.003 and D22S278 a Max LOD 3.1] (Kelsoe et al., 2001; DeLisi et al., 2002).

Furthermore, the high incidence of identified deletions located within 22q13.12 to 22qter in individuals with similar clinical phenotypes has led to the recognition of a separate condition known as 'chromosome 22q13 deletion syndrome' (also known as Phelan-McDermic Syndrome). In addition to the main clinical characteristics, delayed development and learning disability, secondary features commonly described are behavioural problems including autistic-like traits and seizures (Phelan et al., 2001). Consistent with this syndrome are singular reports of individuals with cytogenetic abnormalities, e.g. inverted duplications, shown to disrupt intervals along chromosome 22q13. Of relevance, the main clinical manifestations often described for these individuals are severe psychiatric abnormalities (i.e. a diagnosis of BPD, schizophrenia or psychosis) and delayed development (Failla et al., 2007; Pramparo et al., 2008).

Homozygosity mapping is a technique which has been used successfully to identify recessive genetic risk factors for a variety of clinical phenotypes. In a recent study performed by Paisan-Ruiz and colleagues, consanguineous families from India and Pakistan presenting with recessive dystonia-parkinsonism (which includes psychiatric features) were genome-wide screened for shared HBD intervals. Interestingly, homozygosity on chromosome 22q13 was found to be shared by affected members from three families and consequently mutations in the gene *PLA2G6* were identified (Paisan-Ruiz et al., 2008). The reported shared HBD region overlaps with intermittent HBD intervals detected in the present study. This hints at the possibility that the chr22q13 region may commonly be homozygous in individuals from the Indian/Pakistan population with shared recent ancestry, and that mutated recessive alleles in genes harboured within this interval may cause or be risk factor for an assortment of clinical disorders.

The screening of the promoter and coding regions of *ATF4, GPR24* and *CACNG2* did not reveal any apparent mutations in affected family members. It is still possible that mutations in intronic regulatory regions of these genes underlie this recessive disease. Furthermore, several alternative candidate genes for this specific phenotype are located on chromosome 22q13. For example, *ADSL* encodes the protein adenylsuccinate lyase, a deficiency in which causes a selectively neuronopathic disorder with psychomotor retardation, epilepsy and autistic-like features as leading traits (Race et al., 2000). Moreover *ADSL*, was a second gene along with *GPR24,* significantly associated with both SZ and BPD in Scottish and Faeroe Island disease populations (Severinsen et al., 2006a; Severinsen et al., 2006b). Mutation screening of these and other promising candidate genes within 22q12-3-13.3 and 2p24.3-25.1 may lead to the discovery of causative mutations associated with this rare phenotype.

CHAPTER 4

INVESTIGATION OF A COMPLEX CHROMOSOMAL ABNORMALITY AND THE DISRUPTED BREAKPOINT GENE *ABCA13*

ACKNOWLEDGEMENTS FOR CHAPTER 4

Clinical data was collected by Douglas Blackwood and Walter Muir. The database of sample information was managed by Margaret van Beck. The Lothian Birth Cohort control samples were kindly provided by Ian Deary and colleagues. The sequencing of exons encoding the TMDs in 100 cases and 100 controls was performed by Alan Maclean. TaqMan assays were performed by Alison Condie, Angie Fawkes, Angela White and William Hawkes at the Wellcome Trust Clinical research facility (WT-CRF).

Sequence analysis and a structural model of the T4031A variant was performed by Dinesh Soares. In silico predictions of the functional/pathological consequences of the newly identified non-synonymous variants were performed by Ben Pickard. CNV screening using BAC arrays was performed by Gloria Tam, Thomas Fitzgerald and Richard Redon at the Sanger institute, Cambridge. Linkage analysis was conducted by Douglas Blackwood and statistical analysis of the replication genotype data was performed by Allan McRae and Peter Visscher.

4. INVESTIGATION OF A COMPLEX CHROMOSOMAL ABNORMALITY AND THE DISRUPTED BREAKPOINT GENE *ABCA13*

4.1 Preface

A complex chromosomal rearrangement was previously identified in a patient with severe and chronic schizophrenia. The three breakpoints were positioned within the regions of 7q21.11, 7p12.3 and 8p23. The breakpoint interval on 7q21.11 houses no potential candidate genes whereas the locus on 7p12.3 directly disrupts the gene, *ABCA13*. To determine if *ABCA13* is the only gene disrupted, and to locate the precise breakpoint within *ABCA13*, the breakpoint regions on chromosomes 8p and 7p were further analyzed by Fluorescence in situ Hybridisation (FISH).

4.2 Results

4.2.1 Fine mapping breakpoint regions on chromosome 8p and 7p

Cloned bacterial artificial chromosome (BAC) RP11-18L2 located on 8p23.1 was found to translocate to the derived chromosome 7. This indicated that the breakpoint was proximal to the *defensin* gene cluster region (8p23.2) previously suspected as the breakpoint locus. Systematic FISH analysis of BACs and fosmids located downstream of this area identified BACs RP11-429B7 and RP11-179A8 and fosmid G248P87290G10 as giving a signature 'split hybridization signal', i.e. translocating to the derived 7 as well as remaining on the derived chromosome 8. A FISH image of the breakpoint fosmid G248P87290G10 is shown in figure 4.1 These clones indicate that the breakpoint region on chromosome 8p23.1 does not directly disrupt any genes. However, *PPP1R3B* (NM_024607) a gene which encodes for a protein phosphatase 1 subunit, and *THEX1* (NM_153332) encoding a RNA exonuclease, lie approximately 8 kB centomeric and 4 kB telomeric, respectively, from the breakpoint locus, as illustrated in figure 4.2.

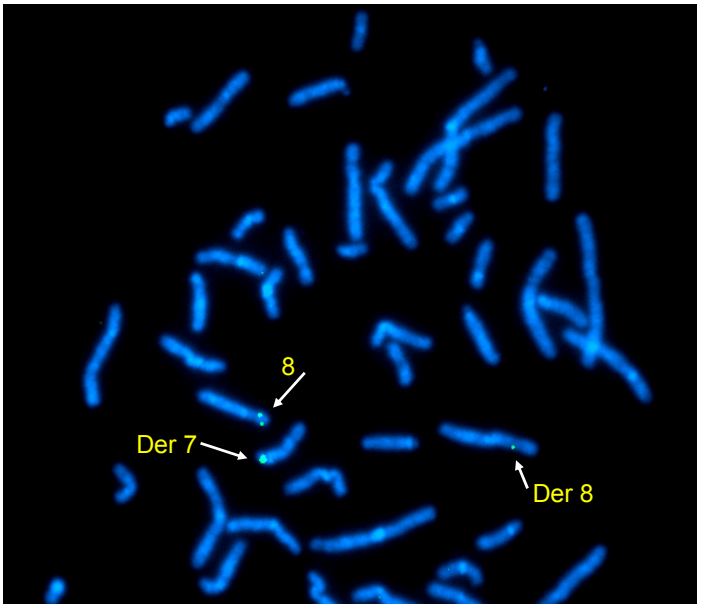

Figure 4.1 The breakpoint-spanning fosmid G248P87290G10 on chromosome 8. In the individual with the complex cytogenetic abnormality, this breakpoint-spanning fosmid shows three signals (green fluorescence) located on the derived chromosomes 8p, 7q and normal 8p.

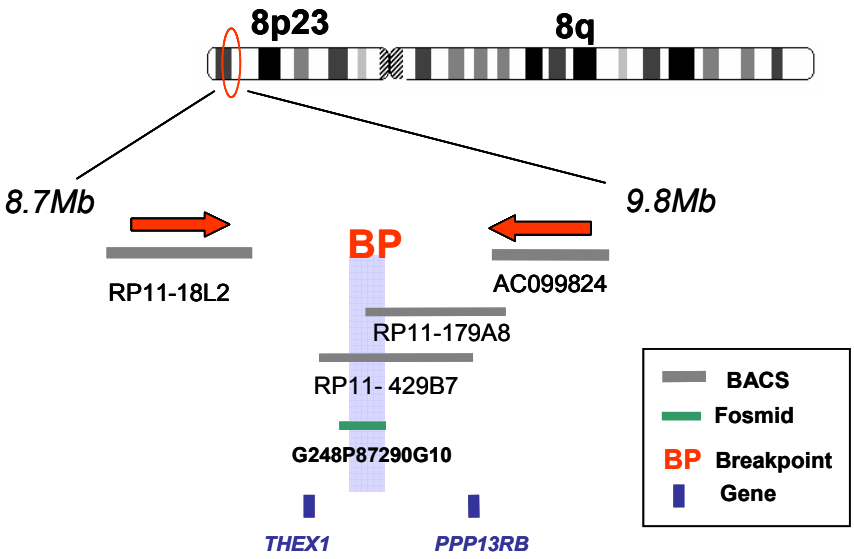

Figure 4.2 BACs and fosmids used to define the breakpoint on chromosome 8p23.1. The genes *PPP1R3B* and *THEX1* are indicated in blue.

Cytogenetic mapping of the region previously identified on chromosome 7p12.3 indicated that two fosmids were broken, G248P8188G7 and G248P85542D8 (G248P8188G7 shown in figure 4.3) Moreover, the breakpoint locus was found to be between fosmids G248P82942G4 and G248P87241B7 which would indicate disruption of *ABCA13* in the vicinity of exons 30 and 31, as illustrated in figure 4.4. This disruption is predicted to result in a truncated transcript which is likely to be degraded due to nonsense-mediated decay mechanisms. All breakpoint-defining BAC and fosmid clones and their cytogenetic and physical location are listed in table 4.1

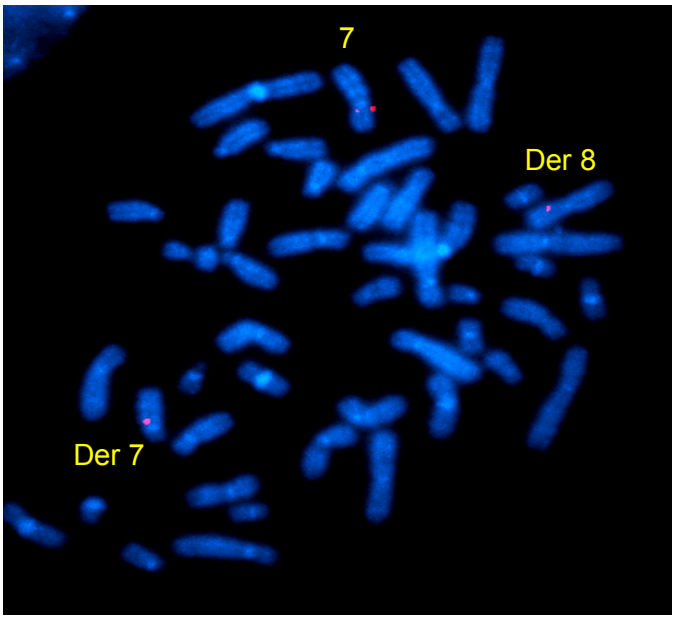

Figure 4.3 Breakpoint fosmid 188G7 on chromosome 7. Three signals (red fluorescence) are detected on the derived chromosomes 7 and 8 and normal 7 in the patient with the cytogenetic abnormality.

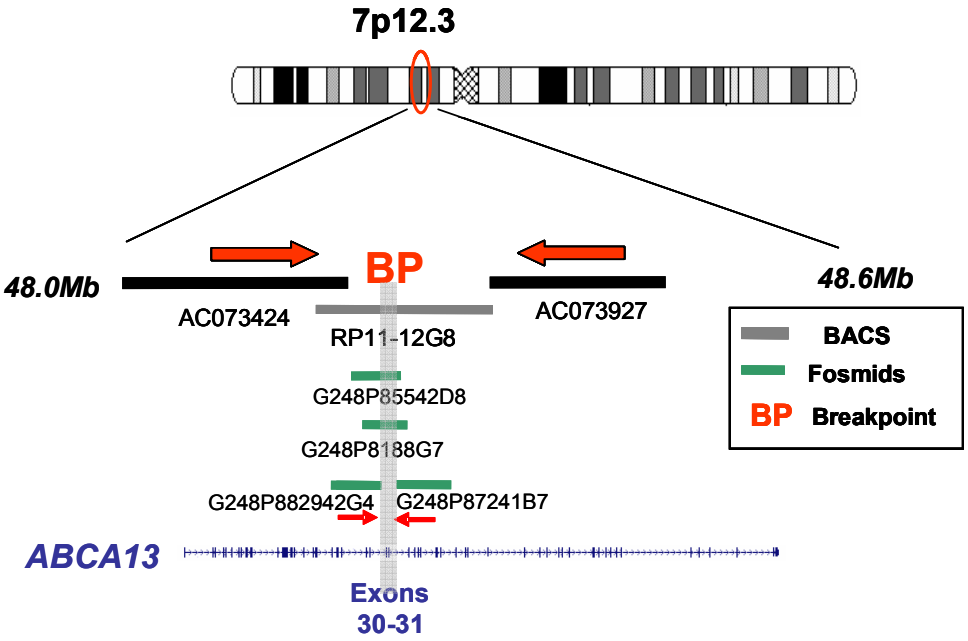

Figure 4.4 BACs and fosmids used to define the breakpoint on chromosome 7p12.3. The breakpoint is positioned between fosmids G248P82942G4 and G248P87241B7 in the vicinity of exons 30 and 31.

Cytogenetic Position	Breakpoint BAC clone	Breakpoint fosmid clone
8p23.1	RP11-429B7	
8p23.1		G248P87290G10
7p12.3	RP11-12G8	
7p12.3		G248P8188G7
7p12.3		G248P85542D8
7q21.11	AC092444	

Table 4.1 Summary of identified breakpoint BAC and fosmid clones

4.2.2 Re-sequencing exons of the *ABCA13* gene encoding functional domains in cases of schizophrenia and controls

The *ABCA13* locus has not previously been associated with psychiatric disorders. We therefore hypothesized that *ABCA13* might make a wider contribution to psychiatric illness through rare, moderate- to high-penetrance variants identifiable in the population only through direct mutation detection. Nineteen key exons (from a total of 62) encoding the two nucleotide binding domains (NBDs), two transmembrane domain clusters (TMDs) and a hydrophobic dipping region (HDR) were amplified using genomic DNA PCR and then re-sequenced in 100 unrelated cases diagnosed with schizophrenia of both sporadic and familial origin. In addition, 100 matched healthy controls were also screened to assess the frequency of ultra-rare benign variants in the general population. A total of thirty-two new variants were identified, 20 within coding regions and 12 within flanking intronic sequences as listed in table 4.2. The majority of novel non-synonymous variants (resulting in amino acid substitutions and hence having potential functional significance) were unique to the case population, whereas synonymous or intronic variants not affecting amino acid sequence showed no such bias as indicated in table 4.3.

To assess the distribution of potential mutations in both the general population and across three major psychiatric illnesses, bespoke TaqMan assays were used to genotype selected, highly conserved, non-synonymous coding variants in much larger genomic DNA sample cohorts of patients with schizophrenia, bipolar disorder, and major depression as well as healthy controls. The case cohorts used was not biased towards individuals with a strong family history. Further evidence that these potential rare mutations are significantly associated with illness was sought by conducting family segregation analysis. Based on these assessments, that is, variant frequency differences between cases and controls, co-segregation of variants with illness in extended families and evolutionary conservation of the mutated residues; I postulate that nine of these variants are potentially pathogenic (discussed in section 4.2.2.4).

Domain	Chr7 location bp NCBI Build 36.1	Base change	AA change	Type	MAF cases	MAF controls
TMD1	48,382,318	G→A	**R3604Q**	missense	A: 0.0050	A: 0.0000
TMD1	48,382,333	A→C	**H3609P**	missense	C: 0.0050	C: 0.0000
TMD1	48,382,337	A→C	P3610P	synonymous	C: 0.0096	C: 0.0000
TMD1	48,382,337	A→T	P3610P	synonymous	T: 0.0048	T: 0.0037
TMD1	48,382,619	T→G	**S3704R**	missense/splice variant	G: 0.0050	G: 0.0000
TMD1	48,384,364	C→T		intronic	T: 0.0095	T: 0.0160
TMD1	48,384,474	A→G		intronic	G: 0.0045	G: 0.0000
TMD1	48,384,623	T→C		intronic	C: 0.0048	C: 0.0053
TMD1	48,398,156	G→A		intronic	A: 0.0523	nd
TMD1	48,398,232	G→C		intronic	C: 0.0048	nd
NBD1	48,399,292	C→G	L3861L	synonymous	G: 0.0000	G: 0.0052
NBD1	48,399,322	T→C	T3871T	synonymous	C: 0.0000	C: 0.0052
NBD1	48,413,738	C→T		intronic	T: 0.0092	nd
NBD1	48,420,643	C→T		intronic	T: 0.1651	T: 0.2067
NBD1	48,420,683	A→G	**T4031A**	missense	G: 0.0050	G: 0.0000
NBD1	48,420,731	C→G	L4047V	missense	G: 0.0169	G: 0.0104
NBD1	48,420,834	C→G		intronic	G: 0.1651	G: 0.2067
HDR	48,465,394	T→C	P4260P	synonymous	C: 0.0000	C: 0.0052
HDR	48,465,399	A→G	**H4262R**	missense	G: 0.0050	G: 0.0000
TMD2	48,518,027	C→T	R4454C	missense	T: 0.0142	T: 0.0156
TMD2	48,518,057	C→A	L4464M	missense	A: 0.0095	A: 0.0208
TMD2	48,526,874	A→G	**T4550A**	missense	A: 0.0050	A: 0.0000
TMD2	48,526,994	C→T	**R4590W**	missense	T: 0.0000	T: 0.0050
TMD2	48,527,112	C→G		intronic	G: 0.0286	G: 0.0161
TMD2	48,530,327	C→G	P4648A	missense	G: 0.0000:	G: 0.0050
NBD2	48,534,459	A→G	R4707R	synonymous	G: 0.0500	G: 0.0526
NBD2	48,534,520	C→T	**R4728X**	nonsense	T: 0.0050	T: 0.000
NBD2	48,538,544	C→T		intronic	T: 0.0000	T: 0.0153
NBD2	48,538,545	C→T		intronic	T: 0.0000	T: 0.0052
NBD2	48,597,311	A→G	**I4841V**	missense	G: 0.0040	G: 0.0000
NBD2	48,597,317	C→T	**R4843C**	missense	T: 0.0000	T: 0.0050
NBD2	48,604,841	C→A		intronic	A: 0.0519	A: 0.0789

MAF cases and controls calculated from discovery resequencing data.
Genomic position based on NCBI build 36.1. AA, amino acid; MAF, minor allele frequency;
NBD, nucleotide binding domain; TMD, transmembrane domain, HDR, hydrophobic dipping region.

Table 4.2 Novel variants identified from re-sequencing 100 cases with schizophrenia and 100 healthy controls. The functional domain, genomic location, base and amino acid change, type of variant and minor allele frequencies are listed.

	Case specific	Shared	Control specific
non synonomous	8	3	3
synonomous	1	2	3
Intronic	1	6	2

Table 4.3 The frequency of novel variants in cases, controls or both populations. A bias in the number of novel non-synonymous variants unique to the case population is evident. Data for three intronic variants were not obtained for the control population and these are therefore not included.

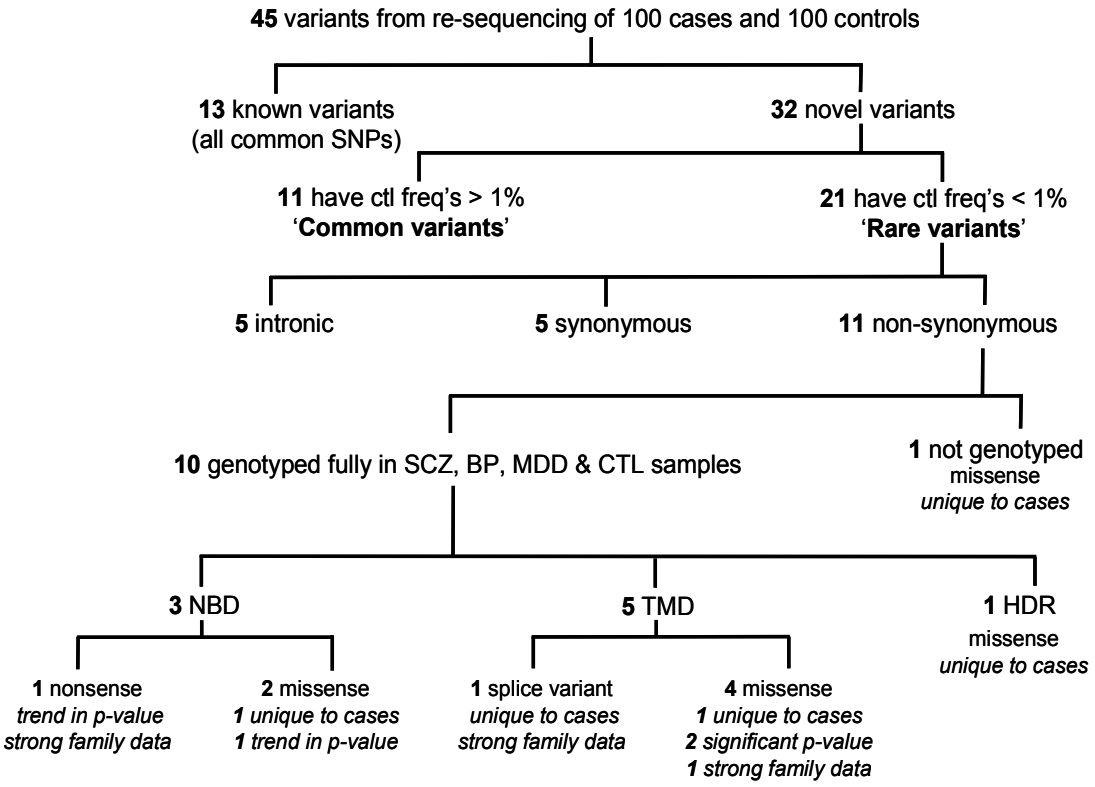

Figure 4.5 Flow chart of findings initiated from the screening of exons encoding the functional domains of *ABCA13*. The chart outlines the strategy and results used to assess potential pathogenic nature of variants.

Figure 4.5 presents a flow chart as a means to visualise the mutation detection strategy and results. The ensuing sections present the results in order of variant class.

4.2.2.1 Analysis of Known SNPs

In addition to the 32 novel variants, thirteen known SNPs were detected in the screened case and control populations. As shown in table 4.4, the MAFs estimated for these variants range between 0.05 (5%) to 0.47 (47%) in the control population, indicating that these variants fall into the class of common polymorphisms. Furthermore, none showed a statistically significant difference in genotype or allele frequencies between the case and control cohorts.

4.2.2.2 Novel intronic and synonymous variants

Twelve novel intronic variants and six novel synonymous (silent) variants were identified from re-sequencing. Five of the 12 intronic variants have MAFs lower than 1% in the case populations and hence can be classified as rare. Data for the control population was not obtained for three intronic variants and 2 variants were found unique to controls and 1 unique to cases. The difference in minor allele frequencies (MAF) between cases and controls was not found to be significant for the remaining 6 intronic variants. Nor was there any evidence supporting that any of these variants may disrupt splice motif sequences.

Recent theoretical studies suggest that silent mutations, i.e. synonymous variants, which involve the substitution of a common codon for a rare codon, may affect the kinetics of translation and hence co-translational folding processes and ultimately efficacy of protein function (Karlin and Mrazek, 1996; Supek and Vlahovicek, 2005; Kimchi-Sarfaty et al., 2007). Of the 6 novel silent mutations detected, four (P3610P, L3861L, T3871T, P4260P) were found to be unique to either the case or control populations (shown in table 4.2). However, the difference in allele frequencies between cases and controls is not statistically significant and none of the base changes introduce a rare

codon. Taken together, this evidence would suggest that these synonymous silent variants are not pathogenic.

4.2.2.3 Novel non synonymous variants discounted as pathogenic

Three non-synonymous variants located within the second transmembrane domain, were identified but subsequently discounted as potentially pathogenic. A non-conservative substitution from a highly conserved arginine to cysteine (R4454C) located within a loop of the second TMD, was detected in 3 cases and 3 control individuals. Consistent with this apparent lack of bias between case and control groups, R4454C was found not to segregate with illness in a large family with schizoaffective disorder, bipolar disorder and MDD, as shown in figure 4.6. Similarly, two conservative amino acid substitutions, L4464M and L4047V, were detected in 2 cases and 4 controls, and 4 cases and 2 controls, respectively. All three of these variants have an allele frequency above 1% in the control population (table 4.2) and are likely neutral polymorphisms.

4.2.2.4 The detection of potentially pathogenic variants.

Eleven non-synonymous variants were detected in the screening phase with MAFs lower than 1%. However, two of the eleven variants (P4648A and I4841V) both conservative substitutions, are of unknown pathogenic status. P4648A positioned in a transmembrane loop of the second TMD, was detected in the heterozygous state in one control individual. This residue change is conservative and genotyping larger case and control cohorts did not identify any additional carriers. Hence it is likely that P4648A is an ultra-rare benign variant. The second variant, I4841V, results in a conservative substitution from isoleucine to valine positioned within the second NBD. This variant was detected in the heterozygous state in an individual identified as a T4031A carrier (T4031A discussed below).

Domain	SNP	Base change	AA change	Type	MAF seq.cases	MAF seq.controls	MAF controls†
TMD1	rs1526093	A→G		intronic	G 0.176	G 0.158	G 0.132
NBD1	rs17132289	A→T	Y3796F	nonsynonymous	T 0.047	T 0.073	T 0.083
NBD1	rs7780299	C→T		intronic	T 0.110	T 0.120	nd
NBD1	rs 6978753	G→A		intronic	A 0.385	A 0.385	A 0.438
NBD1	rs17548783	C→T	A4037A	synonymous	C 0.459	T 0.476	C 0.442
TMD2	ENSSNP7713259	A→G		intronic	G 0.032	G 0.052	nd
TMD2	ENSSNP13252658	G→A	K4609K	synonymous	A 0.032	A 0.052	nd
TMD2	ENSSNP13252659	C→T	C4619C	synonymous	T 0.032	T 0.052	nd
TMD2	rs34364517	A→G		intronic	G 0.032	G 0.052	nd
NBD2	rs1316349	G→T		intronic	T 0.058	T 0.071	T 0.092
NBD2	rs7778411	G→C		intronic	C 0.298	C 0.342	C 0.264
NBD2	rs10243913	G→A		intronic	A 0.399	nd	nd
NBD2	rs10046546	A→G		intronic	G 0.316	nd	nd

MAF cases and controls calculated from resequencing 100 schizophrenics and controls; nd = no data;

† denotes data obtained from either HapMap or Perlegen data bases

Table 4.4 Known SNPs detected from the sequencing of case and control populations. The MAF calculated for the sequenced case and control cohorts is listed. The final column presents data pertaining to control individuals obtained from either the HapMap or Perlegen databases. No significant differences between frequencies for cases and controls were found

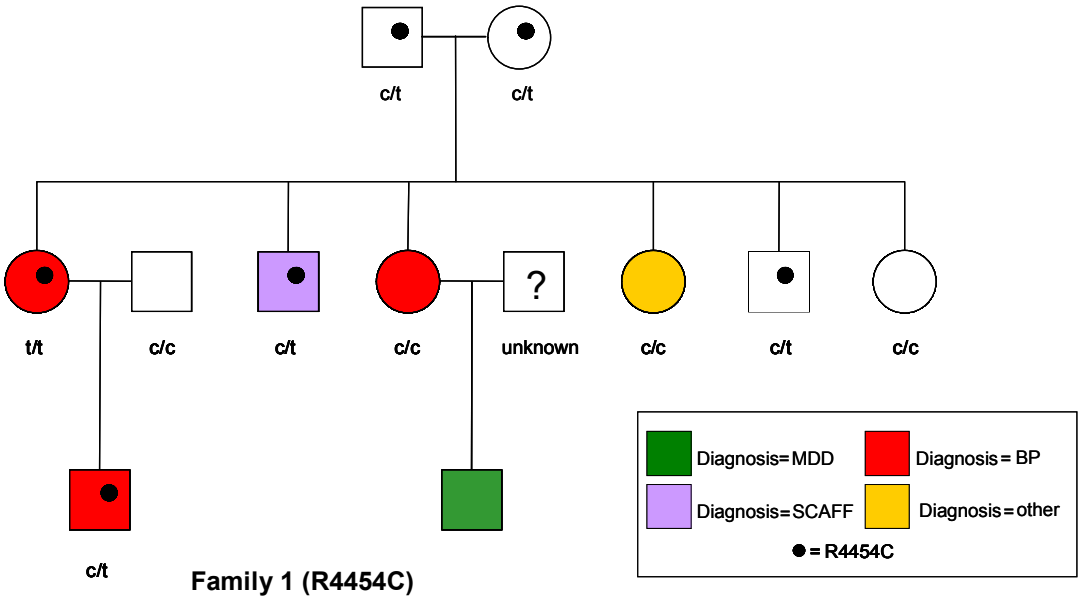

Figure 4.6 Family pedigree carrying the TMD2 non-synonymous variant R4454C. The T allele is the mutant allele and does not segregate with illness. 'Unknown' denotes unknown phenotype and '?' represents unknown genotype.

As the base change for I4841V in exon 57 (NBD2) and for T4031A in exon 40 (NBD1) are located within two different LD blocks, these variants are not in high LD with one another. I4841V was not found in any other control or case sequenced, and so its status as a potential risk variant or benign ultra-rare polymorphism is unknown.

The investigation of the remaining nine non-synonymous variants identified by screening has provided evidence that these variants are disease liability factors. The details of the nine variants are provided in table 4.5 and discussed in succession below.

Mutation 1: T4031A

The missense mutation T4031A, a non-conservative change of a phylogenetically conserved threonine residue to alanine in the first nucleotide binding domain, was identified in the heterozygous state in one individual with schizophrenia. The presence of this variant was confirmed by cloning the PCR product followed by sequencing as shown in figure 4.7a.

The frequency of the T4031A mutation was determined by genotyping DNA from cases of schizophrenia, bipolar disorder and MDD as well as two healthy control groups. A total of 1 case with schizophrenia and 3 cases with bipolar disorder in a total case population of 2208 samples were found to be heterozygous. In contrast, this variant was absent in 2362 control individuals assayed. Therefore the minor allele frequencies (MAF) for T4031A is 0.009 combined cases and 0.000 controls resulting in a p-value of P=0.052, [or P=0.1 replication data only] (Fisher's exact test, one-tailed) which demonstrates a trend towards significance. An estimation of the strength of the effect of a genetic variant on the disease phenotype is often expressed as an odds ratio (OR), i.e. the ratio of the odds of manifesting the disease in carriers of the risk allele to the odds of manifesting the disease in noncarriers. Due to an absence of this variant in the control populations, the OR for this mutation is calculated as infinity.

Table 4.5 Putative pathogenic variants identified from the initial screening of the *ABCA13* gene and subsequent genotyping in larger cohorts of cases and controls

Variant	Domain	Exon	Genomic position	Base change	Conservation AA	AA change	Type	No. total cases	Phenotype	No. controls	Allele freq. cases	Allele freq. controls	P-value	Odds Ratio (95% CI)
1	NBD1	40	48,420,683	A→G	RH, D, R, M, Ch	T4031A	missense	4 (2162)	1/1119 SCZ, 3/678 BP, 0/365 MDD	0 (2362)	0.0009	0.0000	0.052	infinity
2	NBD2	54	48,534,520	C→T	RH, D, R, M, Ch	R4728X	nonsense	11 (2158)	5/1104 SCZ , 5/680 BP,1/374 MDD	5 (2370)	0.0025	0.0010	0.076	2.4 (0.8-7.0)
3	NBD2	57	48,597,317	C→T	RH, D, R, M, Ch	R4843C	missense	19 (1870)	12/915 SCZ, 5/619 BP, 2/336 MDD	7 (1125)	0.005	0.003	0.130	1.6 (0.7 to 4.0)
4	TMD1	33	48,382,619	T→G	RH, D, R, M, Ch	S3704R	splice variant	1 (1706)	1/951 SCZ, 0/496 BP, 0/259 MDD	0 (1039)	0.0003	0.0000	n/a	infinity
5	TMD1	33	48,382,333	A→C	RH, D, R, M, Ch	H3609P	missense	28 (1707)	13/957 SCZ, 10/488 BP, 5/262 MDD	9 (1039)	0.0085	0.0043	0.048	1.9 (0.9-4.0)
6	TMD1	33	48,382,318	G→A	RH, D, R, M,	R3604Q	missense	1 (1766)	1/941 SCZ, 0/494 BP, 0/331 MDD	1 (1051)	0.0003	0.0005	n/a	0.5 (0.03 to 9.5)
7	TMD2	52	48,526,874	A→G	RH, D, R, Ch	T4550A	missense	19 (1708)	10/961 SCZ, 8/482 BP, 1/265 MDD	3 (1038)	0.0056	0.0014	0.013	3.8 (1.1-12.7)
8	TMD2	52	48,526,994	C→T	RH, D, R, M, Ch	R4590W	missense	17 (1946)	6/974 SCZ, 7/622 BP, 4/350 MDD	5 (1071)	0.0044	0.0023	0.148	1.9 (0.7 to 5.1)
9	HPR	43	48,465,399	A→G	RH, R, M, Ch	H4262R	missense	1 (1817)	1/937 SCZ, 0/562 BP, 0/318 MDD	0 (1080)	0.0003	0.0000	n/a	infinity

Genomic position based on NCBI Build 36.1
Brackets denote total number of samples genotyped
SCZ schizophrenia, BP Bipolar disorder, MDD major depressive disorder
conservation: RH rhesus monkey, D, dog, R rat, M mouse, Ch chicken
P values calculated using Fisher's exact test (one tailed). n/a, not applicable; CI, 95% confidence interval.
NBD, nucleotide binding domain; TMD, transmembrane omain clusters; HDR, hydrophobic dipping domain

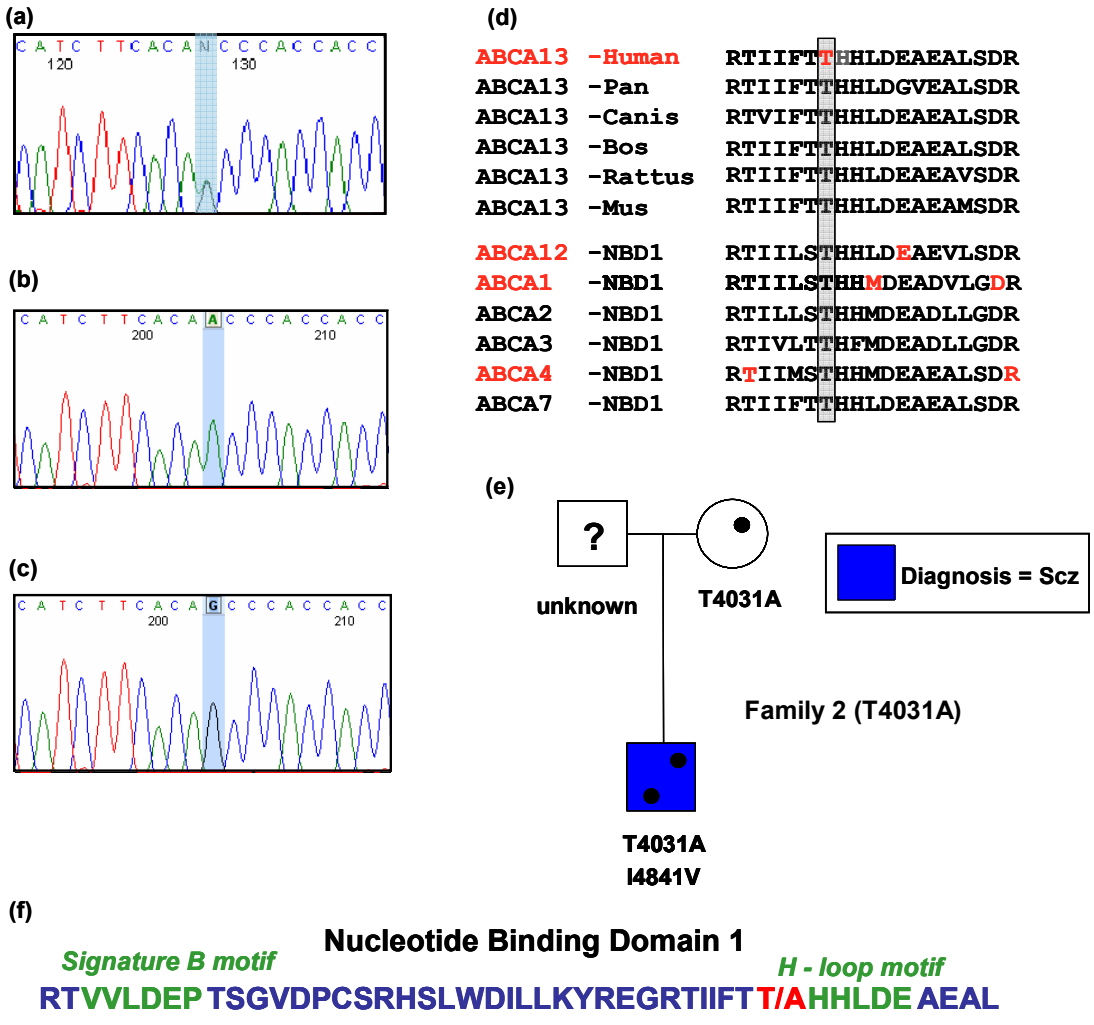

Figure 4.7 Sequence traces, amino acid position and conservation and family pedigree of the T4031A variant. Trace chromatogram of the heterozygous state as identified from sequencing gDNA in a case with schizophrenia (a), and cloned wild-type allele (b) and cloned mutant allele (c) resulting from the bacterial cloning and sequencing of the heterozygote PCR products. The mutated base is shaded blue. Conservation of the wildtype threonine amino acid across species (top) and among closely related ABCA protein family members (d). Previously reported pathological ABCA subfamily NBD mutations are shown in red. Family pedigree carrying T4031A and indicating possible compound heterozygote effect with I4841V (e). Location of the mutated T4031A (red) within the first NBD and neighbouring a conserved H-loop motif (f). 'Unknown' denotes unknown phenotype and '?' represents unknown genotype.

Follow-up family studies led to the identification one small family in which the proband is heterozygous for T4031A and another non-synonymous variant I4841V. The proband's mother who is not affected, carries T4031A but not I4841V showing that T4031A is not a *de novo* germ line mutation (figure 4.7e).

T4031A, as indicated in figure 4.7f, is situated immediately adjacent to the highly conserved functional H-loop Histidine residue and also in proximity of other functional motifs required for direct ATP-binding. Indeed, the H-loop histidine residue (H4032), adjacent to T4031 has been referred to as the "linchpin" of ATP hydrolysis in NBDs because it is essential for holding together all required parts of a complicated network of interactions between ATP, water molecules, Mg^{2+}, and amino acids (Zaitseva et al., 2005). Dinesh Soares evaluated the consequence of the T4031A mutation on protein structure and function by means of sequence analysis and a structural model (figure 4.8). The results suggested it is likely that the loss of two critical hydrogen bonds by substitution from a normally conserved and buried threonine residue to the less bulky alanine adjacent to the H-loop His4032, and within a complex network of inter-residue-bonding interactions, will perturb local structure. Hence, optimal ATPase activity, and consequently allocrite translocation is likely to be compromised (Soares personal communication).

Mutation 2: R4728X

A nonsense mutation, R4728X, located 19 amino acids before the start of the second nucleotide binding domain and within the highly conserved A-loop motif (*A*romatic residue interacting with the *A*denine ring of *A*TP), was detected in one case with schizophrenia (figure 4.9). This variant was confirmed by a restriction digest assay, as shown figure 4.8b. Transcripts containing nonsense mutations are frequently degraded through 'nonsense-mediated decay' which typically, like the original chromosomal abnormality, result in reduced gene dosage.

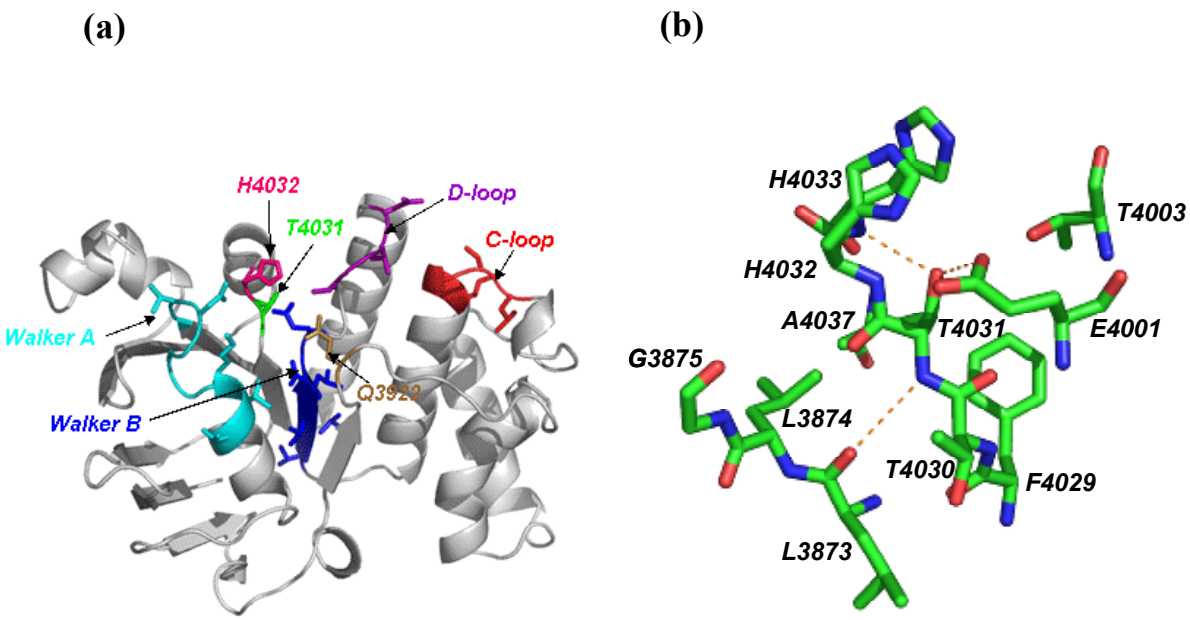

Figure 4.8 The location of T4031 and ATP-binding site on 3D-model. (a) A representation of the 3D-model, with the side-chains of ATP-binding motifs and mutated residue T4031A (green) shown; ATP-signature motifs colour coded and labelled; secondary structure assigned by STRIDE. (b) Close-up view of T4031 hydrogen bonds indicated by dashed orange lines. The buried side-chain hydroxyl group of T4031 forms a potential "loop-stabilising" hydrogen bond with the backbone nitrogen of H4033 and additionally with the catalytic Walker B amino acid E4001. The backbone-backbone hydrogen bond between T4031 and L3873 is also shown. Other amino acid residues proximal to T4031 (5 Å sphere radius) are also shown and labelled (colour code: carbon atoms = green; oxygen atoms = red; nitrogen atoms = blue; hydrogen atoms are not shown for clarity). Vicinal functional residues H4032 (H-loop), G3875 (Walker A), and E4001 (Walker B) can be seen in this representation.

Figure and legend reproduced by kind permission of D. Soares (unpublished).

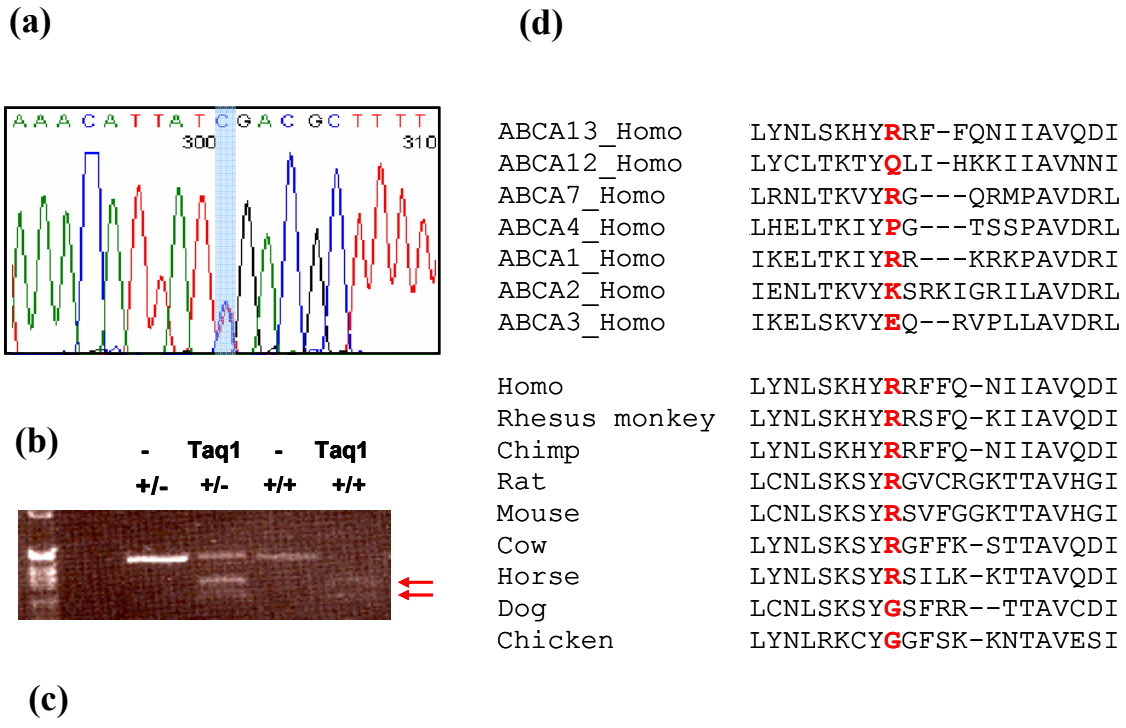

Figure 4.9 Sequence trace, restriction digest, position and conservation of R4728X. (a) Chromatogram of the heterozygous individual with schizophrenia as identified from sequencing. The mutated base is shaded blue. (b) Restriction digest of PCR product confirming the presence of the base change. The homozygous wildtype allele is fully cleaved by the taq1 enzyme producing a product of 200 and 300 bps (red arrows). In contrast, only one allele of the heterozygous mutant DNA is cleaved producing a product of 500bp as well as the 200 and 300 bps products. (c) Location of the mutated R4728X variant 19 AA before the start of the second NBD and within the A-loop motif. Amino acids shown in blue represent the start of the NBD and residues coloured green correspond to the highly conserved Walker a motif. (d). ABCA sub-family and species conservation of the wild-type arginine (shown red) amino acid. The arginine residue is highly conserved between orthologues but displays more variability between ABCA sub-family members.

Indeed, the equivalent amino acid has been shown to be mutated in the *ABCC6* gene causing pseudoxanthoma elasticum - a multi-organ disorder characterised by ectopic mineralisation of connective tissues (Bergen et al., 2007).

In a larger population study of 2193 cases, 4 R4728X heterozygotes were found in cases diagnosed with schizophrenia, 1 with schizophrenia co-morbid with mental retardation (MR), 4 with bipolar disorder, 2 with MDD. One control individual in the initial 1327 control sample group was also found to be a heterozygous carrier. Typing of a second control population, composed of 1043 individuals from the 1936 Lothian Birth Cohort, identified 4 further carriers. However, neither population of controls had been formally screened for psychiatric diagnoses or family history of psychiatric illness and the mental health of controls is therefore unknown.

Consequently, the MAF is calculated to be <1% (0.0025 cases; 0.0010 controls), relating to an OR of 2.4 (Confidence Interval [CI] 0.8-7.0) and a p-value of P=0.076, (fisher's exact test, one tailed) again indicating a trend in significance. Follow-up studies of relatives of carrier cases indicate that R4728X shows clear co-segregation with illness in two multiplex families presenting with bipolar disorder and MDD and two small families with schizophrenia and MDD (figure 4.10a-d).

Haplotype background of T4031A and R4728X

Single nucleotide polymorphisms in the region of T4031A and R4728X were sequenced in relatives and probands with these variants. The conserved patterns of nearby SNPs observed in the sequence of 4 carriers of T4031A and 20 carriers of R4728X imply that the two mutant alleles each arose once on a common (but different) haplotype background. This suggests all present-day cases of these two mutations are descended from two British/European ancestors. As shown in figure 4.11, the haplotypes cover a genomic region which may form one large LD block or two smaller LD blocks relating the two functional halves (TMD/NBD1 and TMD/NBD2) of the transporter.

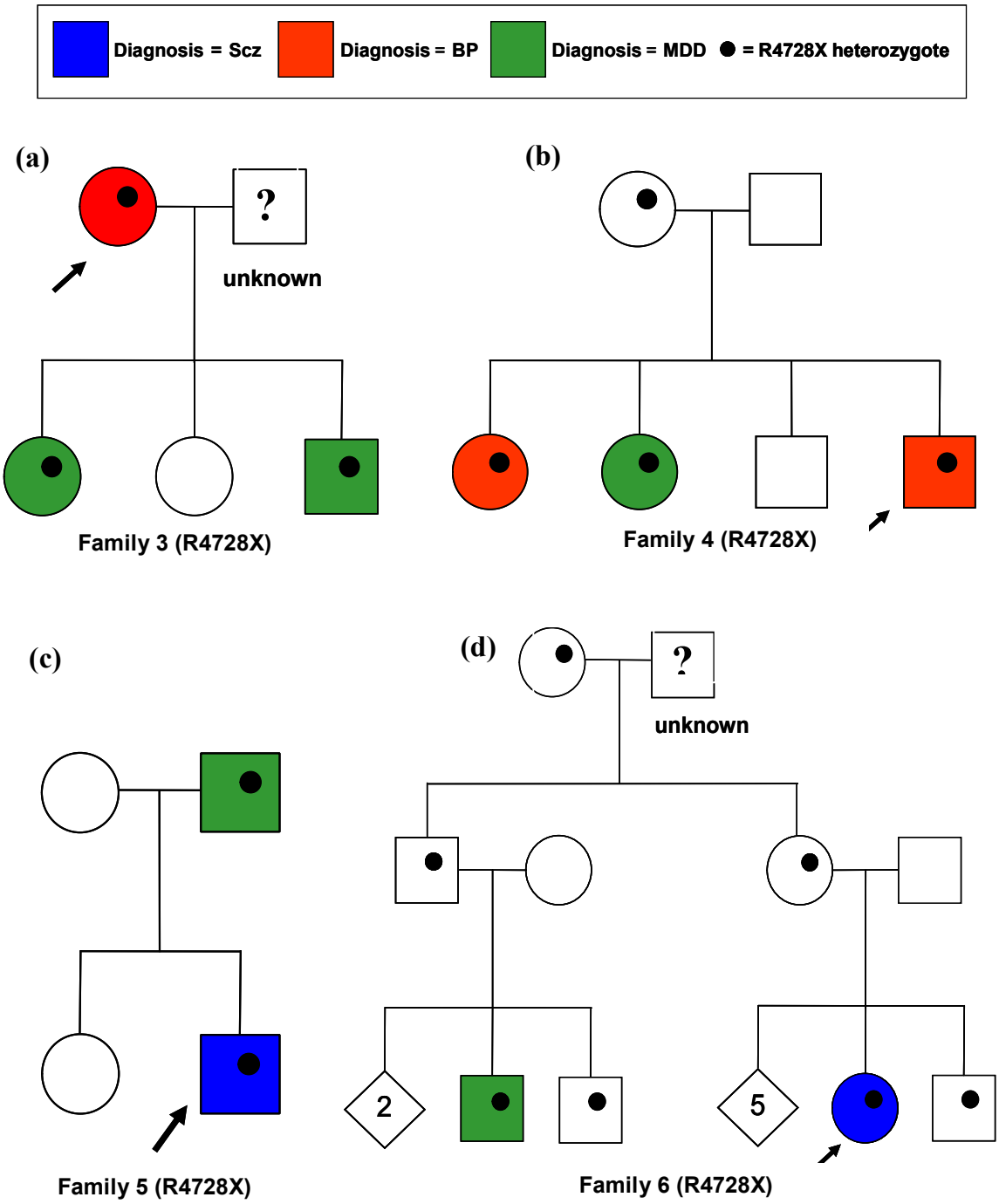

Figure 4.10 Co-segregation of R4728X with illness in four pedigrees. Arrows denote probands. Diamond shapes and numbers within represent the number of non-affected individuals. 'Unknown' denotes unknown phenotype and '?' represents unknown genotype.

(a)

SNP	rs1526093 ‡	rs17132289‡	rs 6978753	T4031A	rs17548783‡	rs1316349‡	R4728X	rs7778411‡	rs10243913	rs10046546
Location	48,377,763	48,399,261	48,414,116	48,420,683	48,420,703	48,538,589	48,534,458	48,597,191	48,625,307	48,625,315
Allele R4728X	G*	A	A*	A	C*	G	C*	C*	G*	A
Allele T4031A	A	A	G	G*	T	G	T	-	-	-

LD BLOCK 1 LD BLOCK 2

* denotes minor allele

‡ denotes SNPs used for haplotype frequency analysis

(b)

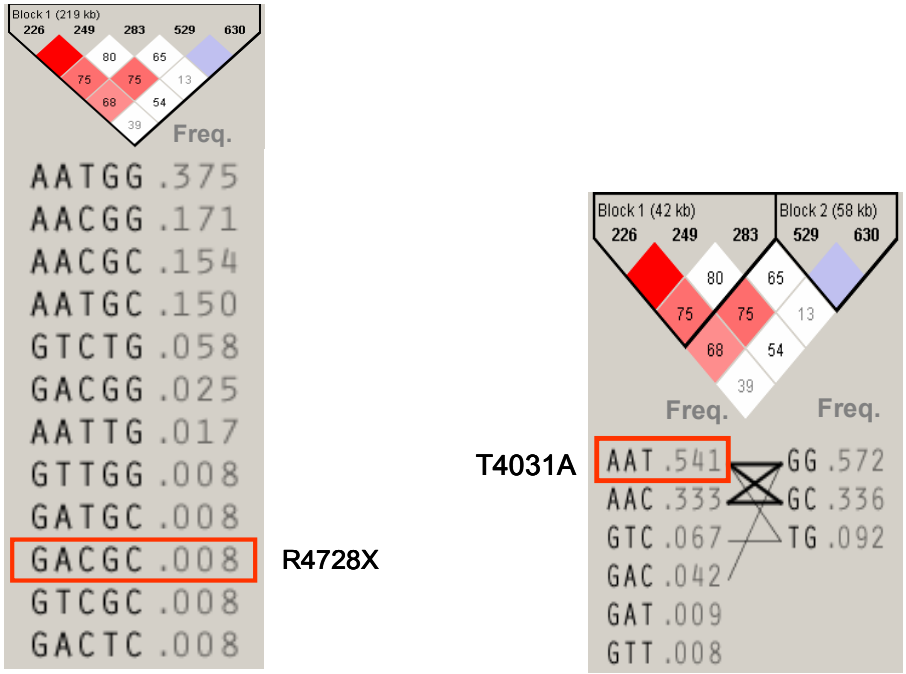

Figure 4.11 Conserved background haplotypes carrying the R4728X and T4031A mutations. (a) SNP ID, genomic location and alleles comprising the two background haplotypes. * denotes the haplotype carrys the MAF and ‡ indicates the 5 SNPs used for haplotype frequency analysis. (b) The frequency of the R4728X or T4031A background haplotypes in the general population based on data from 5 SNPs and 3 SNPs respectively (red rectangles).

The nonsense mutation is carried on a haplotype spanning the entire sequenced region; however, the T4031A is carried on a shorter haplotype spanning only the first LD block. To investigate how common these haplotypes are in the general population, in phase data from five known SNPs (rs1526093, rs17132289, rs17548783, rs1316349, rs7778411) were down loaded for 30 CEPH trios from HapMap Phase II build 125 (http://www.hapmap.org.). The frequency of the 5 SNP R4728X-carrying haplotype was found to be less than 10% in the general population. In contrast, based on data pertaining to 3 SNPs only (figure 4.11b), T4031A is carried on a background haplotype far more common (~54%).

Mutation 3: R4843C

The third novel variant positioned within the NBDs, R4843C, was initially detected in one control individual. This non-conservative amino acid substitution from arginine to cysteine, occurs proximal to the signature ABC motif and is highly conserved between species (Figure 4.12). To assess whether this variant was a benign ultra-rare variant, a further 1870 cases and 1125 controls samples were genotyped (Table 4.5). Nineteen cases, 12 schizophrenia, 5 BP and 2 MDD, and 7 controls were identified and confirmed as heterozgotes. The frequency of R4843C is therefore estimated to be 0.005 for cases and 0.003 controls, p= 0.13, resulting in an OR of 1.6 (CI 0.7 to 4.0).

Follow-up studies of proband relatives led to the identification of three small families (presented in figure 4.13) and co-segregation with illness was observed in two of the three families. In the first family, the mother of the proband has bipolar disorder and the proband schizoaffective disorder and both are heterozygous for R4843C. Neither of the parents in family 8 is affected. However, the father is a carrier and there is family history of suicide on the paternal side. In family 9 the mother of the proband who has bipolar disorder and an affected sibling with depression were found not to have the variant.

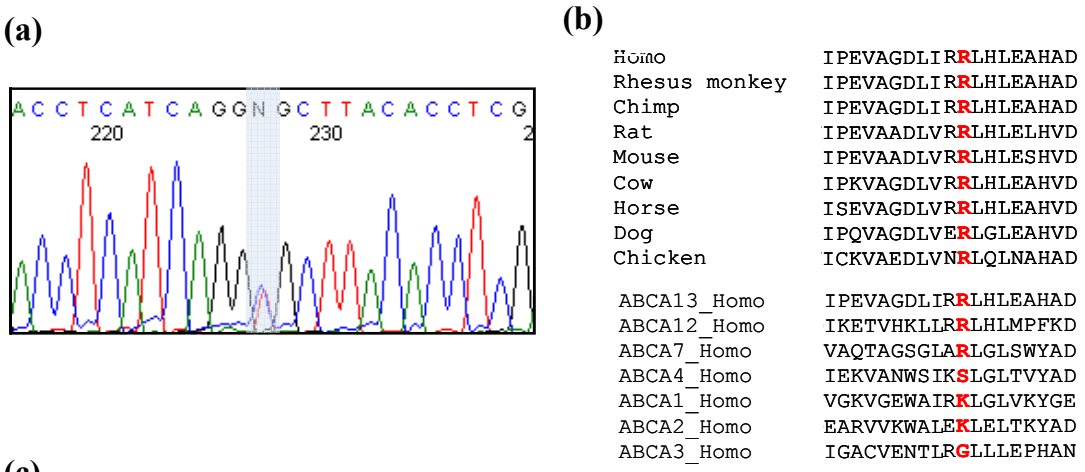

Figure 4.12 Sequence trace, amino acid position and conservation of R4843C. (a) Sequence chromatogram of heterozygous mutant for R4843C. (b) ABCA subfamily and species conservation of the wildtype arginine (shown red) amino acid. The arginine residue is phylogenetically highly conserved. (c) Amino acid sequence showing location of the variant.

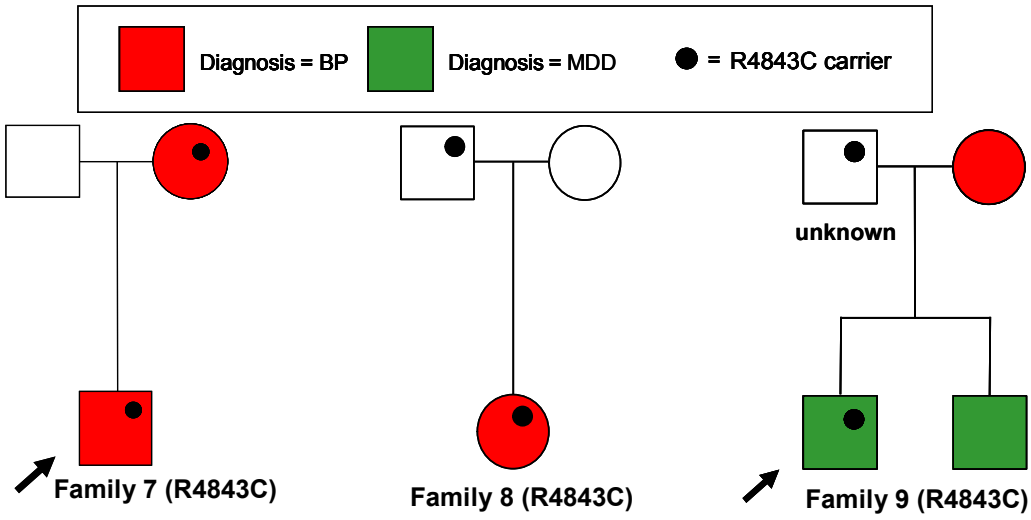

Figure 4.13 Small families carrying the R4843C variant. In family 7 the mother and proband are both affected and carriers. The parents in family 8 are both not affected, however, the father is a carrier and there is family history of suicide on the paternal side. R4843C does not appear to segregate in family 9 as both the mother and a sibling are affected but not carriers of R4843C.

However, no information is available regarding the father's phenotype. Multiple genetic risk variants may contribute to these clinical phenotypes in addition to R4843C inherited from the father.

Mutation 4: S3704R

The non-conservative amino acid substitution of a serine to arginine (S3704R) located within a transmembrane loop of the first TMD, was detected in the heterozygous state in one proband from a large family with schizophrenia and MDD (Figure 4.14). Genotyping large case-control cohorts revealed no further cases (0/1763 samples) or controls (0/1039) to be heterozygous carriers. Moreover, S3704R was found to co-segregate with illness in this large family, as shown in figure 4.14e. It is clear, however, that S3704R does not show full penetrance as several asymptomatic family members were found to be heterozygous.

In addition to its amino acid substitution, this mutation introduces a novel cryptic splice donor site as assessed using the Berkeley Drosophila Genome Project splice site predication tool (http://www.fruitfly.org/seq_tools/splice.html). The introduction of a novel donor splice site potentially results in a transcript with a downstream frameshift and premature stop codon. Calculated MAFs for S3704R are 0.0003 cases, 0.000 controls, p= 0.62 (Fisher's exact test, one tailed), and OR infinity. Hence, S3704R displays all the typical features of a rare Mendelian, highly penetrant, deleterious mutation.

Mutations 5: H3609P

H3609P positioned within transmembrane loops of the first TMD, was initially identified in 3 cases of schizophrenia and one control. This variant involves a non-conservative amino acid substitution of a highly conserved histidine to proline. A sequence chromatogram, amino acid position and conservation for H3609P is presented in figure 4.15.

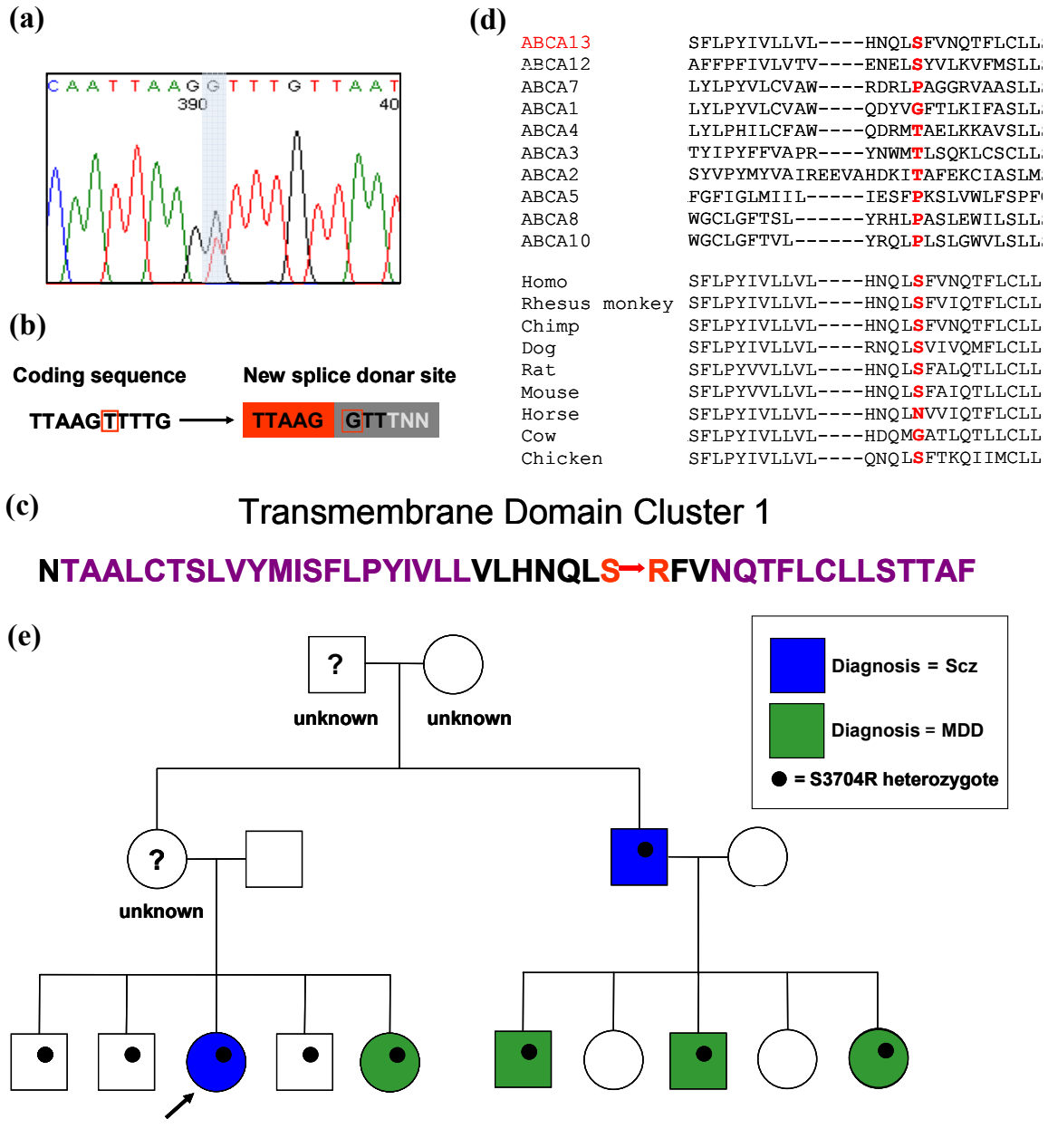

Figure 4.14 Sequence chromatogram, splice variant sequence, amino acid position, conservation and segregation of S3704R with illness in a large pedigree. (a) Sequence chromatogram of heterozygous mutant for S3704R. (b) Schematic of novel splice donor site. (c) Position of amino acid substitution in the first TMD. Transmembrane domains are coloured purple. (d) ABCA subfamily and species conservation of the wildtype serine (shown red). The serine residue is highly conserved between species. (e) Family pedigree in which S3704R co-segregates with illness. The black dot denotes a S3704R heterozygote. 'Unknown' denotes unknown phenotype and '?' represents unknown genotype.

(a)

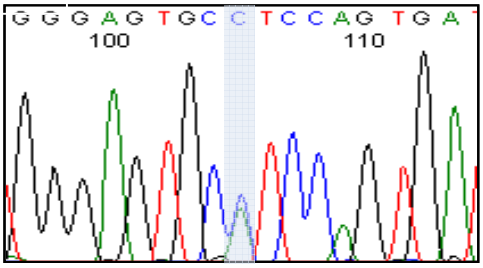

(b)

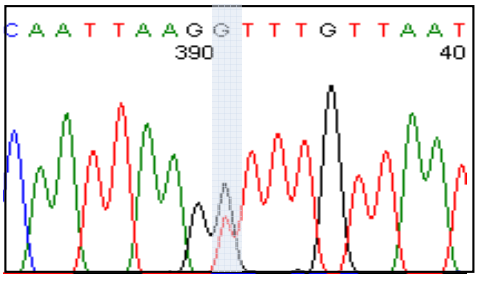

(d)

Homo	EQEIQIEEYM**R**MMGV**H**PVIHFLAWFLEN
Rhesus monkey	EQEIQIEEYL**R**MMGV**H**PMTHFLAWFLEN
Chimp	EQEIQIEEYM**R**MMGV**H**PVIHFLAWFLEN
Dog	ERQTQIEEYM**R**MMGV**H**STVLFLAWFLEN
Rat	EREIQIEEYM**R**IMGL**H**PVIHFLSWFLEN
Mouse	EREIQIEEYM**R**MMGL**H**PTIHFLSWFLEN
Horse	EREIQIEEYM**R**MMGV**H**PTIHFLAWFLEN
Cow	EREIQLEEYM**R**MMGV**H**PAVHFLAWFLEN
Chicken	EREIHLEEYM**K**TMGV**H**PAIHFFAWFLEN
ABCA13	EQEIQIEEYM**R**MMGV**H**PVIHFLAWFLEN
ABCA12	EKDLRLHEYM**K**MMGV**N**SCSHFFAWLIES
ABCA7	EKETRLRDTM**R**AMGL**S**RAVLWLGWFLSC
ABCA1	EKEARLKETM**R**IMGL**D**NSILWFSWFISS
ABCA4	EKELRLKETL**K**NQGV**S**NAVIWCTWFLDS
ABCA3	EKERRLKEYM**R**MMGL**S**SWLHWSAWFLLF
ABCA2	EKEHRLKEVM**K**TMGL**N**NAVHWVAWFITG
ABCA5	EKEKKIKEFL**K**IMGL**H**DTAFWLSWVLLY
ABCA8	RERKRMKALM**T**MMGL**R**DSAFWLSWGLLY
ABCA10	RERGKFKKLM**T**VMGL**R**ESAFWLSWGLTY

(c)

Transmembrane Domain Cluster 1

KLVYEQEIQIEEYMR→QMMGVH→PPVIHFLAWFLENMAVLTISS

Figure 4.15 Sequence chromatogram, amino acid position and conservation of H3609P and R3604Q. (a) Sequence chromatogram of heterozygous mutant for H3609P. (b) Sequence chromatogram of heterozygous mutant for R3604Q (c) Position of amino acid substitutions in the first TMD. Transmembrane domains are coloured purple. (d) ABCA sub-family and species conservation of the wildtype histidine and arginine residues (shown red). Both amino acids are highly conserved between species but show less conservation between ABCA sub-family members.

Genotyping a total of 1707 cases and 1039 controls samples revealed 27 cases and 9 control individuals were heterozygous and one individual with bipolar disorder homozygous for H3609P. Allele frequencies for H3609P in the case population (0.0085) and control population (0.0043) shows a statistical significant difference, p=0.048 (Fisher's exact test, one tailed), and correspond to an OR of 1.9 (CI 0.9-4.0). Furthermore, analysis of nearby SNPs in a limited number of unrelated carriers suggests that, like T4031A or R4728X, H3609P may have arisen on a common haplotype background (data not shown).

Segregation in eight small families with schizophrenia, bipolar disorder and MDD indicated that H3609P was inherited by every case investigated and that H3609P displays incomplete penetrance (figure 4.16). In three multiplex pedigrees more than one affected sibling was identified. Three male siblings with schizophrenia (family 11), one male sibling with schizophrenia and one female sibling with MDD (family 14) and three female siblings, two of which have bipolar disorder and one MDD (family 17) were all found to be H3609P heterozygotes.

The remaining five families consist of two parents and an affected child, in three of which both parents are unaffected (families 13, 15, 18). In the fourth single child family (family 12) the father has MDD and carries H3609P. In the fifth family (family 16) the mother was diagnosed with BP but does not have the variant, whereas the father, with a diagnosis of alcoholism, was found to be a carrier. This finding does not indicate a lack of H3609P segregation with illness as evident from the other families but could suggest that a risk factor associated with bipolar disorder illness from the mother differs from risk for schizophrenia from the father.

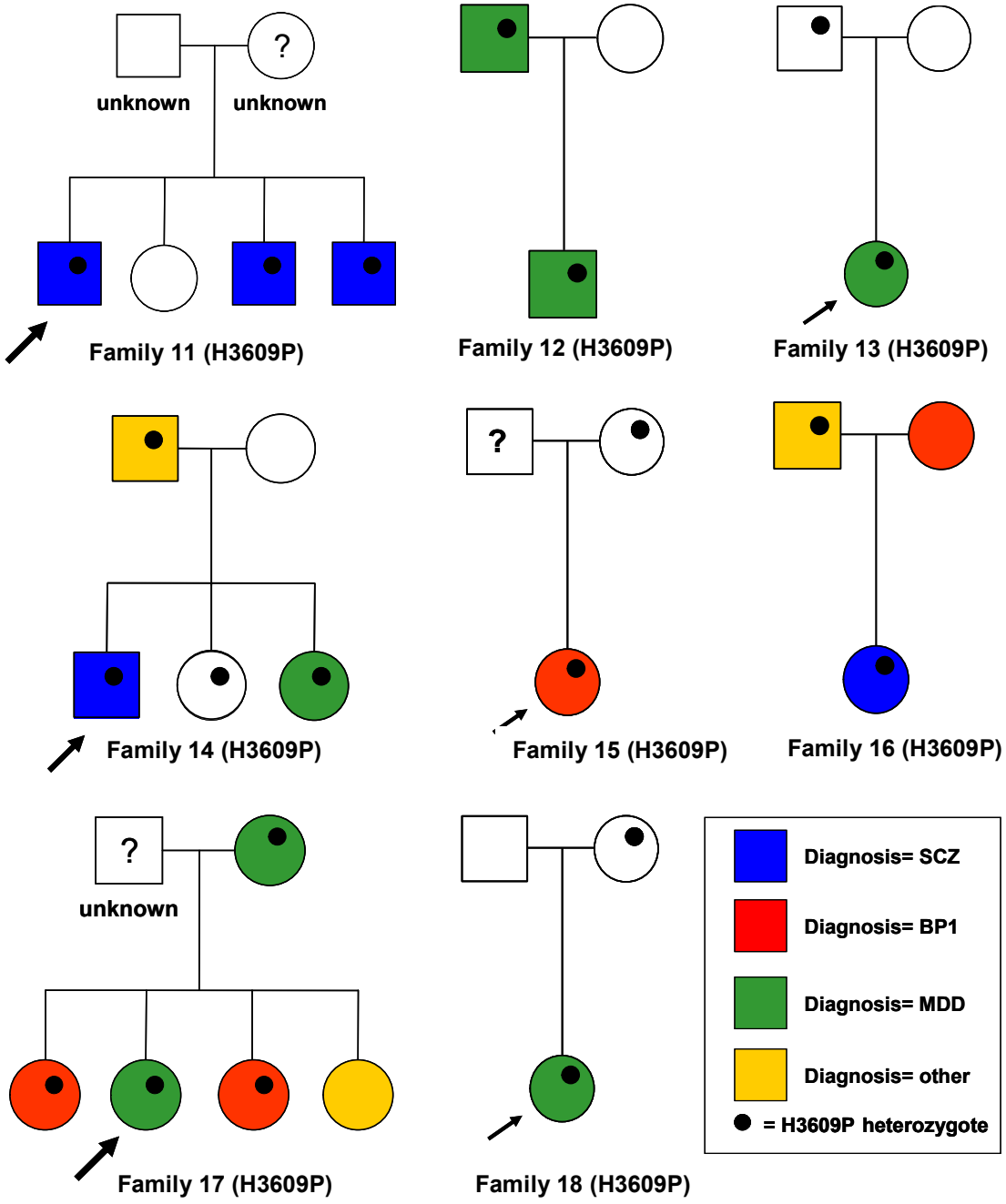

Figure 4.16 Family pedigrees carrying H3609P. The probands are denoted by a black arrow. Unknown indicates the phenotype is unknown and a question mark denotes unknown genotype. "Other" diagnoses are: major depression -single episode; minor depression; generalised anxiety disorder and alcoholism. Arrows indicate probands. Unknown denotes unknown phenotype and '?' represents unknown genotype.

Mutations 6: R3604Q

A third variant positioned within transmembrane loops of first the TMD, R3604Q, was initially identified in one patient with schizophrenia (figure 4.15). R3604Q, a non-conservative substitution of arginine to glutamine, was not found in any additional cases (total genotyped 1766) but present in one control out of 1051 sampled. Therefore, the difference in allele frequency between cases and controls (cases 0.0003, controls 0.0005) was found not to be statistically significant. The proband with schizophrenia initially detected with R3604Q belongs to a small family presenting with illness as shown in figure (4.17). The father and two siblings with affective disorders schizophrenia were found to be R3604Q heterozygotes.

Mutations 7: T4550A

T4550A results in a non-conservative amino acid substitution from threonine to alanine (figure 4.18). This variant, positioned within the third transmembrane spanning domain, was initially detected in the heterozygous state in one case with schizophrenia. A total of 1708 cases and 1038 controls were typed, leading to the identification of a further 18 heterozygous cases and 3 heterozygous controls individuals.

The difference in allele frequencies between the two cohorts (0.0056 cases, 0.0014 controls) was found to be significant ($p=0.013$, Fisher's exact test, one-tailed), corresponding to a moderately high OR of 3.8 (CI 1.1-12.7). Furthermore, two small pedigrees, one with two affected siblings with schizophrenia, were found to carry T4550A (figure 4.18d).

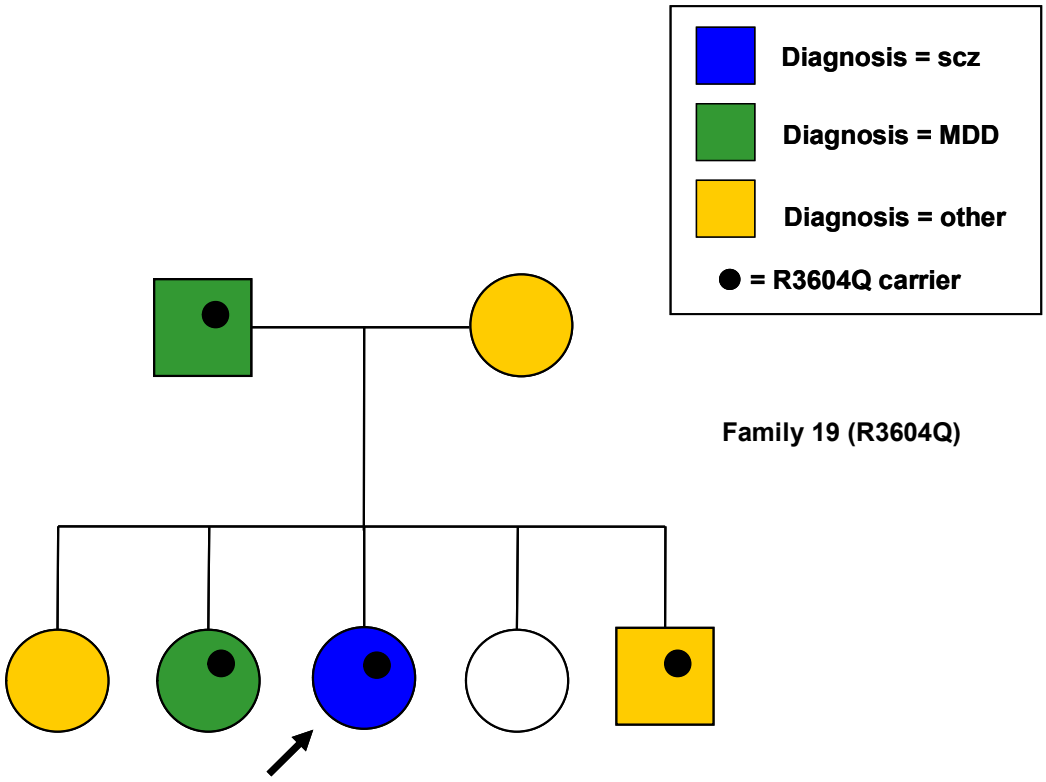

Figure 4.17 Family pedigree carrying R3604Q. The proband is denoted by a black arrow. "Other" diagnoses are: major depression - single episode, minor depression, generalised anxiety disorder and alcoholism.

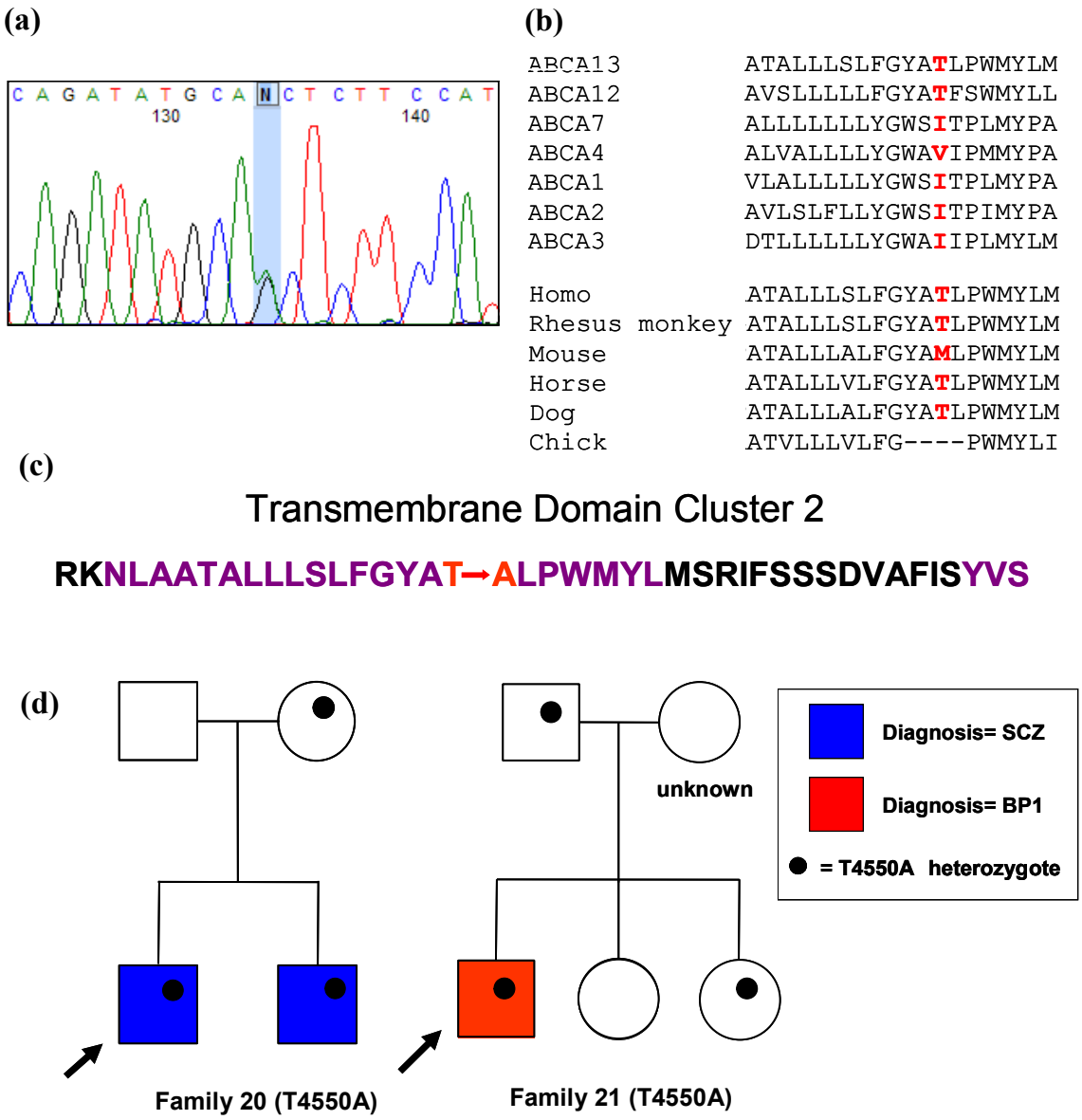

Figure 4.18 Sequence chromatogram, amino acid position, AA conservation and segregation of T4550A. (a) Sequence chromatogram of heterozygous mutant for T4550A. (b) ABCA sub-family and species conservation of the wildtype threonine residue (shown red). T4550A is less conserved between ABCA family members (c) Position of amino acid substitution in the second TMD. Transmembrane domains are coloured purple. (c) Two small families identified withT4550A. The variant was found to be carried by two siblings with schizophrenia in one small family and in one proband with bipolar disorder and two individuals not affected in a second family.

Mutations 8:R4590W

A second novel variant located within TMD2, R4590W, is also positioned within a transmembrane-spanning domain (figure 4.19c). The wild-type arginine is highly conserved phylogenetically and in its mutated state substituted by a tryptophan residue (figure 4.19b). R4590W was originally identified in one control individual. Subsequent genotyping indicated a total of 17 cases (out of 1946 cases sampled) and 5 controls (out of 1071 genotyped) were heterozygous for R4590W. This relates to an OR 1.9 (CI 0.7 to 5.1). However, the frequency difference, 0.0044 cases and 0.00223 controls, is not significant (p=0.148). No pedigrees were available for follow-up segregation analysis.

Mutations 9:H4262R

Finally, another low frequency variant, H4262R, located distal to the hydrophobic dipping region (HDR) was found only in one individual with schizophrenia and in an unaffected sibling in a total of 1817 cases and 1080 controls (figure 4.20b). This variant results in an amino acid change from a highly conserved histidine residue to an arginine amino acid, as shown in figure 4.20. While this substitution involves residues from the same basic group, arginine is classified as very basic whilst histidine has a relatively weak affinity for hydrogen atoms and is only partly positive at neutal pH. Therefore, although this variant may potentially perturb tertiary structure, in the absence of further data, e.g. strong familial segregation, clear association cannot be confirmed.

The locations of all nine putative pathogenic mutations discussed above are summarised in figure 4.21. There is no apparent clustering of variants in any one functional domain.

(a)

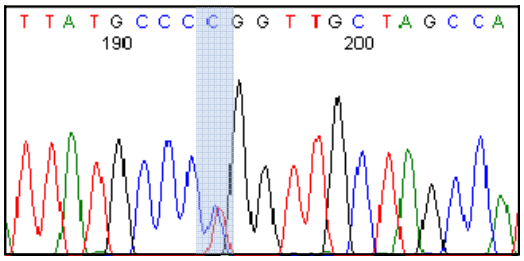

(b)

```
ABCA13          IFGLCTMLITIMPRLLAIIS-KAK
ABCA12          FFGINSIVSLSVVYFLSKEKPNDP
ABCA7           FIGINGSMATFVLELFSD-----Q
ABCA4           FIGINSSAITFILELFEN----NR
ABCA1           FIGINGSVATFVLELFTD-----N
ABCA2           FIGITATVATFLLQLFEHD----K
ABCA3           LSGIATFLMVTIMRIPAV------

Homo            IFGLCTMLITIMPRLLAIISKAK
Rhesus monkey   IFGLCTILITVMPRLLAIISKAK
Mouse           IFGLCTSLMTTMPRLLAIISKAQ
Horse           IFGLCTSLMTIMPRLLAIISKAQ
Dog             IFGLCTTLMTIMPRLLAMVSKAQ
Chick           VFGLCTFLVTLLPRILAIISKAQ
```

(c)

Transmembrane Domain Cluster 2

AFISYVSLNFIFGLCTMLITIMPR→WLLAIISKAKNLQNIYDVLKW

Figure 4.19 Sequence chromatogram, amino acid position and conservation of R4590W. (a) Sequence chromatogram of heterozygous mutant for R4590W. (b) ABCA subfamily and species conservation of the wildtype arginine residue (shown red). (c) Position of amino acid substitution in the second TMD. Transmembrane domains are coloured purple.

(a)

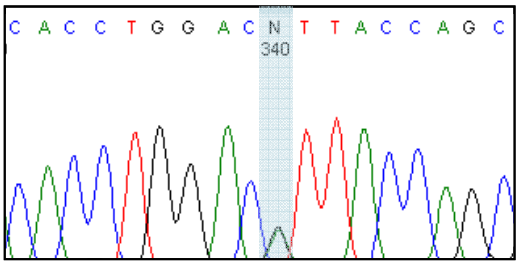

(b)

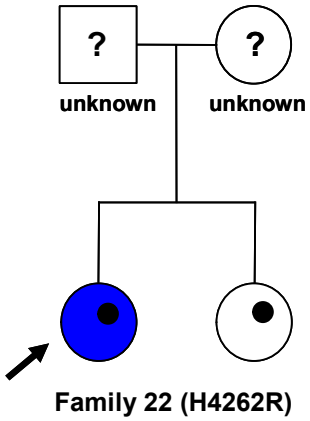

(c)

Hydrophobic Dipping Region

ADLLLPVLFVALAMGLFMVRPLATEYPPLRLTPGH→RYQRAETYFF

Figure 4.20 Sequence chromatogram, amino acid position and pedigree with H4262R. (a) Sequence chromatogram of heterozygous mutant for H4262R. (b) Small pedigree identified with two H4262R heterozygotes. (c) Position of amino acid substitution in intracellular loop after the hydrophobic dipping region. Residues shown purple indicate membrane dipping region.

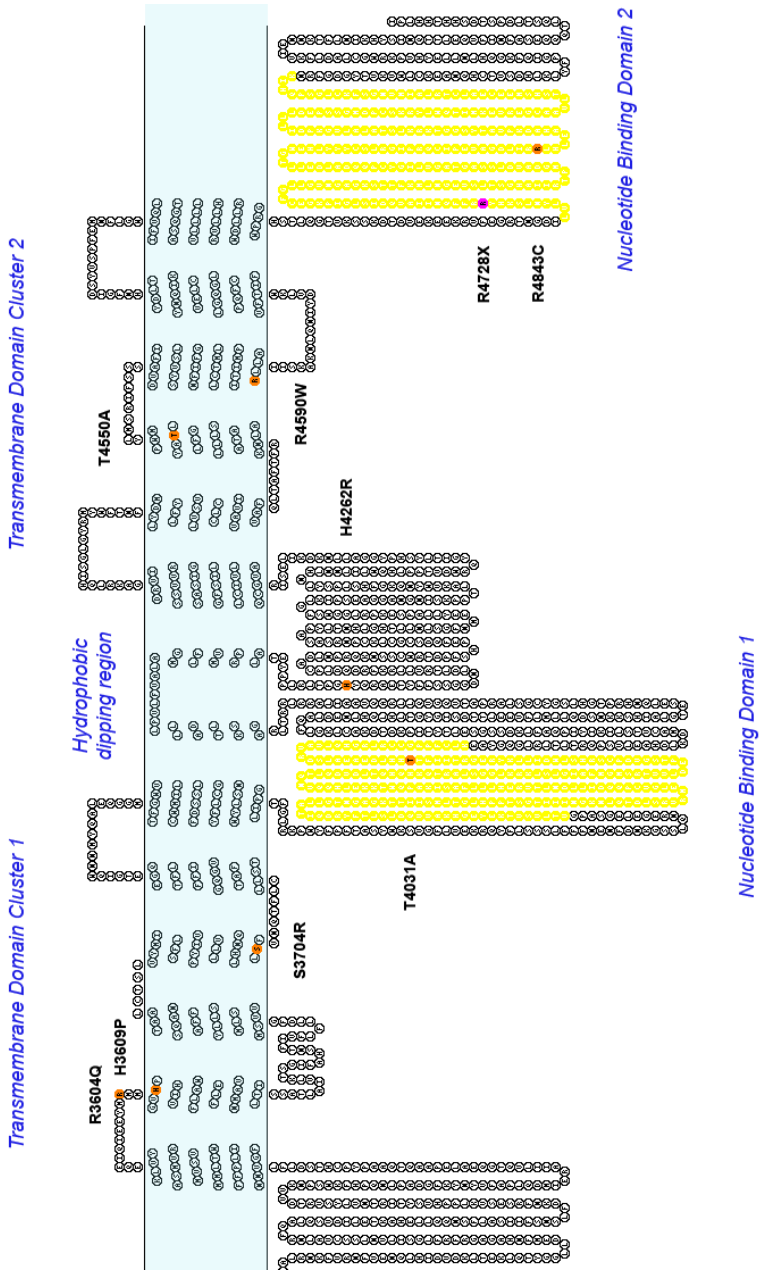

Figure 4.21 Schematic representation of the functional domains within ABCA13 and the locations of the identified putative mutations. The long N-terminal cytoplasmic tail and 3' C-terminus are not depicted. The mutations do not appear to cluster in any one functional domain. Representation based produced using the TOPO2 protein modeling program (Johns S.J.,TOPO2, Transmembrane protein display software, http://www.sacs.ucsf.edu/TOPO2/).

4.2.2.5 Further assessment of the pathogenic nature of identified coding variants

The potential pathological nature of the nine point mutations was suggested by type of variant, conservation of mutated residues, differences in allele frequencies between cases and controls, and variant segregation in affected family members. Furthermore, the consequences on protein structure and function of one variant, T4031A, were predicted by means of sequence analysis and a structural modelling. To assess further the nature of the identified amino acid substitutions, Ben Pickard examined eight of the nine potential mutations (the R4728X nonsense mutation was omitted), the two additional non-synonymous variants with as yet unknown status, and three non-synonymous 'potential control' polymorphisms within *ABCA13* using the computational models PolyPhen, PMUT and Panther PSEC. These computational tools aim to predict the pathological consequences of mutated residues within a protein sequence.

The results showed discrepencies in predications between the models, as indicated in table 4.6 (Pickard, B. unpublished observation). However, there was a trend towards the control variants (common non-synonymous amino acid changes) being predicted as neutral or benign by two of the models and the variants with significant ORs showing pathological likelihood. No putative pathogenic variant was predicted to be damaging/deleterious by all three models and only one tool (Panther) recognised the significance of the T4031A substitution, although this tool over-estimated the pathological nature of the control variants. An important consideration for future studies is to clarify the functional outcome of the identified putative pathogenic variants using direct biochemical or functional assays.

4.2.2.6 Cases carrying multiple rare risk variants

A total of 6 cases were found to be compound heterozygotes for two risk variants (listed in table 4.7) and a further affected individual biallelic for H3609P. In contrast, all controls carriers were found to be monoallelic. Unfortunately, follow-up family studies of these individuals could not be performed.

		Results from pmut				Results from PolyPhen		Results from Panther	
Variant	AA	Odds ratios	NN output	Reliability	Prediction	PSIC difference	Prediction	subPSEC	Pdeleterious
1	T4031A*	infinity	0.291	4	NEUTRAL	1.486	BENIGN	-6.443	0.969
3	R4843C	1.6 (0.7 - 4.0)	0.901	8	PATHOLOGICAL	2.257	PROBABLY DAMAGING	-2.934	0.484
4	S3704R	infinity	0.730	4	PATHOLOGICAL	1.613	POSSIBLY DAMAGING	No result	
5	H3609P	1.9 (0.9 - 4.0)	0.949	8	PATHOLOGICAL	2.734	POSSIBLY DAMAGING	-3.320	0.579
6	R3604Q	0.5 (0.03 - 9.5)	0.721	4	PATHOLOGICAL	1.357	BENIGN	-4.415	0.805
7	T4550A	3.8 (1.1 - 12.7)	0.328	3	NEUTRAL	1.238	BENIGN	-3.013	0.503
8	R4590W	2.4 (0.8 - 7.0)	0.992	9	PATHOLOGICAL	2.257	PROBABLY DAMAGING	No result	
9	H4262R	infinity	0.567	1	PATHOLOGICAL	2.284	PROBABLY DAMAGING	-3.123	0.531
	P4648A		0.448	1	NEUTRAL	2.100	PROBABLY DAMAGING	-3.949	0.721
	I4841V		0.056	8	NEUTRAL	0.620	BENIGN	-3.114	0.528
	L4047V		0.209	5	NEUTRAL	1.017	BENIGN	-4.132	0.756
	R4454C		0.928	8	PATHOLOGICAL	2.257	PROBABLY DAMAGING	-4.460	0.812
	L4464M		0.038	9	NEUTRAL	0.792	BENIGN	-3.550	0.634
			http://mmb2.pcb.ub.es:8080/PMut/			http://genetics.bwh.harvard.edu/pph/		http://www.pantherdb.org/tools/csnpScoreForm.jsp	

Table 4.6 In silico prediction of the functional/pathological consequences of all 13 newly identified non-synonymous variants. Eight of these variants have association/family evidence consistent with a role in psychiatric illness, 2 are of unknown status (P4648A and I4841V) and 3 are putative polymorphisms (L4047V, R4454C, L4464, MAF>1%) and included as negative controls. The R4728X nonsense mutation was not included. The red shading in the odds ratio column highlights the variants associated with risk. Results are shown for the three *in silico* predictive tools used; Pmut, PolyPhen and Panther, and are colour-coded (grey for moderate evidence and red for strong evidence) for predicted pathological consequence. * denotes the T4031A variant predicted to be pathogenic by means of structural modelling. Analysis performed by B. Pickard.

Individual	Variant 1	Variant 2	Diagnosis
1	T4031A	T4550A	SCZ
2	T4031A	T4550A	BP1
3	T4031A	I 4841V	BP1
4	H3609P	R4590W	BP1
5	H3609P	R4590W	BP1
6	H3609P	T4550A	BP1
7	H3609P	H3609P	SCZ

SCZ, schizophrenia; BP1, bipolar disorder 1.

Table 4.7 Affected individuals identified as being biallelic for risk variants. Six individuals are compound heterozygotes and one case homozygous for H3609P. Although the risk status of I4841V is unknown, details are included.

Intriguingly, these biallelic affected individuals all present with more serious diagnoses (bipolar disorder I or schizophrenia) and hence provide support that for the supposition that rare variant allelic interactions across *ABCA13* potentially increase susceptibility to, and severity of, psychiatric illness.

4.2.2.7 Association and linkage analysis

The rarity of these variants makes significant p-values difficult to achieve even in sizeable populations. Nevertheless, two risk variants (T4550A and H3609P) show significant individual genotype p-values and two (T4031A and R4728X) demonstrate a trend towards significance. However, to avoid a potential bias in estimates of the effect size, p-values for individual variants were also calculated for the frequency data derived from the secondary 'replication' TaqMan genotyping stage alone, i.e. the sequencing discovery sample numbers were excluded. Table S1, appendix 2, presents these corrected p-values for all cases per variants as well as p-values calculated for each variant for Scz, BP and MDD separately.

The Chi Square test ($\chi 2$) was used to calculate the collective significance of the burden of all newly identified nonsynonymous variants with a minor allele frequency of less than 0.01. Total numbers included 31 mutated alleles in 12175 control individuals and 101 mutated alleles in 16739 joint case individuals, giving a significant global p-value of <0.0001 (1 tailed, sequencing and TaqMan genotyping data combined). Moreover, excluding the initial discovery sequencing data to ensure an unbiased estimate, the global p-value remains significant 0.00026 (corrected TaqMan replication frequency data only). This corresponds to an OR of 2.1: 95% CI lower limit 1.5 (TaqMan replication frequency data only).

Similarly, using the same inclusion criteria but also including a family carrying a CNV located with *ABCA13* (discussed in section 4.23), a non-parametric single point linkage analysis which estimates identity by descent (IBD) between all pairs of affected relatives in 15 families, gave a combined Z score of 4.13, a Kong and Cox LOD score of 3.86

($p=1.26 \times 10^{-5}$) (Kong and Cox, 1997). These results indicate significant linkage of *ABCA13* mutations with psychiatric phenotypes within families.

4.2.2.8 Exploring potential gender effects

Positive associations for schizophrenia and bipolar disorder are commonly reported to be gender-specific. To evaluate whether for each of the potentially pathogenic non-synonymous risk variants there is an obvious over-representation in either gender, the percentage of male and female heterozygote carriers was compared to an approximate percentage of males and female genotyped. Table 4.8 lists the percentages calculated for variants detected in more than one case. Three variants, R4728X, T4550A and R4843C, indicate a potential bias in gender, although the scope for interpretation of data from such small numbers is limited. R4728X was identified in 4 male cases and 7 female cases even though the percentage of affected males typed (55%) were higher than females (45%). Conversely, T4550A and R4843C show a potential over-representation of male cases carriers to females cases (14 male, 5 female). This may be explained, in part, by a larger percentage of male cases successfully typed (T4550A 59.5% vs 50.5%; R4843C 55.2% vs 44.8%).

4.2.3 The identification of a CNV within *ABCA13*

Further evidence lending support for the *ABCA13* locus harboring rare pathogenic variants comes from the identification of a copy number variant (CNV) showing segregation in a large pedigree with schizophrenia and MDD, presented in figure 4.22. This CNV was detected in a whole genome CNV screen of schizophrenia cases and controls. Using a custom oligo array (Agilent technologies) with 34036 probes covering 1.5 Mb spanning *ABCA13,* an 11kb intronic hemizygous deletion positioned between exons 55 and 56 within *ABCA13* was confirmed to be present in 7 out of 11 family members (Tam et al., unpublished data). One family member diagnosed with MDD who does not carry this variant is therefore presumed a phenocopy. We postulate that this rare structural variant confers risk through the disruption of regulatory regions.

Variant	female (N) %	males (N) %
T4031A		
case carriers	(1) 25	(3) 75
control carriers	0	0
total genotyped cases	45.3	54.7
total genotyped controls*	35.8	64.2
R4728X		
case carriers	(7) 63.6	(4) 36.3
control carriers	(3) 60	(2) 40
total genotyped cases	45.0	55.0
total genotyped controls*	35.8	64.2
H3609P		
case carriers	(12) 42.9	(16) 57.1
control carriers	(6) 66.6	(3) 33.3
genotyped cases plates	40.5	59.5
control plates	35.8	64.2
T4550A		
case carriers	(5) 26.3	(14) 73.6
control carriers	(1) 33.3	(2) 66.6
genotyped cases plates	40.5	59.5
control plates	35.8	64.2
total	38.9	61.1
R4590W		
case carriers	(8) 47.1	(9) 52.9
control carriers	(2) 40	(3) 60
genotyped cases plates	44.8	55.2
control plates	35.8	64.2
R4843C		
case carriers	(5) 26.3	(14) 73.6
control carriers	(3) 42.9	(4) 57.1
genotyped cases plates	44.8	55.2
control plates	35.8	64.2

* Minus LBC control cohort

Table 4.8 Comparison of percentage of males and females carrying risk variants. The mean percentage of males and females on case and control plates successfully genotyped are listed as a comparison. Variants are listed only if more than one case was detected. Bracketed numbers are the total number of cases identified for each variant.

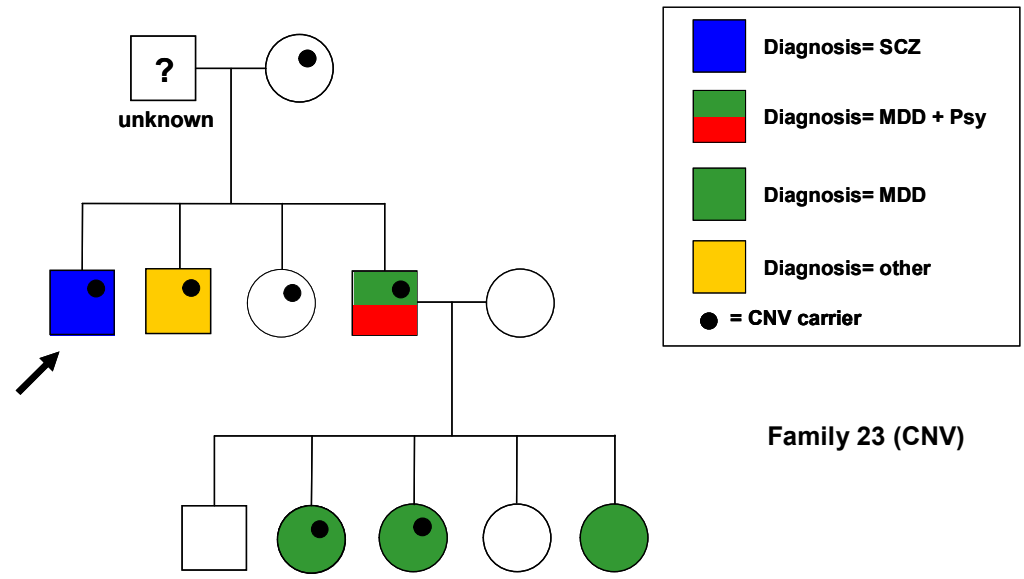

Figure 4.22 Pedigree of family carrying the 11 kb intronic CNV deletion. Heterozygote carriers are marked with the black dot. Unknown genotype and phenotype are denoted by a question mark and unknown respectively. "Other" diagnoses are: major depression - single episode, minor depression and generalized anxiety disorder (GAD).

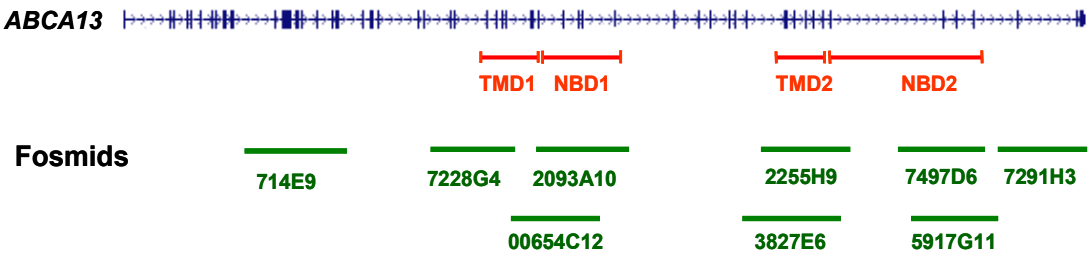

Figure 4.23 Schematic illustration of fosmid clones used to investigate a possible deletion in an individual with schizophrenia. The exons sequenced encoding the functional domains are highlighted in red.

4.2.4 An affected individual homozygous for rare alleles

An individual with schizophrenia screened for mutations within exons 32-40, 43 and 42-59 was found to be homozygous for all known and new SNPs detected. Moreover, this individual was found to be homozygous for three rare alleles (MAF <0.05), suggesting a possible deletion on one chromosome along this sequence. To clarify whether this individual carried a deletion, FISH was performed using fosmids located within *ABCA13* in addition to two BACs outside of the *ABCA13* locus, and on interphase nuclei from control individuals as well as the case. Figure 4.23 schematically illustrates the location of the BAC/fosmid clones hybridized in relation to sequenced regions.

Two fluorescent signals were consistently detected for all *ABCA13* clones and control BACs as shown in figure 4.24. However, for the adjacent fosmids G248P85917G11 and G248P87497D6 there appeared to be a reduced signal on one chromosome 7, suggestive of a small deletion. Further analysis using material from control individuals also indicated this reduced signal, suggesting signal variation to be inherent to the fosmids clones rather than a reduction in chromosomal material specific to the case. DNA from this affected individual was further analysed for deletions using the custom oligo array (agilent technologies) described above and performed at Sanger. No evidence was found for copy number variants (CNVs) over the *ABCA13* locus, indicating that a deletion is not the cause of homozygosity in this individual.

Extended tracts of homozygosity may reflect the phenomenon of uniparental disomy (UPD) in which a child inherits two copies of a chromosome or chromosome segments from one parent. To investigate whether this individual may have UPD, microsatellite markers positioned along chromosome 7 were genotyped. The case was found to be homozygous for 5 (inter-dispersed) markers and heterozygous for 13 markers including the marker D7S519 nearest to *ABCA13*, shown in figure 4.25. In concert, these data disprove the hypothesis that homozygosity for variants located within *ABCA13* evident in this one individual arises from a deletion or UPD. Nonetheless, this individual may be homozygous for an as yet unidentified mutation which confers risk for schizophrenia.

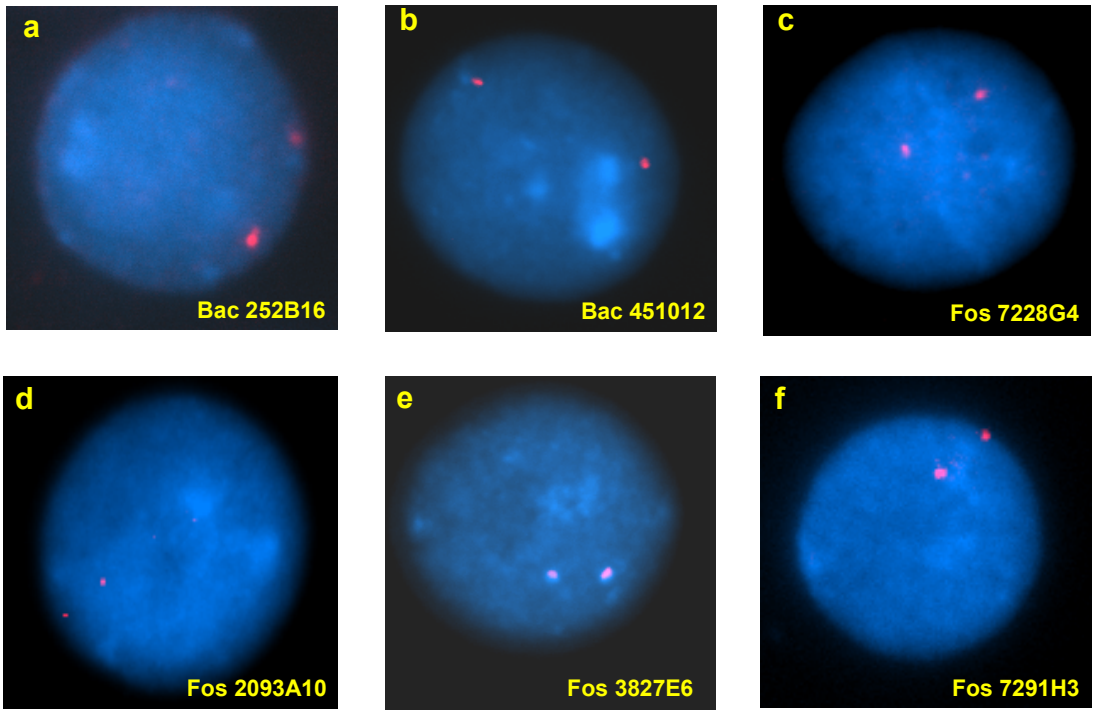

Figure 4.24 Interphase nuclei hybridized with fosmid and BAC DNA in an individual with schizophrenia and a potential deletion. Control BACs located outside *ABCA13* (a & b), fosmids positioned within *ABCA13* (c-f). Two signals are clearly seen for all clones.

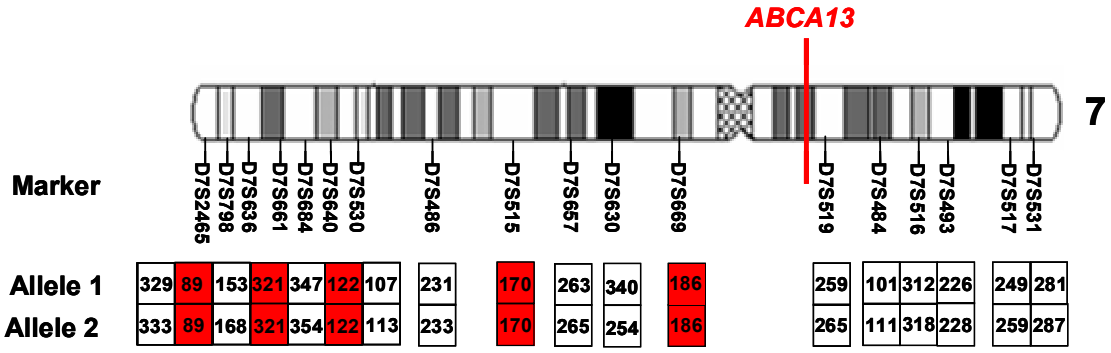

Figure 4.25 Microsatellite marker genotyping on chromosome 7 in an individual with schizophrenia. Homozygous markers shaded red, heterozygous markers not filled. The locations of the microsatellites and *ABCA13* are depicted schematically along the chromosome.

4.3 Discussion

This chapter reports the fine mapping of a cytogenetic abnormality resulting in the disruption of the *ABCA13* gene in an individual with chronic schizophrenia and the identification of rare coding sequence variants positioned within *ABCA13* as a cause of schizophrenia, bipolar disorder and major depressive disorder. The findings indicate both association of rare variants with disease in the population and linkage of these variants within families. Further, the investigation of an affected individual displaying homozygosity over the *ABCA13* locus led to the conclusion that a deletion within this region and UPD of chromosome 7 were not causative factors associated with the clinical phenotype.

4.3.1 Cytogenetics and the chromosome 7 region in disease

The identified breakpoint region on chromosome 8p23.1 did not directly disrupt any annotated transcripts but was in close proximity to two genes, *PPP1R3B* which encodes a protein phosphatase 1 subunit, and *THEX1* which encodes a RNA exonuclease. Protein phosphatase-1 proteins have a diverse range of functions in mammalian cells. PPP1R3B, a serine/threonine-specific phosphoprotein phosphatase regulatory sub-unit, however, targets PP1 to glycogen synthase. Thus it regulates and is necessary for PP1 glycogen metabolism (Ceulemans et al., 2002). Moreover, PPP1R3B is expressed ubiquitously including in astrocytes at glutamatergic synapses in the brain. Consequently it may play an important role in an activity-dependent metabolic 'tagging' process – a signaling mechanism hypothesized to be important for synaptic plasticity mechanisms (Pellerin and Magistretti, 1994). The close proximity of the breakpoint, which could disrupt regulatory mechanisms controlling PPP1R3B expression, in conjunction with the functional role of this sub-unit in the brain, suggests that PPP1R3B should not be dismissed as potentially contributing to the pathology of disease.

Cytogenetic analysis of the breakpoint interval on chromosome 7p12.1 indicated that *ABCA13* was disrupted in the vicinity of exons 30 and 31. The resulting mutated protein is predicted to be truncated by approximately 50% of its normal sequence and to lose both pairs of functional domains. Even if the extremely long N-terminal cytoplasmic tail were a separate transcript product as suggested, the promoter regulatory motifs and initial exon(s) adjacent to the functional domains, which are necessary for translation of a functional transporter, would be absent from the disrupted protein product. Furthermore, it is possible that if *ABCA13* were to encode for two half transporter transcripts, the second distal transporter might still be transcribed. However, unpublished data indicate that only a 'full transporter' *ABCA13* transcript encoding for two transmembrane clusters and NBDs are expressed in mouse and human brain tissue (investigated in chapter 5; R. Cannon, personal correspondence). The position of the breakpoint is therefore likely to result in lack of functional protein product from the disrupted allele and thus is consistent with the hypothesis of haploinsufficiency, i.e. insufficient gene product for normal cellular function, underlying the clinical outcome.

Chromosome 7 is a hot-spot for chromosomal abnormalities associated with autistic spectrum disorders (ASD). Breakpoint sites along chromosome 7, reported for ASD and other clinical phenotypes, are predominately clustered on the long q-arm (Scherer et al., 2003; Vorstman et al., 2006). Nonetheless, two cases with ASD are reported to have cytogenetic abnormalities in the region of 7p12. Wolpert and colleagues describe an affected individual with a 20Mb duplication spanning 7p11-p14 (Wolpert et al., 2001). In contrast, a reciprocal inversion on chromosome 7 with the p-arm breakpoint identified at 7p12 was detected in a second case of ASD (Warburton et al., 2000; Vorstman et al., 2006). As far as the author can ascertain, both these abnormalities include, or are very close to, the *ABCA13* locus, and hence they provide some additional evidence of potential region-specific dosage effects leading to neuropsychiatric conditions. As yet, other than the individual described in the present chapter, no further cases of cytogenic disruptions in this interval in individuals schizophrenia, bipolar disorder or MDD have been reported.

4.3.2 Linking cytogenetics and rare variants: lessons from autism spectrum disorder

Ultra-rare causal and risk variants detected within candidate genes originally identified by chromosomal disruptions, e.g. *NLGN3*, *NLGN4, SHANK3*, and *CNTNAP2*, have previously been reported for neuropsychiatric disorders. In recent years, research into the genetics of ASD has led to the identification of inherited and de novo mutations in genes implicated in specific common biological processes. For example, a *de novo* frameshift mutation and an inherited missense mutation within the genes *NLGN4* and *NLGN3* respectively were detected in two pairs of brothers with Autism or Aspergers syndrome (Jamain et al., 2003). In a large family with mental retardation, Autism or Aspergers syndrome, a 2 base pair deletion resulting in a premature stop codon within *NLGN4* was found to segregate with all three disorders (Laumonnier et al., 2004). Moreover, a single base pair deletion in *CNTNAP2* was found in every affected individuals from a large Amish pedigree with cortical dysplasia–focal epilepsy (CDFE) syndrome - a heterogeneous condition characterized by intractable seizures and autism (Strauss et al., 2006). These rare deleterious variants were all found in the homozygous state in affected individuals, supporting a recessive, highly penetrant causal nature.

In two candidate, and cytogenetically disrupted ASD genes, *SHANK3* and *CNTNAP2*, rare variants were detected in the heterozygous state. In a first resequencing study of *SHANK3*, nine inherited missense mutations, one de novo missense mutation and two *de novo* CNVs were identified as unique to the case population (Moessner et al., 2007). A second screen, performed on different case and control cohorts, revealed seven rare inherited missense mutations detected in ASD cases only (Durand et al., 2007). Furthermore, 13 highly conserved missense mutations (8 predicted deleterious) within *CNTNAP2* were found unique to individual or multiple cases and at an allele frequency lower than 0.00025 (1/4000) (Bakkaloglu et al., 2008). Four of the non-synonymous variants reported for *CNTNAP2* were identified in pedigrees with more than one affected individual and three of these showed segregation with ASD in the affected first-degree relatives. Of interest, these variants show not only inheritance from unaffected parents

but incomplete penetrance, i.e. carried in non-affected relatives. Moreover, although the collective rate of these variants was up to two-fold higher in cases compared to controls, owing to their rarity the difference in frequencies did not achieve a statistical threshold for an association.

The fact that such heterozygous rare risk variants were identified in the same gene (*CNTNAP2*) found to be disrupted in cases with cytogenetic abnormalities and in which a deleterious homozygous frameshift mutation segregates in a large affected pedigree indicates that multiple types of causal/risk variants within one gene can contribute to the pathogenesis of a disease (Fernandez et al., 2004; Strauss et al., 2006; Bakkaloglu et al., 2008). These studies also highlight that both private mutations and inherited rare risk variants evident in more than one case result in a spectrum of neurobehavioural phenotypes. This phenotypic heterogeneity in conjunction with variable expressivity, is postulated to be due to the expression of mutations being modulated by other protective or liability alleles or non-genetic factors (Laumonnier et al., 2004).

4.3.3 Rare variants in psychiatric illness

With respect to schizophrenia and bipolar disorder, putatively pathological ultra-rare non-synonymous variants have been reported in *DISC1* (Disrupted in Schizophrenia-1), *PCM1* (pericentriolar material 1 protein) and in genes known to cause Wolfram syndrome (WS) and Darier disease (DD), two diseases frequently co-morbid with mood disorders (Kato, 2001; Song et al., 2008). *DISC1*, a breakpoint gene disrupted in large Scottish family with schizophrenia, bipolar disorder and MDD, is emerging as the best supported candidate gene for schizophrenia. An initial mutation detection study of *DISC1* identified a four nucleotide C-terminal frame-shift deletion predicted to encode a protein truncation near the C-terminus. This mutation was present in two affected siblings presenting with schizophrenia and schizoaffective disorder and their asymptomatic father, but not carried by two siblings with MDD and one sib with schizotypal disorder (Sachs et al., 2005). However, a subsequent re-sequencing study by

Green and co-workers did not find this mutation in 655 schizophrenia cases but did find it in two of 694 blood donor controls without known history of psychiatric diseases (Green et al., 2006).

A third screen of *DISC1* using 288 cases with schizophrenia and 288 controls was performed by Song and colleagues (Song et al., 2008). Seven heterozygous missense variants were found unique to the case population, 1 variant detected only in control individual and 6 variants found in both cases and controls. Subsequent genotyping of a larger control population revealed 5 missense mutations remained unique to the case cohort (three non-conservative AA substitutions, 2 moderately conserved between species and 1 found in more than one case) and a further 2 variants had a significant difference in frequencies between cases and controls. Unfortunately, the relatives of probands were not investigated, and hence whether these variants are inherited or segregate with disease is as yet unknown.

Pericentriolar material 1 protein (*PCM1*), a protein binding partner of *DISC1*, was screened for rare mutations in 32 individuals with schizophrenia and 219 white control samples. One novel rare nonsense mutation was detected in the heterozygous state in an individual with schizophrenia and absent in the control population. This null mutation was subsequently found to be carried by the proband's affected mother and one sibling with schizoaffective disorder but not carried in seven unaffected members of the maternal and paternal sibship (Kamiya et al., 2008).

Darier's disease (DD) is a rare autosomal dominantly inherited dermatological disease frequently accompanied by neurological disorders such as mild mental retardation, epilepsy and psychiatric illness. The mutated gene, *ATP2A2*, identified as causing Darier's disease maps to 12q23–q24.1 and encodes a sarcoplasmic/endoplasmic reticulum calcium pump that plays a role in intracellular calcium signalling (Sakuntabhai et al., 1999). The screening of *ATP2A2* in cases with neuropsychiatric phenotypes with and without DD has produced mixed results. For example, a screen of the gene in 19

probands with DD, ten of which presented with neuropsychiatric symptoms, detected 17 different coding variants and missense mutations. Intriguingly, the mutations, identified in the patients with neuropsychiatric features, showed non-random clustering in the 3' half of the gene (Jacobsen et al., 1999). In contrast, a second screen of DD cases with neuropsychiatric phenotypes did not find an association between a specific class and differential spread of mutations in DD cases with neuropsychiatric features, and resequencing *ATP2A2* in a cohort of bipolar cases failed to identify any non-synonymous variants (Ruiz-Perez et al., 1999; Jacobsen et al., 2001). These latter findings are in accordance with results from pedigree analysis of DD families showing incomplete co-segregation of bipolar disorder and Darrier's disease (Green et al., 2005). Together, this would suggest that mutations within *ATP2A2* on their own are insufficient to confer major risk for psychiatric illness, but supports instead that the DD locus is in linkage disequilibrum with, as yet unidentified, highly penetrant autosomal dominant risk factors.

Wolfram syndrome (WFS1) is a rare autosomal recessive neurodegenerative disorder characterized by the presence of diabetes mellitus and optic atrophy, although additional symptoms such as sensori-neural hearing impairment and psychiatric features are reported to be common in WFS1 patients. The *WFS1* gene encodes a glycoprotein predominately localized in the endoplasmic reticulum whose function is currently unknown (Takeda et al., 2001). Homozygous deleterious mutations (usually null mutations and unique to a family) within *WFS1* give rise to clinically heterogeneous WFSL phenotype. However, heterozygous carriers in WFS1 families are 26-fold more likely to require psychiatric hospitalization for major depression than non-carriers (Swift et al., 1998; Swift and Swift, 2005). Mutation detection studies in patients with psychiatric disorders have led to the identification of over 20 rare missense mutations, although the causality of some of these variants is hard to interpret as several of studies did not include control samples. Furthermore, case control studies of three common coding variants indicate a significant association with suicide attempts and completions (Crawford et al., 2002; Adolfo Sequeira, 2003). The private nature of most of the

identified mutations suggests that multiple but very rare variants within *WFS1* may be major risk factors for MDD and other psychiatric disorders.

4.3.4 The nature of the *ABCA13* rare variants discovered: penetrance issues, variable expressivity, and mutation effects

In the present study, 9 putative pathogenic coding mutations within highly conserved functional regions of *ABCA13* were identified. Follow-up studies did not find evidence for any mutation being *de novo* but showed segregation for 5 of the variants, R4728X, S3704R, H3609P, R3604Q and T4550A, within 15 families with severe psychiatric conditions. Moreover, segregation analysis indicated incomplete penetrance of variants, a finding anticipated from the lack of concordance in monozygotic twins and consistent with previous rare variant studies of complex neuropsychiatic diseases discussed above. It is worthy of note however, that some second generation members of pedigrees may be too young to express a disease phenotype and that this might be a contributing factor to a proportion of the variable expressivity.

The occurrence of the same mutations in individuals with phenotypes across the psychiatric spectrum supports an overlap of aetiologies for these disorders consistent with previous findings. For example, the phenotypic heterogeneity caused by a single mutation within ASD candidate genes (discussed above) and a single cytogenetic lesion disrupting *DISC1* in a large multiplex family (Blackwood et al., 2001). However, numerous candidate gene SNP-tag studies have reported the association of a SNP or haplotype with one specific psychiatric diagnosis. For example, different common haplotypes or variants within the genes *NPAS3* and *GRIK4* are associated with both bipolar and schizophrenia (Pickard et al., 2005a; Pickard et al., 2006). Collectively, these findings, would suggest that multiple genetic mechanisms in conjunction with environmental factors may differentially influence liability to develop a clinical phenotype.

Rare variants in other ABCA sub-family members give rise to variable phenotypes. For the majority of cases, and unlike the present findings, different mutations within the same gene results in distinct clinical diseases. For instance, loss of function mutations in *ABCA12* carried in the homozygous or as compound heterozygous state cause a severe form of a keratinization disorder known as harlequin ichthyosis, whereas homozygous and heterozygous missense mutations located in the first NBD result in a milder form of the disorder- lamellar ichthyosis type 2 (Kaminski et al., 2006). Similar to *ABCA12*, homozygous and compound heterozygote mutations in *ABCA1* result in Tangier disease, (TD) a severe form of HDL deficiency while rare heterozygous alleles cause low levels of high-density lipoprotein cholesterol (HDL-C) a factor which contributes to developing coronary artery disease (Bodzioch et al., 1999; Brooks-Wilson et al., 1999; Slatter et al., 2008). Furthermore, mutation analysis suggests that where they occur may determine the type of clinical presentation. For example, clusters of mutations localized within the first extracellular domain and the C-terminus are associated with a cardiovascular phenotype, whereas mutations which cluster near to or within the first NBD frequently coincide with splenomegaly (Kaminski et al., 2006).

In a third ABCA member, *ABCA4*, sequence variations cause a variety of degenerative retinal dystrophies, e.g. Stargardt disease (STGD), cone-rod dystrophy type 3 (CRD3), retinitis pigmentosa type 19 (RP19) and age-related macular degeneration (AMD), which vary in clinical severity. Again, there appears to be a broad correlation between class of mutation(s) and severity of retinal disease which has led to the formulation of the 'residual activity model' in which the level of residual ABCA4 protein activity/function is hypothesized to determine clinical phenotype (van Driel et al., 1998; Rozet et al., 1999). However, the complexity of the genotype/phenotype correlation is also illustrated by the observation that a small number of the same rare homozygous and complex alleles (compound heterozygote) have been identified in patients with different phenotypes (Allikmets, 2000; Kitiratschky et al., 2008).

These findings suggest that the distribution of variants, class of mutation and allele status, i.e. heterozygote, compound heterozygote or homozygote, in mutated ABCA sub-family members all may be factors influencing disease expression. The spread of rare variants detected in the current screen of *ABCA13* does not show any clear clustering of mutations. As the majority of these variants were found in individuals presenting with schizophrenia, bipolar disorder or MDD, there is no evidence supporting that mutation location influences clinical expression. However, as only exons encoding the functional domains were screened it is still possible that a distribution bias in variant type, which may correlate to variable disease presentation, exists.

Missense mutations can give rise to dominant negative effects through an altered gene product that interferes with the wild type protein function. The location of the identified missense mutations within the encoded ABCA13 protein suggests that pathology can result either from inactivation of the nucleotide binding domains or through the modification of the properties of the channel. In contrast, null mutations, such as a truncated protein resultant from premature stop codon or cytogenetic disruption are predicted to cause illness through either haploinsufficiency owing to 'nonsense-mediated decay' of the truncated allele's transcript or a gain-of-function effect whereby the truncated protein product gains a new and abnormal function. The present results suggest that both the missense mutations and the potentially 'null' nonsense and splice variant mutations contribute to all three clinical phenotypes and therefore there is no apparent effect of class of mutation or functional mechanism on clinical outcome. Furthermore, it is as yet unclear from the data whether severe, null homozygous mutations within *ABCA13* cause either a lethal or clinically distinct severe phenotype.

Previously identified heterozygous null alleles have not always been found to be causally related to disease. For instance, a splice variant within the gene *ciliary neurotrophic factor* (*CNTF*) predicted to result in a truncated protein has been reported not to be associated with a variety of neurological and psychiatric disorders (Takahashi et al., 1994; Van Vught et al., 2007). However, their findings differ from the present

results in two important ways. First, the *CNTF* null allele was originally identified in the homozygous state in 4 out of 151 controls and 5 out of 240 neurological disease subjects and hence had a higher frequency in the control population than cases. Second, the null allele occurs in more than 2% of the general population and so may be classified as a polymorphism rather than rare variant. The *CNTF* null allele also highlights that mutation effects are protein-specific and dependent on the disrupted function of the gene product with specific cells.

Premature termination codons introduced by random mutation may not always terminate at the optimal efficiencies expected of naturally occurring stop codons. Examples exist whereby the translation of a significant proportion of the growing polypeptide chain continues beyond the termination codon – a process known as read-through (Fox, 1987). In mammalian genes there is some evidence that the translation termination signal might be influenced by its context and more specifically by the bases following the nonsense codon (McCaughan et al., 1995). This observation has been proposed as one explanation as to why nonsense mutations located in a conserved region of the cystic fibrosis transmembrane conductance regulator (*CFTR*/*ABCC7*) are phenotypically less severe (Fearon et al., 1994). Using in vitro and in vivo studies of termination signals in mammalian systems, McCaughan and co-workers (1995) found that efficiency of termination was biased by the fourth and fifth base immediately adjacent to UAG. Their data suggested that UAGC was a relatively weak termination signal, as is the sequence introduced by the nonsense mutation within *ABCA13*. However, signal effectiveness was found to be greatly increased if the fifth base were G. As the *ABCA13* nonsense mutation is followed by the bases CG, we would predict that termination does occur with some efficiency.

Furthermore, a consequence of read-through at an opal (UGA) stop codon is the insertion of a selenocysteine amino acid into the polypeptide chain (Lee et al., 1989). The *ABCA13* nonsense mutation is located within a highly conserved A-loop motif (*A*romatic residue interacting with the *A*denine ring of *A*TP) of the second NBD, and the mutated arginine residue is immediately adjacent to the aromatic residue tyrosine which

interacts with the adenosine ring of ATP (Ambudkar et al., 2006). If read-through were to occur, the substitution of the arginine for an inserted selenocysteine may well have an effect on local chemistry, thereby disrupting ATP-binding.

Taken together, these observations suggest that the R4728X nonsense mutation should have a significant effect on *ABCA13* function either through null or loss of function mechanisms. However, the detection of R4728X in 5 control individuals, suggests that the associated estimated risk is more in line with a less penetrant 'risk' missense mutation. One explanation for this discrepancy may be that the R4728X mutation is sufficient to contribute to risk alone whereas some of the missense mutations identified may contribute to risk in an additive manner as discussed below. This suggestion would also be consistent with the evident familial segregation of R4728X with illness, which is less prominent (as would be expected if two or more risk variants needed to be transmitted together) for the missense mutations.

4.3.5 Interacting variants in psychiatric illness

In the current study nine mutations were found in the heterozygous state consistent with a model of dominant inheritance. The majority of cases identified were heterozygotes, but one affected individual was found to be a homozygous for the missense mutation H3609P. Whether this individual belongs to a family where consanguinity has occurred, i.e. a state in which there is higher likelihood of recessive risk alleles being inherited, is unfortunately at present unknown.

What is unique to this study and thus far not described in schizophrenia, bipolar or MDD research, is the identification of cases carrying more than one putative risk variant, e.g. compound heterozygotes, and the fact that these individuals present with more severe phenotypes. From this observation we can hypothesis two important issues. One, interactions between rare risk variants across a gene may be a common mechanism which, in an additive manner, contributes to susceptibility to psychiatric illness. Evidence supporting multiplicative allele interaction comes from a candidate gene study

of *NPAS3* in which several common risk-increasing and protective haplotypes were identified with clear frequency differences between the bipolar/schizophrenia case and healthy control cohorts. These were shown to interact with each other, dictating the net genetic risk of psychiatric illness (Pickard et al., 2008a). Two, the additive effects of multiple rare risk alleles may also result in a more severe clinical outcome and hence may increase penetrance, i.e. the presence of non-affected carriers evident in affected families. In this model, similar to findings for the other ABCA family proteins described above, the severity of the clinical phenotype would correlate with genetic load.

4.3.6. Odds ratio estimates for common and rare variants

Odds ratios calculated for common and rare variants known to contribute to complex diseases such as breast cancer and colorectal cancer are suggested to have different distributions. For common variants ORs are usually below 2 and based on observations from a range of recent publications cited by Bodmer and Bonilla, have an estimated mean OR of 1.36. In contrast, for rare variants most have ORs above 2 with a mean estimated as 3.74 (Bodmer and Bonilla, 2008). The observed ORs in the current study range between 0.5 to infinity, and, excluding variants unique to cases or found in one case and control only, have a mean OR of 2.32. Moreover, two variants, T4550A (OR 3.8 CI 1.1-12.7) and R4728X (OR 2.4 CI 0.8-7.0) have ORs above 2, and a further three variants, H3609P (OR 1.9 CI 0.9-4.0), R4590W (OR 1.9 CI 0.7 to 5.1)) and R4843C (OR 1.6 CI 0.7 to 4.0), with values between 1.6-1.9.

Using the calculated ORs and associated IC intervals as an estimate of penetrance may explain in part why some mutations, e.g R4728X, provide more evidence of concordant segregation within families as opposed to variants with lower ORs. However, in contrast to the view as argued by Bodmer and Bonilla, that owing to low penetrance, rare risk variants do not give rise to a familial concentration of cases – the present findings indicate that the penetrance of some rare variants must be sufficiently high (0.5) to show

familial concentration that is similar to standard mendelian segregation (Bodmer and Bonilla, 2008).

4.3.7. How do the findings fit with current models of complex genetic disease?

Rare sequence variants are known to have an important role in the multifactorial inheritance of common diseases such as breast cancer, colorectal cancer (CRC) and Alzheimer's disease. Using these diseases as a model of the contribution of rare variants to complex disease, it has become clear that the term 'rare variant' covers two categories of mutation. First, the classical rare deleterious familial mutations are analogous to the type of mutation detected for Mendelian diseases. These mutations are predominately null private mutations, show strong familial aggregation have high penetrance and very low frequencies (>0.1). The second type of variant, as reviewed by Bodmer and Bonilla, have a higher frequency in the case population (0.1% to 2-3%) and ORs of 2 or above; are carried in one or more affected individuals but do not show familial concentration, i.e. are sporadic in nature, and in the majority are missense mutations of unknown clinical significance (Bodmer and Bonilla, 2008). It is important to note that both types of rare variant would not be detected by whole-genome studies and are suggested to be population-specific, both properties having important consequences for confirmatory candidate gene studies.

Although the present data does not fit exactly into the two classes described for these diseases (e.g. MAFs calculated are all <0.5% and clear familial segregation for R4728X which has an OR of 2.4) there is evidence supporting some dichotomy. For instance, S3704R conforms to the first class of null, private mutation, with high penetrance apparent from familial segregation and a very low estimated frequency. Conversely, the missense mutations H3609P, T4550A and R4590W show characteristics more typical for the second class of rare variant: for example, being detected in controls and having moderate ORs, less familial concentration and higher observed frequencies. Thus these

data are the first to lend support to a genetic architecture of psychiatric disorders comparable to other common, genetically complex and heterogeneous diseases.

Genes identified as rare variant contributors are commonly discussed in terms of their mutation load. Owing to the rarity of these variants, a global or combined p-value is typically reported as evidence of association. In the present study the summation effects of all coding risk variants resulted in a global p-value of 0.000025. However, mutation detection studies of major genes for other complex disorders, for example *BRCA1/BRCA2* and breast cancer, have subsequently led to the identification of hundreds of different rare pathogenic mutations (Walsh et al., 2006). Therefore, it is plausible that the re-sequencing of additional *ABCA13* exons may result in the detection of further mutations and hence indicate increased association of *ABCA13* with disease risk.

Furthermore, as indicated by SNP-tagging association studies of *DISC1*, rare variant genes may also harbour common, small-effect, modulating risk alleles (Hennah et al., 2008). Indeed, in a case-control GWA study of bipolar individuals, a common SNP located within *ABCA13*, was in the top 500 most significant associations (Blackwood et al., personnal communication) It is possible, therefore, that the potential collective effect of rare *ABCA13* mutations and common variants may explain a considerable proportion of psychiatric illness.

The current results strongly support the rare variant hypothesis of complex common diseases and implicate *ABCA13* as a gene of large effect. With the advancement of re-sequencing technologies, comprehensive mutation detection studies of *ABCA13* and other appropriately selected candidate genes will reveal the extent to which rare mutations contribute to psychiatric illness. Concurrently, the discovery of rare highly penetrant variants may enable the development of preventative disease screening in addition to providing insight into biological pathways critical to disease development.

4.3.8. The function of ABCA13 and its potential involvement in biological processes

All ABCA proteins functionally characterized to date are known to shuttle lipid molecules across cellular membranes (Albrecht and Viturro, 2007). The presence in ABCA13 of a conserved C-terminal motif known to be shared among the lipid transporting group adds weight to its likely role in this process (Fitzgerald et al., 2004). Over a 1000 different lipid species exist in eukaryotic cells and, in addition to being structural components of cellular membranes, different species have key roles in processes such vesicular trafficking, signal transduction and transcriptional regulation (D'Angelo et al., 2008; van Meer et al., 2008). While the precise substrate/allocrite for the ABCA13 transporter remains to be identified biochemically, abnormalities in lipid metabolism have been strongly implicated as a potential underlying pathology in psychiatric illnesses, as discussed in chapter 1.

Lipid metabolism and movement of specific lipid species to appropriate cellular compartments is a highly regulated mechanism which, when disrupted in a global or local manner, could impact on a number of diverse biological processes. The most plausible of these processes to underlie psychiatric phenotypes are defects in intracellular signalling pathways, oxidative stress, synaptic function and myelination. In recent years, polyunsaturated fats and complex lipids such as arachidonic acid and sphingolipids have received attention owing to their role as second messengers in proliferation, differentiation, apoptosis, and inflammation. For example, as a second messenger, arachidonic acid (AA) can act as a retrograde signal modulating LTP, or activate protein kinase C (PKC) which in turn is able to interact with the NMDA receptors suggesting a role in neuronal excitability and neuroplasticity (Williams et al., 1989). Similarly, inositol phospholipids are involved in the intracellular second messenger inositol-1, 4,5-triphosphate (IP3) and diacylglycerol (DAG) pathways which are endogenous activators of PKC (Lenox and Wang, 2003). Interestingly both IP3 and DAG are hypothesized to be downstream components of a signaling pathway directly affected by lithium, an anti-manic agent used to treat bipolar patients (Quiroz et al.,

2004). Furthermore, both lithium and a second mood-stabilising drug, valproic acid, are reported to have their therapeutic effects via decreased AA turnover (Chang et al., 1996; Chang et al., 2001).

Oxidative stress is a pathological process whereby an excessive increase in reactive oxygen species (ROS) and reactive nitrogen species (RNS) by mitochondrial dysfunction can cause cell death and tissue damage. A number of publications have implicated free radicals and oxidative stress in schizophrenia pathology (Yao et al 2005). Sphingolipids such as ceramide have been shown to play an important role in receptor mediated signal cascades but also in the generation of ROS and RNS through regulation of antioxidant enzymes (Won and Singh, 2006). In parallel, ROS and RNS regulate sphingolipid metabolism through regulating enzymes responsible for their metabolism. Hence, sphingolipid metabolism and redox homeostasis are regulated in a bidirectional manner which when disrupted may cause a pathological state.

The proper composition of cellular membranes is critical for the normal function and compartmentalization of ion channels and synaptic receptors. Ion channel activity has been shown to be modulated by direct interaction with membrane lipids. For instance, phosphatidylinositol 4,5-bisphosphate (PIP_2) serves as an obligate cofactor of inward rectifying (Kir) potassium channel activity (Tucker and Baukrowitz, 2008). Moreover, membrane-protein interaction between the negatively charged phosphate group in membrane lipid molecules and voltage-gated potassium channels is essential for channel activation (Schmidt et al., 2006).

Neurotransmitter receptors are predominately concentrated and precisely localized in specific microdomains within the neuronal membrane called lipid rafts (Simons and Ikonen, 1997). These cholesterol- and sphingolipid-enriched microdomains are proposed to act as an assembly for clusters of receptors and components of receptor-activated signalling cascades. Disruption of lipid rafts through, for example, the depletion and enrichment of cholesterol decreases optimal neurotransmitter agonist potency at GABA

and nicotinic acetylcholine (nACh) receptors, whilst the integrity of the lipid rafts appear to be also necessary for the maintenance of normal synaptic morphology and dendritic spine density (Sooksawate and Simmonds, 2001; Hering et al., 2003). Furthermore, *in vivo* and *ex vivo* studies indicate endogenous neuronal cholesterol biosynthesis, turnover and transport impair hippocampal paired pulse facilitation (PPF) and LTP and hence has a significant effect on synaptic plasticity. As cholesterol is also known to bind directly to a number of transmembrane ion channels, enzymes and receptors, it is as yet unclear whether such modulated synaptic function is a result of direct interaction or indirect disturbance of lipid raft composition (Haines, 2001).

Antidepressants and antipsychotic drugs are also reported to affect receptor function at lipid raft micro-domains. For example, the antidepressants desipramine, fluoxetine, and reboxetine and the antipsychotics fluphenazine, haloperidol, and clozapine were found to co-localize with the ligand-gated serotonin 5-HT3 receptors in raft-like domains. The concentrations of these psychopharmacological drugs within the domain was strongly associated with the inhibitory potency against serotonin-induced cation currents (Eisensamer et al., 2005)**.** Moreover, treatment with the antidepressants desipramine and fluoxetine has been shown to result in the movement of $G\alpha_s$ out of lipid rafts and into a closer association with adenylyl cyclase and thus thereby potentially modulating cAMP signaling cascades (Donati and Rasenick, 2005). Taken together, these findings indicate that antidepressants and antipsychotics might exert some of their therapeutic efficacy by altering a component of the membrane that is associated with lipid rafts.

A third body of research supports a link between fatty acids and neurotransmitter function. Animal and clinical studies suggest that fatty acid supplementation mediates its therapeutic effects through modulation of the serotonin $(5\text{-HT})_2$ receptor complex. For example, omega-3 fatty acid enhances the 5-HT responsivity as measured by the magnitude of 5-HT amplification on ADP-induced platelet aggregation (Yao et al 2004). Using a rodent model, omega-3 fatty acid and omega-6 fatty acid supplementation has been shown to alter 5-HT receptor and transporter binding and implicated to modulate

the biogenic amine metabolism (Hibbeln and Salem, 1995; Farkas et al., 2002). Likewise, fatty acid deficient diets differentially affect dopamine D2 receptor binding and significantly decrease dopamine concentrations (Hibbeln and Salem, 1995; Zimmer et al., 2000). Although the molecular mechanisms underlying these effects are currently unknown, these observations suggest that the fatty acid supplementation consistently shown to ameliorate the clinical symptoms of psychiatric disorders may be mediating its therapeutic effect via modulation of neurotransmitter function.

Finally, myelination-the formation of a myelin sheath around the axons of neurons, is essential for the fast propagation of action potentials and the maintenance of axonal integrity. The myelin sheath is a specialised, lipid-rich domain of the glial cell plasma membrane, synthesised by oligodendrocytes in the CNS. This cellular membrane is composed of a specific subset of lipids and proteins the assembly of which is tightly regulated in time and place (Simons and Trotter, 2007). Molecular abnormalities of myelin and consequential white matter deficits are an attractive candidate pathological process for schizophrenia. Reduced levels of the major structural phospholipids of myelin have been found in several regions of the brain in schizophrenic patients. Moreover, microarray analysis and transcriptomic investigation indicate down regulation of oligodendroglia and myelin biosynthesis genes associated with psychiatric disorders (Schmitt et al., 2004; Segal et al., 2007; Smesny et al., 2007; Sokolov, 2007; Tkachev et al., 2007).

The timescale of myelination, beginning prenatally and with full maturation occurring during adolescence and early adulthood, is consistent with the neurodevelopmental profile of schizophrenia, whilst a global impairment in white matter activity is in keeping with the disconnection hypothesis of schizophrenia which posits a failure in "the integration of functionally specialized systems". It is therefore not inconceivable that a deficit in specific lipid species may underlie abnormalities impacting upon the process of myelination either alone, or in conjunction with, disruption of other biological

processes and that these pathological abnormalities contribute to the expression of psychiatric illness.

Many pertinent questions regarding *ABCA13* cellular function remain currently unanswered. Important future considerations should include the analysis of lipid species translocated and ABCA13 subcellular localization and cellular distribution in brain. Furthermore, the elucidation of putative protein binding partners may reveal ABCA13's involvement in local cellular pathways or biological systems; and thus suggest new directions for research in the quest to find rationally based treatments and preventative strategies for some of the most common and disabling psychiatric disorders.

To conclude, the identification of multiple rare coding mutations among unrelated cases and found to segregate in pedigrees provides both biological evidence and epidemiological support for the causal role of *ABCA13* in psychiatric disease. These discoveries also present significant novel insight into the genetic architecture of psychiatric disorders consistent with molecular models and previous findings of other complex diseases. Furthermore, *ABCA13*'s candidacy provides not only a starting point for further examination of pathological pathways and processes but opens up exciting possibilities for the development of new therapies of schizophrenia, bipolar disorder and depression.

CHAPTER 5

ANALYSIS OF *ABCA13* EXPRESSION

ACKNOWLEDGEMENTS FOR CHAPTER 5

Advice on Immuno-histochemistry techniques and analysis of expression was kindly provided by and Dr. Rachel James (Centre for Neuroscience, University of Edinburgh) and Professor J. Bell and Dr. Robert Walker (Neuropathology Unit, University of Edinburgh).

5. ANALYSIS OF *ABCA13* EXPRESSION

5.1 Preface

Chapter 4 presented data providing strong evidence supporting the hypothesis that *ABCA13* is a highly penetrant risk factor for psychiatric illness. However, the exact function of ABCA13, its role in biological pathways and expression in human brain are still unknown. With an aim to explore these issues, the expression profile of *ABCA13* transcripts in cell lines and human tissue and ABCA13 protein subcellular localization and cellular distribution in human post-mortem brain were examined.

5.2 Results

5.2.1 RT- PCR of human ABCA13 in cell lines and brain tissue

Pairs of oligonucleotide primers were designed across exons encoding for the large N-terminal transmembrane domain, first transmembrane domain cluster, middle of protein between TMD/NBD1 and TMD/NBD2, and second transmembrane domain cluster depicted in figure 5.1a. The spread of primer pairs across the gene would identify any potential disparities in expression across the gene – an important consideration as other members of the ABC gene family can exist in different splice forms or can even produce transcripts encoding just 'half' of the gene.

RT-PCR was performed on cDNA derived from two human neuroblastoid cell lines LAN5 and SH-SY5Y, two human glioblastoma cell lines U373 and MOG, an embryonic human kidney cell line HEK293 human lymphocytes and human blood RNA. In addition, cDNA from post-mortem human hippocampus and frontal cortex was analysed for expression of a short and long transcript located within the middle of the protein.

ABCA13 was found to be expressed only in the glioblastoma U373 cell line across all regions of the transcript analysed, as shown in figure 5.1.b.

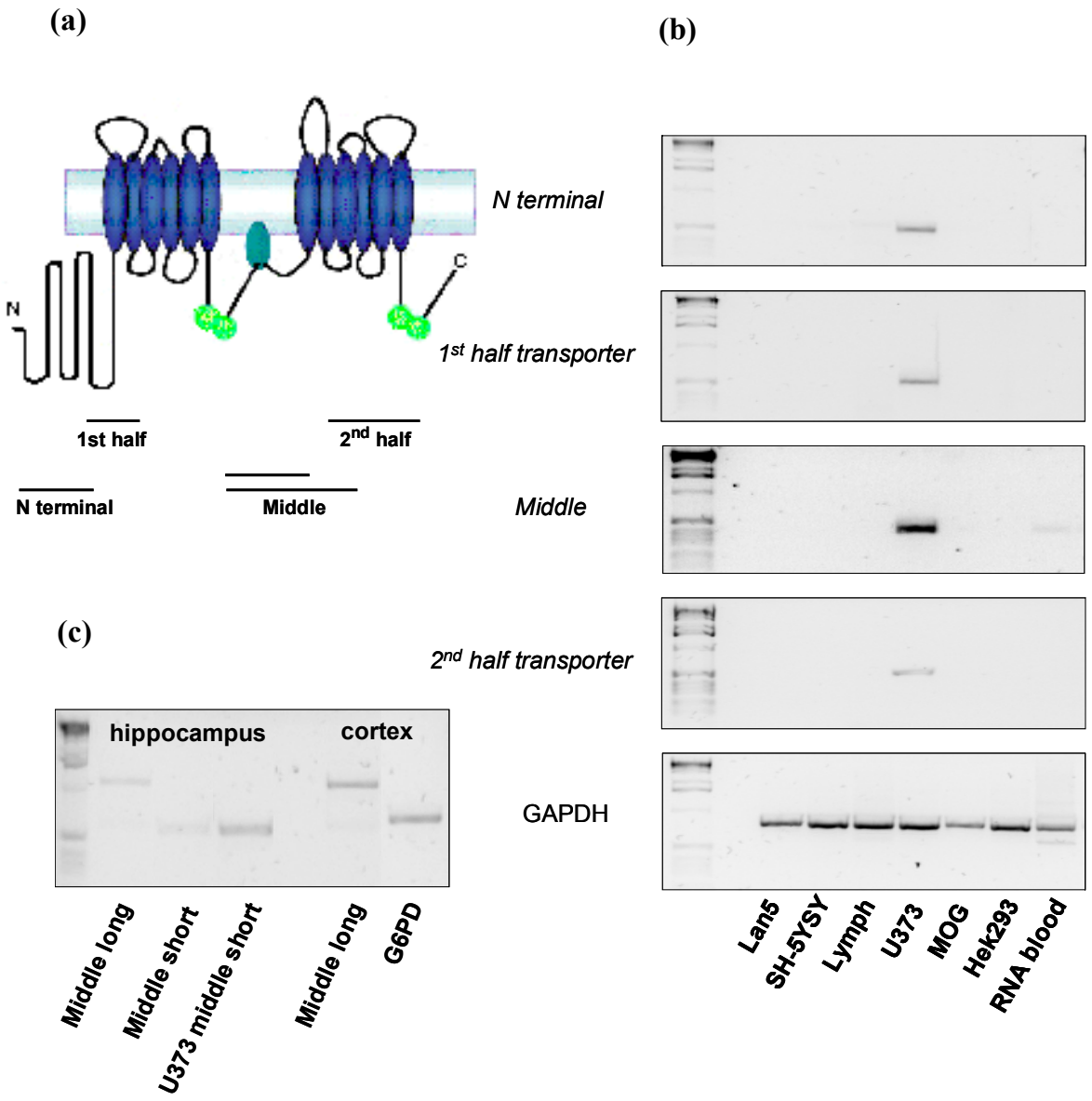

Figure 5.1 Human *ABCA13* expression in cell lines and human tissue. (a) Schematic representation of ABCA13 showing regions examined by RT-PCR. (b) *ABCA13* mRNA transcript expression assessed in cell lines, lymphocytes and human blood. GAPDH was used as a positive control. (c) *ABCA13* mRNA transcript expression in post-mortem tissue from the hippocampus and frontal cortex. *ABCA13* expression in the U373 cell line and G6PD expression in the cortex were used as positive controls.

There was no evidence for differential region-specific gene expression which could arise on account of the existence of multiple isoforms. *ABCA13* was shown not to be expressed in human blood or lymphocytes. Unfortunately, this means that future studies potentially investigating reduced expression of *ABCA13* RNA or protein in cases identified with mutations cannot be performed. However, *ABCA13* mRNA transcripts were found to be expressed in human hippocampus and frontal cortex tissue, indicating that *ABCA13* is a brain-expressed gene.

5.2.2 IHC analysis of ABCA13 in human post mortem brain sections

The RT-PCR expression profiling technique has the limitation that expression in specific cell types and subcellular domains within human brain regions can not be resolved. To further examine further the distribution of ABCA13 protein in brain, IHC was performed using transverse sections of the rostral medulla oblongata and coronal sections of the human frontal cortex and hippocampus. ABCA13 expression was analysed using a rabbit anti-human affinity purified polyclonal antibody (ABCA13 870) raised against a C-terminal amino acid sequence not homologous with any of the cloned proteins belonging to the ABC family.

A negative control (absence of primary antibody) and a positive control (primary antibody Glial Fibrillary Acidic Protein [GFAP] – an astrocyte marker) were performed on every IHC run. Omission of a primary antibody resulted in tissue sections without any visible DAB reaction product, indicating that the protocol used did not result in any non-specific background signal.

In all nuclei of the medulla oblongata, e.g. lateral vestibular nucleus, inferior olivary nucleus, hypoglossal nucleus and dorsal motor nucleus of the vagus, ABCA13 870 immunoreactivity was observed in glia cells and large neurons, localized primarily to the cell cytoplasm, shown in figure 5.2. It is possible that a similar pattern of staining might be observed if an antibody does not bind specifically to protein peptide sequence. To

assess the specificity of the ABCA13 870 antibody, IHC was performed using pre-immune serum taken from the animal prior to immunization. This pre-immune serum should bind to proteins within brain tissue in a non-specific manner, and hence characterize non-specific immunoreactivity.

Immunoreactivity for ABCA13 870 was found to differ from non-specific reactivity for the corresponding antiserum. For example, as indicated in figure 5.2b and d, pre-immune serum reactivity was evident in the nuclei of cells and prominent within the white matter tracts of the medial lemniscus. In contrast, ABCA13 870 reactivity was frequently observed to be absent from the nuclei of large neurons and within white matter tracts, shown in figure 5.2a and c. ABCA13 870 reactivity, however, was seen in cells interspersed between the tracts of white matter.

ABCA13 870 reactivity was consistently found in neuronal and glial cells in all layers of the frontal cortex. As indicated in figures 5.3a, b and 5.4a, reactivity was predominately restricted to the cytoplasm and in some cells immuno-positive staining was clearly observed to be localized to the endoplasmic reticulum. Furthermore, in the white matter underlying the neocortex grey matter, ABCA13 870 reactivity was seen in all types of glial cells, i.e. astrocytes, oligodendrocytes and microglia, as shown in figure 5.3b.

In the hippocampus ABCA13 870 immunoreactivity was evident in the cytoplasm of large mossy fibre neurons and smaller polymorphic cells within the hilus, and pyramidal cells of the CA4, CA3, CA2 and CA1 subfields (figure 5.5c). Moreover, prominent cytoplasmic staining was observed in the granule cells of the granule cell layer (GCL) of the dentate gyrus, shown in figure 5.5a.

A second antibody specificity test – the pre-absorption of the ABCA13 870 antibody with the immunizing peptide prior to IHC - was conducted using sections of the hippocampus only.

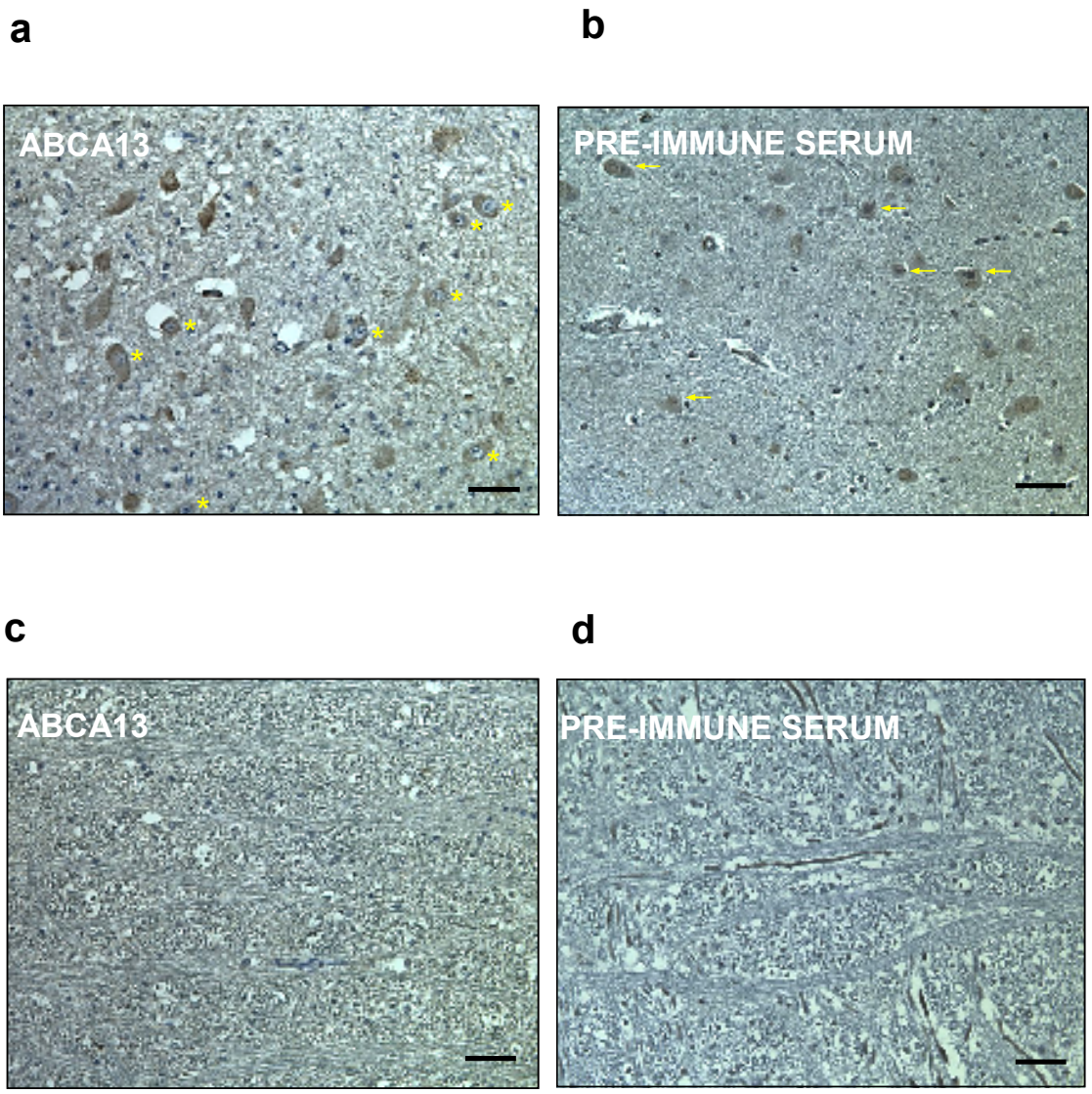

Figure 5.2 ABCA13 870 antibody and corresponding pre-immune antiserum immunoreactivity in the medulla oblongata. (a) ABCA13 870 antibody reactivity in the dorsal motor nucleus of the vagus. (b) Pre-immune antiserum reactivity in inferior olivary nucleus. ABCA13 870 reactivity (c) and pre-immune antiserum reactivity (d) in white matter tract of the medial lemniscus. ABCA13 870 reactivity was however observed in cells interspersed between the white matter tracts Yellow stars indicate large neurons in which reactivity is absent from cell nuclei. Yellow arrows show DAB stained non-specific reactivity in nuclei of neurons. Images captured at 160 magnification. The black bar represents 50μm.

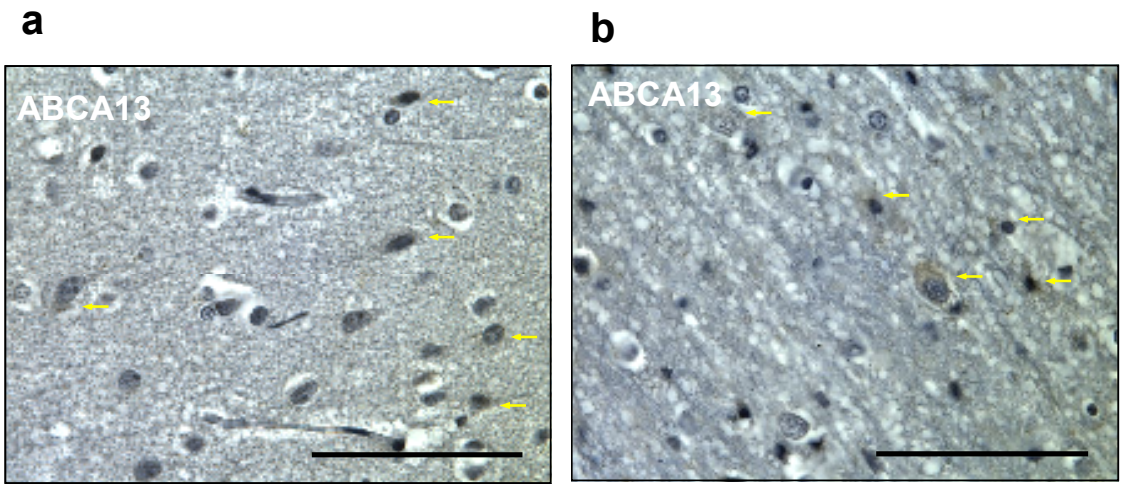

Figure 5.3 High magnification images of ABCA13 870 antibody reactivity in layers 2 and 6 and the underlying white matter of the frontal cortex. ABCA13 870 antibody reactivity in layer 2 (a) and layer 6 merging into the underlying white matter (b). Yellow arrows indicated DAB stained reactivity. Images captured at 400 magnification. The black bar represents 50µm.

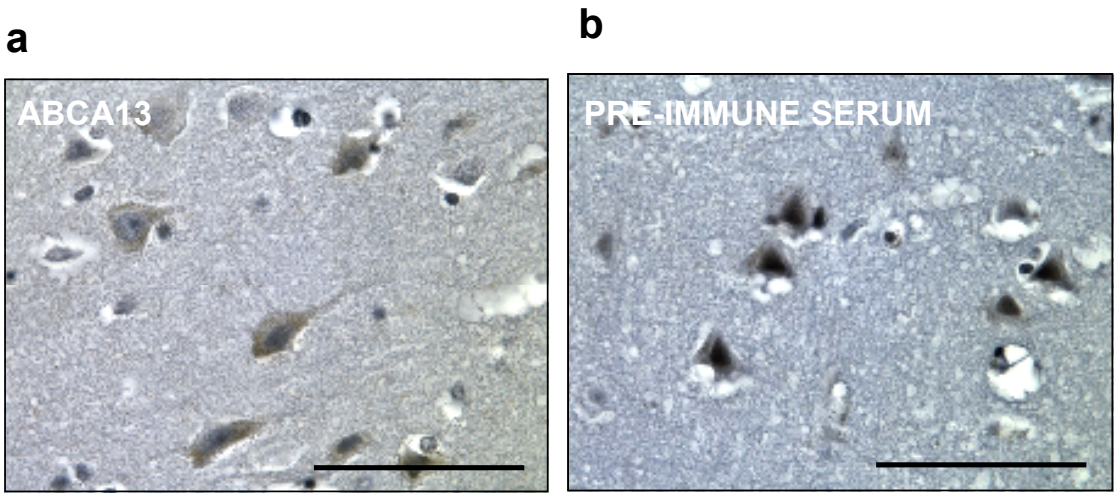

Figure 5.4 High magnification images of ABCA13 870 antibody and corresponding pre-immune antiserum immunoreactivity in layer 3 of the frontal cortex. (a) ABCA13 870 antibody immuno-postive staining appears to localize to the cell cytoplasm. (b) pre-immune serum reactivity apparent in the cytoplasm and nucleus of neurons. Images captured at 400 magnification. The black bar represents 50µm.

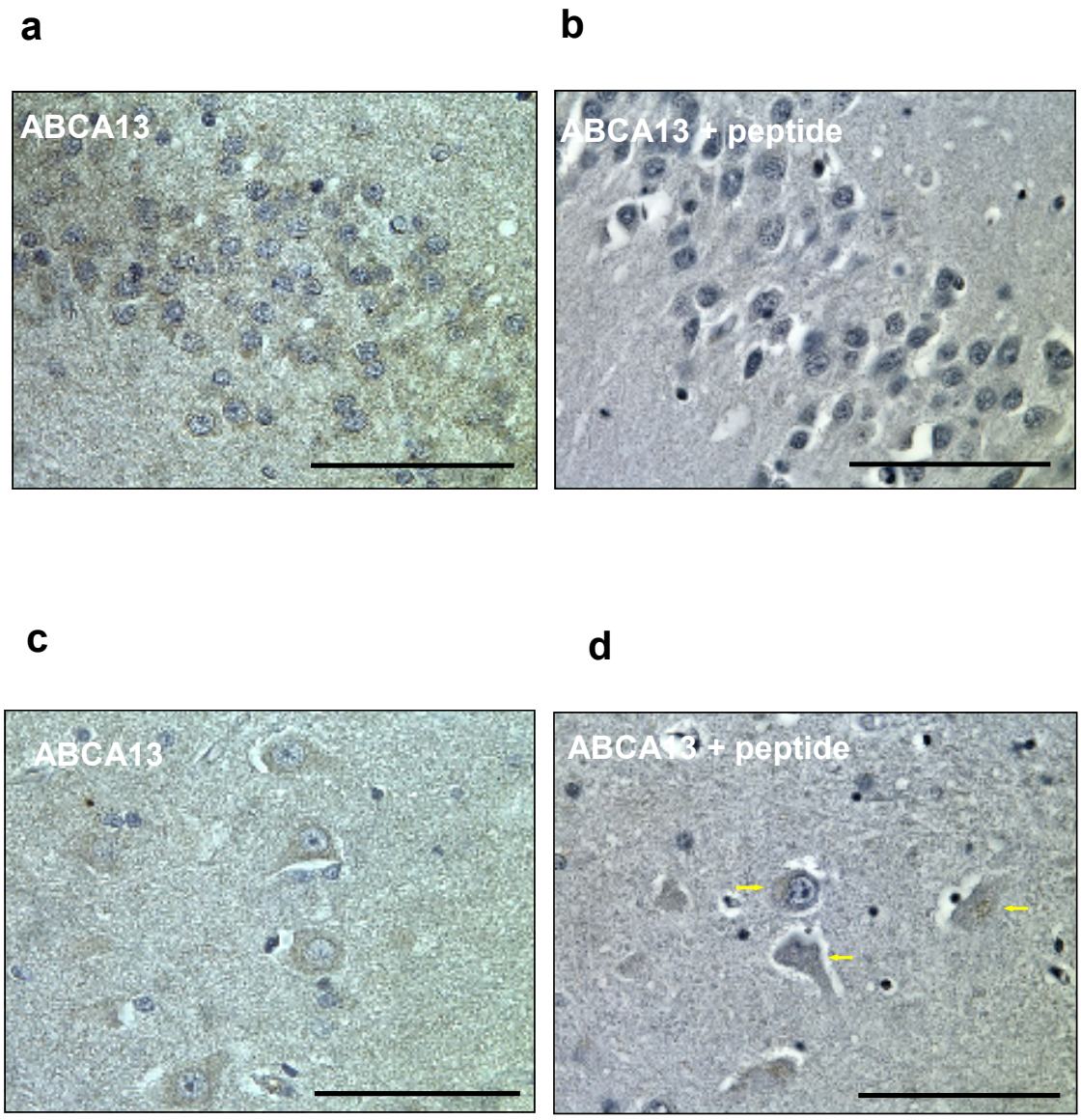

Figure 5.5 ABCA13 870 antibody and corresponding pre-immune antiserum immunoreactivity in the dentate gyrus and hilus of the hippocampus. (a) High magnification image of ABCA13 870 reactivity in the GCL of the DG and (b) ABCA13 870 blocked with pre-absorbed peptide in the DG. (c) ABCA13 870 reactivity in the hilus of the hippocampus and (d) after blocking with pre-absorbed peptide. The black bar represents 50μm.

This control assay should block specific immunoreactivity for ABCA13 and hence an absence of DAB reactivity would indicate primary antibody specificity.

Immuno-positive staining in the granule cells of the dentate gyrus was found to be almost completely absent following peptide pre-absorption (shown in figure 5.5b) suggesting that ABCA13 870 immunoreactivity within the granule cells represents genuine ABCA13 expression. Indeed, this finding is consistent with IHC data investigating abca13 expression in mouse brain (R. Cannon, North Carolina Research Triangle, USA; personal communication). However, reduced immuno-positive ABCA13 870 staining in the large mossy fiber neurons in the hilus and pyramidal cells of the CA regions was still observed after peptide incubation, shown in figure 5.5d. This would suggest that in addition to what appears to be to specific ABCA13 immunoreactivity in the granule cells, the ABCA13 870 antibody also cross-reacts with additional epitopes resulting in non-specific binding in these regions.

As the peptide pre-absorption control condition was not conducted prior to ABCA13 870 IHC in other brain sections, it is unclear whether the ABCA13 870 immunoreactivity observed and described above is indeed specific, i.e. indicative of real ABCA13 expression, or unspecific binding. Future experiments, including this control peptide pre-absorbtion control condition performed in other brain region sections and examining the immunoreactivity profile of additional human ABCA13 antibodies, will help to clarify the extent to which the ABCA13 870 antibody is specific for ABCA13.

5.3 Discussion

This chapter describes the investigation of *ABCA13* mRNA and protein expression in cell lines, human blood and brain tissue. RT-PCR assays indicated *ABCA13* to be expressed in one human-derived oligodendrocyte/astrocytoma cell line and post-mortem frontal cortex and hippocampus brain tissue. IHC performed using a polyclonal antibody which was assayed for ABCA13 protein specificity by means of two control conditions,

suggested that ABCA13 is localized to the cytoplasm of granule cells of the dentate gyrus. However, these experiments also indicated that the ABCA13 870 antibody binds to non-specific epitopes making the interpretation of ABCA13 expression difficult to determine.

5.3.1 ABCA13 expression in human and mouse tissues

Human expression studies

One previous study has investigated *ABCA13* mRNA expression in human derived cell lines and tissues. Prades and colleagues performed tissue profiling (which included multiple tissues from different brain regions including the hippocampus and frontal cortex) of all major transcripts which encode for the six predicted isoforms of human ABCA13. They found that expression of transcripts one and two, the full length isoform and an isoform which includes the functional domains but is missing the long N terminal tail, was highest in human trachea, testis and bone marrow. The remaining four transcripts were undetected in any tested tissues, and transcript expression was absent in brain (Prades et al., 2002). These results contrast with the present data, which indicated that in the two brain regions assayed – the hippocampus and frontal cortex - *ABCA13* mRNA is expressed.

In the same study Prades and coworkers also examined by means of real time PCR *ABCA13* expression in a panel of tumor cell lines. They report that expression was detected highest in one leukemia (SR), one prostrate (DU-145) and three CNS tumor cell lines (SNB-19, U251, SF-539) (Prades et al., 2002). One of these CNS tumor cell lines, U251, is suggested to be derived from the U373 human glioblastoma cell line, which was tested and found to express *ABCA13* in the present study. However, the present findings also indicated that in this glioblastoma cell line, transcripts relating to different regions of *ABCA13* were all consistently expressed. This finding supports the notion that, like all other *ABCA* sub-family members, *ABCA13* encodes for a full transporter

and not two half transporters – an issue which has important consequences for the functional interpretation of potential pathogenic mutations.

The aforementioned study did not test transcript expression in human blood or lympohctyes extracted from blood. To perform functional assays assessing the potential consequences of mutations using samples taken from mutation carriers, ABCA13 is needed to be expressed in the sampled tissues. Unfortunately, the current results did not detect any expression in human blood and lymphocytes, the easiest tissue to obtain from human subjects, and hence such function studies can not be conducted.

Rodent studies

One study conducted by Barros et al., (2003) has comprehensively investigated *Abca13* mRNA distribution in mouse tissues. Expression was reported to be highest in the submaxillary gland, epididymus, ovary, and thymus, however *Abca13* was also detected in brain, eye, liver, lung, heart, skeletal muscle, pancreas, kidney, thyroid, bone marrow, spleen, testis, prostrate, uterus and mouse embryo at lower levels, suggesting that *Abca13* is widely expressed (Barros et al., 2003). As discussed by the authors, the ubiquitous expression of *Abca13* is also observed with *ABCA1* - a gene/protein that when mutated is known to cause HDL-deficiency syndromes. Expression studies of *Abca1* have reported a lack of consistency between high levels of mRNA expression and corresponding protein expression. This has led to the suggestion that, like many ABC transporters, post-transcriptional modulation is a likely mechanism regulating ABCA1 protein expression. Indeed, although inconsistencies between *Abca13* mRNA and protein expression have not yet been investigated, post-transcriptional modification has also been suggested as an important mechanism potentially regulating Abca13 protein expression (Barros et al., 2003).

More recent unpublished research, performed by individuals in the same group, has used fluorescent IHC to examine Abca13 expression in mouse brain. They report that among

other regions of the brain, Abca13 is highly expressed in neurons of the locus ceruleus in the brain stem and granule cells of the dentate gyrus. Furthermore, high resolution analysis clearly indicates Abca13 to be localized to the cytoplasm and predominately in a subcellular domain corresponding to the golgi apparatus or endoplasmic reticulum (Cannon et al., personal communication).

These observations are consistent with the current results and highlight that ABCA13 is potentially expressed in a region in which new neurons are generated throughout adulthood. This process known as adult neurogenesis, and its link to psychiatric illness, is discussed in some detail in chapters 7 and 8. However, it is interesting to note and relevant to the current findings that in a recent study a biomarker of neural stem and progenitor cells (NPCs) located within the dentate gyrus and which give rise to newly generated mature cells was identified as a complex mixture of saturated and/or mono-unsaturated fatty acids and related compounds (Manganas et al., 2007). As yet, the functional relevance of these lipid molecules for the control of proliferation and differentiation of NPCs remains to be elucidated. However, as ABCA13 putatively transports one or more lipid species across membranes, its expression within granule cells of the dentate gyrus leaves open the interesting possibility that disruption of ABCA13 function may have a detrimental affect upon neurogenesis.

5.3.2 Expression profile and function of other ABCA sub-family members

Most ABC transporters belonging to the ABCA sub-class are reported to be expressed in a broad spectrum of tissues. However, their individual expression profiles, cellular localisation and consequential specific function within lipid secretory pathways influence why, when such genes are mutated, a diverse range of phenotypic diseases are caused. For example, mutations within *ABCA4* give rise to retinal diseases including Stargardt disease, cone-rod dystrophy, retinitis pigmentosa and age-related macular degeneration. The ABCA4 protein is highly expressed within the outer segment disk membrane of rod and cone photoreceptors located within the retina. It is proposed to act

as an outwardly directed flippase transporting a chromophore of the visual pigment rhodopsin (*all-trans* retinaldehyde), and hence its activity is likely to be involved in the recycling of *all-trans* retinal released from the photobleached rhodopsin during the retinoid cycle (Wenzel et al., 2007).

In contrast, genetic defects in *ABCA12* cause two hereditary dermatological keratinization disorders, harlequin ichthyosis and lamellar ichthyosis type 2. ABCA12 is expressed in many tissues but within the keratinocytes of the upper epidermal layers of human skin it is localised to the membranes of secretory intracellular lipid storage organelles called lamellar granules. Abnormal localisation of glucoceramide within cultured keratinocytes from harlequin ichthyosis patients suggests that ABCA12 is involved in the intracellular translocation of spingolipids within the lamellar granules during the process of kerotinocyte differentiation (Kaminski et al., 2006).

ABCA1 and ABCA2 are both highly expressed in brain, are implicated in brain lipid homeostasis and have been linked to neurodegenerative diseases of the brain. ABCA1 is expressed in multiple brain cell types albeit with significant cell and region expression differences. Evidence from rodent studies suggests that Abca1 plays a significant role in the lipidation and homestatic concentrations of apoE and in addition, may be a principal modulator of neurotoxic amyloid-β peptide production and amyloid desposition - histological symptoms of Altheimer's disease (AD) (Hirsch-Reinshagen et al., 2004; Kim et al., 2008). Conversely ABCA2 is reported to be expressed almost exclusively in oligodendrocytes within human brain matter and located within oligodendrocytes at the subcellular membranes of the endolysomal compartment and Golgi apparatus. ABCA2 is therefore postulated to have a role in intracellular lipid trafficking and may be important in the regulation of neural sphingolipid transport (Hirsch-Reinshagen et al., 2004; Kim et al., 2008). However, like ABCA1, ABCA2 has been indicated by genetic and biological studies to be linked to the pathology of AD as well as temporal lobe epilepsy (Mace et al., 2005; Arion et al., 2006).

Several ABCA transporters are known to be expressed in multiple cellular membranes. For instance ABCA1 is reported to be localised to the plasma membrane, golgi apparatus and lysosomal membranes in a variety of cell types, ABCA3 to the plasma membrane, lamellar bodies and lysosomes of alveolar pneumocytes, and ABCA5 to the golgi apparatus and lyosmomes within leydig cells of the testis (Wenzel et al., 2007). Differential subcellular localisation and hence the potential to influence distinct lipid pathways in different cells and tissues may explain how mutations in one transporter may give rise to various, phenotypically distinct, clinical disorders, e.g. ABCA1 is causally linked to Tangiers disease as well as being implicated to have a role in AD.

The unpublished findings by Cannon et al. indicate Abca13 is localised to the ER in spinal neurons in mice. The endoplasmic reticulum is the main cellular compartment of lipid synthesis suggesting that ABCA13 many be involved in the transport and hence appropriate delivery of lipid molecules to other organelles/membranes. However, ABCA13, like ABCA1, may be expressed in different compartments in various cell types. Future experiments investigating ABCA13 subcellular distribution in a variety of tissue may provide more insight into its functional involvement in lipid secretory pathways and potential propensity to cause disease.

Another characteristic of ABC proteins is that they do not appear act in isolation but instead are postulated to function as components of multi-unit complexes (Buechler et al., 2002; Munehira et al., 2004). Given the general broad range of tissues that express ABCA proteins it is likely that tissue-specific interacting partners might define a larger spectrum of biological activities associated with each transporter. Furthermore, in conjunction with differential subcellular distribution, cell-specific interaction with other proteins might also be a major factor influencing disease expression.

The evidence presented in this chapter, that ABCA13 is expressed in human brain, is just the beginning of our understanding of the potential function of ABCA13 and consequential psychiatric disease molecular pathology. Future research involving

conditional gene targeting, IHC co-localisation studies and protein binding assays may provide much needed insight into the potential tissue-specific roles, specific lipid species transported and physical interacting protein binding partners of ABCA13.

CHAPTER 6

A CASE-CONTROL ASSOCIATION STUDY OF A VARIANT WITHIN THE 3'UTR OF *GRIK4* AND BIPOLAR DISORDER

ACKNOWLEDGEMENTS FOR CHAPTER 6

The insertion/deletion (indel) variant was originally genotyped by J. Boyd in 259 bipolar disorder cases and 196 control individuals. To increase sample size I genotyped a further 160 cases and 27 controls before re-analysing the entire data set. The indel replication study was conducted by B. Pickard. To ensure that genotyping calls were consistent between both studies, I performed a second and independent call of all replication samples using the Genemapper program. The modeling of the RNA secondary structure was performed by R.S. Hamilton and I. Davis and allelic expression analyses by B. Pickard, as stated in the text. Figures 6.1 and 6.2 were produced by B. Pickard.

6. A CASE-CONTROL ASSOCIATION STUDY OF A VARIANT WITHIN THE 3'UTR OF *GRIK4* AND BIPOLAR DISORDER.

6.1 Preface

In a tagging SNP case-control association study, a haplotype located within 3'UTR *GRIK4* was found to be negatively associated with bipolar disorder (Pickard et al., 2006). Subsequent screening of the 3'UTR region in bipolar protective haplotype homozygous carriers revealed a 14bp deletion (ss79314275) segregating with the SNP haplotype.

6.2 Results

A case-control association study of the insertion/deletion (indel) variant was performed by genotyping 356 individuals diagnosed with bipolar disorder and 286 healthy control individuals. A significant difference between the groups was found (p=0.00000273 genotype, p=0.00000019 allele), as indicated in table 6.1a. No significant deviation from Hardy-Weinberg Equilibrium (HWE) was evident in the control population. However, deviation from HWE was found for the bipolar disorder samples, consistent with other findings reporting strong association in a disease group. The corresponding Odds Ratios (ORs) of 2.16 (95% confidence interval [CI]: 1.61-2.90) insertion allele and 0.46 deletion allele (95% CI: 0.34-0.62) could equally be interpreted to support the hypothesis that the insertion is a risk variant or, alternatively, that the deletion has a protective effect. However, as the deletion allele is rarer than the insertion allele (del frequency 0.24 controls, 0.13 cases; ins frequency 0.76 controls, 0.87 cases) and the original SNP association study showed association for a protective rather than risk haplotype, we prefer to describe the finding as a protective effect (figure 6.1). Moreover, as both genotype and allele p-values calculated in the present study are more significant than the Expectation Maximisation (EM) predicted haplotype p-values calculated in the

original SNP association study, this suggests that the indel is either in higher LD with the causal variant or is the actual variant itself.

Due to a significant overlap in samples typed for both the initial SNP association and the initial indel study, a replication study on an independent Scottish cohort of 376 controls and 274 bipolar disorder cases was performed by B. Pickard (Pickard et al., 2008b). Consistent with the findings above, a significant negative association for both deletion genotype (p=0.0166) and allele (p=0.0107) was shown (table 6.1b). However, although the frequency of the deletion allele was found to be similar between studies for controls (0.23), it was present at a slightly higher frequency in bipolar disorder cases (0.17). Hence, the calculated OR for the deletion allele is less pronounced OR0.69 (95% CI: 0.52-0.92) than in the first study.

Combining the two data sets results in an OR of 0.47 (95%CI: 0.36-0.62) for heterozygotes and an OR of 0.33 (95%CI: 0.18-0.58) for homozygous deletion individuals (table 6.2). The increased protection (reflected by a lower OR) for homozygotes suggests that the protective effect is additive or dose-dependent and implies that the underlying 'protective' mechanism may be transcript regulation, resulting in an increase in mRNA or protein expression.

Deletions in the 3'UTR region are postulated to affect RNA secondary structures which consequently may determine mRNA stability (Chen et al., 2006). Russell Hamilton and IIan Davis modeled RNA secondary structures across species predicted for the insertion and deletion alleles to establish whether the RNA sequence variation is functionally important. They concluded that the INS and DEL containing RNAs produce two distinct populations of secondary structures which potentially have functional consequences (Pickard et al., 2008b).

a)

	Control	Bipolar	Total
Genotype			
DEL/DEL	20	11	31
DEL/INS	95	67	162
INS/INS	171	278	449
		p=0.00000273	
Allele			
DEL	135	89	224
INS	437	623	1060
		p=0.00000019	
Freq. allele del	*0.24*	*0.13*	

b)

	Control	Bipolar	Total
Genotype			
DEL/DEL	25	6	31
DEL/INS	121	81	202
INS/INS	230	274	417
		p=0.0166	
Allele			
DEL	171	93	264
INS	581	455	1036
		p=0.0107	
Freq. allele del	*0.23*	*0.17*	

Table 6.1 Insertion/deletion genotyping results from individuals diagnosed with bipolar disorder and unaffected controls in the original study a) and replication study b). Chi-square derived p-values and the frequency of the deletion allele are shown.

	Control	Bipolar	Total
Genotype			
DEL/DEL	45	17	62
DEL/INS	216	148	364
INS/INS	401	465	886
Total	662	630	1292
		p=0.00000043	
Allele			
DEL	306	182	488
INS	1018	1078	2096
Total	1324	1260	2584
		p=0.00000002	
Freq. allele del	*0.23*	*0.14*	

Table 6.2 The combined data set from the original and replication association study. Chi-square derived p-values and the frequency of the deletion allele are shown.

To explore the potential effect of mRNA regulation on transcript expression, Ben Pickard examined mRNA allelic expression using a PCR-based assay in two cells lines and post-mortem hippocampal and cerebral cortical tissue from heterozygous individuals with no history of psychiatric illness.

His results indicated that in cDNA from naturally heterozygous neuroblastoma cell line (SHSY-5Y), and human embryonic kidney HEK293 cell line transfected with GFP-*GRIK4* fusion expression constructs, there was a marked predominance of the deletion allele mRNA indicating its increased relative abundance. This over-representation of the deletion-carrying transcript (calculated to be approximately 40% above the insertion allele) was also found in human hippocampal tissue, although frontal cortex tissue did not show the same clear bias (figure 6.2). The finding that *GRIK4* mRNA transcripts carrying the deletion are relatively more abundant supports the hypothesis that the genetic protective effect is mediated through increased kainate receptor expression.

6.3 Discussion

This chapter reports a highly significant association between a deletion in the 3'UTR variant of *GRIK4* and protection against bipolar disorder. Further evidence in the form of RNA secondary structure analysis of the insertion and deletion alleles and mRNA allelic expression studies indicating increased over-representation of the deletion-carrying transcript provide some support that protection afforded by the deletion may result from mRNA regulation.

In the field of common disease genetics there has been some debate as to whether some positive associations found in case-control studies may result from population stratification effects (Cardon and Palmer, 2003; Freedman et al., 2004). The term population stratification pertains to differences in allele frequencies between cases and controls attributable to diversity in background population rather than association of genes with disease.

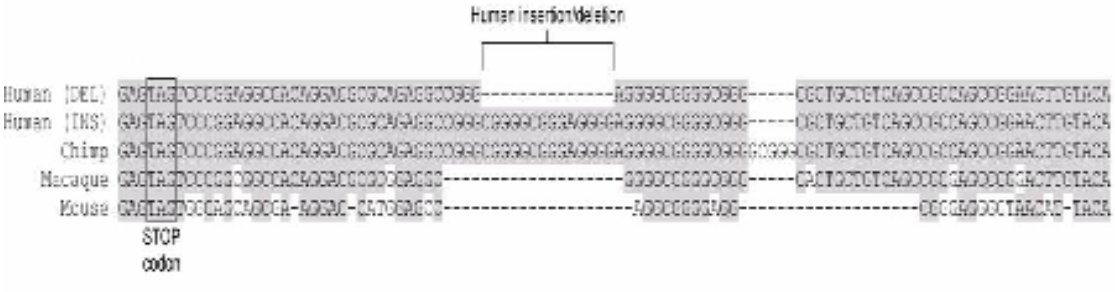

Figure 6.1 Alignment of *GRIK4* 3'UTR deletion/insertion in human, chimp, macaque and mouse. Figure taken from Pickard at al., 2008 (figure 1).

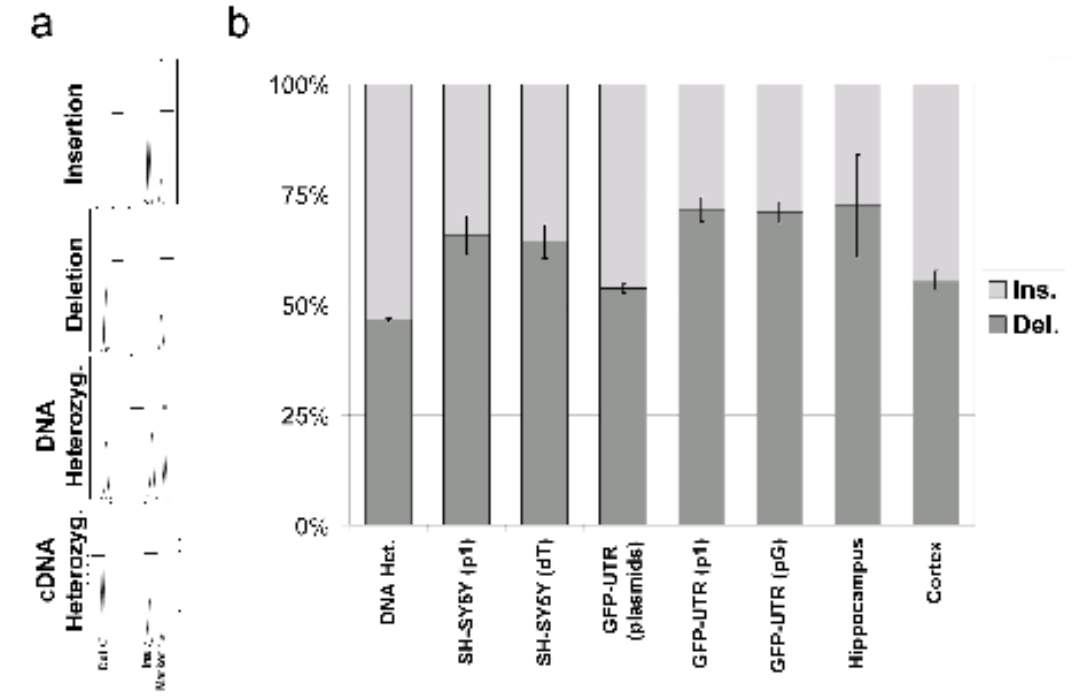

Figure 6.2 Relative expression levels of the deletion and insertion *GRIK4* alleles as determined by a fluorescently labelled PCR reaction. a) Representative examples from the PCR assay. b) Proportions of the insertion and deletion forms in SHSY-5Y genomic DNA (n=3), cDNA samples from SHSY-5Y (two separate RT primers, n=6), pre-transfection insertion/deletion expression plasmid mix (assay replicated 3 times), cDNA from HEK293 cells transfected with the insertion/deletion expression plasmid mix (two separate RT primers, n=5) and cDNA from heterozygote control human hippocampus (3 samples) and cortex (5 samples). Error bars indicate the standard error of the mean. Figure taken from Pickard et al., 2008, figure 2.

In the current study, the case-control cohorts consisted of cases and controls from North East and South East Scotland, a stable population which shows little evidence of stratification (WTCCC, 2007). Moreover, this cohort has been extensively genotyped in case-control studies of candidate genes producing both negative and positive results, suggesting a lack of cohort-dependent frequency bias.

It is a common observation that the odds ratio of a disease variant is usually overestimated in the study that first reports the association (Lohmueller et al., 2003). This bias, known as the 'winner's curse', relates to the power of the initial test for association, i.e. low powered studies of a variant of genuine but low to moderate association results in an effect size that is biased upwards (Zollner and Pritchard, 2007). The estimated effect size for the deletion allele in the present study was indeed found to be slightly higher in the initial study than replication study (ORs 0.46 versus 0.69). However, a significant difference between cases and controls was still ascertained in the replication study, so providing independent support that carriers of the deletion allele have a reduced chance of developing bipolar disorder.

In addition to the original SNP association study performed in our lab, two further case-control studies of *GRIK4* have been conducted. Shibata and colleagues typed 24 common SNPs across *GRIK4* in 100 unrelated Japanese individuals with schizophrenia and a hundred control subjects. They found no evidence for an association with either single markers or two SNP haplotypes (Shibata et al., 2006). Likewise, Li et al. typed 5 SNPs, including the three originally found to be associated with schizophrenia in the Scottish population, in 288 cases of schizophrenia and controls from the Chinese population. Again, single SNP and haplotype analysis revealed no statistically significant association (Li et al., 2008). These findings, which contrast with the present results, may be explained by number of factors. First, the study by Shibata and coworkers was of a modest size and may not have had the power to detect risk effects associated with an OR of 1.5 (0.65). Second, the 5 SNPs investigated by Li and colleagues may not be in LD with the protective haplotype and therefore do not 'tag' the

indel variant. Third, the cases investigated in both studies had a diagnosis of schizophrenia and not bipolar disorder. Finally, the prevalence of the protective haplotype (composed of rs513548, rs2282586 and rs1944522) which tags the indel variant was analyzed using phased HapMap data for European, African and Asian populations. The results indicate that the haplotype is very rare in the Asian population (Eur: 0.22, Afr.: 0.17, Asi.:0.02), and hence a significant association in the Japanese and Chinese populations would not be expected (B. Pickard, unpublished observation).

The current findings from European population based genome-wide case-control SNP scans of bipolar disorder have also failed to identify *GRIK4* as a risk-susceptibility gene. One explanation for this disparity is that the SNPs typed on the arrays actually fail to tag the indel variant. For example, the 500K affymetrix chip used in the Wellcome Trust Case Consortium (WTCCC, 2007) scan has only one SNP (rs2282586) of the original associated protective haplotype, and this SNP in isolation showed only moderate significance in the original Scottish study. Future case-control studies of *GRIK4,* whether investigating the associated indel directly or the 3 SNP haplotype in proxy with the variant, are needed to confirm the present findings and to assess further the prevalence of the indel variant in non-Asian populations.

Further evidence supporting *GRIK4* candidacy in mental illness comes from pharmacogenetic research. The Sequenced Treatment Alternatives to Relieve Depression (STAR*D) clinical trial investigated associations between genetic variation in 68 candidate genes (chosen for their role in major neurotransmitter systems or potential pharmacological pathways) and outcome of antidepressant treatment (Paddock et al., 2007). Using a two phase study design, 768 markers were initially typed in a discovery cohort composed of 1,199 individuals diagnosed with major depressive episodes and treated for 14 weeks with the selective serotonin reuptake inhibitor (SSRI) citalopram. The second wave genotyping was conducted using a cohort of 617 treated patients with depression and a comparison group of 634 unmediated controls. Two markers located within the *HTR2A* gene (encoding a serotonin receptor) and *GRIK4* were found to

exceed nominal significance for association with treatment response or remission in each phase (illustrated in figure 6.3). Interestingly, the associated SNP (rs1954787) positioned within the first intron of GRIK4 is a component of the extended haplotype associated with schizophrenia in the original Scottish SNP case-control study. However this SNP, located in the proximal portion of *GRIK4*, is not in strong linkage disequilibrium with the associated bipolar haplotype or indel variant.

To determine the nature of the observed association, Paddock and colleagues analyzed *GRIK4* marker frequencies in cases and comparison controls. This revealed that only non-responders (to treatment) differed significantly from healthy controls and that significant differences in frequencies existed for 12 markers which span an interval in the distal portion of GRIK4 covering several LD blocks (figure 6.3).

Moreover, multiple regression analysis of the same genotype data set performed by Laje et al. (unpublished observation) also revealed that a co-morbid condition, anxious depression, showed independent associations with *GRIK4* (Paddock et al., 2007*)*. Whether some of these multiple independent associations are driven by the indel variant is as yet unknown. However, these results strongly imply that multiple, common variants in *GRIK4* may have functional consequences relevant to psychiatric illness.

The 3'untranslated region of mRNA is recognized as having an essential role in the posttranscriptional regulation of gene expression. Unlike 5'UTR mRNA sequences which contain highly conserved translational regulatory elements, the 3'UTR sequence has less evolutionary constraints. Hence 3'UTR sequence variation is postulated to be responsible for determining time- and location-specific processes such as nuclear transport, polyadenylation, subcellular targeting, and translation efficacy, as well as mRNA degradation (Conne et al., 2000).

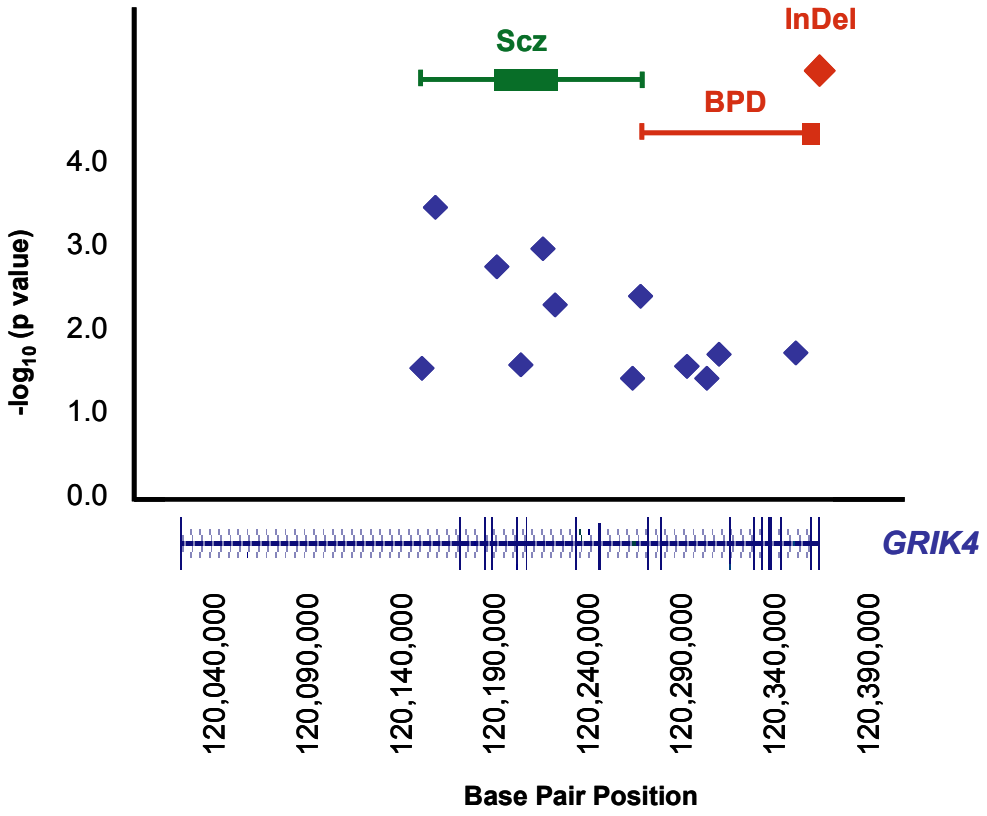

Figure 6.3 Schematic representations of multiple positive associations of *GRIK4* with antidepressant treatment and with schizophrenia and bipolar disorder. Blue diamonds represent 12 independent significant marker associations found for cases of MDD non-responsive to citalopram, as reported by the STAR*D study. Positive association of extended (green bracketed lines) and core (green filled rectangles) with schizophrenia and bipolar disorder, as reported by Pickard et al., 2006, are also indicated. The position of the protective indel (red diamond) is shown. The negative $\log_{10}$ values of the respective p values are plotted on the y axis. Physical positions based on UCSC 2006, dbSNP build129 and *GRIK4* gene structure is shown on the x axis. Figure based on data provided in figure 2 (Paddock at al., 2007).

The associated 14bp indel in *GRIK4* is positioned in an interval termed the upstream sequence (USS) located between the translational termination codon and the upstream core polyadenylation signal. Regulatory motifs and mRNA secondary structures in this region can affect transcript stability through adenylate/uridylate-rich element (ARE)-mediated mRNA decay, interaction with trans-acting factors, and by cleavage site protection. The indel region does not contain AU-Rich elements (AREs) and so this process is unlikely to contribute to the functional mechanism. This region is however AG-rich, a feature linked to an increased likelihood of single-stranded RNA conformation. Indeed, the consensus structure of the insertion sequence indicates that several regions exist as single strands including a single-stranded region comprising an internal loop, and thus these sites are potential targets for protein factor or miRNA binding (Pickard et al., 2008b).

One well documented example of mRNA stabilization resulting from trans-acting proteins binding to cis-acting elements is that of iron-responsive elements (IRE's) found in genes involved in iron metabolism. IREs form a single-stranded stem loop structure with which iron regulatory proteins (IRPs) associate. When cellular iron levels are low, IRP binds the mRNA and stabilizes it by shielding it from cleavage (Grzybowska et al., 2001). Future biochemical experiments investigating the identification of putative factors differentially interacting with *GRIK4* insertion and deletion sequences may provide more insight into the mechanism by which the indel exerts its effects.

A variant in the 3'UTR region of *GRIK2* encoding the kainate receptor subunit GLUR6 has also been associated with disease. Huntington's disease (HD), a neurodegenerative disorder, is caused by an expanded CAG trinucleotide repeat that lengthens a polyglutamine tract near the amino terminus of the huntingtin protein (HTT) (Macdonald, 1993). However, multiple reports of an association between a trinucleotide repeat polymorphism (16TAA) in the 3'UTR of *GRIK2* and age at neurologic onset in HD strongly indicates that *GRIK2*/GLUR6 acts as a modifier of HD pathogenesis. Furthermore, a screen of *GRIK2* in individuals who possess the 16TAA polymorphism

and displayed early onset HD, failed to identify coding variants or an ancestral haplotype in LD with the 3'UTR polymorphism. This suggests that the 3'UTR allele is itself responsible for the modifier effect (Zeng et al., 2006). The functional mechanisms of this modifier allele have yet to be elucidated. Nonetheless, post-transcriptional mRNA editing of kainate receptor subunits GLUR5 and GLUR6 at specific TMD sites are known to have a functional impact on receptor channel currents (Lerma et al., 2001).

We propose that the associated *GRIK4* deletion has its effect through mRNA stability, and hence may influence KA1 protein abundance either globally or in specific subcellular locations, i.e. neuronal dendrites. Consequently, this may potentially shift kainate subunit stoichiometry and thus the functional properties of kainate receptors at glutamatergic synapses.

CHAPTER 7

CHARACTERISATION OF GRIK4/KA1 PROTEIN EXPRESSION IN HUMAN BRAIN

ACKNOWLEDGEMENTS FOR CHAPTER 7

Advice on Immunohistochemistry techniques and analysis of expression was kindly provided by Dr. Rachel James (Centre for Neuroscience, University of Edinburgh) and Professor J. Bell and Dr. Robert Walker (Neuropathology Unit, University of Edinburgh).

.

7. Characterisation of KA1 expression in human brain

7.1 Preface

The previous chapter discussed the identification of a deletion in the 3'UTR of *GRIK4*/KA1 as a protective factor for bipolar disorder. This associated *GRIK4* variant is hypothesized to exert its effect through mRNA stability and hence may influence KA1 protein abundance either globally or in specific subcellular locations. To investigate this issue, KA1 protein expression was first characterized in regions of the human brain commonly reported to be involved in the expression of psychiatric illness.

7.2 Results

7.2.1 Antiserum specificity

The current study examined KA1 protein expression in human post-mortem brain using sections of the frontal cortex, cerebellum, amygdala hippocampus and parahippocampal regions provided by the Edinburgh University MRC Sudden Death Brain and Tissue Bank. KA1 expression was determined using an affinity-purified antibody 272, raised in rabbit against a human C-terminal amino acid sequence not homologous with any of the other cloned subunits belonging to the kainate receptor family.

To assess whether this antibody binds to a protein species of similar molecular weight as human KA1, immunoblotting was performed. Western blot analysis using the 272 antiserum showed two major immunoreactive bands of approximately 105 kDa and 210 kDa in human glioblastoma cell line U373 and human neuroblastoma cell line SH-SY5Y as well as one faint band (~ 105 kDa) in a protein lysate from homogenised mouse brain (figure 7.1). The molecular mass of the 105 kDa corresponds closely with that predicted from the cloned cDNA sequence (Werner et al., 1991), and hence provides evidence that the 272 antibody is specific for KA1.

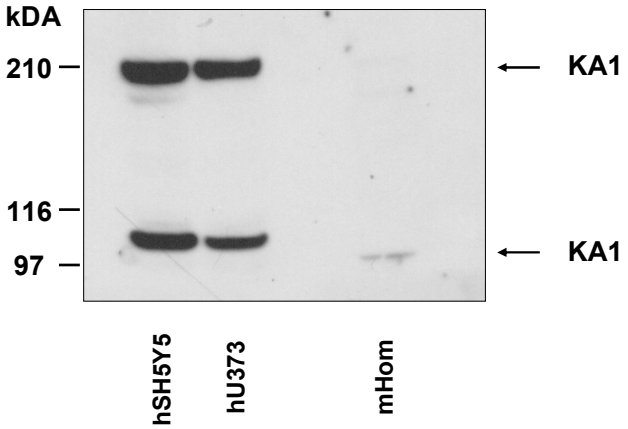

Figure 7.1 KA1 detection in human cell lines and mouse brain. The peptide used for immunization (rKA1) shares no homology with the C-terminus of other members of the kainate receptor subunit/binding protein families. Protein lysates were prepared from human hU373 and hSH-SY5Y cell lines as well as mouse brain protein homogenate (mHom). Two immunoreactive bands of approximately 105 kDa and 210 kDa were detected, with the 105kDa molecular species consistent with the size predicted from the cloned cDNA. Numbers on the left represent size standards in kilodaltons (kDa).

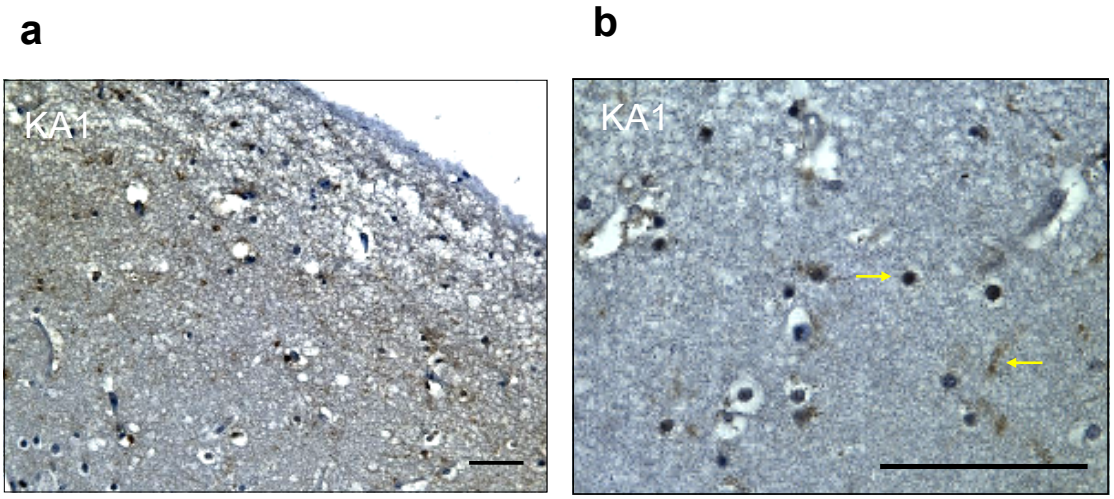

Figure 7.2 KA1 protein expression in layer 1 of the frontal cortex. Images captured at low x160 magnification (a) and at high x400 magnification (b). Arrows indicate the brown DAB immunoreactivity for KA1 evident in glial cells and neuronal dendrites. The black bar represents 50µm.

The presence of a second band may be due to dimerization of the protein, as no other KA1 isoforms are known to exist; or alternatively, may represent a mature glycosylated form as previously described (Darstein et al., 2003).

7.2.2 Frontal cortex

Histology was performed using coronal sections taken in a parasagittal plane of the frontal cortex. A negative control (absence of primary antibody) and a positive control (primary antibody Glial Fibrillary Acidic Protein [GFAP] – an astrocyte marker) were performed on every IHC run. Omission of a primary antibody resulted in tissue sections without any visible DAB reaction product. Conversely, the use of α-GFAP as a positive control demonstrated that the IHC protocol was fully optimized, and facilitated the identification of glial cells, primarily astrocytes, within specific tissue regions.

The cerebral cortex is typically composed of six cell layers numbered from the outer surface of the cortex (pia mater) to the underlying white matter. In layers 2-6 the principal neuronal cells are excitatory and release glutamate as their primary neurotransmitter. Layer 1 of the frontal cortex is an acellular neuronal layer predominately composed of glial cells, dendrites and axons of cells located in deeper layers and white matter corticocortical fibers. KA1 immunoreactivity was evident in all three kinds of glial cell types, i.e. astrocytes, oligodentrocytes and microglia, and in between the cells in axonal/dendritic processes, shown in figure 7.2.

KA1 DAB staining was also found in the cell bodies of glial cells and small neuronal spherical cells (including granular cells) as well as dendritic processes in layers 2 and 4, (also know as the superficial and deep molecular layers), shown in figure 7.3. KA1 immunoreactivity in processes was more prevalent in layer 4, which may reflect the fact that layer 4, unlike layer 2, has interneurons that are excitatory and glutamatergic. Similarly, immunoreactivity in layer 3 was most prominent in glia and the processes of pyramidal shaped neurons. However, some neurons also showed cytoplasmic and nuclear staining, as shown in figure 7.4a.

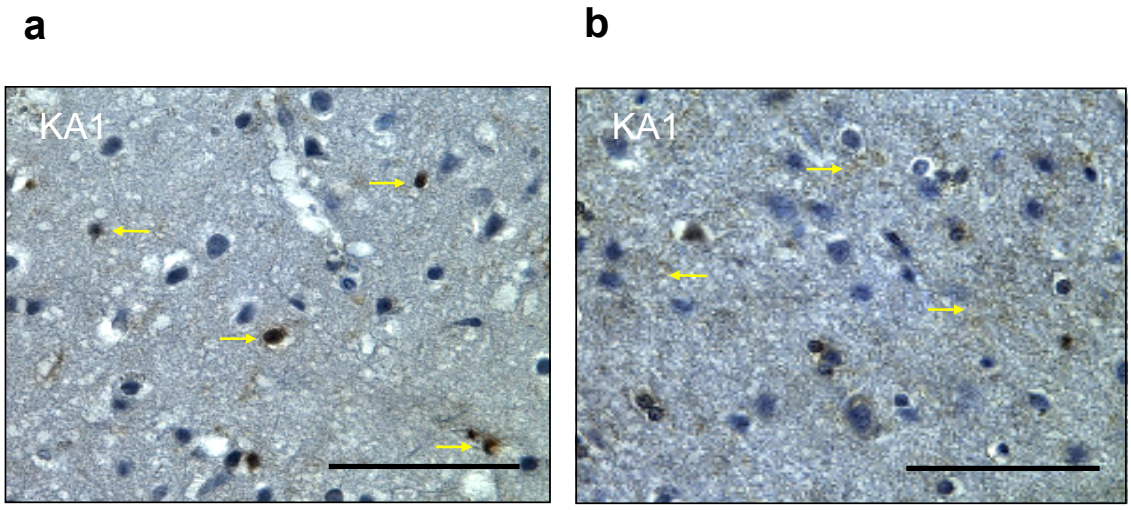

Figure 7.3 KA1 protein immunoreactivity in layers 2 and 4 of the frontal cortex. Glial cells, small spherical neuronal cells (which are likely to include granular cells), and dendrites express KA1 in layer 2 (a) and layer 4 (b). Yellow arrows in (a) indicate immunoreactive positive granular cells and in (b) immunoreactivity for dendritic processes. The black bar represents 50μm.

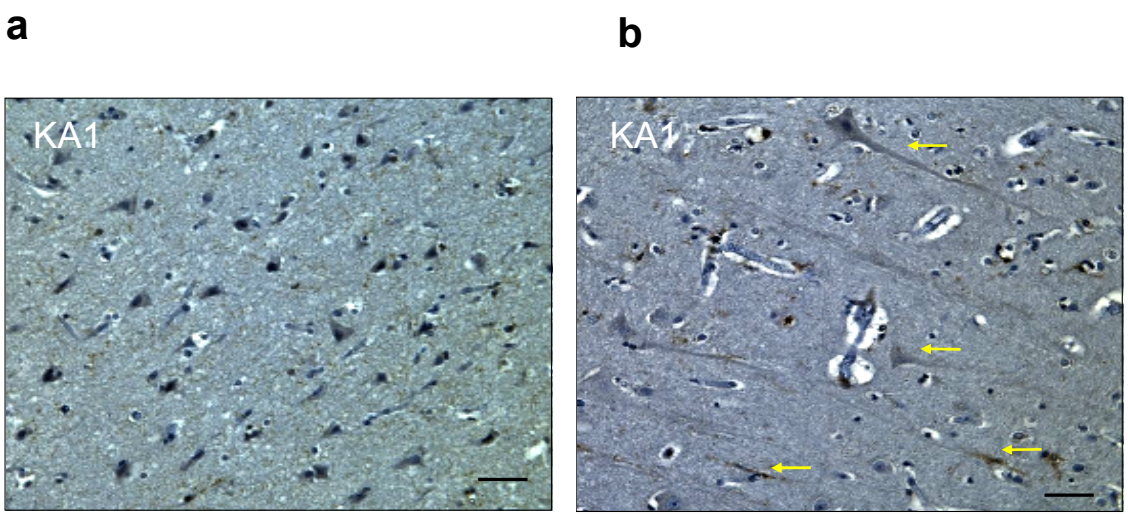

Figure 7.4 KA1 protein immunoreactivity in layers 3 and 5 of the frontal cortex. Neuronal and glial cells express KA1 in layer 3 (a) and layers 5 (b). Yellow arrows in indicate immunoreactive positive pyramidal cells and dendritic/axonal arborizations. The black bar represents 50μm.

This pattern of staining was also found in layer 5, which is comprised of large pyramidal shaped neurons, and layer 6 – a multiform layer composed of a heterogeneous variety of neurons (shown in figures 7.4b and 7.5). In addition, glial cells of the white matter underlying the neocortex show strong KA1 and GFAP antibody reactivity, demonstrated in figure 7.6. The KA1 Immuno-positive signal was strongest in the cell bodies of glial cells and dendritic connections between cell bodies.

7.2.3 Cerebellum

The cerebellar cortex is divided histologically into three layers: the outer molecular layer, purkinje cell layer and inner granular cell layer (GCL). This three layer structure consists of 5 primary types of neurons: excitatory granular cells and inhibitory stellate, basket, purkinje and golgi cells. In addition to these neuronal cell types, a discrete population of radial glial cells (Bergmann cells) located within or near the purkinje cell layer, are hypothesized to be potential stem cells. Afferent axons which terminate in the cerebellar cortex synapse upon either excitatory mossy fiber terminals in the granular layer or climbing fibre connections located in close proximity to the purkinje cells.

KA1 immunoreactivity was identified in three primary regions of the cerebellar cortex: punctate staining the granular cell layer, purkinje cell layer and sparse dendritic processes in the molecular layer. The immunoreactivity found in the granular cell layer is evident as sporadic circular clusters/blobs (10-20μm) located within the superficial portion of the layer, as shown in figures 7.7 and 7.8. This staining is consistent with the location of golgi cell axon terminals. However, only a proportion of putative golgi cells show this strongly immuno-positive signal. Interestingly, this specific expression pattern has also been described for GluR5 (a kainate receptor subunit which can form a functional channel with KA1) and mGluR2/3 (metabotropic glutamate receptor subunits) and is in accordance with the suggestion that golgi cells can be segregated into two groups based on the presence or absence of glutamate receptors (Ohishi et al., 1994; Lerma et al., 2001).

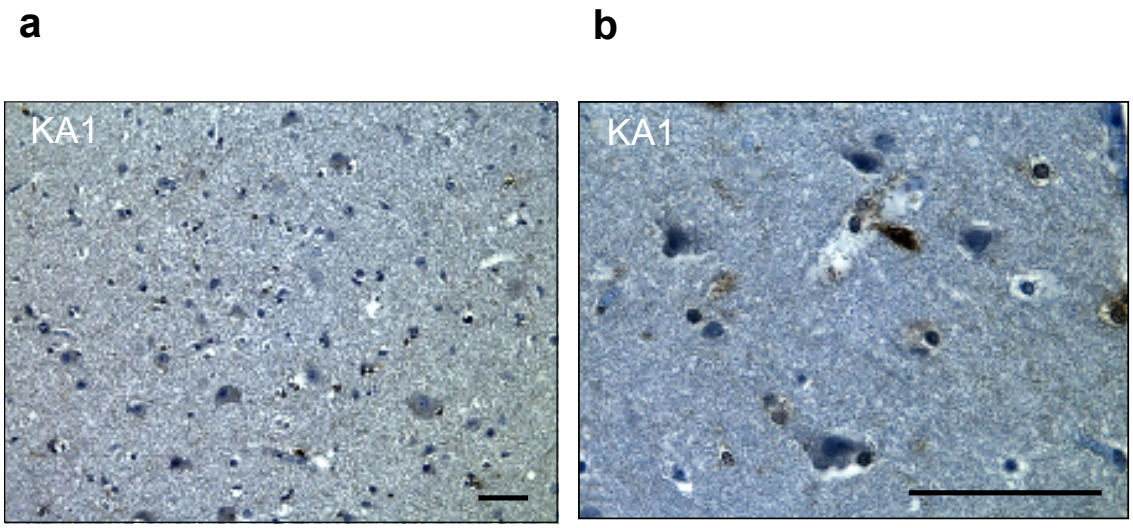

Figure 7.5 KA1 protein immunoreactivity in layer 6 of the frontal cortex. (a) Image captured at low x160 magnification, and (b) at high x400 magnification. Immunopositve staining is predominately in glial cells, sporadic cell bodies and processes of neurons. The black bar represents 50μm.

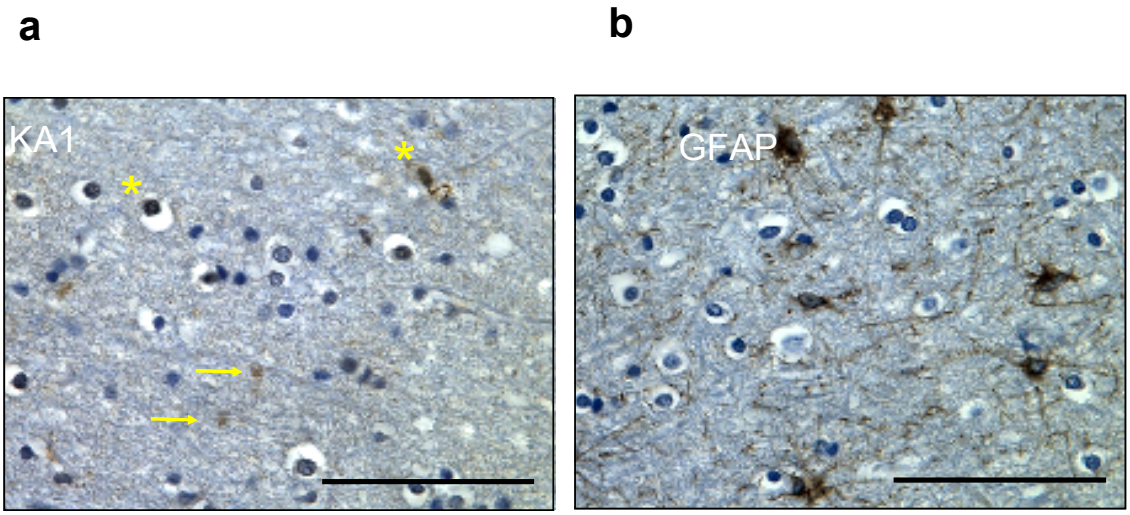

Figure 7.6 Protein immunoreactivity for KA1 and GFAP in the white matter underlying the neocortex. Immuno-positive staining for KA1 (a) and for GFAP (b). Yellow stars indicate immunoreactivity for large glial cells, likely to be astrocytes and oligodendrocytes. Yellow arrows point to immuno-positive fibrils. The black bar represents 50μm.

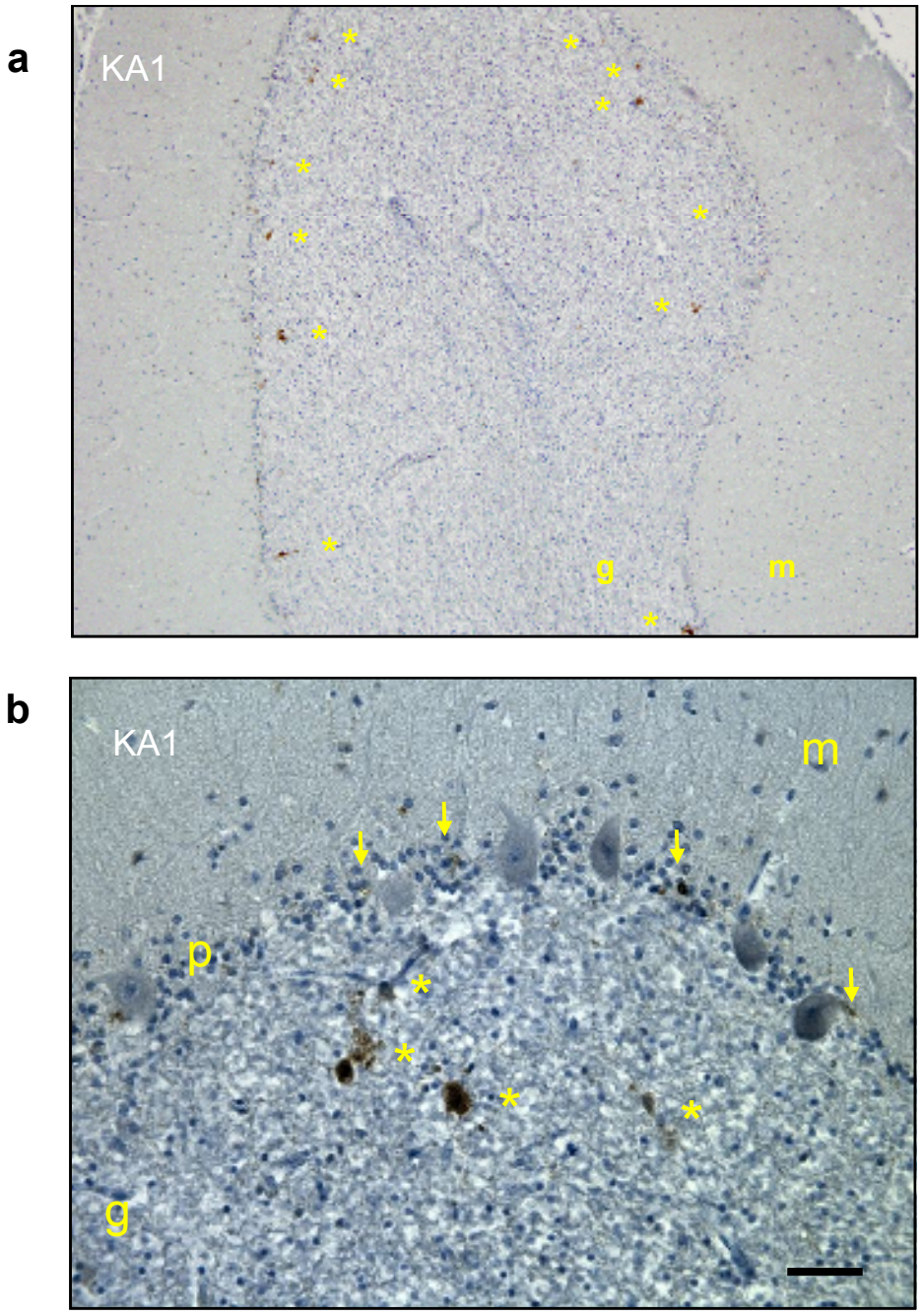

Figure 7.7 Protein immunoreactivity for KA1 in the cerebellar cortex. Images captured at low x100 magnification (a), and at a higher x160 magnification (b). Yellow stars point to strong immuno-reactive staining in the superficial portion of the granular layer. Yellow arrows indicate staining in cells which putatively may be Bergmann glia. The black bar represents 50μm. (g, granular layer; p, purkinje cells; m, molecular layer).

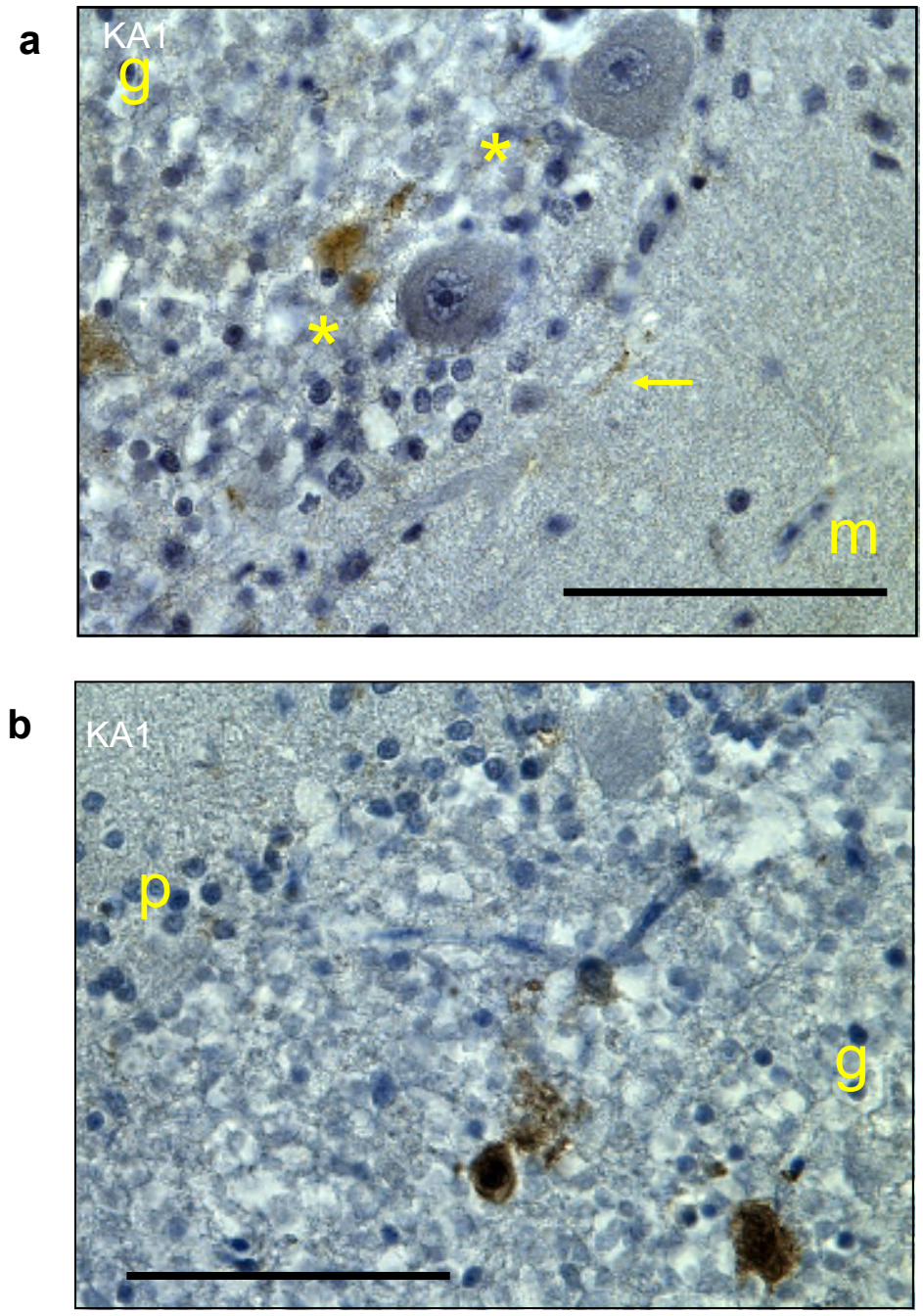

Figure 7.8 High magnification images of KA1 protein immunoreactivity in the cerebellum. (a) High magnification image showing KA1 staining in the superficial granular layer (yellow stars) and dendrites in the molecular layer (arrow). (b) Image demonstrating strong KA1 immunoreactivity in the granular layer, consistent with golgi cell staining. The black bar represents 50μm. (g, granular layer; p, purkinje cells; m, molecular layer).

A proportion of the purkinje cells showed weak to moderate cytoplasmic immunoreactivity, indicated in figure 7.7.b. Strong but sporadic immuno-positive staining was however observed in small cells and dendrites positioned in close proximity to the purkinje cells, shown in figures 7.7b and 7.8. Immuno-positive staining for GFAP, a marker of astrocytes, indicates that these cells may be Bergmann glia (figure 7.9). Furthermore, dendritic arborizations in the purkinje cell layer and superficial molecular layer may be dendrites of the Bergmann glia or processes of golgi cells and purkinje cells.

7.2.4 Amygdala

The amygdala, a component of the limbic system, is a mass of subcortical grey matter involved in the processing of emotive experience. It is comprised of multiple nuclei surrounded by cortex which has a characteristic six layer structure analogous to the neocortex. KA1 immunoreactivity was observed as weak cytoplasmic staining in large neurons within nuclei. However, there was no evidence for axonal/dendritic KA1 expression in these cells. Immunoreactivity was more prominent within the cytoplasm of large neurons within layers 3, 5 and 6 of the cortex, as shown in figure 7.10. Moreover, the staining of glial cells, i.e. astrocytes, oligodendrocytes and microglia, was similar to that observed in frontal cortex and cerebellum tissue.

7.2.5 The hippocampal formation

7.2.5.1 The hippocampus

The hippocampal formation is a group of cytoarchitectonically distinct adjoining regions including the hippocampus, dentate gyrus (DG) and parahippocampal areas such as subiculum, entorhinal and perirhinal cortices. These regions, in concert with other limbic structures, are intrinsically involved in cognitive processes such as memory formation, spatial coding and context dependent integration of information.

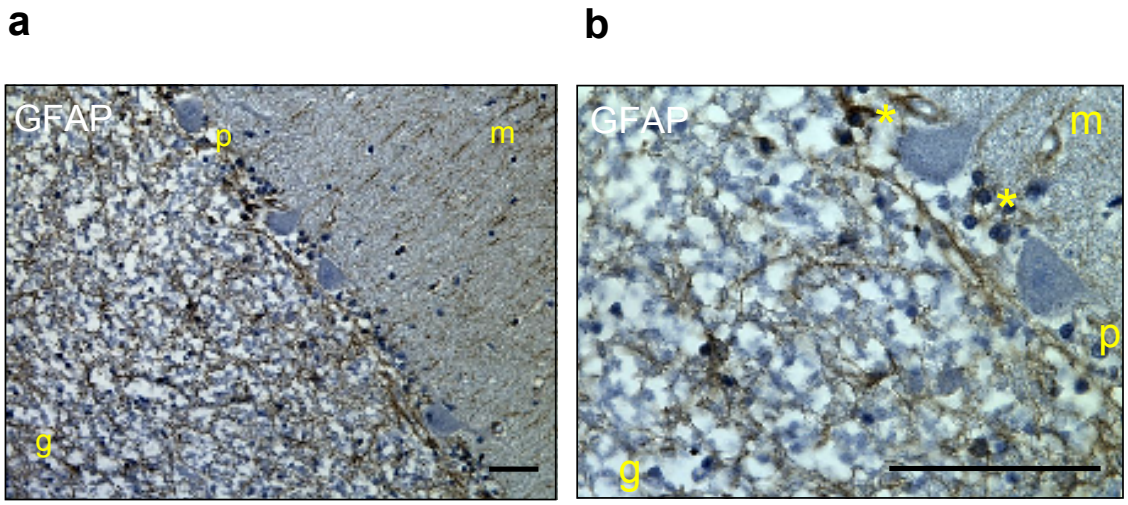

Figure 7.9 Protein immunoreactivity for GFAP in the cerebellar cortex. Images captured at low x16 magnification (a) and at high x400 magnification (b). Yellow stars indicate brown immunoreactivity for GFAP in Bergmann glial cells located in close proximity to the large purkinje cells. The black bar represents 50µm. (g, granular layer; p, purkinje cells; m, molecular layer).

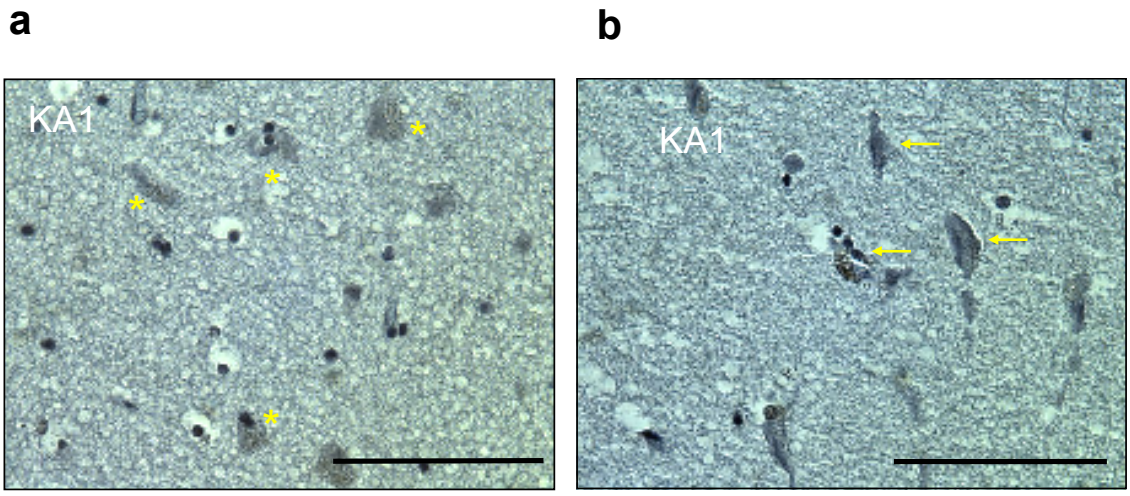

Figure 7.10 Protein KA1 immunoreactivity in cortical layers surrounding deeper nuclei of the amygdala in (a) Layer 3 of the amygadala cortex, and (b) large neurons of layer 5 or 6. Yellow stars and arrows indicate immuno-positive staining predominantly within the ER of cells.

Within the hippocampus proper, the main subdivisions are the Cornu ammonis (CA) fields (CA1, CA2, CA3 and CA4), and the alveus – a layer composed of white myelinated fibers which borders the lateral ventricle. The major afferent pathway to the hippocampus is the perforant path. The axons of the perforant path arise principally in the superficial layers of the entorhinal cortex and project to the granule cells of the dentate gyrus and pyramidal cells of the CA1 and CA3. Likewise, the axons of the granule cells within the DG extend via the hilus to CA3 pyramidal cells, forming a second main pathway - the mossy fibre pathway. In turn the pyramidal cells of the CA3 are the source of major input to the CA1 (the Schaffer collateral pathway). Collectively these three pathways have been termed the 'trisynaptic circuit' and represent a major portion of the functional circuitry of the hippocampal formation, as schematically illustrated in figure 7.11.

KA1 immunoreactivity was observed in the dendritic processes of the granule cells located within the inner and outer molecular layer (stratum moleculare) of the dentate gyrus (presented in figure 7.12a). Strong but sporadic staining was evident in the DG granule cell nuclei and dendrites, with no obvious variation in regional distribution. However, as shown in figure 7.13a, weaker and more diffuse cytoplasmic staining was also observed in a proportion of the granule cells. Immunoreactivity for GFAP, a marker of astrocytes, indicated that astrocytes are located within the granule cell layer (GCL) as well as clustering along the GCL inner border, the subgranular zone, adjoining the hilus (figure 7.12b). As the size and shape of these glial cells are similar to granule cells, it is possible that some immuno-positive KA1 cells within the DG are in fact astrocytes.

The hilus, the inner region of the dentate gyrus, is a polymorphic cell region composed of small neurons, glial cells and large mossy fibre neurons which synapse with granule cell axons and CA3 pyramidal cells. Strong KA1 immunoreactivity was observed in the cell body and processes of a small number of these mossy fibre neurons, evident in figure 7.14a.

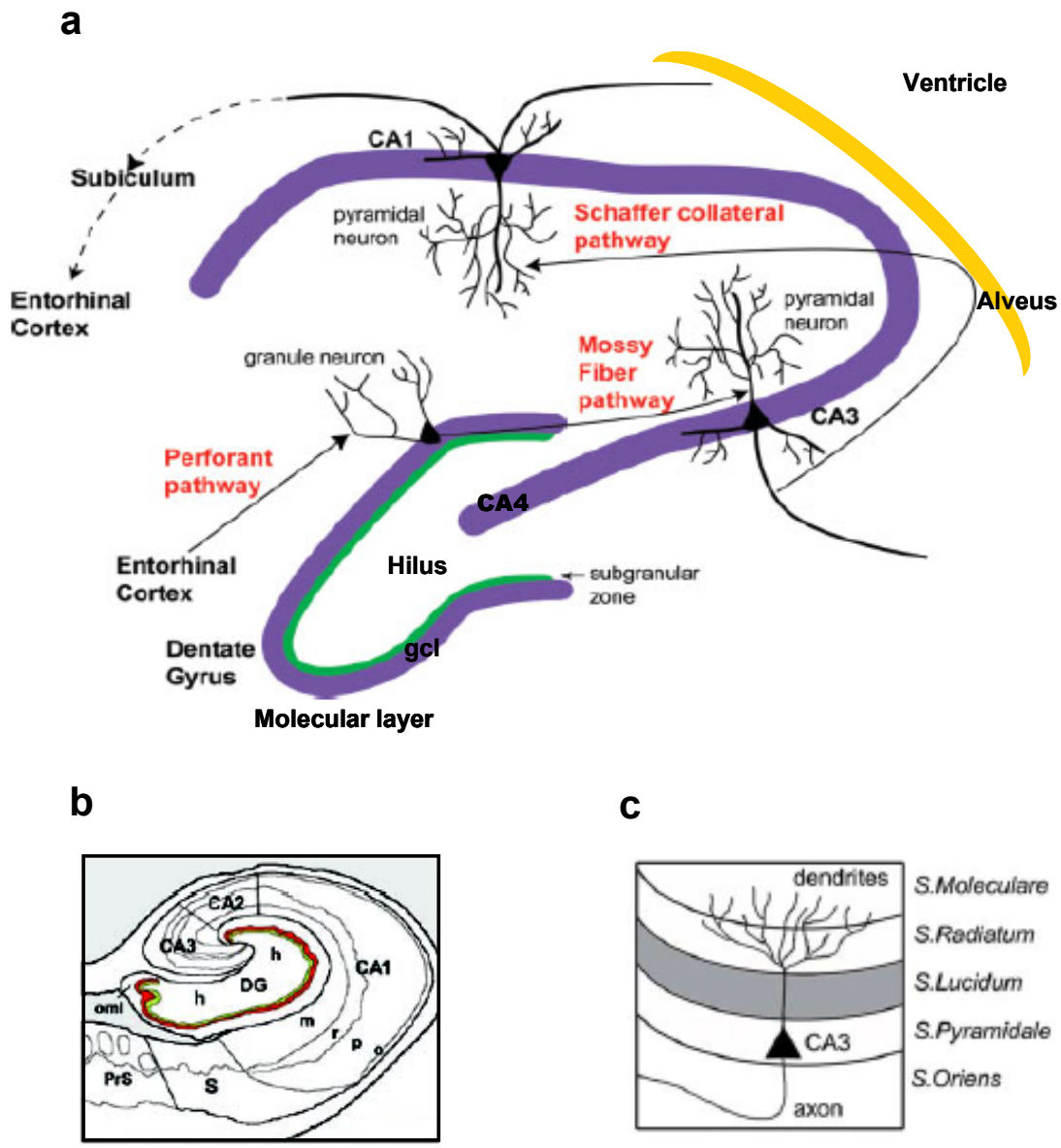

Figure 7.11 Schematic illustration of the hippocampal formation and major pathway circuitry. (a) Structure and cyto-architecture of the hippocampus and DG. Figure adapted from (McCaffery et al., 2006) figure 1. (b) Diagram of a human tissue section illustrating the strata in the CA fields. Diagram adapted from Talbot et al. 2004, figure 4A. (c) Schematic illustration of CA3 strata. Figure adapted from (Jaskolski et al., 2005), figure 2. DG, dentate gyrus; h, hilus; m, stratum lacunosum-moleculare; o, stratum oriens; oml, outer molecular layer; p, stratum pyramidal; PrS, presubiculum; r, stratum radiatum; S, subiculum.

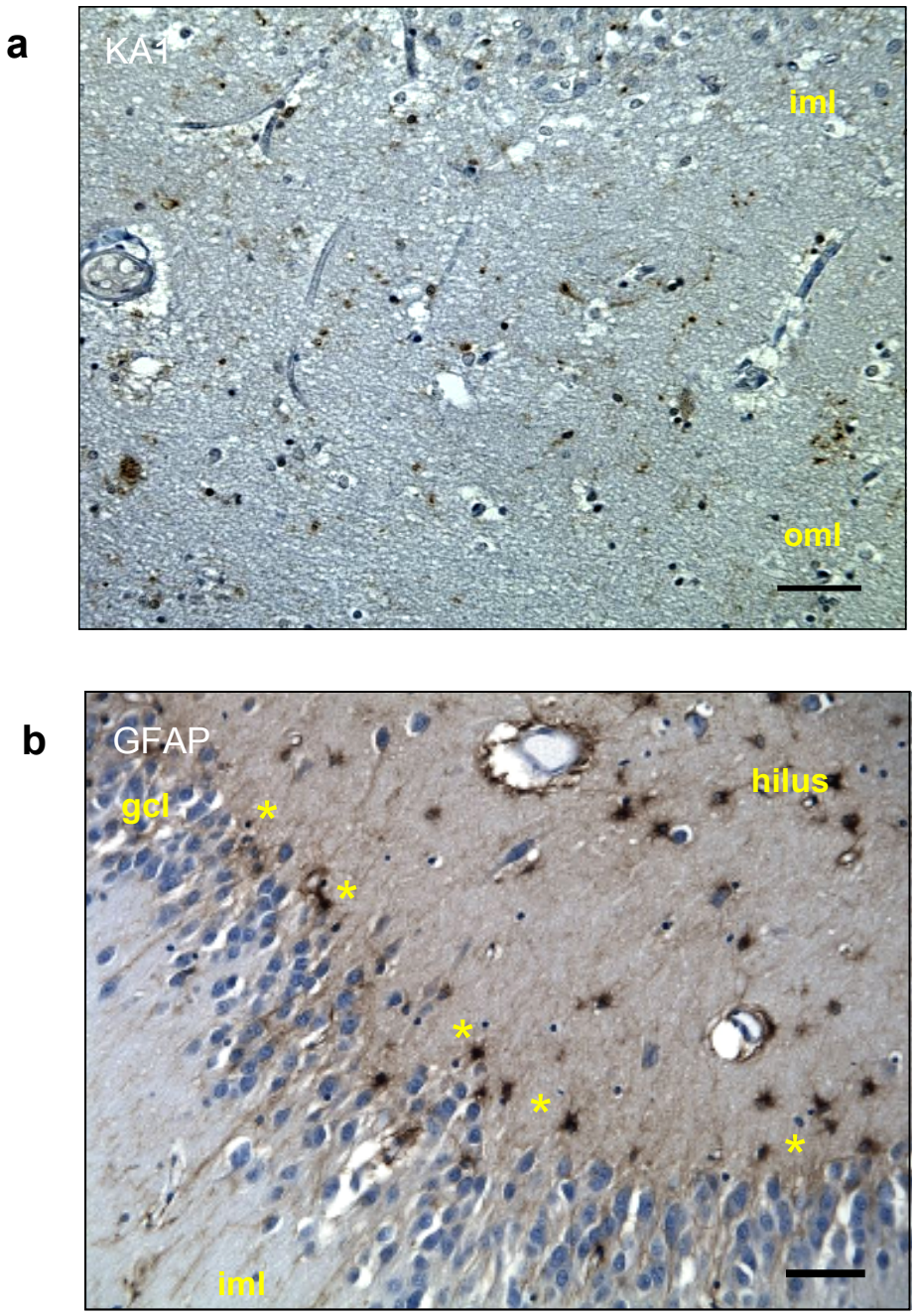

Figure 7.12 KA1 and GFAP protein immunoreactivity in the molecular layer and GCL of the dentate gyrus. (a) KA1 expression in dendrites within the molecular layer (stratum moleculare). (b) GFAP expression in the DG hilus, GCL and molecular layer. Yellow stars indicate the clustering of astrocytes in the inner layer of the GCL. The black bar represents 50μm. Iml, inner molecular layer; oml, outer molecular layer; gcl, granule cell layer.

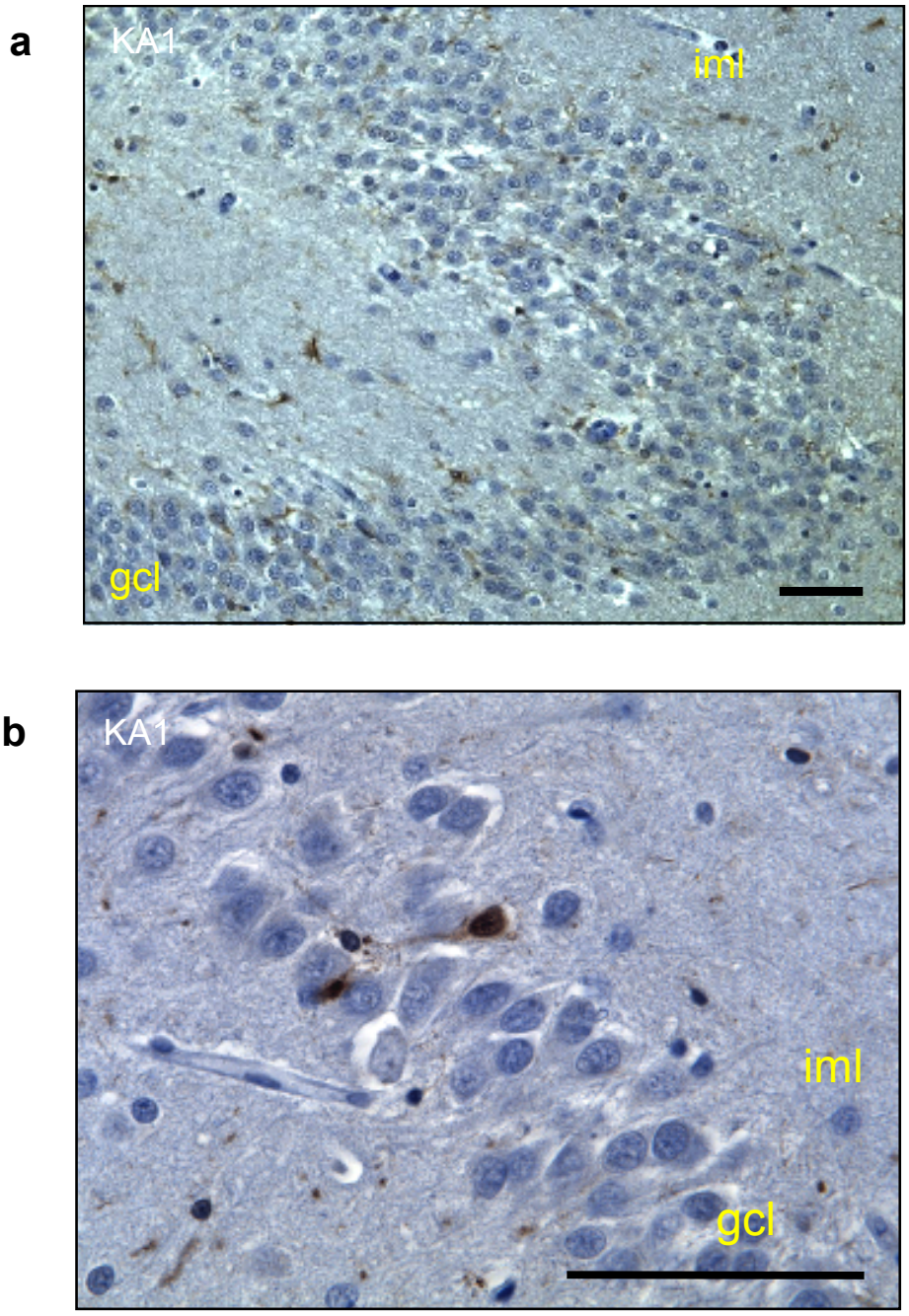

Figure 7.13 KA1 expression in the granular cell layer of the dentate gyrus. Image captured at low x160 magnification (a), and at high x400 magnification (b). Staining is evident in the nucleus, cell body and processes of the granule cells. The black bar represents 50µm. (gcl granular cell layer; iml, inner molecular layer).

Strong reactivity was also observed in neuropil (unmyelinated synaptic processes and terminals interspersed between neurons) in an area consistent with it being mossy fibre connections (figure 7.14). In addition, and similar to other brain regions, glial cells showed a strong immuno-positive signal.

The CA4 field starts within the hilus and curves outwardly until adjoining the CA3 region in the hippocampus proper, indicated in figure 7.11. KA1 immunoreactive expression was observed in the neuropil surrounding the principal cell of this region (the large pyramidal cells) as well as weak cytoplasmic staining within the pyramidal cells themselves (figure 7.14b).

This pattern of expression is retained within the CA3 and CA2 fields. The strongest and most diffuse immuno-positive signal was observed in the neuropil among pyramidal cells and the stratum lucidum (l) of the CA3 field, a region in which mossy fibre cells synapse with the apical dendrites of CA3 pyramidal cells (figure 7.15a). Moderate signal localised to the cytoplasm of pyramidal cells provides support for the hypothesis that KA1 is expressed post-synaptically in neurons as well as pre-synaptically in mossy fibre cells. Immunoreactivity was also evident in the processes of CA3 pyramidal cells located in the stratum radiatum. In addition, the observed punctate dendritic expression in the stratum oriens (CA3 pyramidal basal dendrites) suggests that KA1 may also be present at CA3 to CA3 associational, and CA3 to CA1 Schaffer collateral, connections. KA1 immunoreactivity in the CA2 region, although consistent with the CA3 expression pattern, was more punctate and less pronounced, as shown in figure 7.15b.

Weak staining in the cell bodies of a small number of CA1 pyramidal cells was also observed. Stronger immunoreactive signal was evident in processes either between the pyramidal cells in the pyramidal stratum or throughout the stratum radiatum of the CA1 field, as shown in figures 7.16 a and b).

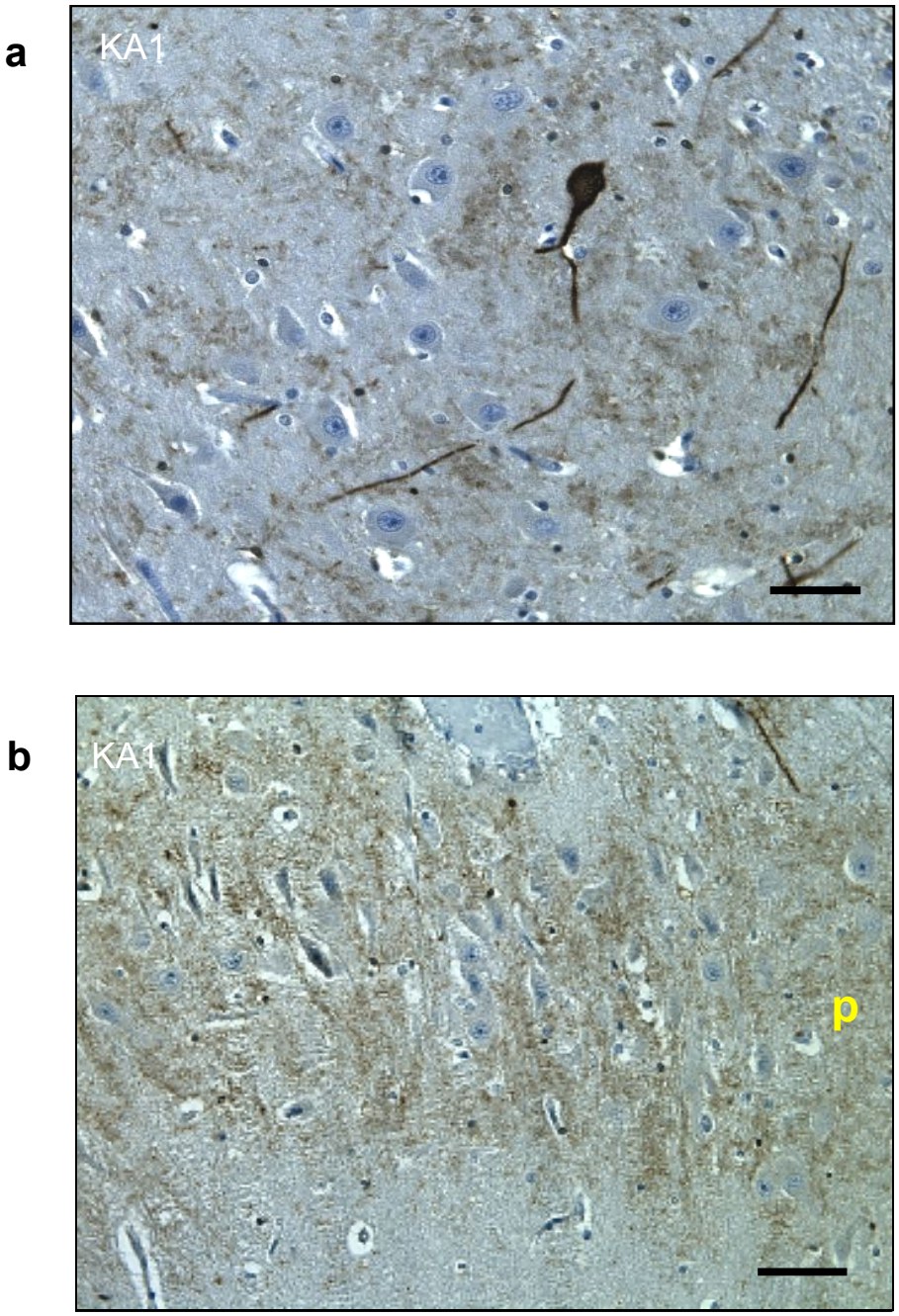

Figure 7.14 KA1 expression in the DG hilus and CA4 region. (a) Low magnification of KA1 expression in the hilus. The large immuno-positive cell is a mossy fibre neuron and the brown background staining is reactivity for neuropil. (b) Low magnification image of KA1 neuropil immunoreactivity in the CA4 field. The black bar represents 50µm. p, pyramidal cell layer.

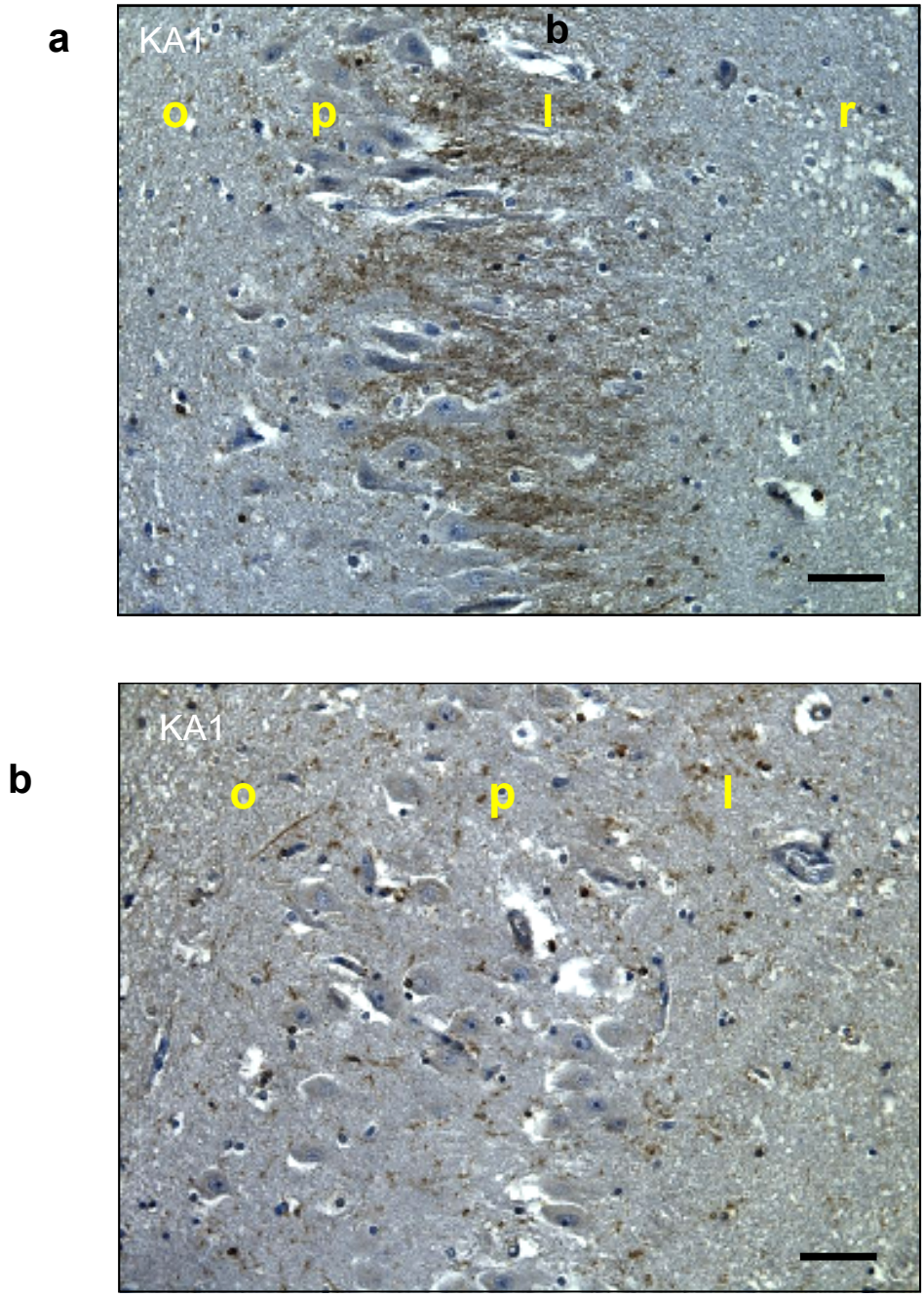

Figure 7.15 KA1 expression in the CA3 and CA2 fields. KA1 immunoreactivity in strata oriens, pyramidial and radiatum of CA3 (a) and CA2 (b). The strongest signal was observed in the stratum lucidum of the CA3 region. The black bar represents 50μm. l, stratum lucidum; o, stratum oriens; p, stratum pyramidal; r, stratum radiatum.

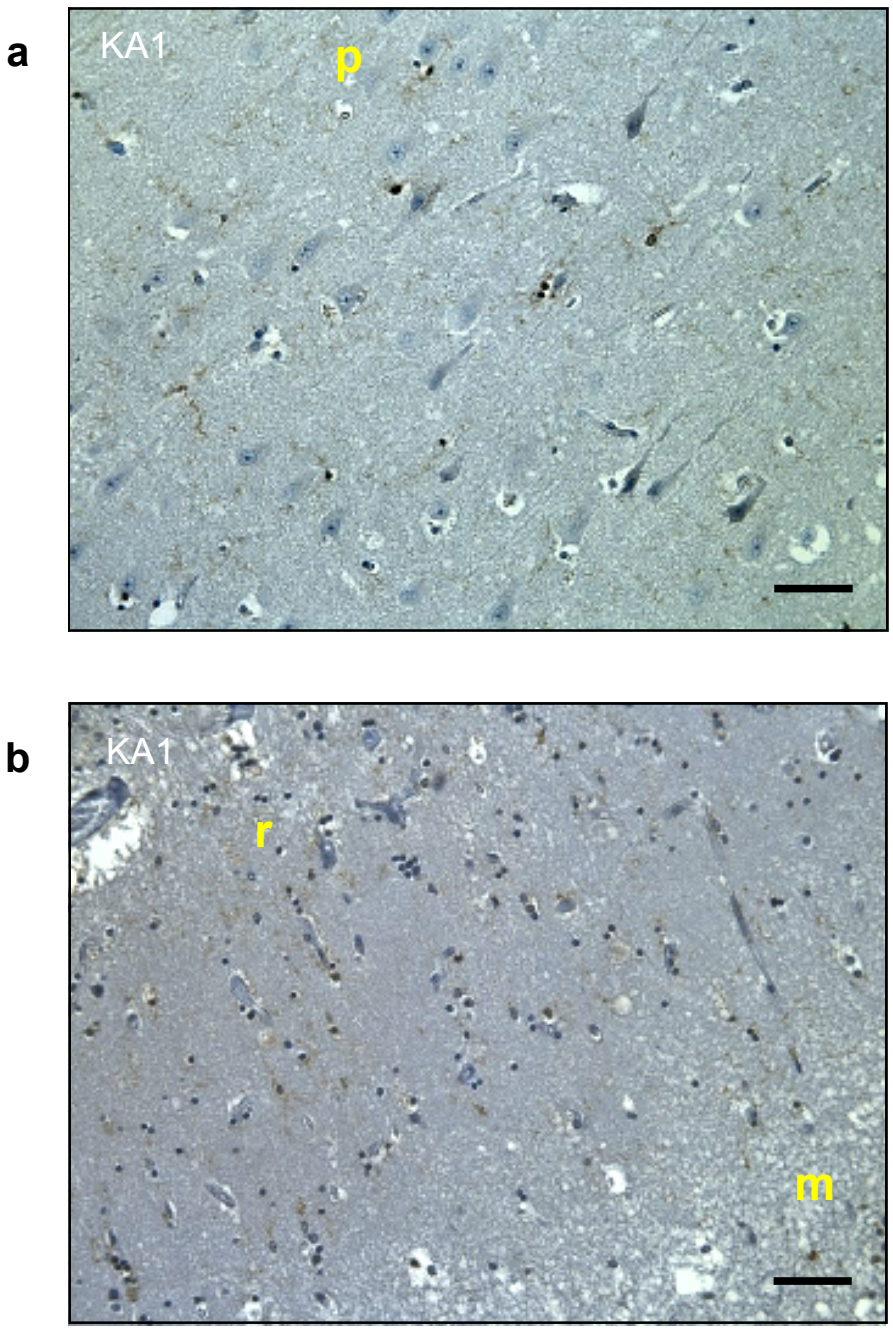

Figure 7.16 KA1 immunoreactivity in the CA1 field. KA1 immunoreactivity in stratum pyramidial (a), and stratum radiatum (b). Signal was most pronounced in processes of the stratum radiatum. The black bar represents 50µm. p, stratum pyramidal; m, stratum lacunosum-moleculare.

Punctate signal corresponding to KA1 expression in processes and glial cells was evident in the stratum lacunosum-moleculare adjoining the stratum radiatum (figure 7.16b). However, in contrast to the CA3/2 regions no immuno-positive staining was observed in the stratum oriens.

The alveus is a layer of white fibres, predominately mossy fibres, covering the ventricular surface of the hippocampus. It is comprised of white matter tracts and glial cells such as astroctyes, oligodenrocytes and microglia and the processes of neurons located in deeper layers. KA1 immunoreactivity was prominent in glial cells of all sizes, dendritic processes as well as in regions between the cells which may represent KA1 expression in the fibres of white matter (shown in figure 7.17 a).

7.2.5.2 Parahippocampal regions

The parahippocampal regions, composed of the subiculum, presubiculum, postsubiculum, entorhinal and perirhinal cortices, are located adjacent to the hippocampus. The pyramidal cell layer architecture of the CA1 field continues into subiculum which in turn adjoins to the pre- and post- subiculum pyramidal layers. Prominent KA1 immunoreactivity was observed in dendrites/processes within the pyramidal layer in the subiculum (figure 7.17b) and to a lesser extent in the pre- and post- subiculum regions.

The cytoarchitecture of the entorhinal cortex (EC) and perirhinal cortex closely resembles the frontal cortex, i.e. being divided into 6 distinct cellular layers. However, unlike the neocortex, the internal granular layer (layer IV) is absent in the EC and instead there is an acellular or plexiform layer (lamina dissecans) (Amaral and Lavenex, 2007). KA1 immunoreactivity was observed in glial and neuronal cells in all layers of the EC.

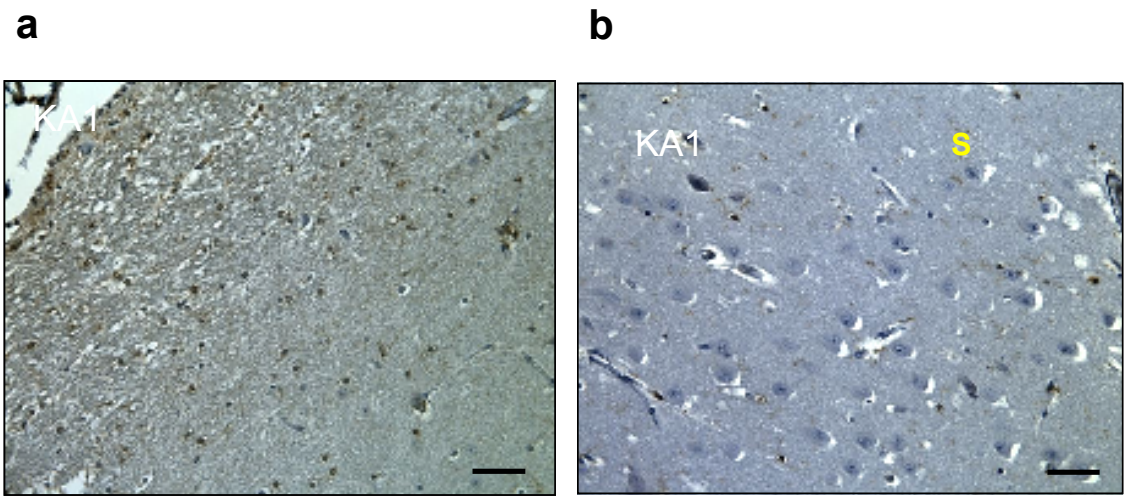

Figure 7.17 KA1 immunoreactivity in the alveus of the hippocampus and subiculum. Low magnification images of KA1 immunoreactivity in the alveus (a) and pyramidal layer of the subiculum (b). Immunoreactivity in the alveus is prominent in glial cells and in regions between the cells whereas in the subiculum KA1 expression is predominately localized to neuronal possesses. The black bar represents 50µm.

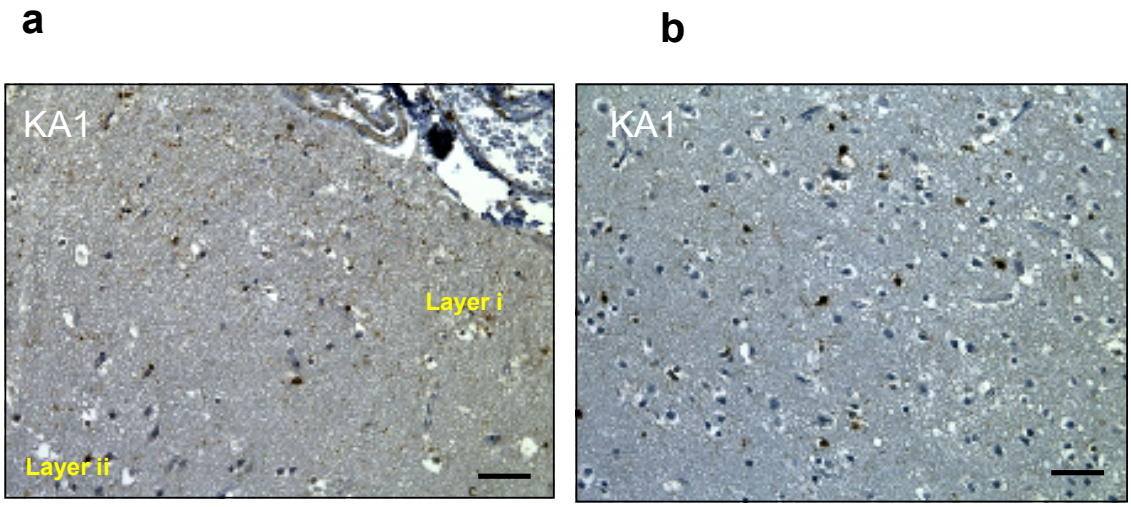

Figure 7.18 KA1 immunoreactivity in layers 1and 2 of the entorhinal cortex. KA1 expression in the acellular layer 1 (a), and granular layer 2 (b), of the entorhinal cortex. The black bar represents 50µm.

The immuno-positive signal in layer 1 of the EC was found to be localized to glial cells and regions, putatively processes, between the glia cells (figure 7.18a). Layer 2 is populated by excitatory medium to large-sized stellate cells and small pyramidal cells, both of which project to the dentate gyrus and CA3. The population of pyramidal cells is reported to be grouped in clusters (cell islands) (Kumar and Buckmaster, 2006; Amaral and Lavenex, 2007). Strong but sporadic cell body and dendritic immunoreactivity was observed in cells of a size which may be either satellite cells or pyramidal cells, as shown in figure 7.18b. However, as there was no evident clustering of the immuno-positive cells, this would suggest that it is the stellate cells that strongly express KA1.

The most numerous neurons in layer 3 are the excitatory pyramidal cells. However this layer also contains other cell types of various sizes and shapes. Strong KA1 immunoreactivity was seen in a number of pyramidal cells, smaller spherical neurons and processes between cells (figure 7. 19a). Layer 4 was not clearly discernible in the EC. Nonetheless, as large and small glial cells were stained immuno-positive throughout the EC, this would suggest that glial cells located within layer 4 also express KA1.

Layer 5 is populated by pyramidal cells, small circular cells and fusiform neurons. In contrast, layer 6 is reported to contain a wide variety of neuronal cell types. The immunoreactive pattern observed was similar in both layers - namely, sporadic staining in the cell body and nuclei of large neurons and smaller spherical cells. Furthermore, a mesh of dendritic processes surrounding the neuronal cells was prominent for KA1 reactivity, evident in figure 7.19b

The 6 cellular bands of the perirhinal cortex are composed of cell populations suggested to be comparable to the neocortex. Glial cells and subtypes of neurons in each layer of the perirhinal cortex showed positive KA1 immunoreactivity. Similar to the staining pattern observed in layer 1 of the neocortex, EC and the alveus, glial cells and processes within the acellular layer 1 of the perirhinal cortex were found to express KA1 (figure 7.20a).

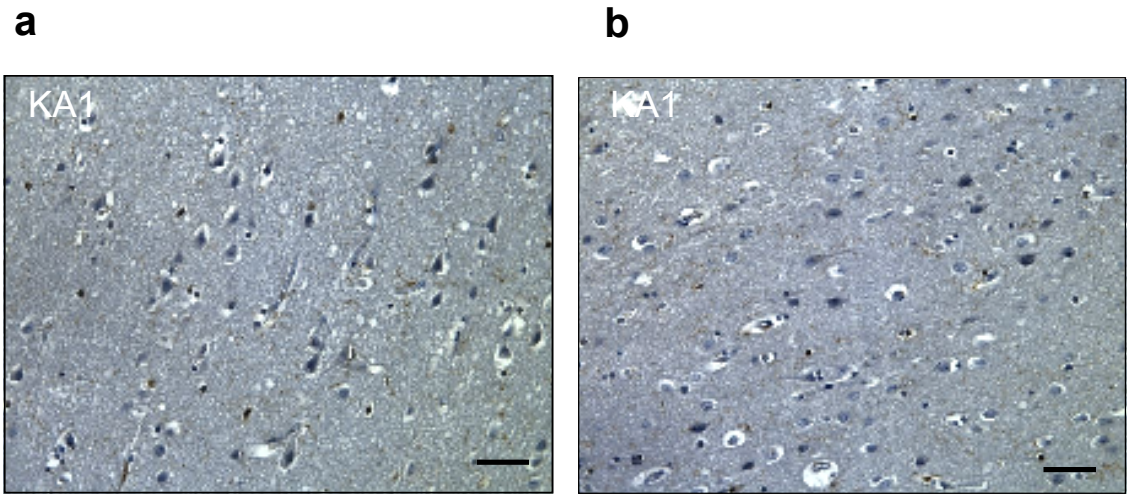

Figure 7.19 KA1 immunoreactivity in layers 3 and 5 and 6 of the entorhinal cortex. KA1 expression in layer 3 (a) and layers 5 and 6 (b) of the entorhinal cortex. Glial cells, the cell bodies and processes of neurons stained immuno-positive. The black bar represents 50μm.

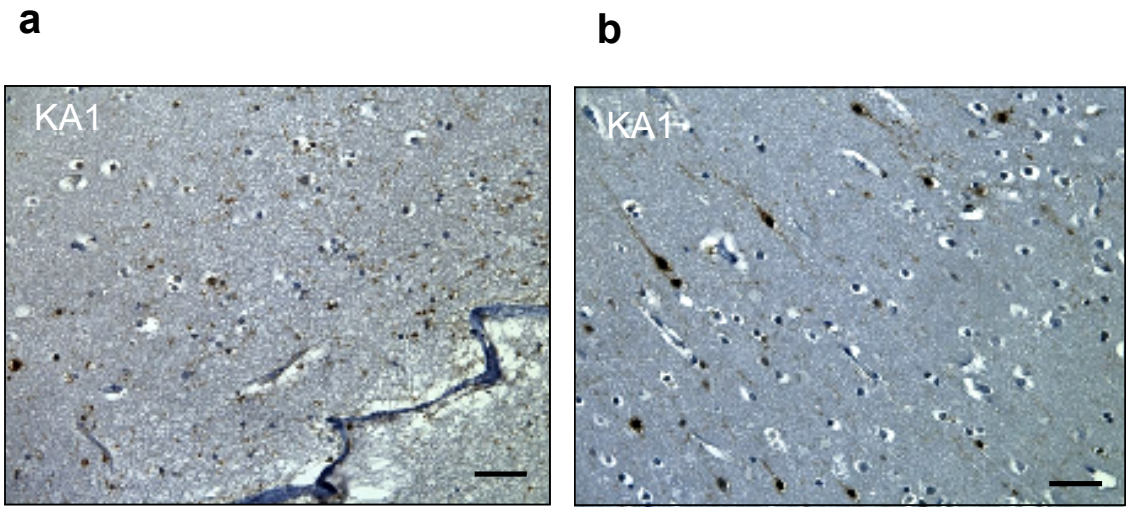

Figure 7.20 KA1 immunoreactivity in layers 1 and 2 of the perirhinal cortex. KA1 expression in layer 1 (a), and layer 2 (b), of the perirhinal cortex. The black bar represents 50μm.

Very strong, distinct reactivity was observed in the granular cell bodies and processes in layer 2, and strong, sporadic staining of spherical shaped cells and axons/dendrites in layer 3 (figure 7.20b and figure 7.21a). In layer 4 of the perirhinal cortex, like layer 2, the cell bodies of some spherical cells, consistent in shape and size of granular cells, and intercalated processes were found to express KA1, as shown in figure 7.21b. Weak cytoplasmic staining of large pyramidal cells and strong staining in smaller neurons was observed in layers 5 and 6. Furthermore, similar to layers 5 and 6 in the EC, a mesh of immuno-positive dendritic processes surrounding the cell bodies was observed, shown in figure 7.21 c and d.

7.3 Discussion

This chapter describes the characterization of KA1 protein expression in paraffin-embedded post mortem brain tissue using a novel polyclonal antibody specific to a carboxy-terminus epitope of the KA1 subunit. KA1 was found to be expressed in glia and specific populations of neuronal cells in all layers of the frontal, entorihinal and perirhinal cortices. In the cerebellum, distinct sporadic immuno-positive staining was observed in the superficial portion of the granular layer and in small cells, putatively Bergmann glia, located in the vicinity of the purkinje neurons. Strong KA1 expression was seen in hippocampus CA3/CA2 pyramidal dendritic neuropil, the processes in the CA1 strata, neuropil of the CA4 region, polymorph cells including glia and mossy fibre neurons of the hilus, and cell body and processes of granular cells in the dentate gyrus. Within these regions, KA1 expression was most prominent in axonal/dendritic processes consistent with localisation to synaptic terminals.

7.3.1 Previous reports of KA1 expression in murine and human brain

Nine studies have previously examined KA1 mRNA or protein expression in the frontal cortex, cerebellum and hippocampus formation, in human and murine brain. Nevertheless, this is the first report of KA1 protein expression using sections of human brain.

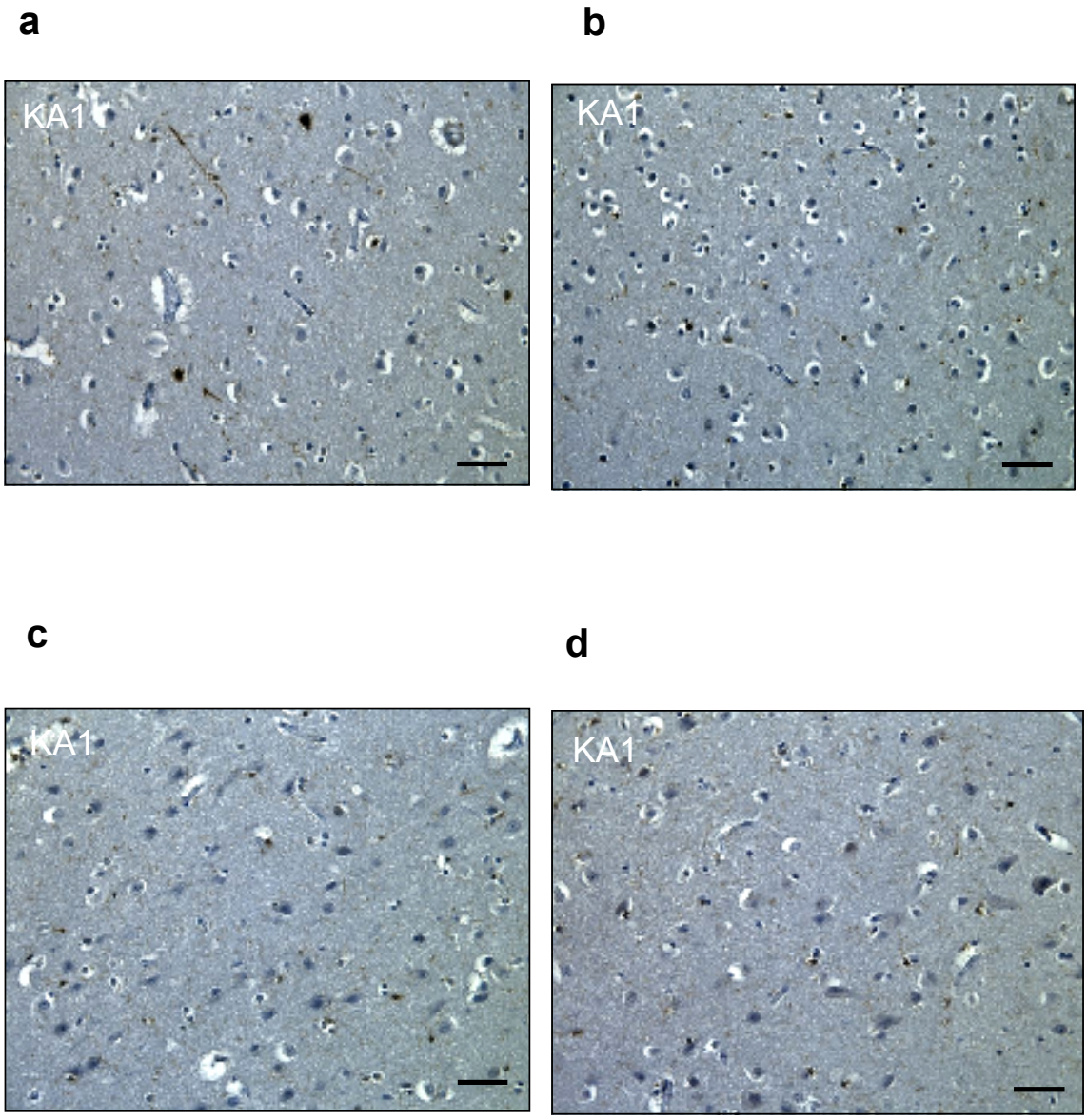

Figure 7.21 KA1 immunoreactivity in layers 3, 4, 5 and 6 of the perirhinal cortex. KA1 expression in layer 3 (a), layer 4 (b), layers 5 and 6 (c and d), of the perirhinal cortex. The cellular composition and hence boundary is difficult to differentiate between layers 5 and 6. Immunoreactivity was consistently observed in glial cells, the cell bodies and processes of neurons. The black bar represents 50μm.

The ensuing sub-sections will discuss similarities and discrepancies in expression profiles between the current and previous findings and highlight novel discoveries specific to this study.

7.3.1.1 Frontal cortex

Five studies have investigated KA1 gene expression in the neocortex of murine brain. Using a polyclonal antibody, Darstein and colleagues reported Ka1 protein expression in neurons scattered throughout layers two and five of mouse cerebral cortex (Darstein et al., 2003). In double Ka1-Cre/lacZ indicator adult transgenic mice, Ka1-Cre immunoreactivity was also observed in layer two and the anterior parts of layers five and six of the cerebral cortex (Kask et al., 2000). Similarly, Weak *Ka1* mRNA expression was also reported in layers two, five and six in rat brain (Werner et al., 1991; Wisden and Seeburg, 1993). Interestingly, this latter study also describes KA1 expression extending into the white matter of the corpus callosum located below the cortical grey matter. A higher resolution examination performed using a Ka1 specific antiserum in rat brain, describes distinct staining in a subset of layer 5 pyramidal neurons and their apical dendrites, as well as lightly stained cells in layers 2, 3 and 4 of the cerebral cortex. Double immuno-fluorescence labeling for KA1 and GABA showed that a subpopulation of GABAergic interneurons in layers 2 and 4 (superficial and deep granular layers) were also Ka1 expressing (Fogarty et al., 2000).

In human brain KA1 mRNA expression has been reported in all cortical laminae of the prefrontal cortex (Meador-Woodruff et al., 2001; Scarr et al., 2005). However, both these studies were of low resolution and gave no details of specific KA1 expressing cell types. In the current study, and consistent with the mRNA studies, KA1 was found to be expressed in all cortical layers. The strongest signal from cell somata was in sub-populations of spherical cells in layers 2 and 4. The majority of these strongly expressing KA1 cells are consistent in shape and size with granular cells. As double labeling was not performed, it is unclear whether the same cells express GABA. However, kainate receptors have been reported both to modulate GABA release at

presynaptic sites and to regulate neuronal GABA receptor expression (Braga et al., 2003; Payne et al., 2008).

In the present study weak cytoplasmic labeling of pyramidal neurons and strong localized axonic/dendritic staining in layers 3 and 5 was clearly observed. These results contrast with the findings by Fogarty and co-workers who describe very distinctive labeling of pyramidal cell somata and apical dendrites which extend into the superficial layers of the rat cortex. This disparity in KA1 immunoreactivity may be due to differences in antibody specificity, in KA1 expression between species or in different cerebral cortical regions.

The current data represent the first description of diffuse KA1 expression in dendritic processes throughout the cortical layers and within the cell bodies of large and small glial cells in the grey matter layers (including acellular layer) and underlying white matter. Kainate receptors have previously been reported to be present in oligodendrocytes, astrocytes and microglia, where they are postulated to be important for mediating glutamate excitoxicity (Matute et al., 2001; Verkhratsky and Kirchhoff, 2007). Moreover, non-synaptic release of glutamate from astrocytes is thought to constitute a potential source of glutamate to activate extrasynaptic kainate receptors (Liu et al., 2004). Thus, the present data raise a number of intriguing questions such as: what is the predominant function of KARs in glia cells; and how, when expression is perturbed, may this contribute to pathological states?

7.3.1.2 Cerebellum

Only three murine studies have reported a consistent signal for KA1 expression in the cerebellar cortex. In mouse sections, Ka1 immunoreactivity was observed in cerebellar purkinje cell bodies and their dendritic arborizations but not in the granule layer or in molecular layer interneurons (Darstein et al., 2003). This pattern of expression was also described in the rat brain by Wilsden and Seeburg (1993). In contrast, Fogarty and colleagues report Ka1 expression in a subset of cells and radial fibres within the molecular layer, in addition to strong Ka1 immunoreactivity in purkinje cell somata and

their dendritic arborizations in rat cerebellum. Double immuno-fluorescence labeling for KA1 and GFAP (a marker of astrocytes) suggested that the radial fibres observed in the molecular layer were Bergmann glia. However the cell bodies of the Bergmann glia were not found to be immuno-positive (Fogarty et al., 2000).

In the current study distinct immunoreactivity was observed in sporadic clusters located within the superficial portion of the granular layer. This pattern of staining, although not previously described for KA1, has been reported for GluR5 and mGluR2/3 (Ohishi et al., 1994; Lerma et al., 2001). The shape, size and position of these clusters is accordant with excitatory GABAergic golgi cells. Double immuno-fluorescence analysis using antibodies for mGluR2/3 and GABA performed by Ohishi and colleagues, confirmed that these putative cell bodies/signal clusters show GABA immunoreactivity. Although the functional consequences of KA1 receptor subunit expression within or in close proximity to (putative) golgi cells remains to be clarified, this finding again supports the hypothesis that kainate receptor activity may influence GABAergic transmission and hence, within the cerebellum, contribute to information processing and integration via feedback mechanisms.

The present results also indicated weak cytoplasmic KA1 expression within purkinje neurons, consistent with previous findings from mouse and rat expression studies. In addition, diffuse immuno positive staining was observed in small spherical cells within the granular and purkinje layers and sparser staining in dendrites positioned within the molecular layer, both in close proximity to purkinje cells. Immunoreactivity for GFAP indicated that the position of the spherical cells is consistent with the location of Bergmann glia. However, the sparse dendritic signal may be the processes of either purkinje or Bergman glia cells. These results contrast with the findings from Fogarty and co-workers which describe strong and diffuse Ka1 expression in a subset of cells and radial glial fibres within the molecular layer in rat brain (Fogarty et al., 2000). However, the fact that KA1 may be expressed in a population of cells in the cerebellum suggested to have a neural stem cell phenotype is an interesting discovery which parallels findings for other brain regions (discussed in section 7.3.1.4).

7.3.1.3 Amygdala

There has been only one study of KA1 expression in the amygdaloid complex. In the rat brain, Ka1 mRNA was found to be absent as examined by low resolution *in situ* hybridization (Werner et al., 1991). Nevertheless, electrophysiological experiments suggest an involvement of kainate receptors in synaptic transmission (Bleakman, 1999). The current findings indicate weak KA1 expression in the cell bodies of large neurons located within amygdala nuclei, and strong immunoreactivity in glia cells in both grey and white matter. Staining in processes was noticeably absent as compared to other brain regions, which could be explained, in part, by the reduced quality of tissue sections.

7.3.1.4 Hippocampus

The distribution of Ka1 mRNA and protein, as reported in the mouse and rat hippocampal formation, is comparable to the current findings. For example, Ka1 expression was found in all CA regions of the hippocampus with the most prominent expression in the CA3 subfield and DG granule cells (Wisden and Seeburg, 1993; Porter et al., 1997; Fogarty et al., 2000; Darstein et al., 2003). One disparity between previous findings and the present data was observed in a study using KA1-Cre/lacZ adult transgenic mice. KA1-Cre immunoreactivity was described as absent in the somata and dendrites of DG granule cells and cell bodies of CA3 pyramidal neurons (Kask et al., 2000). As these results also conflict with other rodent Ka1 expression studies, it is unlikely that this inconsistency is due to differential expression between species but may be the result of aberrant transgene expression pattern or altered intracellular Cre distribution.

Three *In situ* hybridization studies investigating *KA1* mRNA expression in the human hippocampus have been conducted. Wisden and Seeburg observed KA1 expression in all pyramidal cells and found substantially elevated levels in CA3 pyramidal neurons (Wisden and Seeburg, 1993). Whereas Porter and co-workers report that KA1 was detected in the dentate gyrus and CA3 region (Porter et al., 1997). Similarly, Beneyto

and co-workers observed KA1 in all regions examined but, like the two aforementioned studies, did not describe in detail specific strata or KA1 expressing cell types (Beneyto et al., 2007).

Consistent with these findings, the present study demonstrated strong distinct KA1 expression in the dendrites (mossy fibre inputs) located within the stratum lucidum and more sporadic dendritic staining in the stratum radiatum of the CA3 field. The ultrastructural localization of KA1 in these mossy fibre synapses, i.e localization on pre- or post-synaptic sites, has been a matter of some debate. Fogarty et al. (2000) investigated this question by using electron microscopy (EM) on pre-embedded, Ka1 immunostained rat brain sections of the CA3 subfield. They showed that labeling was present in dendritic structures that were post-synaptic to axon terminals within the stratum radiatum. They also report that mossy fibre terminals (pre-synaptic) and the post- synaptic dendritic spines within the stratum lucidum were devoid of label.

In contrast, Darstein and co-workers performed immunogold EM on hippocampal mouse sections stained for Ka1. They reported immunogold labeling on pre-synaptic, mossy fibre boutons, and to a lesser degree, postsynaptic spines within the stratum lucidum. Furthermore, labeling with 5nm 2 gold particles, which gives an increased spatial resolution, indicated a major KA1 peak in distribution on the presynaptic membrane and a smaller peak of distribution near to the post-synaptic membrane in both synaptic and extrasynaptic zones (Darstein et al., 2003). Unfortunately, the resolution of immunostaining in the current study is too low to determine ultrastructure localization. However, KA1 was shown to be clearly expressed in both CA3 pyramidal cells and mossy fibre neurons.

In the current study, weak KA1 staining of pyramidal neurons and stronger labeling of processes with the pyramidal cell layer and throughout the stratum radiatum of the CA1 subfield was observed. The stratum radiatum within the CA1 is described as the suprapyramidal region in which CA3 to CA1 Schaffer collateral afferent connections are

located. This region is also rich in a variety of inhibitory interneurons such as basket and radial trilaminar cells. Administration of kainate (KA), the agonist of this receptor type, has been reported to cause a reduction in GABAergic inhibition in CA1 pyramidal neurons as revealed by a decrease of evoked GABAergic IPSCs. Whether this inhibitory effect is mediated by presynaptic KARs localized on GABAergic terminals on CA1 pyramidal cells is still a matter of debate (Lerma, 2003). However, administration of KA in submicromolar concentrations produces the opposite effect, i.e. an increase in spontaneous GABAergic IPSCs, and this GABAergic facilitation has been proposed to occur through the activation of somatodendritic KARs located on interneurons (Vincent and Mulle, 2008). Again, double labeling experiments using KA1 and neurotransmitter specific marker antibodies, might reveal the class of cell in which KA1 is expressed within the strata of the CA1 subfield.

The present results also clearly indicate that KA1 is expressed in all regions of the mossy fibre pathway, i.e. apical dendrites, somata and axons of the granular cells, mossy fibre neurons in the hilus, mossy fibre terminals in the CA3 field and mossy fibre white matter tracts in the alveus. Of particular interest is the evident KA1 distribution within the granule cells and along the subgranular zone (SGZ) in the dentate gyrus. It is in this specific region that adult neurogenesis occurs, i.e. the generation of new neurons in the adult brain. Granule neurons are generated throughout life from two populations of neural progenitor cells located within the DG which can be identified according to their specific morphologies and expression of sets of molecular markers.

Type 1 progenitor cells have radial processes spanning the granule cell layer and express nestin, SOX2 (Sry-related HMG box transcription factor) and GFAP (Zhao et al., 2008). In the current study, immunohistochemistry performed using a GFAP specific antibody on hippocampal sections indicated that there may be some positional overlap in GFAP and KA1 expressing cells. Type 2 progenitor cells have short processes, do not express GFAP but are SOX2-positive. A recent study has shown that a single, type 2 progenitor cell can give rise to both a neuron and glial cells, i.e. these cells have stem cell

properties (Suh et al., 2007). The distribution of KA1 in cells at the SGZ raises the intriguing possibility that KA1 is expressed in one or both types of neural progenitor cell and is in line with finding that KA1 is potentially expressed in Bergmann glia – a stem cell population in the cerebellum. Important future considerations should include co-localisation studies of KA1 and neurogenesis/stem cell specific molecular markers within human hippocampal and cerebellum sections.

The proliferation and differentiation of neural progenitor granule cells are both processes which may result in aberrant neurogenesis when disrupted. However, equally important is the migration and functional integration of the newly-born granule neurons into the mossy fibre circuitry. Recent evidence suggests that during development KARs may be involved in axon navigation. For example, filopodial motility is reported to be differentially regulated by kainate receptors in hippocampal mossy fibres in the developing neonatal mouse brain (Tashiro et al., 2003). Furthermore, similar to the process of synaptogenesis during development, synapse formation and activity dependent re-modelling of synapses are critical factors determining appropriate functional connectivity. Indeed, the specialized synapses of mossy fibres (known as 'thorny excrescences') are described to have numerous morphological types of terminal, and this morphological variation has been proposed to reflect different maturational stages of connections formed by newly generated granule cells (Gould, 2007). The expression profile of KA1, in conjunction with its functional role at mossy fibre terminals, leaves open the possibility that KA1 (within a KAR complex) may play a part in the migration and synaptic integration of newly generated neurons. Future research exploring this exciting avenue, for example histological and electrophysiological investigation of Ka1 transgenic mice, might provide further insight into these possibilities.

7.3.1.5 Parahippocampal regions

Two studies have examined KA1 mRNA expression within regions of the parahippocampus in sections of rat and human tissue. KA1/Ka1 was detected at a moderate level in both the subiculum and EC (Wisden and Seeburg, 1993; Beneyto et al., 2007). Furthermore, human KA1 was found to be distributed throughout all 6 layers of the perirhinal cortex, consistent with the present results (Beneyto et al., 2007). As yet the cellular organization of the perirhinal cortex and consequential direct afferents to other hippocampal regions has not been fully characterized (Liu and Bilkey, 1998). However, the current findings indicated prominent KA1 immunoreactivity in cells within layer 2 of the EC, a region which is known to provide a direct input (the perforant path projection) to the CA1 and CA3 subfields as well as the dentate gyrus.

7.3.2 Discrepancies between studies: advantages and disadvantages of IHC

The disparity in reports of KA1 expression evident in previous studies and compared to the current findings may reflect a difference in species-specific expression. In addition, there may be subtle differences between KA1 mRNA and protein localization. Nevertheless, discrepancies might also arise on account of the technique used to examine KA1 expression profile. For example, *in situ* hybridization and quantitative autoradiography are techniques which have a low spatial resolution and a high background signal which may make weaker sporadic cell staining difficult to interpret. An advantage of IHC is that labeling is of a higher resolution, enabling localized cell and subcellular distribution to be determined. Conversely, a disadvantage to IHC is the possibility that the KA1 antibody cross reacts to structurally similar epitopes such as different isoforms or other KAR subunits. This may be one explanation as to why the IHC study by Fogarty et al., (2000) report differences in expression both to, other studies performed using rat brain and to the current findings. However, an additional control test, not performed in this study, would be to pre-absorb the KA1 primary antibody with the appropriate (unique) immunizing peptide, which should consequently block any specific immunoreactivity.

7.3.3 Expression patterns of kainate receptor subunits in the brain

Kainate receptors are tetrameric combinations of five subunits (GluR5-7, KA1, KA2) of which only GluR5-7 can form functional homomeric cationic channels. The auxillary subunits, KA1 and KA2 must co-assemble with the principal subunits for functional expression on the plasma membrane. Within the brain, KAR subunit composition is suggested to be highly heterogeneous, with different combinations giving rise to native kainate receptors that have distinct physiological and pharmacological properties (Jaskolski et al., 2005). All receptor subunits are expressed widely throughout the adult central nervous system and show distinct overlapping patterns of mRNA and protein expression. To add to the complexity of KAR subunit distribution, GluR5-7 undergo alternative splicing and/or mRNA editing and these iosforms may also be differentially distributed in cell populations and subcellular sites.

KA2, GluR6 and GluR7 are described as having a widespread pattern of distribution in human brain tissue (Porter et al., 1997; Chittajallu et al., 1999). In contrast, it is suggested that GluR5 shows a more limited expression profile. In the present study, the most comprehensive investigation of KA1 mRNA or protein distribution in human brain, KA1 was indicated to be expressed in both glia and subsets of neuronal cells in every brain region examined.

All five subunits are reported to be present in layers 2-5 in human frontal and entorhinal cortices. KA1 and GluR7 were found to be expressed at the highest levels in the frontal cortex and similarly KA1, KA2 and GluR7 highest in the EC (Meador-Woodruff et al., 2001; Scarr et al., 2005; Beneyto et al., 2007). In the cerebellum KA2 and GluR6 are strongly expressed throughout the granular cell layer but are absent in the purkinje cells or the molecular layer, whereas GluR7 mRNA is expressed in some cells in the molecular layer (putatively stellate/basket cells) as well as at low levels in purkinje and granule cells. The expression patterns of GluR5 and KA1 show some overlap, e.g. purkinje cells and sporadic labeling in a specific subgroup of cells (putatively golgi

cells) located within the superficial portion granular cell layer. This would suggest that in these particular cells KA1 assembles with GluR5 to form a functional receptor.

The heterogeneous nature of kainate receptor subunit composition is also apparent in the human hippocampus at both a cellular and subcellular level. KA1, KA2, and GluR6 mRNA are all reported to be expressed in pyramidal cells within the CA1 and CA3 subfields and granule cells of the dentate gyrus (Porter et al., 1997). However, electrophysiological studies in conjunction with *in situ* histology examination suggests that, unlike KA1, GluR6 and KA2 are predominately localized to the post synaptic site at mossy fibre contacts in the CA3 stratium lucidum (Pinheiro and Mulle, 2008). GluR5 and GluR7 subunits have an even more distinct regional pattern. GluR5 is expressed in the CA1 and CA3 but not in the dentate gyrus. In contrast, GluR7 is expressed in the dentate gyrus and at low levels in cells within the stratium oriens and CA3 subfield (Porter et al., 1997). Figure 7.22 summarizes the current findings for KA1 and schematically illustrates distribution of GluR5-7 and KA2 in the hippocampal formation.

7.3.4 The function of KARs and KA1

As introduced in section 1.4.3.3 of chapter 1, kainate receptors are involved in short term synaptic plasticity mechanisms, synaptic integration and long-term modulation of neurotransmission. KARs located at post-synaptic sites directly mediate excitatory transmission, while pre-synaptic KARs typically modulate neurotransmitter release through noncanonical signalling pathways (Lerma, 2006). Furthermore, activation of kainate receptors is reported to produce bi-directional modulation of both excitatory and inhibitory transmission, i.e. low to moderate activation enhances transmission, whereas stronger activation inhibits transmission (Huettner, 2003).

These diverse functions require the appropriate subcellular localization of native KARs (comprised of particular subunits) within specific functional domains of neurons (see Lerma 2003; Heuttner 2003 and Pinheiro and Mulle 2008., for comprehensive reviews).

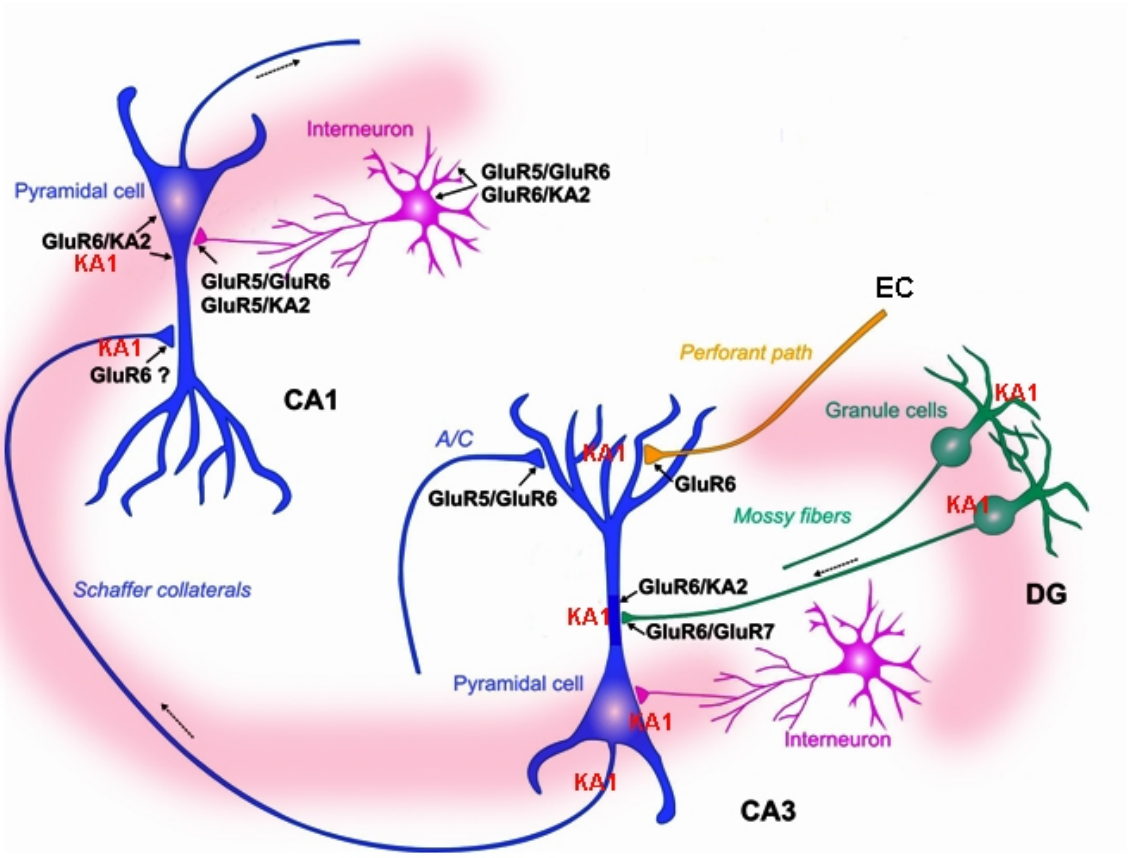

Figure 7.22 Schematic representation summarizing KAR subunit expression in the hippocampus and dentate gyrus. Figure adapted from Vincent and Mulle, 2008, figure 1. The distribution of KA1, as determined in the present study, is shown (KA1 coloured red). Differences in ultra-structure subcellular localization are not indicated.

However, it is not yet known if it is the assembly of specific combinations of subunits which determines subcellular localization.

KAR mediated synaptic function is reported to be particularly important for hippocampal mossy fibre - CA3 (MF-CA3) long-term potentiation and normal synaptic plasticity. Plasticity mechanisms at these synapses are fundamentally different from other regions. For example, induction of mossy fibre LTP is independent of NMDA activation and is expressed presynaptically (Harris and Cotman, 1986; Nicoll and Schmitz, 2005).

The use of transgenic mice has begun to provide some insight into which receptor subunits are involved in the different functions of kainate receptors in this region. Contractor and colleagues investigated the electrophysiological properties at MF-CA3 synapses in KA1 knockout and Ka1/Ka2 double knockout mice. They found that paired pulse and frequency facilitation in these mice was normal, suggesting that an absence of KA1, or both subunits, does not alter presynaptic kainate function. However, mossy fibre LTP was found to be impaired in Ka1/Ka2 double KO mice. Furthermore, in $Ka1^{-/-}$ mice, $EPSC_{KA}$ was not observed with normal high synaptic stimulation but could be observed using a train of high frequency stimuli. This suggested that the distribution of post-synaptic KARs is localised to the peri-synaptic regions and hence is abnormal in $Ka1^{-/-}$ mice. Together these results led the authors to hypothesise that Ka1 and Ka2 together control functional surface expression of KARs and Ka1 controls synaptic localization at MF-CA3 synapses (A. Contractor, Personal communication).

From the distribution profile of KA1 in the human hippocampal formation presented in this chapter, it is evident that KA1 is expressed in regions involved in neuronal processing within all three pathways forming the trisynaptic circuit- the major route of information transfer commonly considered to underlie memory consolidation. It is possible therefore, that alterations in KA1 expression not only have a significant effect

upon CA-MF transmission, as discussed above, but could also influence information processing within other regions of the hippocampal circuitry. This in turn may have physiological consequences on network activity outside of the hippocampus, which potentially may underlie aberrant facets of cognition.

CHAPTER 8

A GENOTYPE EXPRESSION CORRELATION STUDY OF KA1 IN HUMAN BRAIN

ACKNOWLEDGEMENTS FOR CHAPTER 8

The Genotyping of tissue from the twelve subjects investigated was performed by Ben Pickard. The coding of samples was carried out by Robert Walker (Neuropathology Unit, University of Edinburgh).

.

8. A genotype expression correlation study of KA1 in human brain

8.1 Preface

The previous two chapters described the identification of an insertion/deletion (indel) in the 3'UTR of *GRIK4/*KA1 as a protective factor for bipolar disorder, and the subsequent characterization of KA1 protein expression in human brain sections. As we have shown that *GRIK4* mRNA transcripts carrying the deletion are relatively more abundant, we hypothesise this variant may also result in differential protein distribution and abundance. To that end, this chapter reports the results of a genotype/protein correlation using brain tissue from individuals asymptomatic for psychiatric illness genotyped for the associated 3'UTR deletion variant.

8.2 Results

8.2.1 Quantification of KA1 expression

Brain tissue donated from the Edinburgh University Human brain bank was genotyped for the ins/del variant. Five heterozygote indels, 6 homozygote insertions and 1 homozygote deletion were matched for age, gender and cause of death. Details pertaining to these samples and the demographic profile of each genotype group are presented in tables 8.1 and 8.2. Paraffin embedded post mortem human coronal sections of the hippocampus and parietal frontal cortex were received coded and the study performed blinded.

In the hippocampus, areas analyzed were the molecular layer and granular cell layer of the dentate gyrus, alveus, hilus, CA4, CA3 and CA1 subfields. In the frontal cortex, immunopositive cell counts in layers 1- 4 were analysed separately. Due to the difficulty in distinguishing between layers 5 and 6, these strata were classified as one region. Immunopositive axons/processes, neuronal and glial counts were quantified within circles of 100μm radii taken from 5-10 images randomly selected from each region of interest using a minimum of 2 slides per individual.

Case Identifier	Gender	Age	PMI (h)	Brain pH	Genotype	Cause of Death
SD004/06	F	52	64	6.40	DEL/DEL	Acute myocardial infarct
SD006/06	M	40	48	6.20	INS/INS	Acute myocardial infarct
SD007/05	M	37	92	nd	INS/DEL	Acute myocardial infarction
SD014/05	F	59	48	nd	INS/DEL	Subarachnoid haemorrhage
SD016/06	M	25	92	6.60	INS/INS	Internal bleeding. Rupture of thoracic aorta (RTA)
SD019/05	F	51	115	6.30	INS/INS	Hypertensive heart disease & cirrhosis
SD019/06	M	20	37	5.55	INS/DEL	Hyperglycaemic coma
SD021/05	F	48	50	6.50	INS/INS	Pulmonary thromboembolism
SD022/06	M	53	51	6.30	INS/INS	Acute myocardial infarct
SD025/05	M	28	39	7.50	INS/DEL	Suspension by a ligature
SD036/05	M	50	61	7.30	INS/DEL	GI haemorrhage & liver failure
SD041/05	M	24	51	6.30	INS/INS	Fatal poisoning with alcohol

Table 8.1 Details of individual samples used for the genotype correlation study. Gender, age, post mortem interval (PMI), pH, genotype and cause of death listed. (DEL/DEL), homozygous deletion; (INS/DEL), heterozygous; (INS/INS) homozygous insertion; RTA, road traffic accident.

	hom del (*n* =1)	het (*n* =5)	hom ins (*n* =6)
Mean age: yr (range)	52	38.3 (20-59)	40.2 (24-53)
Gender ratio: male/female	0/1	4/1	4/2
Mean PMI: hr (range)	64	55.4 (37-92)	67.8 (50-115)
Mean Brain pH	6.4	6.8	6.4

Table 8.2 Genotype Group Demographics. Mean age, gender ratio, mean post mortem interval (PMI) and mean brain pH listed for each genotype group. The number of samples in each group is listed in brackets.

Immunopositive glial cells, i.e. astrocytes, oligodendrocytes and microglia, were examined separately from neuronal counts in the hilus, CA4, CA3 and CA1 of the hippocampus and layers 3 and 5 of the frontal cortex. Neuronal positive counts included immunopositive labelled processes as well as cell somata and nuclei. Neuropil staining in the hilus, CA4 and CA3 subfields was assessed semi-quantitatively using a colour deconvolution technique in Image J (Ruifrok and Johnston, 2001). Details of this method are presented in chapter 2, section 2.5.4.1.

8.2.2 Genotype/protein correlation in the hippocampus

The mean hippocampal cell counts and neuropil percentages calculated for each sample are presented in table 8.3. One sample (SD016/06 genotyped homozygous insertion) had to be excluded from the analysis of all hippocampal regions owing to torn tissue sections. Data for a second sample (SD014/05 genotyped heterozygous) was also not obtained for the CA4, CA3, CA1 sub-regions on account of poor tissue quality. The mean cell counts and neuropil percentages per genotype group are listed in table 8.4.

A summary of the *P* and *F* values associated with hippocampal cell count and neuropil immunoreactivity percentage differences between the groups is provided in table 8.5. A significant difference in immunoreactive cell counts between the homozygous insertion (hom ins) group and heterozygous/homozygous deletion (het/hom del) or heterozygous (het) groups was found in the direction predicted for the granular cell layer of the dentate gyrus (het + hom del vs hom ins, $F = 25.07$, [1,10], $P = 0.0005$; het vs hom ins, $F = 25.51$, [1,10], $P = 0.0005$) , and CA3 pyramidal cells (het + hom del vs hom ins, $F = 6.35$, [1,9], $P = 0.018$; het vs hom ins, $F = 11.93$, [1,9], $P = 0.0055$) [one way ANOVA, one tailed], shown in table 8.5 and graph 8.1 a and b). Moreover, comparison of homozygous insertion versus heterozygotes alone genotypes indicated a trend in increased protein expression in heterozygotes in CA3 dendritic neuropil ($H = 2.16$, $P = 0.07$), CA4 pyramidial cells ($F = 2.26$, [1,8], $P = 0.09$), CA1 pyramidal cells ($F = 2.16$, [1,8], $P = 0.09$), and immunoreactivity in the alveus ($F = 2.19$, [1,8], $P = 0.09$), [one way ANOVA and nonparametric Kruskal-Wallis Test, one tailed] (Graphs 8.1 c and d).

Table 8.3 Hippocampal cell count and neuropil percentage means per individual sample. Standard errors are shown.

Sample	ML Gial cells	ML Neuronal	DG Granular	Alveus	Hilus Neuronal	Hilus glial	CA4 Neuronal	CA4 glia	CA3 pyramidal	CA3 glial	CA1 pyramidal	CA1 glial	Hilus Neuopil	CA4 Neuopil	CA3 neuropil
SD025/05	12.3 ± 1.2	1.9 ± 0.5	7.2 ± 0.6	15.3 ± 0.9	5.7 ± 0.6	19.4 ± 1.8	7.7 ± 0.8	19.6 ± 1.7	20.4 ± 1.9	14.4 ± 1.2	12.1 ± 1.1	11.0 ± 1.2	6.3	5.2	9.8
SD022/06	5.9 ± 0.6	0.3 ± 0.1	3.3 ± 0.4	9.2 ± 0.6	3.3 ± 0.5	13.3 ± 1.3	5.0 ± 0.9	15.3 ± 1.6	16.0 ± 1.5	7.7 ± 0.7	3.9 ± 0.5	7.0 ± 1.0	3.0	1.5	3.0
SD041/05	9.5 ± 1.4	6.9 ± 1.0	4.6 ± 0.4	17.6 ± 1.6	7.4 ± 0.8	16.3 ± 1.4	10.3 ± 1.1	17.0 ± 1.7	12.5 ± 1.4	5.7 ± 0.5	6.7 ± 0.8	6.1 ± 0.9	1.4	0.8	4.0
SD019/05	12.9 ± 1.5	8.3 ± 0.8	5.4 ± 0.7	6.7 ± 0.7	9.2 ± 1.0	10 ± 1.0	9.5 ± 1.2	11.5 ± 1.3	16.4 ± 1.0	8.3 ± 0.6	14.8 ± 1.5	12.1 ± 1.6	1.8	3.1	3.9
SD016/06	nd	nd	nd	nd	nd	nd	nd	nd	nd	nd	nd	nd	nd	nd	nd
SD036/05	9.3 ± 0.8	14.5 ± 1.4	7.9 ± 0.7	17.4 ± 1.6	16.7 ± 1.6	8.6 ± 0.9	20.7 ± 1.9	8.2 ± 0.7	19.7 ± 1.7	22.7 ± 1.7	14.3 ± 1.4	9.7 ± 1.0	3.6	6.5	11.1
SD004/06	11.0 ± 1.2	4.5 ± 0.5	7.1 ± 1.0	9.9 ± 1.0	6.8 ± 0.8	17.0 ± 1.5	10.5 ± 1.1	12.4 ± 1.3	12.9 ± 1.0	9.9 ± 0.8	8.4 ± 0.7	10.5 ± 1.1	4.1	3.6	2.0
SD006/06	7.7 ± 0.8	10.1 ± 0.9	4.3 ± 0.4	11.2 ± 1.1	14.5 ± 1.4	5.3 ± 0.5	18.2 ± 1.7	7.9 ± 0.7	12.0 ± 1.1	13.8 ± 1.5	7.9 ± 1.0	8.5 ± 1.3	0.7	2.6	3.1
SD021/05	5.5 ± 0.7	4.8 ± 0.6	5.8 ± 0.7	7.4 ± 0.5	9.5 ± 1.1	12.7 ± 1.1	12.8 ± 1.1	13.4 ± 1.2	10.2 ± 1.0	14.3 ± 1.2	8.8 ± 1.1	8.2 ± 0.8	6.7	7.5	1.3
SD019/06	5.3 ± 0.6	7.7 ± 1.0	10 ± 1.1	10.4 ± 0.8	11.5 ± 1.2	6.3 ± 0.9	15.7 ± 1.4	5.1 ± 0.7	4.8 ± 0.9	18 ± 2.1	13.4 ± 1.1	6.5 ± 0.7	3.8	1.0	2.3
SD014/05	9.1 ± 0.8	8.1 ± 0.8	7.1 ± 0.8	nd	11.3 ± 1.2	9.0 ± 1.0	nd	nd	nd	nd	nd	nd	1.4	nd	nd
SD007/05	10.7 ± 0.9	15.0 ± 1.5	9.2 ± 0.8	13.8 ± 1.2	22.4 ± 2.0	14.5 ± 1.5	24.4 ± 2.2	15.7 ± 1.4	16.4 ± 1.4	26.3 ± 2.3	7.9 ± 0.7	7.5 ± 0.8	10.5	17.3	22.3

	Hom insertion (*n*=6)		Het + hom del (*n*=6)		Het (*n*=5)		Hom deletion (*n*=1)	
	Mean	SEM	Mean	SEM	Mean	SEM	Mean	SEM
Molecular layer neuronal	6.08	1.69	8.62	2.15	9.44	2.43	4.50	0.56
Molecular layer glia	8.30	1.35	9.62	0.99	9.34	1.16	11.00	1.16
Dentate gyrus granule cells	4.69	0.43	8.09	0.50	8.28	0.57	7.10	0.93
Alveus	10.42	1.96	13.36	1.31	14.23	1.32	9.9	1.03
Hilus neuronal	8.78	1.81	12.40	2.56	13.52	2.82	6.8	0.78
Hilus glia	11.52	1.92	12.47	2.14	11.56	2.38	17.00	1.50
Hilus Neuropil abundance	2.70	1.07	4.94	1.28	5.12	1.55	4.06	1.49
CA4 neuronal	11.16	2.16	15.82	3.99	17.16	3.59	10.50	1.09
CA4 glia	13.02	1.58	12.22	2.37	12.17	2.59	12.40	1.31
CA4 Neuropil abundance	3.11	1.16	6.65	2.55	7.40	3.11	3.64	1.68
CA3 neuronal	9.95	1.72	18.34	2.60	20.35	2.34	10.30	0.89
CA3 glia	13.42	1.20	14.94	2.51	15.45	3.12	12.92	0.98
CA3 Neuropil abundance	3.05	0.47	9.49	3.69	11.36	4.11	2.04	0.13
CA1 neuronal	8.42	1.80	11.22	1.19	11.93	1.27	8.40	0.72
CA1 glia	8.38	1.02	9.05	0.80	8.68	0.92	10.50	1.08

Table 8.4 Hippocampal cell count and neuropil percentage means per genotype group. Values are shown for homozygous insertion group (Hom insertion), heterozygous and homozygous deletion group, Heterozygous group (het) and homozygous group (hom deletion). Red values indicate significance difference between groups or a trend towards significance.

	het + hom del vs hom ins		het vs hom ins	
	P value	*F* value	P value	*F* value
Molecular layer neuronal	0.20	0.81	0.14	1.29
Molecular layer glia	0.22	0.65	0.29	0.34
Dentate gyrus granule cells	0.00050	25.07	0.00050	25.51
Alveus	0.13	1.47	0.09	2.19
Hilus neuronal	0.15	1.23	0.10	2.00
Hilus glia	0.38	0.11	0.50	0.00
Hilus Neuropil abundance	0.11	1.72	0.12	1.66
CA4 neuronal	0.13	1.54	0.09	2.26
CA4 glia	0.40	0.07	0.41	0.06
CA4 Neuropil abundance	0.13*		0.16*	
CA3 neuronal	0.018	6.35	0.0055	11.93
CA3 glia	0.31	0.26	0.28	0.37
CA3 Neuropil abundance	0.17*		0.07*	
CA1 neuronal	0.12	1.59	0.09	2.16
CA1 glia	0.32	0.24	0.42	0.04

Table 8.5 P and *F* values associated with hippocampal cell counts and neuropil immunoreactivity percentages. * denotes non parametric analysis. Red values indicate significance or a trend towards significance. Parametric tests performed, one-way ANOVA (one-tailed) and non-parametric, Kruskal-Wallis (one-tailed).

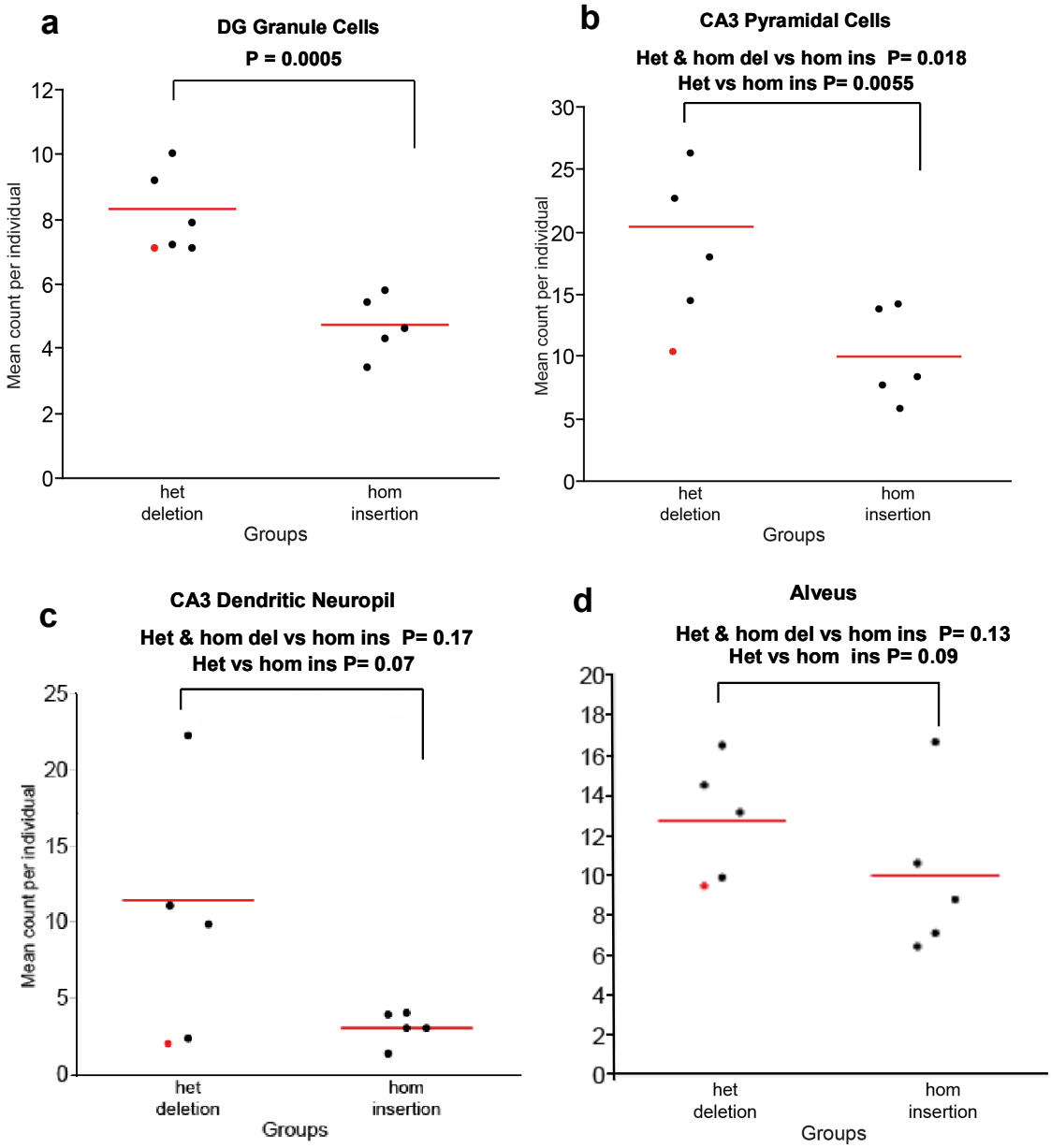

Graph 8.1 Genotype effect on mean cell counts and neuropil abundance in the hippocampus. Granule layer cell in the dentate gyrus; (b) CA3 pyramidal layer; (c) CA3 dendritic neuropil; (d) Alveus. Red dot indicates the homozygous deletion individual. Red line indicates the mean of each group. Het, heterozygous group; het & hom, heterozygous group plus the one homozygous deletion individual; hom ins, homozygous insertion group. Differences between genotype groups for the DG cell layer, CA3 pyramidal cells and alveus regions were tested using one-way ANOVAs – a parametric test. A non-parametric, Kruskal-Wallis (one-tailed) test was employed for the CA3 dendritic neuropil region.

Figure S1, appendix 3 provides an example of increased KA1 expression in the CA3 region evident in a heterozygous carrier as compared to homozygous insertion carrier.

All neuronal cell counts and neuropil abundance percentage means were found to be higher in the deletion allele groups than the homozygous insertion group, shown in table 8.4. Table 8.6 and graph 8.2 summarise the percentage increase in KA1 expression associated with the deletion groups in quantified neuronal and glial cell regions. The mean of means for all neuronal regions analysed together indicates a 75% and 92% increase in the het/hom group and het group, respectively. This analysis includes values calculated for the alveus region as dendritic processes as well as glial cells were counted. In contrast, counts of just glial cells in the molecular layer, hilus, CA4, CA3 and CA1 were found to be similar between groups. Consequently, the mean increase in KA1 expression associated with the deletion allele groups for glial count regions was found to be low (7.4 het/hom and 5.0 het).

The individual *P* values calculated for the differences between groups in each region, presented in table 8.5 and discussed above, were not corrected for multiple testing. However, assuming a more conservative level of significance ($\alpha = 0.01$), the genotype effect observed for the granule cell layer in the dentate gyrus and pyramidal cells in the CA3 still remain significant. Owing to the small numbers analysed in each neuronal region - making reaching statistical significance hard to reach - the observed percentage increase in all neuronal count regions strongly suggests that a genotype effect is predominant in neuronal associated expression.

Analysis of confounding variables was assessed by the non-parametric Spearman's rank correlation test. Table 8.7 presents the Pearson correlation coefficient P-values (two tailed) calculated for genotype, gender, age, PMI, pH and hippocampal counts. No correlation was found between genotype, gender, PMI and pH. However, a significant correlation was indicated between gender and age. As the groups were matched for age and gender this correlation is unlikely to be confounding.

	% ins hom vs het + hom	% ins hom vs het
Neuronal		
Molecular layer neuronal	41.78	55.26
Dentate gyrus granule cells	72.49	76.55
Hilus neuronal	41.23	53.99
Hilus Neuropil abundance	83.33	89.63
CA4 neuronal	41.75	53.76
CA4 Neuropil abundance	113.83	137.94
CA3 neuronal	84.32	104.52
CA3 Neuropil abundance	211.14	272.45
CA1 neuronal	33.25	41.69
Alveus*	28.21	36.56
All regions neuronal mean % increase	**75.13**	**92.24**
Glial		
Molecular layer glia	15.90	12.53
Hilus glia	8.25	0.03
CA4 glia	-6.22	-6.53
CA3 glia	11.40	15.12
CA1 glia	7.88	3.58
All regions glial cell mean % increase	**7.44**	**4.95**

* counts in the alveus include glia cells and neuronal dendritic processes

Table 8.6 Percentage increase in KA1 expression calculated for the deletion groups relative to the insertion group per hippocampal region.

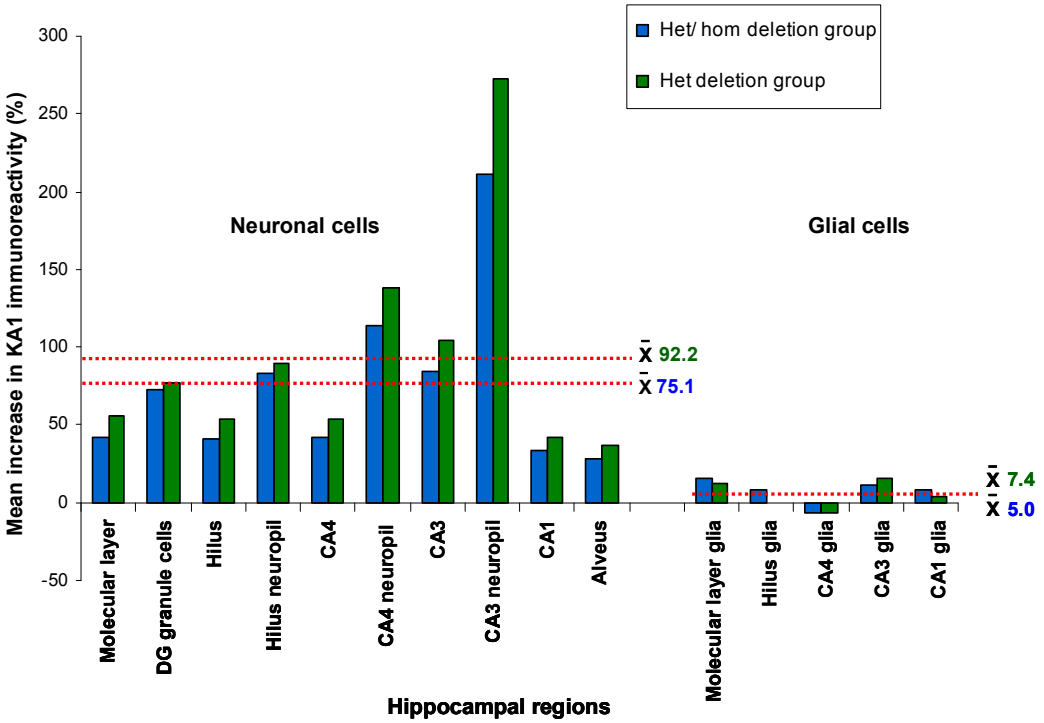

Graph 8.2 The deletion allele increases KA1 immunoreactivity in neuronal cells in the hippocampus. Red dashed lines indicate the mean of neuronal and glial cell regions in the two deletion allele groups. Het/hom, heterozygous group plus one homozygous deletion individual.

Table 8.7 Analysis of genotype, gender, age, PMI, pH and hippocampal counts. Correlations are given as Pearson correlation coefficient P-values (two tailed). Red values indicate significant p-values (not corrected for multiple testing). PMI, post mortem interval; DG, dentate gyrus; neu, neural counts; ML molecular layer.

	Genotype	Gender	Age	PMI	pH	DG	ML neu	ML glia	Alveus	Hilus neu	Hilus glia	CA4 neu	CA4 glia	CA3 neu	CA3 glia	CA1 neu	CA1 glia	Hilus %	CA4 %	CA3 %
Genotype	-	0.567	0.663	0.587	0.597	0.001	0.390	0.442	0.260	0.200	0.297	0.250	0.797	0.036	0.624	0.200	0.635	0.222	0.200	0.122
Gender		-	0.021	0.514	0.745	0.827	0.600	0.594	0.030	0.504	0.944	0.420	0.939	0.349	0.674	0.656	0.118	0.730	0.958	0.241
Age			-	0.666	0.660	0.359	0.962	0.838	0.178	0.880	0.687	0.700	0.863	0.742	0.321	0.757	0.187	0.601	0.773	0.746
PMI				-	0.988	0.973	0.206	0.060	0.444	0.323	0.954	0.612	0.909	0.848	0.351	0.497	0.188	0.621	0.235	0.303
pH					-	0.938	0.941	0.161	0.151	0.946	0.200	0.986	0.177	0.417	0.003	0.557	0.140	0.246	0.044	0.004

Four region-specific KA1 counts were also found to be significantly correlated with either gender or tissue pH. Cell counts in the alveus were significantly correlated with gender (P =0.03), and CA3 neuronal cell counts (P =0.003), CA4 and CA3 neuropil percentages (P =0.04, P =0.004) with tissue pH. Both the alveus and CA3 neuropil quantified regions showed a trend in significance between genotype groups. However, as genotype was found not to correlate with gender or pH, it is improbable that these differences in counts are due to gender and pH as confounding variables.

8.2.3 Genotype/protein correlation in the frontal cortex

Mean frontal cortex cell counts calculated for each sample are presented in table 8.8. One sample, SD019/05 genotyped homozygous insertion, was excluded from the analysis of layers 3 - 6 owing to the poor quality of tissue sections. The mean cell counts for all strata per genotype group are listed in table 8.9.

P and F values calculated for cell count differences between the groups are summarized in table 8.10. A significant difference in immunoreactive cell counts between the homozygous insertion (hom ins) group and heterozygous/homozygous deletion (het/hom del) or heterozygous (het) groups was found in the direction predicted for layer 1 (het/hom del vs hom ins, H = 5.77, P = 0.0058; het vs hom ins, H = 4.80, P = 0.014) [nonparametric Kruskal-Wallis Test, one tailed], shown in graph 8.3a).

A significant difference between the groups was found also for layer 2 heterozygote group versus homozygous insertion (F = 3.49, [1,9], P = 0.047, one way ANOVA one tailed) which showed only a trend in significance when comparing the heterozygous/homozygous deletion group with the insertion group (F = 3.14, [1,10], P = 0.054 one way ANOVA one tailed) indicated in graph 8.3b. Furthermore, a trend towards significance was also observed for layer 4 (het/hom del vs hom ins, F = 2.97, [1,10], P = 0.06; het vs hom ins, F = 2.55, [1,10], P = 0.07, one way ANOVA one tailed).

Sample	Layer 1	layer 2	layer 3 neuronal	Layer 3 glia	Layer 4	Layers 5 & 6 neuronal	Layers 5 & 6 glia
SD025/05	19.8 ± 1.5	21.8 ± 1.6	5.9 ± 0.5	17.3 ± 1.8	8.7 ± 0.8	6.7 ± 0.5	21.1 ± 1.2
SD022/06	14.2 ± 1.2	11.7 ± 1.0	4.5 ± 0.4	15.5 ± 1.3	3.5 ± 0.4	4.0 ± 0.3	13.9 ± 1.0
SD041/05	20.5 ± 1.5	16.0 ± 1.1	11.6 ± 0.9	16.7 ± 1.3	8.5 ± 0.7	12.9 ± 1.0	20.5 ± 1.5
SD019/05	18.1 ± 1.4	16.9 ± 1.2	nd	nd	nd	nd	nd
SD016/06	19.5 ± 1.4	20.9 ± 1.6	7.4 ± 0.5	18.2 ± 1.3	10.5 ± 0.9	10.5 ± 0.8	21.8 ± 1.5
SD036/05	30.9 ± 2.3	50.8 ± 3.7	16.8 ± 1.2	19.3 ± 1.3	19.1 ± 1.3	17.9 ± 1.3	27.8 ± 2.0
SD004/06	30.4 ± 2.1	28.4 ± 2.2	9.6 ± 0.7	23.6 ± 1.7	16.1 ± 1.4	11.9 ± 0.9	25.6 ± 1.9
SD006/06	29.5 ± 2.4	45.9 ± 3.6	15.2 ± 1.1	24.7 ± 1.7	18.6 ± 1.3	18.2 ± 1.2	26.0 ± 1.9
SD021/05	17.9 ± 1.4	31.6 ± 2.2	16.3 ± 1.3	18.5 ± 1.4	12.5 ± 0.9	16.9 ± 1.2	20.6 ± 1.5
SD019/06	21.0 ± 1.5	34.9 ± 2.4	13.0 ± 1.0	12.7 ± 1.0	13.6 ± 1.2	14.1 ± 1.1	18.3 ± 1.4
SD014/05	29.6 ± 2.3	31.2 ± 2.3	16.1 ± 1.2	19.3 ± 1.5	16.4 ± 1.3	15.5 ± 1.1	20.9 ± 1.4
SD007/05	45.3 ± 3.5	57.6 ± 4.0	20.2 ± 1.4	21.9 ± 1.4	27.0 ± 1.7	19.5 ± 1.4	25.2 ± 1.8

Table 8.8 Frontal cortex cell count means per individual sample. Standard errors are presented. Counts performed using x160 layer 2 and x400 layer 4 magnifications.

	Hom insertion		Het + hom del		Heterzygous only		Homozygous del	
	Mean	SEM	Mean	SEM	Mean	SEM	Mean	SEM
Layer 1	19.94	2.10	29.49	3.73	29.30	4.57	30.41	2.17
Layer 2	23.82	5.20	37.44	5.65	39.25	6.56	28.40	3.20
Layer 3 neuronal	11.00	2.06	13.58	2.12	14.39	2.40	9.56	0.71
Layer 3 glia	18.73	1.59	19.02	1.56	18.10	1.55	23.63	1.72
Layer 4	10.74	2.47	16.85	2.76	17.01	3.05	16.08	1.38
Layers 5 & 6 neuronal	12.48	2.52	14.28	1.89	14.75	2.21	11.88	0.91
Layer 5 & 6 glia	20.57	1.94	23.18	1.47	22.69	1.70	25.63	1.90

Table 8.9 Frontal cortex cell count means per genotype group. * denotes non-parametric analysis. Red values indicate significance or a trend. Values are shown for homozygous insertion group (Hom insertion), heterozygous and homozygous deletion group, Heterozygous group (het) and homozygous group (hom deletion). Red values indicate a significance difference between groups or a trend towards significance.

	het + hom del vs hom ins		het vs hom ins	
	P value	*F* value	P value	*F* value
Layer 1	0.008*		0.014*	
Layer 2	0.054	3.14	0.047	3.49
Layer 3 neuronal	0.21	0.69	0.17	1.06
Layer 3 glia	0.45	0.02	0.39	0.08
Layer 4	0.06	2.97	0.07	2.55
Layers 5&6 neuronal	0.29	0.34	0.26	0.46
Layer 5 &6 glia	0.15	1.19	0.22	0.68

Table 8.10 P and *F* values associated calculated for frontal cortex cell counts. * denotes non-parametric analysis. Red values indicate significance or a trend towards significance. Parametric tests performed, one-way ANOVA (one-tailed) and non-parametric, Kruskal-Wallis (one-tailed).

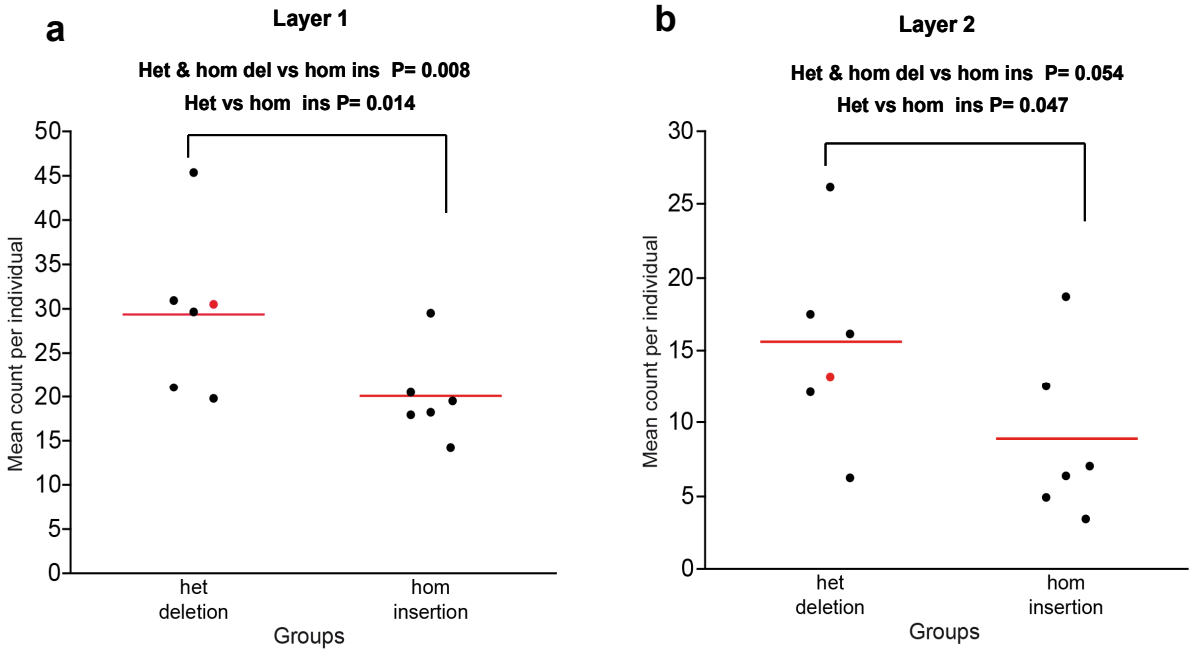

Graph 8.3 Genotype effect on mean cell counts in the frontal cortex. Genotype effects found for (a) layer 1 and (b) layer 2. Red dot indicates the homozygous deletion individual. Red line indicates the mean of each group. Het, heterozygous group; het & hom, heterozygous group plus the one homozygous deletion individual; hom ins, homozygous insertion group. . Differences between genotype groups for layer 1 mean counts were tested using one-way ANOVAs – a parametric test. A non-parametric, Kruskal-Wallis (one-tailed) test was performed for layer 2 mean counts .

Consistent with the results for the hippocampus, all neuronal cell counts means were found to be higher in the deletion allele groups than the homozygous insertion group, as shown in table 8.9. A summary of the percentage increase in KA1 expression associated with the deletion groups estimated separately for neuronal and glial cell regions is presented in table 8.11 and graph 8.4. The mean for all neuronal regions analysed together indicates a 40% and 44% increase in the het/hom group and het group, respectively. This analysis included values calculated for layer 1 as immuno-positive dendritic processes were counted in addition to glial cells. Again similar to the hippocampus, counts of immunopositive glial cells in layers 3 and 5/6 were observed to be similar between groups and the mean increase in KA1 expression associated with the deletion allele groups for glial count regions was found to be low (7% het/hom and 3% het group alone).

Table 8.10 presents the Pearson correlation coefficient P-values (two tailed) calculated for genotype, gender, age, PMI, pH and frontal cortex counts. No correlation was found between frontal cortex genotype counts and gender, age, PMI or pH.

8.3 Discussion

This chapter reports the findings of a genotype expression correlation investigating the candidate gene *GRIK4*. A significant correlation was found for DG granule and CA3 pyramidal cells in the hippocampus and layer 1 immunoreactivity in the frontal cortex. Neuronal and neuropil expression in all regions quantified was observed to be higher in the deletion groups than the insertion group, showing a mean 75-92% increase in expression in the hippocampus and 40-43% increase in the frontal cortex. Collectively, these findings were found to be consistent with our hypothesis that this deletion variant exerts a protective effect against bipolar disorder through increased KA1 protein abundance in neuronal cells in key brain regions.

	% ins hom vs het + hom	% ins hom vs het
Neuronal		
Layer 1*	47.89	46.94
Layer 2 x16	57.18	64.78
Layer 3 neuronal	23.45	30.81
Layer 4 x40	56.89	58.38
Layers 5 & 6 neuronal	14.42	18.19
All regions neuronal mean % increase	**39.97**	**43.82**
Glial		
Layer 3 glia	1.55	-3.63
Layer 5 & 6 glia	12.68	10.3
All regions glial mean % increase	**7.12**	**3.34**

* counts in layer 1 include glia cells and neuronal dendritic processes

Table 8.11 Mean percentage increase in frontal cortex KA1 expression estimated for the deletion allele groups relative to the insertion group.

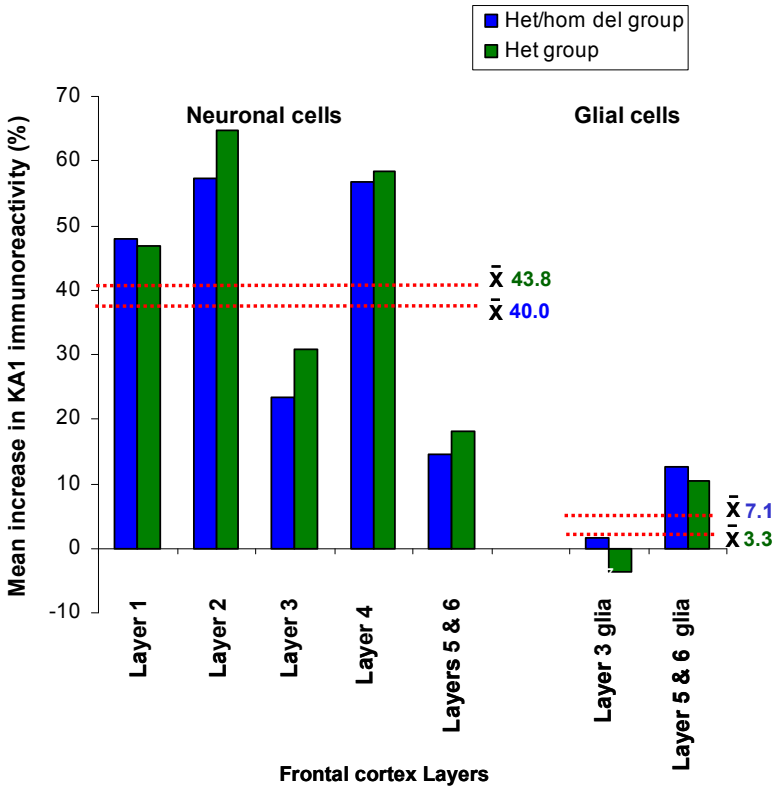

Graph 8.4 The deletion allele increases KA1 immunoreactivity in neuronal cells in the frontal cortex. Red dashed lines indicate the mean of neuronal and glial cell regions in the two deletion allele groups

Table 8.12 Analysis of genotype, gender, age, PMI, pH and frontal cortex cell counts. Correlations are given as Pearson correlation coefficient P-values (two tailed). Red values indicate significant p-values (not corrected for multiple testing). PMI, post mortem interval; neu, neural counts.

	Genotype	Gender	Age	PMI	pH	Layer 1	Layer 2	layer 3 neu	layer 3 glia	layer 4	lay 5&6 neu	lay 5&6 glia
Genotype	-	0.567	0.663	0.587	0.597	0.050	0.107	0.426	0.902	0.119	0.571	0.303
Gender		-	0.021	0.514	0.745	0.851	0.989	0.553	0.382	0.783	0.630	0.857
Age			-	0.666	0.660	0.668	0.551	0.551	0.202	0.618	0.762	0.722
PMI				-	0.988	0.562	0.837	0.611	0.247	0.190	0.519	0.240
pH					-	0.631	0.988	0.748	0.609	0.931	0.717	0.310

8.3.1. Abnormalities in KAR subunit expression in individuals with psychiatric illness

As discussed in chapter 1, a number of studies have reported abnormal kainate receptor (KAR) subunit expression in the hippocampus, parahippocampus and frontal cortex regions in cases of psychiatric illness. However, unlike the current study which assessed a genotype-specific effect in tissue from asymptomatic control subjects, these previous investigations compared expression in post mortem brains of individuals with schizophrenia and affective disorders with comparison control groups. With respect to the hippocampus, Kerwin and colleagues using the technique of quantitative autoradiography, first reported a reduction of kainate subtype binding in mossy fibre CA3/4 zone in the left hippocampus, and bilateral losses in dentate gyrus and parahippocampal regions in tissue from schizophrenic individuals (Kerwin et al., 1990). Those regions indicated to have reduced KA binding are consistent with the areas found in the current study to show lower KA1 expression in the insertion group. However, the technique used by Kerwin et al. localizes KA receptor binding and hence does not provide any information concerning specific KAR subunits.

Three studies have subsequently examined alterations in specific KAR subunit expression in the hippocampal formation of healthy controls and cases. Porter and coworkers found reduced KA2 and GluR6 mRNA expression in the dentate gyrus granule cells and CA2/3 subfield in brains. Unfortunately, KA1 expression was not considered abundant enough to quantify differences between cases and controls. A second study reported a 30-35% reduction in the density of $GluR_{5,6,7}$ immunoreactivity in dendrites found in both stratum radiatum and stratum moleculare of sectors CA3 and CA2, as well as proximal and middle portions of CA1 in schizophrenic brain. Nonetheless, no difference was found between control and the bipolar disorder group and the dentate gyrus was not examined (Benes et al., 2001).

In contrast, Beneyto and colleagues analyzed mRNA transcript expression of all five KAR subunits in the hippocampus and parahippocampal regions in tissue from

individuals with schizophrenia, bipolar disorder and MDD. They report a significant reduction in GluR6 in the entorhinal cortex (EC) in bipolar disorder individuals and a significant decrease in GluR5 expression in the perirhinal cortex associated with all three psychiatric phenotypes. Alterations in KAR subunit expression was not observed in the hippocampus, and KA1 expression did not differ significantly between the groups (Beneyto et al., 2007).

In the frontal cortex four papers report changes in KAR subunit transcript expression associated with schizophrenia. Meador-Woodruff et al. reported a shift in subunit stoichiometry, with increased expression of GluR7 mRNA and decreased KA2 mRNA in both infragranular and supragranular layers of the prefrontal cortex (Meador-Woodruff et al., 2001). Furthermore, Garey and co-workers, found a significant reduction in numerical density of neurons immunopositive to GluR6 and GluR7 in layers 2-6 of the orbitofrontal cortex of chronic schizophrenics, whereas Scar and colleagues observed a significant decrease in GluR5 expression in all layers of the frontal cortex but no changes in GluR6, GluR7, KA1 and KA2 (Scarr et al., 2005; Garey et al., 2006). Conversely, decreases in both GluR7 and KA1 mRNA in the left superior gyrus of neuroleptic-free schizophrenic individuals were found by Sokolov. This study quantified expression by performing RT-PCR assays, and so alterations in laminae distribution, i.e. concordant with the present findings, were not investigated. Interestingly, Sokolov also reported a negative correlation between the subunit mRNA and time without neuroleptic medication before death suggesting that kainate receptor subunit mRNAs decline rapidly after drug withdrawal (Sokolov, 1998).

These findings led to a number of observations pertinent to the current results. First, a potential confound to most of these post mortem studies is the possible effects of past antipsychotic exposure. Indeed, animal studies have suggested that KAR subunit transcripts are altered after chronic antipsychotic treatment – a finding which provides additional evidence for a link between KAR function and psychiatric illness (Meador-Woodruff et al., 1996; Schmitt et al., 2003). The present study avoided this potential

confound by analyzing expression in asymptomatic individuals naive to antipsychotic medication.

Second, various assessments of frontal cortex KAR subunit expression associated with psychiatric illness have led to inconsistent results. It is possible that these discrepancies may be due to different neocortical areas examined, to different techniques used to quantify expression in laminae, potential confounding variables such as antipsychotic exposure, or alternatively sub region-specific changes in subunit expression.

A third observation is that all studies reporting alterations in KAR subunit expression in the hippocampus consistently found decreases in subunit abundance. This would suggest that a reduction in specific subunits which may result in an 'unfavorable' shift in kainate receptor subunit composition (at least in the hippocampus) might be the underlying mechanism giving rise to illness. Such a hypothesis is in accordance with the current results – namely a decrease in KA1 expression found for the insertion genotype is positively associated with bipolar disorder. Furthermore, unlike the previous studies in which groups were based on genotype rather than phenotype status, the present study provides a direct link between a causal factor, i.e. genetic risk factor, subunit expression differences and a psychiatric disorder. Future examination of identified genetic risk variants in other KAR subunits and subunit expression abundance in postmortem brain tissue may provide further insight into underlying factors contributing to the findings of previous positive reports.

8.3.2 Genotype-specific KA1 increases in neuronal cells, dendrites and neuropil

In the current study a difference between the deletion allele and insertion groups in two regions, the granule cell layer in the dentate gyrus and CA3 hippocampal pyramidal cells, remains statistically significant after assuming a more conservative level of significance ($\alpha = 0.01$). An intrinsic limitation to this study is the small number of individuals examined, especially when samples cannot be included in some sub-regions owing to torn tissue sections. This makes statistical significance difficult to achieve and

hence complicates the interpretation of apparent, but not statistically significant, quantified differences in expression counts. However, the data clearly indicate that for all neuronal associated expression, i.e. neuronal cell soma, processes and dendrite, but not glial cells, in both the hippocampus and frontal cortex the deletion allele groups had higher immunopositive counts than the insertion group.

The fact that this effect was not evident for glial cell regions suggests two possible explanations. First, the deletion allele increases KA1 mRNA abundance globally, but in glial cells there is an opposing mechanism leading to increased KA1 degradation. Such a mechanism might be the availability of GluR5-7 subunits with which KA1 forms functional and stable kainate receptors. A second possibility is that KA1 longevity is increased in specific subcellular locations, e.g. neuronal processes/dendrites. Such a localised cellular effect might be influenced by factors such as synaptic activity within neuronal pathways (Steward and Wallace, 1995).

In addition to neuronal soma and processes, KA1 expression was also found to show a genotype-specific increase in CA3/4 neuropil abundance. This finding is worth considering in the context of the 'reduced neuropil hypothesis' of schizophrenia forwarded by (Selemon et al., 1995). The theory, based on morphometric analysis of the prefrontal cortex and quantitative studies of neuronal densities in brains from schizophrenic patients, proposes that disturbances in cognitive functioning in schizophrenia may be mediated by a process which involves atrophy of neuronal processes, giving rise to deficits in neuronal connections (Selemon and Goldman-Rakic, 1999). Although in the current study absolute levels of neuropil were not quantified, the results are consistent with the hypothesis that altered expression of a protein involved in plasticity processes at neuronal connections (neuropil) may give rise to abnormalities in neuronal processing which in turn may contribute to the expression of psychiatric disease.

8.3.3 Genotype/KA1 expression in DG and link to neurogenesis

A striking KA1 expression genotype effect was found for the granule cell layer in the dentate gyrus. As discussed in chapter 7, it is in this region that adult hippocampal neurogenesis occurs resulting in the functional integration of new born neurons within the mossy fibre pathway. Adult hippocampal neurogenesis has been consistently shown to be increased under conditions known to ameliorate psychiatric symptoms, e.g. administration of antidepressants, mood stabilizers and cognitive enhancers, and conversely decreased under states of stress, a precipitating factor for psychiatric illnesses (Scharfman and Hen, 2007). Consequently, this has led to adult neurogenesis being considered a factor in the pathogenesis and course of mood disorders and schizophrenia.

The most compelling evidence supporting this hypothesis is that the blockade of hippocampal neurogenesis inhibits the therapeutic-like effects of most physical and chemical anti-depressant treatments, and antidepressants increase the level of several growth factors, e.g. brain derived growth factor (BDNF) and vascular endothelial growth factor EGV, which themselves have pro-neurogenic properties (Krishnan and Nestler, 2008). However, the dependence of behavioral effects of antidepressants on adult neurogenesis is also known to be influenced by factors such as species, genotype, the nature of antidepressants, and the type of behavioural paradigms assessed (Zhao et al., 2008). Consequently, this has led to the speculation that antidepressants may exert their behavioural effects through both neurogenesis-dependent and neurogenesis-independent pathways, and that neurogenesis-dependent processes are likely to be influenced by hippocampal network activity (Sahay and Hen, 2007).

The biological investigation of *DISC1* and *NPAS3*, two candidate genes for schizophrenia, provides further support for aberrant neurogenesis contributing to hippocampal aspects of psychiatric disease. For example, DISC1-deficient cells in the subventricular zone exhibit an increase in neuritic sprouting and neuronal migration resulting in aberrant morphological development, mis-positioning of new dentate

granule cells as well as defects in axonal targeting and development of mossy fibre synaptic outputs (Duan et al., 2007; Faulkner et al., 2008). In contrast, *NPAS3* knockout mice display a marked attenuation in adult hippocampal neural precursor cell proliferation (Pieper et al., 2005).

The significant correlation between the protective allele within *GRIK4* for bipolar disorder and increased immunopostive counts in the DG granule cell layer and CA3 pyramidal/mossy fibre CA3 terminals, hint at the possibility that the protective effect may be through an adult hippocampal neurogenesis related mechanism. Although further research is needed to investigate the role of KA1 in adult neurogenesis, the present results add to the emerging evidence that hippocampal neurogenesis might be a 'biological convergent point' upstream of primary genetic defects in the pathogenesis of psychiatric illnesses.

8.3.4 Stress, psychiatric illness and a role for KA1

Epidemiological and behavioural studies strongly suggest that environmental stress (acting concurrently with genetic factors) is an environmental precipitating factor to the development of psychiatric disorders. During stressful situations and episodes of high arousal, the hypothalamic-pituitary-adrenal (HPA) axis becomes activated, resulting in, among other physiological processes, corticosterone/glucocorticoid (GC) release from the adrenal cortex into the circulatory system. The surprising discovery that glucocorticoid receptors are highly expressed in the rodent hippocampus and possibly at lower levels in the frontal cortex, has led to the conjecture that the hippocampus and frontal cortex might regulate aspects of the HPA axis (McEwen, 1980; Sarrieau et al., 1986; Sanchez et al., 2000).

Extensive studies using both acute and chronic stress/steroid protocols have revealed that corticosteroids can inhibit postnatal and adult DG granule cell proliferation. Elevation of corticosterone (glucocorticoid) levels by the activated hypothalamic-pituitary-adrenal axis is the main mechanism for stress-mediated suppression of

newborn granule cell proliferation. In addition, moderate durations of stress and high GC exposure in rats and tree shrews cause reversible atrophy of apical dentrites of CA3 pyramidal cells and dentate gyrus neurons and alterations in synaptic terminal structure (Magarinos and McEwen, 1995; Magarinos et al., 1996; McEwen and Magarinos, 1997).

McEwen argues that short-term structural plasticity (dendritic pruning in CA3) and inhibition of neurogenesis are both examples of adaptive 'protective' mechanisms that could reduce the impact of glutamate and glucocorticoids in causing more permanent damage to the hippocampus (McEwen, 1999). What is pertinent to the current research is that KA1 activity, through pre-synaptic mechanisms at mossy fibre terminals, is postulated to be critical to the process of reversible atrophy of CA3 apical dendrites (McEwen, personal communication). Although this research is still in its infancy, this intriguing finding links KA1 function to the physiological processes activated during chronic stressful states and mechanisms by which the hippocampus adapts to short term disturbances. It is exciting therefore, that the current findings - showing association between bipolar disorder (characterized by episodes of depression and elevated mood states) and alterations in KA1 expression at the same critical hippocampal regions - are complimentary to McEwen's research implicating KA1 as a potential mood disorder factor.

8.3.5 Differential KA1 expression and neural circuits

Neurodevelopmental disorders are hypothesized to be caused by neuronal dysfunction. One theory forwarded by Ramocki and Zoghbi, posits that neuropsychiatric phenotypes arise owing to failure of neuronal homeostasis (Ramocki and Zoghbi, 2008). Neurons are dynamic entities which must constantly adapt to changing external and internal stimuli through, for example, the remodeling and pruning of synaptic connections. Neuron-specific changes resultant from aberrant alterations in protein function or expression, are likely to affect neuronal networks.

Ramocki and Zoghbi argue that neurons within affected networks must make homeostatic responses to establish or re-establish "a proper balance of excitation and inhibition" (Ramocki and Zoghbi, 2008). Consistent with this concept is the model proposed by Sudhof (2008) to explain the physiological consequences of mutations in neuroligins and neurexins associated with autism spectrum disorders (ASD) (Sudhof, 2008). Neuroligins and neurexins are trans-synaptic cell-adhesion molecules that mediate essential signaling between presynaptic and postsynaptic domains. Sudhof proposes that these proteins are involved in shaping synaptic efficacy and plasticity and hence can alter the balance between excitatory and inhibitory neurotransmission in a subset of neural circuits. Consequently, mutations within neuroligins and neurexins are postulated to result in disturbance of neural network function (Sudhof, 2008).

The distribution of KA1 and its role in synaptic plasticity makes it a key functional candidate for influencing pathway dynamics. It is therefore unsurprising and in total concordance with a 'neuronal homeostasis' hypothesis that the present findings revealed an increase in KA1 correlated with the protective allele in all neuronal regions examined. Alterations in KA1 expression might be a mechanism which contributes to changes in synaptic strength and hence might modify the relative contribution of different synapses and shape the properties of the tri-synaptic pathway or circuitry within the frontal cortex. In turn, cognitive processing associated with circuit activity within these structures could be altered or indeed impaired.

The hippocampus and frontal cortex do not function in isolation from other brain regions. Information flow within interconnecting circuits modulates the processing and function of these structures which consequently underlie the expression of complex behaviour. For example, reciprocal processing within the amygdala and hippocampus mediates the affective component of context-dependent memory formation. Such processing, when disrupted, is hypothesized to be linked to symptoms of post- traumatic stress disorder (PTSD) as well as other affective disorders (Nadel and Jacobs, 1996).

Although only the frontal cortex and hippocampus were examined in the present study, it is possible that the KA1 genotype effect may influence expression and potential plasticity processes in different brain regions. Consequently, this could influence transmission within diffuse series of neural networks interlinking multiple brain structures, and thus give rise to abberant facets of cognition and behaviour. Functional imaging studies investigating a *GRIK4* genotype effect on cognition are currently underway and may provide more insight into region-specific or global deficits in processing.

The present results also raise the possibility that pharmacologically mediated increases in kainate receptor activity, mirroring the protective deletion's effect on expression and potentially circuit activity, might present a therapeutic opportunity for bipolar disorder and other psychiatric illnesses. However, kainate receptor agonists are known to compromise neuronal viability by impeding structural and functional integrity, i.e. they are excitotoxic to neuronal and glial cells (Michaelis, 1998; Konradi and Heckers, 2003). Therefore, a more practical strategy aimed at facilitating kainate receptor function would be the use of drugs that inhibit kainate receptor desensitization. For example, the lectin Concanavalin A (ConA) blocks desensitization in all native as well as cloned KA subtypes by inhibiting conformational changes within the receptor-protein complex (Bunch and Krogsgaard 2008). The development of ConA and other related pharmacological agents which effectuate changes in plasticity mechanisms might lead to important drug discoveries in the treatment of psychiatric diseases.

The findings presented in chapters 6, 7 and 8 are unique in that they provide a direct link between a protective genetic variant, alterations in RNA/protein expression and a potential model of the physiological consequences on synaptic and network activity. This body of research not only provides strong support for the glutamate hypothesis of schizophrenia and mood disorders, but also - as *GRIK4* is likely to be one of many risk factors which may converge in common endpoints- sets a precedent for what might be expected to be discovered for other candidate risk factors. Furthermore, this model does

not exclude the possibility of involvement of interacting physiological systems, e.g. HPA axis, and disturbances in other neurotransmitter systems acting concurrently upon, or down stream from, a primary glutamate synaptic defect. Further research examining the molecular determinants of pathways involved in KA1 function, i.e. a potential role in neurogenesis, GC receptor activation at mossy fiber terminals, and synaptic modulation of pathway dynamics, may provide significant insight into common disrupted processes and thus offer new avenues for effective treatments of psychiatric disease.

CHAPTER 9

GENERAL DISCUSSION

9. GENERAL DISCUSSION

9.1 Review of projects

This thesis has presented research utilizing two powerful genetic approaches in order to identify and subsequently examine, genetically and biologically, candidate genes for psychiatric disease. The first approach (project 1), employing positional mapping in two consanguineous families which presented with a high incidence of disease, aimed to identify recessive loci and putative risk variants. The second approach involved the genetic and biological investigation of the candidate genes, *ABCA13* and *GRIK4* (projects 2 and 3), identified as directly disrupted in patients with schizophrenia who carry complex chromosomal rearrangements.

In this chapter, I will first review very briefly the major findings of each project. This will serve as the background for the subsequent discussion centred on critical questions debated in the field of psychiatric genetics, i.e. the issues of phenotypic heterogeneity, potential risk allele interaction, rare versus common risk variants, protective alleles, and mode of genetic mutations. These questions, and the insight provided by the findings of the thesis are of central importance in efforts to comprehend the composition of genetic risk in the population and thus provide a strong starting point for biological investigations into pathophysiological processes of psychiatric disease.

In the first project, homozygosity mapping was initially performed in a consanguineous family in which five out of six offspring present with schizophrenia, epilepsy or sensori-neural hearing impairment either singly or in combination. Two HBD loci were detected on chromosomes 22q13 and 2p24-25, regions previously implicated to harbour susceptibility factors for psychiatric illness, or hearing loss, respectively. Unfortunately, the sequencing of strong candidate genes within these HBD loci failed to identify any potential causal coding variants.

Homozygosity mapping was subsequently performed in a second, related family with a high incidence of deafness as a means to identify common loci of shared ancestry putatively housing recessive genes for hearing loss. Five HBD loci were identified on chromosomes 1p22.2-1q23.1, 7q21-q31.1, 8q12, 12p13 and 20q13. There was nonetheless, no evident overlap of the HBD intervals detected in the two families suggesting that the underlying causative genetic factors segregating within the two related families are not the same. These identified HBD loci do, however, overlap with non-syndromic deafness loci two of which house known deafness genes.

The primary aim of the second project was to provide additional evidence that the breakpoint gene *ABCA13* is a liability factor for schizophrenia. The fine mapping of the breakpoint regions interrupted by a cytogenetic abnormality carried by a patient with schizophrenia indicated that *ABCA13* is the only gene directly disrupted. The sequencing of exons encoding the highly conserved functional domains commonly mutated in other ABCA sub-family members led to the identification of eight potentially pathogenic, ultra-rare coding variants. Follow-up family and case-control association studies indicated that these variants collectively are strongly associated with increased risk for schizophrenia, bipolar disorder and major depression and show linkage with illness in families. Expression studies indicated that *ABCA13* mRNA is expressed in the human hippocampus and frontal cortex and that ABCA13 protein is expressed in the granule cells of the dentate gyrus.

The third project involved the investigation of the candidate gene, *GRIK4,* initially identified through disruption by a chromosomal abnormality in a patient with severe schizophrenia and mild learning disability. A haplotype within *GRIK4* was previously identified as associated with bipolar disorder. A case-control association study of a common indel variant located in the 3'UTR of *GRIK4* and in LD with the associated haplotype, suggested the deletion allele to be a causal factor exerting a protective effect against bipolar disorder. KA1, the glutamate receptor sub-unit protein encoded by

GRIK4, was found to be expressed in all layers of the human frontal and entorhinal cortices, in the superficial portion of the granular layer and in small cells in the vicinity of purkinje neurons within the cerebellum and at regions involved in neuronal processing within all three pathways forming the trisynaptic circuit within the human hippocampus. A subsequent genotype/protein expression correlation study indicated that KA1 expression within the hippocampus and frontal cortex was significantly increased in subjects carrying the protective deletion allele.

9.2 What do the findings tell us about the genetic architecture of psychiatric illness?

Genetic risk variants and phenotypic heterogeneity

Research into Mendelian disease genes has shown that lesions in one gene can cause several phenotypic traits, i.e. can have a pleiotropic effect, or conversely mutation of several genes, the effects of which converge on commonly disrupted biological processes, can give rise to one clinical phenotype. For example, mutations within *ABCA4* give rise to a variety of retinal dystrophies, as discussed in chapters 4 and 5, and multiple genes are known to cause sensori-neural deafness, as discussed in chapter 3. Both models of gene action have been postulated for common complex disease, and evidence indicates that both theories are relevant to psychiatric illnesses (Dean, 2003; Ramocki and Zoghbi, 2008).

The present findings provide strong evidence that two genes, *ABCA13* and *GRIK4*, contribute to liability of developing bipolar disorder, and hence add support for a model that more than one gene may be an etiological factor for a psychiatric phenotype. There are, however, intriguing differences between the findings of the two present studies. Although research suggests that *GRIK4* may also contribute to risk for schizophrenia (indicated by the chromosomal abnormality and additional associated haplotypes and SNPs discussed in chapter 6), the present results indicate the protective effect afforded

by the common indel variant (and associated haplotype in LD with the variant) *per se* is specific to bipolar disorder (Pickard et al., 2005a; Paddock et al., 2007).

In contrast, multiple rare variants within *ABCA13* were identified in individuals with schizophrenia, bipolar disorder or MDD. Thus the *ABCA13* data support the supposition that one gene and indeed one allele may increase risk for three diagnoses of psychiatric disease. This phenomenon has previously been described for a cytogenetic lesion disrupting *DISC1* which segregates with disease in a pedigree with multiple psychiatric conditions (St Clair et al., 1990; Blackwood et al., 2001). However, the *ABCA13* data suggest that in addition to a major structural mutation which putatively results in a haploinsuffiency, point mutations with potentially less severe consequences on protein function may also contribute to variable clinical phenotypes.

Multiplicative variant interaction

Considerable evidence from animal and human studies suggests that multiple risk genes or alleles are required for the expression of some Mendelian disease such as Waardenburg syndrome and Bardet-Biedl Syndrome (Dean, 2003). Genetic research of breast cancer, a common complex disease, also indicates that multiplicative interaction between rare high penetrant alleles or low penetrant common variants, both in the same or different susceptibility gene, can exist and may give rise to different phenotypes (Stratton and Rahman, 2008).

Within the field of psychiatric genetics, evidence supporting a model of additive allelic interaction has come from studies of common, low penetrance associated SNPs or haplotypes (Pickard et al., 2005a; Baum et al., 2008). The *ABCA13* findings are the first data to suggest that interactions between ultra-rare moderate penetrance risk variants across a gene may be a mechanism which, in an additive manner, contributes to susceptibility to psychiatric illness, and that such additive effects may also be a contributory factor to the severity of clinical outcome. Hence these findings not only set

a precedent for what may be revealed from future studies of candidate genes but also indicate that the mode of gene action underlying psychiatric illness may be similar to other common complex disorders.

Rare versus common alleles

A third issue, historically debated in the field of psychiatric genetics, is the contribution of rare and common alleles to disease risk. The results reported in this thesis provide support both the 'common disease - common allele' hypothesis (associated *GRIK4* indel variant) and 'common disease - rare allele hypothesis' (*ABCA13* rare variants). However the data also provide additional information which extends our current understanding of variant classes.

First, the *ABCA13* results suggest that there are two types of rare variant - moderate penetrance rare coding variants with ORs of 1.6-3.8 and high penetrance, potentially null private mutations which show strong familial aggregation. Again, these findings are consistent with genetic models of other complex diseases such as breast cancer and Alzheimer's disease.

Second, common risk variants as identified by GWAS and SNP tag case-control association studies are reported to have low odds ratios of 1.5 or less. However, the combined *GRIK4* indel association data resulted in an OR of 0.47 for heterozygotes (equivalent to ~ 2 fold risk) is lower, i.e. has a greater effect, than previously predicted for a common allele.

Third, a GWAS scan identified a SNP within *ABCA13* as being in the top 200 SNPs associated with bipolar disorder. This opens the possibility that, similar to *DISC1,* a candidate gene of major effect, *ABCA13* may harbour both rare high penetrance and common low risk alleles. As yet, *GRIK4*, like many other 'common allele' candidate genes, has not been comprehensively screened for rare variants. Forthcoming re-

sequencing efforts focused on these genes will provide crucial insight into the frequency and type of common/rare genetic factors.

Protective alleles

In addition to the identification of rare susceptibility alleles, the findings of this thesis also provide strong support for the existence of protective alleles. To the author's knowledge, the *GRIK4* indel variant is the first actual 'causal' protective variant reported for a psychiatric condition. Rare coding variants identified in only control individuals within candidate genes of major effect, e.g. P4648A in *ABCA13*, have the potential also to be protective. However, owing to the difficulties associated with distinguishing between a benign ultra-rare variant and potential protective allele and the interpretation of pedigree segregation, modeling and functional studies are needed to verify the protective nature of such a candidate variant. Therefore, many unresolved issues regarding the genetics of protective variants remain, such as the typical frequencies of alleles and whether the magnitude of protective effects is similar to that of risk variants.

Types of mutations

The study of other diseases implicates multiple molecular mechanisms by which genetic changes may lead to human disease. Common risk variants as identified by GWAS or SNP-tag case-control studies are often located within non-coding regions. This has led to the supposition that common risk alleles are likely to have to have a regulatory effect upon transcript expression. We hypothesized that the common non-coding indel located in the 3'UTR of *GRIK4* would have a regulatory effect through differential mRNA stability altering *GRIK4* mRNA abundance. The results of RNA and protein indel expression studies presented in this thesis support our hypothesis.

In contrast, cytogenetic lesions which directly disrupt a gene and null point mutations, as identified within *ABCA13*, are thought to result in a state of haploinsufficiency owing to 'nonsense-mediated decay', i.e. produce reduced gene dosage effects. Moreover, missense mutations are predicted to have a direct effect on protein activity either by increasing or reducing the protein's functional efficacy, as suggested by the structural modeling of T4031A *ABCA13* variant. The findings of projects 2 and 3 therefore provide compelling evidence that a variety of mutation 'types' contribute to the expression of psychiatric phenotypes. Bioinformatic, genetic and biological research may further uncover how the consequences of such mutations alter normal gene transcript function and hence lead to a disruption of biological pathways.

9.3 Future research

With the development of new technologies, the genetic study of psychiatric disease is more assessable than ever before. The strategy used to study the candidacy of *ABCA13* has been shown to be highly effective in identifying rare risk variants. Re-sequencing efforts using high throughput, cost efficient platforms such as the Solexa (Illumina), SOLID™ (Applied Biosystems) and 454 Life Science™ (Roche Applied Science) will be invaluable for the comprehensive screening for rare variants of candidate genes either located within mapped loci or previously implicated as pathological. Furthermore, re-sequencing will be necessary to verify whether detected rare variants are specific to a geographic population or indeed to phenotypic groups. As with the present study, this approach should be followed by case-control association studies and pedigree analysis of the any identified coding variants. In parallel, the use of large scale, high throughput whole genome SNP or oligo array chips will aid the identification of rare and/or associated CNVs, whilst follow-up case-control studies using Multiplex Amplicon Quantification (MAQ), qPCR, or cytogenetic assays will provide further information into the contribution to disease risk of rare and common structural variants.

As more genetic risk variants are identified, it will crucial that the functional consequences of mutated alleles are comprehensively explored. Computational modeling and functional analysis will be necessary for predicting the causal genetic mechanism and underlying mode pathology. The biological examination of candidate genes is also a vital step in understanding common disrupted biological mechanisms. The discussion section of each results chapter has already highlighted future experiments which would naturally continue from my studies and which might provide support for, or disprove, speculated theories. Such experiments should include co-localisation studies of candidate genes with synaptic and cell population markers, and the molecular investigation of complexes and physical interactors, thereby giving further insight into functionally relevant molecular pathways.

Animal models of psychiatric illness, candidate gene targeted knock out mice and the use of pharmacological interventions, are other areas of research which have been and may prove particularly productive. For instance, as discussed in chapter 8, using an animal model of stress/depression, KA1 was shown to be critical for the process of reversible atrophy of CA3 apical dendrites within the mossy fibre pathway and hence implicated as a contributing factor in pathophysiological processes. This line of research, complementary to our own findings, may subsequently reveal important aspects of plasticity, circuit and systems related disease mechanisms. Furthermore, the recent generation of *GRIK4*/Ka1 and *Abca13* KO mice strains provide an opportunity for histological, neuroanatomical and phenotypic examination and may prove valuable for the development of pharmacological agents.

An alternative and complementary strategy for investigating potential pathophysiological processes is to employ a top down approach. The study of endophenotypes, e.g. brain structure and activity, cognition and neurophysiology in affected and asymptomatic relatives of probands who carry identified risk factors, will further our knowledge of the effects of high-risk genotypes on phenotypic features. Moreover, such human studies may reveal significant differences, or indeed aspects of

commonality, between risk genotypes, and thus highlight variation or convergence of underlying biological processes. Consequently, the standard definitions of psychiatric disease may evolve as diagnostic categories are adapted to reflect genetic and pathophysiological aetiology, the outcome of which may bring new opportunities for personalized medicine.

9.4 Concluding remarks

The ultimate ambition of genetic studies is the development of effective treatments or preventative strategies by furthering our understanding of the aetiology of disease. This thesis has contributed to this goal through the genetic and biological investigation of candidate genes for psychiatric and neurological disorders. The findings of all three projects, mapped HBD loci, the identification of rare variants within *ABCA13* and the association of common protective allele located within *GRIK4* with increased protein expression in human brain tissue, offer significant potential for future research and provide unique insight into the genetic landscape of psychiatric disorders.

BIBLIOGRAPHY

Abecasis GR, Cherny SS, Cookson WO, Cardon LR (2002) Merlin--rapid analysis of dense genetic maps using sparse gene flow trees. Nat Genet 30:97-101.

Abramoff MD, Magelhaes PJ, Ram SJ (2004) Image Processing with Image J. Biophotonics International 11:36-42.

Adolfo Sequeira (2003) Wolfram syndrome and suicide: Evidence for a role of WFS1 in suicidal and impulsive behavior. American Journal of Medical Genetics Part B: Neuropsychiatric Genetics 119B:108-113.

Albrecht C, Viturro E (2007) The ABCA subfamily--gene and protein structures, functions and associated hereditary diseases. Pflugers Arch 453:581-589.

Allikmets R (2000) Simple and complex ABCR: genetic predisposition to retinal disease. Am J Hum Genet 67:793-799.

Alonso J, Angermeyer MC, Bernert S, Bruffaerts R, Brugha TS, Bryson H, de Girolamo G, Graaf R, Demyttenaere K, Gasquet I, Haro JM, Katz SJ, Kessler RC, Kovess V, Lepine JP, Ormel J, Polidori G, Russo LJ, Vilagut G, Almansa J, Arbabzadeh-Bouchez S, Autonell J, Bernal M, Buist-Bouwman MA, Codony M, Domingo-Salvany A, Ferrer M, Joo SS, Martinez-Alonso M, Matschinger H, Mazzi F, Morgan Z, Morosini P, Palacin C, Romera B, Taub N, Vollebergh WA (2004) Prevalence of mental disorders in Europe: results from the European Study of the Epidemiology of Mental Disorders (ESEMeD) project. Acta Psychiatr Scand Suppl:21-27.

Amaral D, Lavenex P (2007) Hippocampal Neuroanatomy. In: The Hippocampus Book (Anderson P, Morris R, Amaral D, Bliss T, O'Keefe J, eds). Oxford: Oxford University Press.

Ambudkar SV, Kim IW, Xia D, Sauna ZE (2006) The A-loop, a novel conserved aromatic acid subdomain upstream of the Walker A motif in ABC transporters, is critical for ATP binding. FEBS Lett 580:1049-1055.

American Psychiatric Association (2004) Diagnostic and Statistical Manual of Mental Disorders, fourth edition Edition. Washington DC: American Psychiatric Association.

Anderson TW, Darling DA (1952) Asymptotic theory of certain "goodness-of-fit" criteria based on stochastic processes

Annals of Mathematical Statistics 23:193–212. .

Arion D, Sabatini M, Unger T, Pastor J, Alonso-Nanclares L, Ballesteros-Yanez I, Garcia Sola R, Munoz A, Mirnics K, DeFelipe J (2006) Correlation of transcriptome profile with electrical activity in temporal lobe epilepsy. Neurobiol Dis 22:374-387.

Badner JA, Gershon ES (2002) Meta-analysis of whole-genome linkage scans of bipolar disorder and schizophrenia. Mol Psychiatry 7:405-411.

Bakkaloglu B, O'Roak BJ, Louvi A, Gupta AR, Abelson JF, Morgan TM, Chawarska K, Klin A, Ercan-Sencicek AG, Stillman AA, Tanriover G, Abrahams BS, Duvall JA, Robbins EM, Geschwind DH, Biederer T, Gunel M, Lifton RP, State MW

(2008) Molecular cytogenetic analysis and resequencing of contactin associated protein-like 2 in autism spectrum disorders. Am J Hum Genet 82:165-173.
Baldwin CT, Weiss S, Farrer LA, De Stefano AL, Adair R, Franklyn B, Kidd KK, Korostishevsky M, Bonne-Tamir B (1995) Linkage of congenital, recessive deafness (DFNB4) to chromosome 7q31 and evidence for genetic heterogeneity in the Middle Eastern Druze population. Hum Mol Genet 4:1637-1642.
Barrett JC, Fry B, Maller J, Daly MJ (2005) Haploview: analysis and visualization of LD and haplotype maps. Bioinformatics 21:263-265.
Barros SA, Tennant RW, Cannon RE (2003) Molecular structure and characterization of a novel murine ABC transporter, Abca13. Gene 307:191-200.
Baum AE, Akula N, Cabanero M, Cardona I, Corona W, Klemens B, Schulze TG, Cichon S, Rietschel M, Nothen MM, Georgi A, Schumacher J, Schwarz M, Abou Jamra R, Hofels S, Propping P, Satagopan J, Detera-Wadleigh SD, Hardy J, McMahon FJ (2008) A genome-wide association study implicates diacylglycerol kinase eta (DGKH) and several other genes in the etiology of bipolar disorder. Mol Psychiatry 13:197-207.
Benes FM, Todtenkopf MS, Kostoulakos P (2001) GluR5,6,7 subunit immunoreactivity on apical pyramidal cell dendrites in hippocampus of schizophrenics and manic depressives. Hippocampus 11:482-491.
Beneyto M, Kristiansen LV, Oni-Orisan A, McCullumsmith RE, Meador-Woodruff JH (2007) Abnormal glutamate receptor expression in the medial temporal lobe in schizophrenia and mood disorders. Neuropsychopharmacology 32:1888-1902.
Bennett P, Segurado R, Jones I, Bort S, McCandless F, Lambert D, Heron J, Comerford C, Middle F, Corvin A, Pelios G, Kirov G, Larsen B, Mulcahy T, Williams N, O'Connell R, O'Mahony E, Payne A, Owen M, Holmans P, Craddock N, Gill M (2002) The Wellcome trust UK-Irish bipolar affective disorder sibling-pair genome screen: first stage report. Mol Psychiatry 7:189-200.
Bennett RL, Steinhaus KA, Uhrich SB, O'Sullivan CK, Resta RG, Lochner-Doyle D, Markel DS, Vincent V, Hamanishi J (1995) Recommendations for standardized human pedigree nomenclature. Pedigree Standardization Task Force of the National Society of Genetic Counselors. Am J Hum Genet 56:745-752.
Bergen AA, Plomp AS, Hu X, de Jong PT, Gorgels TG (2007) ABCC6 and pseudoxanthoma elasticum. Pflugers Arch 453:685-691.
Berkovic SF, Serratosa JM, Phillips HA, Xiong L, Andermann E, Diaz-Otero F, Gomez-Garre P, Martin M, Fernandez-Bullido Y, Andermann F, Lopes-Cendes I, Dubeau F, Desbiens R, Scheffer IE, Wallace RH, Mulley JC, Pandolfo M (2004) Familial Partial Epilepsy with Variable Foci: Clinical Features and Linkage to Chromosome 22q12. Epilepsia 45:1054-1060.
Berrettini WH (2000) Are schizophrenic and bipolar disorders related? A review of family and molecular studies. Biol Psychiatry 48:531-538.
Blackwood DH, Knight HM (2007) Genetic Predispositions to Stressful Conditions. In: Encyclopedia of Stress, Second Edition Edition (Fink G, ed), pp 141-145. . Oxford: Academic Press.
Blackwood DH, Fordyce A, Walker MT, St Clair DM, Porteous DJ, Muir WJ (2001) Schizophrenia and affective disorders--cosegregation with a translocation at

chromosome 1q42 that directly disrupts brain-expressed genes: clinical and P300 findings in a family. Am J Hum Genet 69:428-433.
Blackwood DHR, Muir WJ (2004) Genetics in relation to psychiatry. In: Companion to Psychiatric Studies, Seventh edition Edition. U.K.: Churchill Livingstone.
Bleakman D (1999) Kainate receptor pharmacology and physiology. Cell Mol Life Sci 56:558-566.
Bodmer W, Bonilla C (2008) Common and rare variants in multifactorial susceptibility to common diseases. Nat Genet 40:695-701.
Bodzioch M, Orso E, Klucken J, Langmann T, Bottcher A, Diederich W, Drobnik W, Barlage S, Buchler C, Porsch-Ozcurumez M, Kaminski WE, Hahmann HW, Oette K, Rothe G, Aslanidis C, Lackner KJ, Schmitz G (1999) The gene encoding ATP-binding cassette transporter 1 is mutated in Tangier disease. Nat Genet 22:347-351.
Boeckmann B, Bairoch A, Apweiler R, Blatter MC, Estreicher A, Gasteiger E, Martin MJ, Michoud K, O'Donovan C, Phan I, Pilbout S, Schneider M (2003) The SWISS-PROT protein knowledgebase and its supplement TrEMBL in 2003. Nucleic Acids Res 31:365-370.
Borowsky B, Durkin MM, Ogozalek K, Marzabadi MR, DeLeon J, Lagu B, Heurich R, Lichtblau H, Shaposhnik Z, Daniewska I, Blackburn TP, Branchek TA, Gerald C, Vaysse PJ, Forray C (2002) Antidepressant, anxiolytic and anorectic effects of a melanin-concentrating hormone-1 receptor antagonist. Nat Med 8:825-830.
Braga MF, Aroniadou-Anderjaska V, Xie J, Li H (2003) Bidirectional modulation of GABA release by presynaptic glutamate receptor 5 kainate receptors in the basolateral amygdala. J Neurosci 23:442-452.
Brooks-Wilson A, Marcil M, Clee SM, Zhang LH, Roomp K, van Dam M, Yu L, Brewer C, Collins JA, Molhuizen HO, Loubser O, Ouelette BF, Fichter K, Ashbourne-Excoffon KJ, Sensen CW, Scherer S, Mott S, Denis M, Martindale D, Frohlich J, Morgan K, Koop B, Pimstone S, Kastelein JJ, Genest J, Jr., Hayden MR (1999) Mutations in ABC1 in Tangier disease and familial high-density lipoprotein deficiency. Nat Genet 22:336-345.
Brown SD, Hardisty-Hughes RE, Mburu P (2008) Quiet as a mouse: dissecting the molecular and genetic basis of hearing. Nat Rev Genet 9:277-290.
Buechler C, Boettcher A, Bared SM, Probst MC, Schmitz G (2002) The carboxyterminus of the ATP-binding cassette transporter A1 interacts with a beta2-syntrophin/utrophin complex. Biochem Biophys Res Commun 293:759-765.
Callenbach PMC, van den Maagdenberg AMJM, Hottenga JJ, van den Boogerd EH, de Coo RFM, Lindhout D, Frants RR, Sandkuijl LA, Brouwer OF (2003) Familial Partial Epilepsy with Variable Foci in a Dutch Family: Clinical Characteristics and Confirmation of Linkage to Chromosome 22q. Epilepsia 44:1298-1305.
Camp NJ, Lowry MR, Richards RL, Plenk AM, Carter C, Hensel CH, Abkevich V, Skolnick MH, Shattuck D, Rowe KG, Hughes DC, Cannon-Albright LA (2005) Genome-wide linkage analyses of extended Utah pedigrees identifies loci that influence recurrent, early-onset major depression and anxiety disorders. Am J Med Genet B Neuropsychiatr Genet 135B:85-93.

Cardno AG, Gottesman, II (2000) Twin studies of schizophrenia: from bow-and-arrow concordances to star wars Mx and functional genomics. Am J Med Genet 97:12-17.
Cardon LR, Palmer LJ (2003) Population stratification and spurious allelic association. Lancet 361:598-604.
Caspi A, Sugden K, Moffitt TE, Taylor A, Craig IW, Harrington H, McClay J, Mill J, Martin J, Braithwaite A, Poulton R (2003) Influence of life stress on depression: moderation by a polymorphism in the 5-HTT gene. Science 301:386-389.
Ceulemans H, Stalmans W, Bollen M (2002) Regulator-driven functional diversification of protein phosphatase-1 in eukaryotic evolution. Bioessays 24:371-381.
Chaki S, Funakoshi T, Hirota-Okuno S, Nishiguchi M, Shimazaki T, Iijima M, Grottick AJ, Kanuma K, Omodera K, Sekiguchi Y, Okuyama S, Tran TA, Semple G, Thomsen W (2005) Anxiolytic- and antidepressant-like profile of ATC0065 and ATC0175: nonpeptidic and orally active melanin-concentrating hormone receptor 1 antagonists. J Pharmacol Exp Ther 313:831-839.
Chakravarti A (1999) Population genetics--making sense out of sequence. Nat Genet 21:56-60.
Chang MC, Grange E, Rabin O, Bell JM, Allen DD, Rapoport SI (1996) Lithium decreases turnover of arachidonate in several brain phospholipids. Neurosci Lett 220:171-174.
Chang MC, Contreras MA, Rosenberger TA, Rintala JJ, Bell JM, Rapoport SI (2001) Chronic valproate treatment decreases the in vivo turnover of arachidonic acid in brain phospholipids: a possible common effect of mood stabilizers. J Neurochem 77:796-803.
Chen JM, Ferec C, Cooper DN (2006) A systematic analysis of disease-associated variants in the 3' regulatory regions of human protein-coding genes II: the importance of mRNA secondary structure in assessing the functionality of 3' UTR variants. Hum Genet 120:301-333.
Chen ZQ, Annilo T, Shulenin S, Dean M (2004) Three ATP-binding cassette transporter genes, Abca14, Abca15, and Abca16, form a cluster on mouse Chromosome 7F3. Mamm Genome 15:335-343.
Chittajallu R, Braithwaite SP, Clarke VR, Henley JM (1999) Kainate receptors: subunits, synaptic localization and function. Trends Pharmacol Sci 20:26-35.
Chiyonobu T, Hayashi S, Kobayashi K, Morimoto M, Miyanomae Y, Nishimura A, Nishimoto A, Ito C, Imoto I, Sugimoto T, Jia Z, Inazawa J, Toda T (2007) Partial tandem duplication of GRIA3 in a male with mental retardation. Am J Med Genet A 143A:1448-1455.
Clapcote SJ, Lipina TV, Millar JK, Mackie S, Christie S, Ogawa F, Lerch JP, Trimble K, Uchiyama M, Sakuraba Y, Kaneda H, Shiroishi T, Houslay MD, Henkelman RM, Sled JG, Gondo Y, Porteous DJ, Roder JC (2007) Behavioral phenotypes of Disc1 missense mutations in mice. Neuron 54:387-402.
Conne B, Stutz A, Vassalli JD (2000) The 3' untranslated region of messenger RNA: A molecular 'hotspot' for pathology? Nat Med 6:637-641.
Cooper AF (1976) Deafness and psychiatric illness. Br J Psychiatry 129:216-226.

Craddock N, Jones I (2001) Molecular genetics of bipolar disorder. Br J Psychiatry 178:S128-133.
Craddock N, O'Donovan MC, Owen MJ (2005) The genetics of schizophrenia and bipolar disorder: dissecting psychosis. J Med Genet 42:193-204.
Crawford J, Zielinski MA, Fisher LJ, Sutherland GR, Goldney RD (2002) Is there a relationship between Wolfram syndrome carrier status and suicide? Am J Med Genet 114:343-346.
Cunningham Owens DG (2004) Clinical psychopharmacology. In: Companion to Psychiatric Studies, Seventh edition Edition (Johnstone E, Lawrie S M, Sharpe M, Freeman CPL ed). UK: Churchill Livingstone.
Curtis D, Vine AE, Knight J (2008) Study of regions of extended homozygosity provides a powerful method to explore haplotype structure of human populations. Ann Hum Genet 72:261-278.
D'Angelo G, Vicinanza M, De Matteis MA (2008) Lipid-transfer proteins in biosynthetic pathways. Curr Opin Cell Biol 20:360-370.
Darstein M, Petralia RS, Swanson GT, Wenthold RJ, Heinemann SF (2003) Distribution of kainate receptor subunits at hippocampal mossy fiber synapses. J Neurosci 23:8013-8019.
Dean M (2003) Approaches to identify genes for complex human diseases: lessons from Mendelian disorders. Hum Mutat 22:261-274.
Dean M, Rzhetsky A, Allikmets R (2001) The human ATP-binding cassette (ABC) transporter superfamily. Genome Res 11:1156-1166.
Deary IJ, Gow AJ, Taylor MD, Corley J, Brett C, Wilson V, Campbell H, Whalley LJ, Visscher PM, Porteous DJ, Starr JM (2007) The Lothian Birth Cohort 1936: a study to examine influences on cognitive ageing from age 11 to age 70 and beyond. BMC Geriatr 7:28.
DeLisi LE, Shaw SH, Crow TJ, Shields G, Smith AB, Larach VW, Wellman N, Loftus J, Nanthakumar B, Razi K, Stewart J, Comazzi M, Vita A, Heffner T, Sherrington R (2002) A Genome-Wide Scan for Linkage to Chromosomal Regions in 382 Sibling Pairs With Schizophrenia or Schizoaffective Disorder. American Journal of Psychiatry 159:803-812.
Devinsky O, Morrell MJ, Vogt BA (1995) Contributions of anterior cingulate cortex to behaviour. Brain 118 (Pt 1):279-306.
Di Rienzo A (2006) Population genetics models of common diseases. Curr Opin Genet Dev 16:630-636.
Donati RJ, Rasenick MM (2005) Chronic antidepressant treatment prevents accumulation of gsalpha in cholesterol-rich, cytoskeletal-associated, plasma membrane domains (lipid rafts). Neuropsychopharmacology 30:1238-1245.
Doris AB, Wahle K, MacDonald A, Morris S, Coffey I, Muir W, Blackwood D (1998) Red cell membrane fatty acids, cytosolic phospholipase-A2 and schizophrenia. Schizophr Res 31:185-196.
Dracheva S, Byne W, Chin B, Haroutunian V (2008) Ionotropic glutamate receptor mRNA expression in the human thalamus: absence of change in schizophrenia. Brain Res 1214:23-34.

Duan X, Chang JH, Ge S, KFaulkner RL, Kim JY, Kitabatake Y, Liu XB, Yang CH, Jorden JD, Ma DK, Liu CY, Ganesan S, Cheng HJ, Ming GL, Lu B, Song H (2007) Disrupted-In-Schizophrenia 1 Regulates Integration of Newly Generated Neurons in the Adult Brain. 130:1146-1158.

Durand CM, Betancur C, Boeckers TM, Bockmann J, Chaste P, Fauchereau F, Nygren G, Rastam M, Gillberg IC, Anckarsater H, Sponheim E, Goubran-Botros H, Delorme R, Chabane N, Mouren-Simeoni MC, de Mas P, Bieth E, Roge B, Heron D, Burglen L, Gillberg C, Leboyer M, Bourgeron T (2007) Mutations in the gene encoding the synaptic scaffolding protein SHANK3 are associated with autism spectrum disorders. Nat Genet 39:25-27.

Eisensamer B, Uhr M, Meyr S, Gimpl G, Deiml T, Rammes G, Lambert JJ, Zieglgansberger W, Holsboer F, Rupprecht R (2005) Antidepressants and antipsychotic drugs colocalize with 5-HT3 receptors in raft-like domains. J Neurosci 25:10198-10206.

Endicott J, Spitzer RL (1978) A diagnostic interview: the schedule for affective disorders and schizophrenia. Arch Gen Psychiatry 35:837-844.

Erbel-Sieler C, Dudley C, Zhou Y, Wu X, Estill SJ, Han T, Diaz-Arrastia R, Brunskill EW, Potter SS, McKnight SL (2004) Behavioral and regulatory abnormalities in mice deficient in the NPAS1 and NPAS3 transcription factors. Proc Natl Acad Sci U S A 101:13648-13653.

Failla P, Romano C, Alberti A, Vasta A, Buono S, Castiglia L, Luciano D, Di Benedetto D, Fichera M, Galesi O (2007) Schizophrenia in a patient with subtelomeric duplication of chromosome 22q. Clin Genet 71:599-601.

Fallin MD, Lasseter VK, Avramopoulos D, Nicodemus KK, Wolyniec PS, McGrath JA, Steel G, Nestadt G, Liang KY, Huganir RL, Valle D, Pulver AE (2005) Bipolar I disorder and schizophrenia: a 440-single-nucleotide polymorphism screen of 64 candidate genes among Ashkenazi Jewish case-parent trios. Am J Hum Genet 77:918-936.

Farkas E, de Wilde MC, Kiliaan AJ, Meijer J, Keijser JN, Luiten PG (2002) Dietary long chain PUFAs differentially affect hippocampal muscarinic 1 and serotonergic 1A receptors in experimental cerebral hypoperfusion. Brain Res 954:32-41.

Fatemi SH, King DP, Reutiman TJ, Folsom TD, Laurence JA, Lee S, Fan YT, Paciga SA, Conti M, Menniti FS (2008) PDE4B polymorphisms and decreased PDE4B expression are associated with schizophrenia. Schizophr Res 101:36-49.

Faulkner RL, Jang MH, Liu XB, Duan X, Sailor KA, Kim JY, Ge S, Jones EG, Ming GL, Song H, Cheng HJ (2008) Development of hippocampal mossy fiber synaptic outputs by new neurons in the adult brain. Proc Natl Acad Sci U S A 105:14157-14162.

Fearon K, McClendon V, Bonetti B, Bedwell DM (1994) Premature translation termination mutations are efficiently suppressed in a highly conserved region of yeast Ste6p, a member of the ATP-binding cassette (ABC) transporter family. J Biol Chem 269:17802-17808.

Feldberg W (1976) Possible association of schizophrenia with a disturbance in prostaglandin metabolism: a physiological hypothesis. Psychol Med 6:359-369.

Fenton WS, Hibbeln J, Knable M (1999) Essential fatty acids, lipid membrane abnormalities, and the diagnosis and treatment of schizophrenia. Biological Psychiatry 47:8-21.
Fernandez T, Morgan T, Davis N, Klin A, Morris A, Farhi A, Lifton RP, State MW (2004) Disruption of contactin 4 (CNTN4) results in developmental delay and other features of 3p deletion syndrome. Am J Hum Genet 74:1286-1293.
Fitzgerald ML, Okuhira K, Short GF, 3rd, Manning JJ, Bell SA, Freeman MW (2004) ATP-binding cassette transporter A1 contains a novel C-terminal VFVNFA motif that is required for its cholesterol efflux and ApoA-I binding activities. J Biol Chem 279:48477-48485.
Fogarty DJ, Perez-Cerda F, Matute C (2000) KA1-like kainate receptor subunit immunoreactivity in neurons and glia using a novel anti-peptide antibody. Brain Res Mol Brain Res 81:164-176.
Fox TD (1987) Natural variation in the genetic code. Annu Rev Genet 21:67-91.
Freedman ML, Reich D, Penney KL, McDonald GJ, Mignault AA, Patterson N, Gabriel SB, Topol EJ, Smoller JW, Pato CN, Pato MT, Petryshen TL, Kolonel LN, Lander ES, Sklar P, Henderson B, Hirschhorn JN, Altshuler D (2004) Assessing the impact of population stratification on genetic association studies. Nat Genet 36:388-393.
Fujita M, Charney DS, Innis RB (2000) Imaging serotonergic neurotransmission in depression: hippocampal pathophysiology may mirror global brain alterations. Biol Psychiatry 48:801-812.
Garey LJ, Von Bussmann KA, Hirsch SR (2006) Decreased numerical density of kainate receptor-positive neurons in the orbitofrontal cortex of chronic schizophrenics. Exp Brain Res 173:234-242.
Gattaz WF, Kollisch M, Thuren T, Virtanen JA, Kinnunen PK (1987) Increased plasma phospholipase-A2 activity in schizophrenic patients: reduction after neuroleptic therapy. Biol Psychiatry 22:421-426.
Gecz J, Barnett S, Liu J, Hollway G, Donnelly A, Eyre H, Eshkevari HS, Baltazar R, Grunn A, Nagaraja R, Gilliam C, Peltonen L, Sutherland GR, Baron M, Mulley JC (1999) Characterization of the human glutamate receptor subunit 3 gene (GRIA3), a candidate for bipolar disorder and nonspecific X-linked mental retardation. Genomics 62:356-368.
Gelder M, Harrison P, Cowen P (2006) Shorter Oxford Textbook of Psychiatry, 5th edition Edition. Oxford: Oxford University Press.
Geyer MA, Vollenweider FX (2008) Serotonin research: contributions to understanding psychoses. Trends Pharmacol Sci.
Gibson J, Morton NE, Collins A (2006) Extended tracts of homozygosity in outbred human populations. Hum Mol Genet 15:789-795.
Glen AI, Glen EM, Horrobin DF, Vaddadi KS, Spellman M, Morse-Fisher N, Ellis K, Skinner FS (1994) A red cell membrane abnormality in a subgroup of schizophrenic patients: evidence for two diseases. Schizophr Res 12:53-61.
Gonzalez-Maeso J, Ang RL, Yuen T, Chan P, Weisstaub NV, Lopez-Gimenez JF, Zhou M, Okawa Y, Callado LF, Milligan G, Gingrich JA, Filizola M, Meana JJ,

Sealfon SC (2008) Identification of a serotonin/glutamate receptor complex implicated in psychosis. Nature 452:93-97.
Gordon D, Abajian C, Green P (1998) Consed: a graphical tool for sequence finishing. Genome Res 8:195-202.
Gottesman II (1991) Schizophrenia genesis: the origins of madness. New York: Freeman.
Gould E (2007) Structural Plasticity In: The Hippocampus Book (Anderson P, Morris R, Amaral D, Bliss T, O'Keefe J, eds), pp 321-342. Oxford: Oxford University Press.
Green E, Elvidge G, Jacobsen N, Glaser B, Jones I, O'Donovan MC, Kirov G, Owen MJ, Craddock N (2005) Localization of bipolar susceptibility locus by molecular genetic analysis of the chromosome 12q23-q24 region in two pedigrees with bipolar disorder and Darier's disease. Am J Psychiatry 162:35-42.
Green EK, Norton N, Peirce T, Grozeva D, Kirov G, Owen MJ, O'Donovan MC, Craddock N (2006) Evidence that a DISC1 frame-shift deletion associated with psychosis in a single family may not be a pathogenic mutation. Mol Psychiatry 11:798-799.
Greinwald JH, Jr., Wayne S, Chen AH, Scott DA, Zbar RI, Kraft ML, Prasad S, Ramesh A, Coucke P, Srisailapathy CR, Lovett M, Van Camp G, Smith RJ (1998) Localization of a novel gene for nonsyndromic hearing loss (DFNB17) to chromosome region 7q31. Am J Med Genet 78:107-113.
Grzybowska EA, Wilczynska A, Siedlecki JA (2001) Regulatory functions of 3'UTRs. Biochem Biophys Res Commun 288:291-295.
Haines TH (2001) Do sterols reduce proton and sodium leaks through lipid bilayers? Prog Lipid Res 40:299-324.
Harlow E, Lane D (1998) Antibodies A Laboratory Manual. New York: Cold Spring Harbour Laboratory Press.
Harris EW, Cotman CW (1986) Long-term potentiation of guinea pig mossy fiber responses is not blocked by N-methyl D-aspartate antagonists. Neurosci Lett 70:132-137.
Harrison PJ (1999) The neuropathology of schizophrenia. A critical review of the data and their interpretation. Brain 122 (Pt 4):593-624.
Harrison PJ, Weinberger DR (2005) Schizophrenia genes, gene expression, and neuropathology: on the matter of their convergence. Mol Psychiatry 10:40-68; image 45.
Hassan MJ, Santos RL, Rafiq MA, Chahrour MH, Pham TL, Wajid M, Hijab N, Wambangco M, Lee K, Ansar M, Yan K, Ahmad W, Leal SM (2006) A novel autosomal recessive non-syndromic hearing impairment locus (DFNB47) maps to chromosome 2p25.1-p24.3. Hum Genet 118:605-610.
Hennah W, Thomson P, McQuillin A, Bass N, Loukola A, Anjorin A, Blackwood D, Curtis D, Deary IJ, Harris SE, Isometsa ET, Lawrence J, Lonnqvist J, Muir W, Palotie A, Partonen T, Paunio T, Pylkko E, Robinson M, Soronen P, Suominen K, Suvisaari J, Thirumalai S, Clair DS, Gurling H, Peltonen L, Porteous D (2008) DISC1 association, heterogeneity and interplay in schizophrenia and bipolar disorder. Mol Psychiatry.

Hering H, Lin CC, Sheng M (2003) Lipid rafts in the maintenance of synapses, dendritic spines, and surface AMPA receptor stability. J Neurosci 23:3262-3271.
Hibbeln JR, Salem N, Jr. (1995) Dietary polyunsaturated fatty acids and depression: when cholesterol does not satisfy. Am J Clin Nutr 62:1-9.
Hirsch-Reinshagen V, Zhou S, Burgess BL, Bernier L, McIsaac SA, Chan JY, Tansley GH, Cohn JS, Hayden MR, Wellington CL (2004) Deficiency of ABCA1 impairs apolipoprotein E metabolism in brain. J Biol Chem 279:41197-41207.
Horrobin DF (1977) Schizophrenia as a prostaglandin deficiency disease. Lancet 1:936-937.
Huettner JE (2003) Kainate receptors and synaptic transmission. Prog Neurobiol 70:387-407.
Ibrahim HM, Hogg AJ, Jr., Healy DJ, Haroutunian V, Davis KL, Meador-Woodruff JH (2000) Ionotropic glutamate receptor binding and subunit mRNA expression in thalamic nuclei in schizophrenia. Am J Psychiatry 157:1811-1823.
ISC ISC (2008) Rare chromosomal deletions and duplications increase risk of schizophrenia. Nature 455:237-241.
Jacobsen NJ, Lyons I, Hoogendoorn B, Burge S, Kwok PY, O'Donovan MC, Craddock N, Owen MJ (1999) ATP2A2 mutations in Darier's disease and their relationship to neuropsychiatric phenotypes. Hum Mol Genet 8:1631-1636.
Jacobsen NJ, Franks EK, Elvidge G, Jones I, McCandless F, O'Donovan MC, Owen MJ, Craddock N (2001) Exclusion of the Darier's disease gene, ATP2A2, as a common susceptibility gene for bipolar disorder. Mol Psychiatry 6:92-97.
Jamain S, Quach H, Betancur C, Rastam M, Colineaux C, Gillberg IC, Soderstrom H, Giros B, Leboyer M, Gillberg C, Bourgeron T (2003) Mutations of the X-linked genes encoding neuroligins NLGN3 and NLGN4 are associated with autism. Nat Genet 34:27-29.
Jaskolski F, Coussen F, Mulle C (2005) Subcellular localization and trafficking of kainate receptors. Trends Pharmacol Sci 26:20-26.
Javitt DC, Zukin SR (1991) Recent advances in the phencyclidine model of schizophrenia. Am J Psychiatry 148:1301-1308.
Jervell A, Lange-Nielsen F (1957) Congenital deaf-mutism, functional heart disease with prolongation of the Q-T interval and sudden death. Am Heart J 54:59-68.
Jorgensen TH, Borglum AD, Mors O, Wang AG, Pinaud M, Flint TJ, Dahl HA, Vang M, Kruse TA, Ewald H (2002) Search for common haplotypes on chromosome 22q in patients with schizophrenia or bipolar disorder from the Faroe Islands. Am J Med Genet 114:245-252.
Kaminski WE, Piehler A, Wenzel JJ (2006) ABC A-subfamily transporters: structure, function and disease. Biochim Biophys Acta 1762:510-524.
Kamiya A, Tan PL, Kubo K, Engelhard C, Ishizuka K, Kubo A, Tsukita S, Pulver AE, Nakajima K, Cascella NG, Katsanis N, Sawa A (2008) Recruitment of PCM1 to the centrosome by the cooperative action of DISC1 and BBS4: a candidate for psychiatric illnesses. Arch Gen Psychiatry 65:996-1006.
Kamnasaran D, Muir WJ, Ferguson-Smith MA, Cox DW (2003) Disruption of the neuronal PAS3 gene in a family affected with schizophrenia. J Med Genet 40:325-332.

Kandel ER, Schwartz JH, Jessell TM (2000) Principles of Neural Science, fourth Edition. New York McGraw-Hill Health Professions Division
Karlin S, Mrazek J (1996) What drives codon choices in human genes? J Mol Biol 262:459-472.
Kask K, Jerecic J, Zamanillo D, Wilbertz J, Sprengel R, Seeburg PH (2000) Developmental profile of kainate receptor subunit KA1 revealed by Cre expression in YAC transgenic mice. Brain Res 876:55-61.
Kathiresan S, Melander O, Guiducci C, Surti A, Burtt NP, Rieder MJ, Cooper GM, Roos C, Voight BF, Havulinna AS, Wahlstrand B, Hedner T, Corella D, Tai ES, Ordovas JM, Berglund G, Vartiainen E, Jousilahti P, Hedblad B, Taskinen MR, Newton-Cheh C, Salomaa V, Peltonen L, Groop L, Altshuler DM, Orho-Melander M (2008) Six new loci associated with blood low-density lipoprotein cholesterol, high-density lipoprotein cholesterol or triglycerides in humans. Nat Genet 40:189-197.
Kato T (2001) Molecular genetics of bipolar disorder. Neurosci Res 40:105-113.
Kelsoe JR, Spence MA, Loetscher E, Foguet M, Sadovnick AD, Remick RA, Flodman P, Khristich J, Mroczkowski-Parker Z, Brown JL, Masser D, Ungerleider S, Rapaport MH, Wishart WL, Luebbert H (2001) A genome survey indicates a possible susceptibility locus for bipolar disorder on chromosome 22. Proc Natl Acad Sci U S A 98:585-590.
Kendler KS (2000) Schizophrenia genetics. In: Kaplan and Sadock's comprehensive textbook of psychiatry (Sadock BJ, Sadock VA, eds), pp p1147-1159. Philadelphia: Lippincott, Williams & Wilkins.
Kendler KS, Neale MC, Kessler RC, Heath AC, Eaves LJ (1993) A longitudinal twin study of personality and major depression in women. Arch Gen Psychiatry 50:853-862.
Kendler KS, Ochs AL, Gorman AM, Hewitt JK, Ross DE, Mirsky AF (1991) The structure of schizotypy: a pilot multitrait twin study. Psychiatry Res 36:19-36.
Kerwin R, Patel S, Meldrum B (1990) Quantitative autoradiographic analysis of glutamate binding sites in the hippocampal formation in normal and schizophrenic brain post mortem. Neuroscience 39:25-32.
Kessler RC, Davis CG, Kendler KS (1997) Childhood adversity and adult psychiatric disorder in the US National Comorbidity Survey. Psychol Med 27:1101-1119.
Kessler RC, McGonagle KA, Zhao S, Nelson CB, Hughes M, Eshleman S, Wittchen HU, Kendler KS (1994) Lifetime and 12-month prevalence of DSM-III-R psychiatric disorders in the United States. Results from the National Comorbidity Survey. Arch Gen Psychiatry 51:8-19.
Kim WS, Weickert CS, Garner B (2008) Role of ATP-binding cassette transporters in brain lipid transport and neurological disease. J Neurochem 104:1145-1166.
Kimchi-Sarfaty C, Oh JM, Kim IW, Sauna ZE, Calcagno AM, Ambudkar SV, Gottesman MM (2007) A "silent" polymorphism in the MDR1 gene changes substrate specificity. Science 315:525-528.
Kirov G, Zaharieva I, Georgieva L, Moskvina V, Nikolov I, Cichon S, Hillmer A, Toncheva D, Owen MJ, O'Donovan MC (2008) A genome-wide association study in 574 schizophrenia trios using DNA pooling. Mol Psychiatry.

Kitiratschky VB, Grau T, Bernd A, Zrenner E, Jagle H, Renner AB, Kellner U, Rudolph G, Jacobson SG, Cideciyan AV, Schaich S, Kohl S, Wissinger B (2008) ABCA4 gene analysis in patients with autosomal recessive cone and cone rod dystrophies. Eur J Hum Genet 16:812-819.
Kleinjan DJ, van Heyningen V (1998) Position effect in human genetic disease. Hum Mol Genet 7:1611-1618.
Kong A, Cox NJ (1997) Allele-sharing models: LOD scores and accurate linkage tests. Am J Hum Genet 61:1179-1188.
Konradi C, Heckers S (2003) Molecular aspects of glutamate dysregulation: implications for schizophrenia and its treatment. Pharmacol Ther 97:153-179.
Krishnan V, Nestler EJ (2008) The molecular neurobiology of depression. Nature 455:894-902.
Kumar SS, Buckmaster PS (2006) Hyperexcitability, interneurons, and loss of GABAergic synapses in entorhinal cortex in a model of temporal lobe epilepsy. J Neurosci 26:4613-4623.
Lander ES, Botstein D (1987) Homozygosity mapping: a way to map human recessive traits with the DNA of inbred children. Science 236:1567-1570.
Lang UE, Puls I, Muller DJ, Strutz-Seebohm N, Gallinat J (2007) Molecular mechanisms of schizophrenia. Cell Physiol Biochem 20:687-702.
Laumonnier F, Bonnet-Brilhault F, Gomot M, Blanc R, David A, Moizard MP, Raynaud M, Ronce N, Lemonnier E, Calvas P, Laudier B, Chelly J, Fryns JP, Ropers HH, Hamel BC, Andres C, Barthelemy C, Moraine C, Briault S (2004) X-linked mental retardation and autism are associated with a mutation in the NLGN4 gene, a member of the neuroligin family. Am J Hum Genet 74:552-557.
Laurier V, Stoetzel C, Muller J, Thibault C, Corbani S, Jalkh N, Salem N, Chouery E, Poch O, Licaire S, Danse JM, Amati-Bonneau P, Bonneau D, Megarbane A, Mandel JL, Dollfus H (2006) Pitfalls of homozygosity mapping: an extended consanguineous Bardet-Biedl syndrome family with two mutant genes (BBS2, BBS10), three mutations, but no triallelism. Eur J Hum Genet 14:1195-1203.
Lavedan C, Licamele L, Volpi S, Hamilton J, Heaton C, Mack K, Lannan R, Thompson A, Wolfgang CD, Polymeropoulos MH (2008) Association of the NPAS3 gene and five other loci with response to the antipsychotic iloperidone identified in a whole genome association study. Mol Psychiatry.
Lee BJ, Worland PJ, Davis JN, Stadtman TC, Hatfield DL (1989) Identification of a selenocysteyl-tRNA(Ser) in mammalian cells that recognizes the nonsense codon, UGA. J Biol Chem 264:9724-9727.
Lencz T, Morgan TV, Athanasiou M, Dain B, Reed CR, Kane JM, Kucherlapati R, Malhotra AK (2007) Converging evidence for a pseudoautosomal cytokine receptor gene locus in schizophrenia. Mol Psychiatry 12:572-580.
Lenox RH, Wang L (2003) Molecular basis of lithium action: integration of lithium-responsive signaling and gene expression networks. Mol Psychiatry 8:135-144.
Lerma J (2003) Roles and rules of kainate receptors in synaptic transmission. Nat Rev Neurosci 4:481-495.
Lerma J (2006) Kainate receptor physiology. Curr Opin Pharmacol 6:89-97.

Lerma J, Paternain AV, Rodriguez-Moreno A, Lopez-Garcia JC (2001) Molecular physiology of kainate receptors. Physiol Rev 81:971-998.
Leutenegger AL, Prum B, Genin E, Verny C, Lemainque A, Clerget-Darpoux F, Thompson EA (2003) Estimation of the inbreeding coefficient through use of genomic data. Am J Hum Genet 73:516-523.
Leutenegger AL, Labalme A, Genin E, Toutain A, Steichen E, Clerget-Darpoux F, Edery P (2006) Using genomic inbreeding coefficient estimates for homozygosity mapping of rare recessive traits: application to Taybi-Linder syndrome. Am J Hum Genet 79:62-66.
Levinson DF (2006) The genetics of depression: a review. Biol Psychiatry 60:84-92.
Lewis CM, Levinson DF, Wise LH, DeLisi LE, Straub RE, Hovatta I, Williams NM, Schwab SG, Pulver AE, Faraone SV, Brzustowicz LM, Kaufmann CA, Garver DL, Gurling HM, Lindholm E, Coon H, Moises HW, Byerley W, Shaw SH, Mesen A, Sherrington R, O'Neill FA, Walsh D, Kendler KS, Ekelund J, Paunio T, Lonnqvist J, Peltonen L, O'Donovan MC, Owen MJ, Wildenauer DB, Maier W, Nestadt G, Blouin JL, Antonarakis SE, Mowry BJ, Silverman JM, Crowe RR, Cloninger CR, Tsuang MT, Malaspina D, Harkavy-Friedman JM, Svrakic DM, Bassett AS, Holcomb J, Kalsi G, McQuillin A, Brynjolfson J, Sigmundsson T, Petursson H, Jazin E, Zoega T, Helgason T (2003) Genome scan meta-analysis of schizophrenia and bipolar disorder, part II: Schizophrenia. Am J Hum Genet 73:34-48.
Li XC, Everett LA, Lalwani AK, Desmukh D, Friedman TB, Green ED, Wilcox ER (1998) A mutation in PDS causes non-syndromic recessive deafness. Nat Genet 18:215-217.
Li Z, He Z, Tang W, Tang R, Huang K, Xu Z, Xu Y, Li L, Li X, Feng G, He L, Shi Y (2008) No genetic association between polymorphisms in the kainate-type glutamate receptor gene, GRIK4, and schizophrenia in the Chinese population. Prog Neuropsychopharmacol Biol Psychiatry 32:876-880.
Liddle PF (1987) The symptoms of chronic schizophrenia. A re-examination of the positive-negative dichotomy. Br J Psychiatry 151:145-151.
Linton KJ, Higgins CF (2007) Structure and function of ABC transporters: the ATP switch provides flexible control. Pflugers Arch 453:555-567.
Liu P, Bilkey DK (1998) Is there a direct projection from perirhinal cortex to the hippocampus? Hippocampus 8:424-425.
Liu QS, Xu Q, Arcuino G, Kang J, Nedergaard M (2004) Astrocyte-mediated activation of neuronal kainate receptors. Proc Natl Acad Sci U S A 101:3172-3177.
Liu XZ, Ouyang XM, Xia XJ, Zheng J, Pandya A, Li F, Du LL, Welch KO, Petit C, Smith RJ, Webb BT, Yan D, Arnos KS, Corey D, Dallos P, Nance WE, Chen ZY (2003) Prestin, a cochlear motor protein, is defective in non-syndromic hearing loss. Hum Mol Genet 12:1155-1162.
Liu YL, Fann CS, Liu CM, Chen WJ, Wu JY, Hung SI, Chen CH, Jou YS, Liu SK, Hwang TJ, Hsieh MH, Chang CC, Yang WC, Lin JJ, Chou FH, Faraone SV, Tsuang MT, Hwu HG (2008) RASD2, MYH9, and CACNG2 Genes at Chromosome 22q12 Associated with the Subgroup of Schizophrenia with Non-Deficit in Sustained Attention and Executive Function. Biol Psychiatry.

Lohmueller KE, Pearce CL, Pike M, Lander ES, Hirschhorn JN (2003) Meta-analysis of genetic association studies supports a contribution of common variants to susceptibility to common disease. Nat Genet 33:177-182.

Macdonald ME, C.M. Ambrose, M.P. Duyao, R.H. Myers, C. Lin, L. Srinidhi, G. Barnes, S.A. Taylor, M. James, N. Groot, H. Macfarlane, B. Jenkins, M.A. Anderson, N.S. Wexler, J.F. Gusella, G.P. Bates, S. Baxendale, H. Hummerich, S. Kirby, M. North, S. Youngman, R. Mott, G. Zehetner, Z. Sedlacek, A. Poustka, A.M. Frischauf, H. Lehrach, A.J. Buckler, D. Church, L. Doucettestamm, M.C. Odonovan, L. Ribaramirez, M. Shah, V.P. Stanton, S.A. Strobel, K.M. Draths, J.L. Wales, P. Dervan, D.E. Housman, M. Altherr, R. Shiang, L. Thompson, T. Fielder, J.J. Wasmuth, D. Tagle, J. Valdes, L. Elmer, M. Allard, L. Castilla, M. Swaroop, K. Blanchard, F.S. Collins, R. Snell, T. Holloway, K. Gillespie, N. Datson, D. Shaw and P.S. Harper (1993) A novel gene containing a trinucleotide repeat that is expanded and unstable on Huntington's disease chromosomes. Cell 72:971-983.

Mace S, Cousin E, Ricard S, Genin E, Spanakis E, Lafargue-Soubigou C, Genin B, Fournel R, Roche S, Haussy G, Massey F, Soubigou S, Brefort G, Benoit P, Brice A, Campion D, Hollis M, Pradier L, Benavides J, Deleuze JF (2005) ABCA2 is a strong genetic risk factor for early-onset Alzheimer's disease. Neurobiol Dis 18:119-125.

Magarinos AM, McEwen BS (1995) Stress-induced atrophy of apical dendrites of hippocampal CA3c neurons: involvement of glucocorticoid secretion and excitatory amino acid receptors. Neuroscience 69:89-98.

Magarinos AM, McEwen BS, Flugge G, Fuchs E (1996) Chronic psychosocial stress causes apical dendritic atrophy of hippocampal CA3 pyramidal neurons in subordinate tree shrews. J Neurosci 16:3534-3540.

Magri C, Gardella R, Valsecchi P, Barlati SD, Guizzetti L, Imperadori L, Bonvicini C, Tura GB, Gennarelli M, Sacchetti E, Barlati S (2008) Study on GRIA2, GRIA3 and GRIA4 genes highlights a positive association between schizophrenia and GRIA3 in female patients. Am J Med Genet B Neuropsychiatr Genet 147B:745-753.

Mah S, Nelson MR, Delisi LE, Reneland RH, Markward N, James MR, Nyholt DR, Hayward N, Handoko H, Mowry B, Kammerer S, Braun A (2006) Identification of the semaphorin receptor PLXNA2 as a candidate for susceptibility to schizophrenia. Mol Psychiatry 11:471-478.

Mandell A, Knapp S (1979) Asymmetry and mood, emergent properties of serotonin regulation. Archives of general psychiatry 36:909-916.

Manganas LN, Zhang X, Li Y, Hazel RD, Smith SD, Wagshul ME, Henn F, Benveniste H, Djuric PM, Enikolopov G, Maletic-Savatic M (2007) Magnetic resonance spectroscopy identifies neural progenitor cells in the live human brain. Science 318:980-985.

Masmoudi S, Tlili A, Majava M, Ghorbel AM, Chardenoux S, Lemainque A, Zina ZB, Moala J, Mannikko M, Weil D, Lathrop M, Ala-Kokko L, Drira M, Petit C, Ayadi H (2003) Mapping of a new autosomal recessive nonsyndromic hearing loss locus (DFNB32) to chromosome 1p13.3-22.1. Eur J Hum Genet 11:185-188.

Matute C, Alberdi E, Domercq M, Perez-Cerda F, Perez-Samartin A, Sanchez-Gomez MV (2001) The link between excitotoxic oligodendroglial death and demyelinating diseases. Trends Neurosci 24:224-230.
McCaffery P, Zhang J, Crandall JE (2006) Retinoic acid signaling and function in the adult hippocampus. J Neurobiol 66:780-791.
McCaughan KK, Brown CM, Dalphin ME, Berry MJ, Tate WP (1995) Translational termination efficiency in mammals is influenced by the base following the stop codon. Proc Natl Acad Sci U S A 92:5431-5435.
McClellan JM, Susser E, King MC (2007) Schizophrenia: a common disease caused by multiple rare alleles. Br J Psychiatry 190:194-199.
McEwen BS (1980) Steroid hormones and the brain: cellular mechanisms underlying neural and behavioral plasticity. Psychoneuroendocrinology 5:1-11.
McEwen BS (1999) Stress and hippocampal plasticity. Annu Rev Neurosci 22:105-122.
McEwen BS, Magarinos AM (1997) Stress effects on morphology and function of the hippocampus. Ann N Y Acad Sci 821:271-284.
McGuffin P, Owen MJ, Farmer AE (1995) Genetic basis of schizophrenia. Lancet 346:678-682.
McGuffin P, Katz R, Watkins S, Rutherford J (1996) A hospital-based twin register of the heritability of DSM-IV unipolar depression. Arch Gen Psychiatry 53:129-136.
McNamara RK, Jandacek R, Rider T, Tso P, Hahn CG, Richtand NM, Stanford KE (2007) Abnormalities in the fatty acid composition of the postmortem orbitofrontal cortex of schizophrenic patients: gender differences and partial normalization with antipsychotic medications. Schizophr Res 91:37-50.
McNamara RK, Jandacek R, Rider T, Tso P, Stanford KE, Hahn CG, Richtand NM (2008) Deficits in docosahexaenoic acid and associated elevations in the metabolism of arachidonic acid and saturated fatty acids in the postmortem orbitofrontal cortex of patients with bipolar disorder. Psychiatry Res 160:285-299.
Meador-Woodruff JH, Davis KL, Haroutunian V (2001) Abnormal kainate receptor expression in prefrontal cortex in schizophrenia. Neuropsychopharmacology 24:545-552.
Meador-Woodruff JH, King RE, Damask SP, Bovenkerk KA (1996) Differential regulation of hippocampal AMPA and kainate receptor subunit expression by haloperidol and clozapine. Mol Psychiatry 1:41-53.
Michaelis EK (1998) Molecular biology of glutamate receptors in the central nervous system and their role in excitotoxicity, oxidative stress and aging. Prog Neurobiol 54:369-415.
Millar JK, Wilson-Annan JC, Anderson S, Christie S, Taylor MS, Semple CA, Devon RS, Clair DM, Muir WJ, Blackwood DH, Porteous DJ (2000) Disruption of two novel genes by a translocation co-segregating with schizophrenia. Hum Mol Genet 9:1415-1423.
Millar JK, Pickard BS, Mackie S, James R, Christie S, Buchanan SR, Malloy MP, Chubb JE, Huston E, Baillie GS, Thomson PA, Hill EV, Brandon NJ, Rain JC, Camargo LM, Whiting PJ, Houslay MD, Blackwood DH, Muir WJ, Porteous DJ

(2005) DISC1 and PDE4B are interacting genetic factors in schizophrenia that regulate cAMP signaling. Science 310:1187-1191.
Millar T, Walker R, Arango JC, Ironside JW, Harrison DJ, MacIntyre DJ, Blackwood D, Smith C, Bell JE (2007) Tissue and organ donation for research in forensic pathology: the MRC Sudden Death Brain and Tissue Bank. J Pathol 213:369-375.
Moessner R, Marshall CR, Sutcliffe JS, Skaug J, Pinto D, Vincent J, Zwaigenbaum L, Fernandez B, Roberts W, Szatmari P, Scherer SW (2007) Contribution of SHANK3 mutations to autism spectrum disorder. Am J Hum Genet 81:1289-1297.
Morris JA, Kandpal G, Ma L, Austin CP (2003) DISC1 (Disrupted-In-Schizophrenia 1) is a centrosome-associated protein that interacts with MAP1A, MIPT3, ATF4/5 and NUDEL: regulation and loss of interaction with mutation. Hum Mol Genet 12:1591-1608.
Mulley JC, Scheffer IE, Harkin LA, Berkovic SF, Dibbens LM (2005) Susceptibility genes for complex epilepsy. Hum Mol Genet 14 Spec No. 2:R243-249.
Munehira Y, Ohnishi T, Kawamoto S, Furuya A, Shitara K, Imamura M, Yokota T, Takeda S, Amachi T, Matsuo M, Kioka N, Ueda K (2004) Alpha1-syntrophin modulates turnover of ABCA1. J Biol Chem 279:15091-15095.
Murray CJ, Lopez AD (1996) Evidence-based health policy--lessons from the Global Burden of Disease Study. Science 274:740-743.
Mustapha M, Salem N, Weil D, el-Zir E, Loiselet J, Petit C (1998) Identification of a locus on chromosome 7q31, DFNB14, responsible for prelingual sensorineural non-syndromic deafness. Eur J Hum Genet 6:548-551.
Nadel L, Jacobs WJ (1996) The role of the hippocampus in PTSD, panic and phobia In: The hippocampus: functions and clinical relevance (Kato N, ed). Amsterdam: Elsevier.
Nakane PK, Pierce J (1967) Enzyme-labeled antibodies: preparations and applications for the localisation of antigens. Journal of Histochemistry and Cytochemistry 14:929-930.
Narayan S, Head SR, Gilmartin TJ, Dean B, Thomas EA (2008) Evidence for disruption of sphingolipid metabolism in schizophrenia. J Neurosci Res.
Nicoll RA, Schmitz D (2005) Synaptic plasticity at hippocampal mossy fibre synapses. Nat Rev Neurosci 6:863-876.
Noponen M, Sanfilipo M, Samanich K, Ryer H, Ko G, Angrist B, Wolkin A, Duncan E, Rotrosen J (1993) Elevated PLA2 activity in schizophrenics and other psychiatric patients. Biol Psychiatry 34:641-649.
O'Connor JA, Muly EC, Arnold SE, Hemby SE (2007) AMPA receptor subunit and splice variant expression in the DLPFC of schizophrenic subjects and rhesus monkeys chronically administered antipsychotic drugs. Schizophr Res 90:28-40.
O'Donovan MC, Craddock N, Norton N, Williams H, Peirce T, Moskvina V, Nikolov I, Hamshere M, Carroll L, Georgieva L, Dwyer S, Holmans P, Marchini JL, Spencer CC, Howie B, Leung HT, Hartmann AM, Moller HJ, Morris DW, Shi Y, Feng G, Hoffmann P, Propping P, Vasilescu C, Maier W, Rietschel M, Zammit S, Schumacher J, Quinn EM, Schulze TG, Williams NM, Giegling I,

Iwata N, Ikeda M, Darvasi A, Shifman S, He L, Duan J, Sanders AR, Levinson DF, Gejman PV, Buccola NG, Mowry BJ, Freedman R, Amin F, Black DW, Silverman JM, Byerley WF, Cloninger CR, Cichon S, Nothen MM, Gill M, Corvin A, Rujescu D, Kirov G, Owen MJ (2008) Identification of loci associated with schizophrenia by genome-wide association and follow-up. Nat Genet.

Ohishi H, Ogawa-Meguro R, Shigemoto R, Kaneko T, Nakanishi S, Mizuno N (1994) Immunohistochemical localization of metabotropic glutamate receptors, mGluR2 and mGluR3, in rat cerebellar cortex. Neuron 13:55-66.

Ohrmann P, Siegmund A, Suslow T, Pedersen A, Spitzberg K, Kersting A, Rothermundt M, Arolt V, Heindel W, Pfleiderer B (2007) Cognitive impairment and in vivo metabolites in first-episode neuroleptic-naive and chronic medicated schizophrenic patients: a proton magnetic resonance spectroscopy study. J Psychiatr Res 41:625-634.

Olney JW, Farber NB (1995) Glutamate receptor dysfunction and schizophrenia. Arch Gen Psychiatry 52:998-1007.

Owen MJ, O'Donovan MC, Gottesman II (2002) Schizophrenia. In: Psychiatric genetics and genomics (McGuffin P, Owen MJ, Gottesman II, eds). Oxford, OX2 6DP.: Oxford University Press,.

Paddock S, Laje G, Charney D, Rush AJ, Wilson AF, Sorant AJ, Lipsky R, Wisniewski SR, Manji H, McMahon FJ (2007) Association of GRIK4 with outcome of antidepressant treatment in the STAR*D cohort. Am J Psychiatry 164:1181-1188.

Paisan-Ruiz C, Bhatia KP, Li A, Hernandez D, Davis M, Wood NW, Hardy J, Houlden H, Singleton A, Schneider SA (2008) Characterization of PLA2G6 as a locus for dystonia-parkinsonism. Ann Neurol.

Park Y, Jo J, Isaac JT, Cho K (2006) Long-term depression of kainate receptor-mediated synaptic transmission. Neuron 49:95-106.

Patil ST, Zhang L, Martenyi F, Lowe SL, Jackson KA, Andreev BV, Avedisova AS, Bardenstein LM, Gurovich IY, Morozova MA, Mosolov SN, Neznanov NG, Reznik AM, Smulevich AB, Tochilov VA, Johnson BG, Monn JA, Schoepp DD (2007) Activation of mGlu2/3 receptors as a new approach to treat schizophrenia: a randomized Phase 2 clinical trial. Nat Med 13:1102-1107.

Payne HL, Ives JH, Sieghart W, Thompson CL (2008) AMPA and kainate receptors mediate mutually exclusive effects on GABA(A) receptor expression in cultured mouse cerebellar granule neurones. J Neurochem 104:173-186.

Peet M, Laugharne J, Rangarajan N, Horrobin D, Reynolds G (1995) Depleted red cell membrane essential fatty acids in drug-treated schizophrenic patients. J Psychiatr Res 29:227-232.

Pellerin L, Magistretti PJ (1994) Glutamate uptake into astrocytes stimulates aerobic glycolysis: a mechanism coupling neuronal activity to glucose utilization. Proc Natl Acad Sci U S A 91:10625-10629.

Petit C (1996) Genes responsible for human hereditary deafness: symphony of a thousand. Nat Genet 14:385-391.

Pettegrew JW, Keshavan MS, Minshew NJ (1993) 31P nuclear magnetic resonance spectroscopy: neurodevelopment and schizophrenia. Schizophr Bull 19:35-53.

Phelan MC, Rogers RC, Saul RA, Stapleton GA, Sweet K, McDermid H, Shaw SR, Claytor J, Willis J, Kelly DP (2001) 22q13 deletion syndrome. Am J Med Genet 101:91-99.

Piatto VB, Nascimento EC, Alexandrino F, Oliveira CA, Lopes AC, Sartorato EL, Maniglia JV (2005) Molecular genetics of non-syndromic deafness. Rev Bras Otorrinolaringol (Engl Ed) 71:216-223.

Pickard BS, Malloy MP, Porteous DJ, Blackwood DH, Muir WJ (2005a) Disruption of a brain transcription factor, NPAS3, is associated with schizophrenia and learning disability. Am J Med Genet B Neuropsychiatr Genet 136B:26-32.

Pickard BS, Millar JK, Porteous DJ, Muir WJ, Blackwood DH (2005b) Cytogenetics and gene discovery in psychiatric disorders. Pharmacogenomics J 5:81-88.

Pickard BS, Thomson PA, Christoforou A, Evans KL, Morris SW, Porteous DJ, Blackwood DH, Muir WJ (2007) The PDE4B gene confers sex-specific protection against schizophrenia. Psychiatr Genet 17:129-133.

Pickard BS, Christoforou A, Thomson PA, Fawkes A, Evans KL, Morris SW, Porteous DJ, Blackwood DH, Muir WJ (2008a) Interacting haplotypes at the NPAS3 locus alter risk of schizophrenia and bipolar disorder. Mol Psychiatry.

Pickard BS, Malloy MP, Christoforou A, Thomson PA, Evans KL, Morris SW, Hampson M, Porteous DJ, Blackwood DH, Muir WJ (2006) Cytogenetic and genetic evidence supports a role for the kainate-type glutamate receptor gene, GRIK4, in schizophrenia and bipolar disorder. Mol Psychiatry 11:847-857.

Pickard BS, Knight HM, Hamilton RS, Soares DC, Walker R, Boyd JK, Machell J, Maclean A, McGhee KA, Condie A, Porteous DJ, St Clair D, Davis I, Blackwood DH, Muir WJ (2008b) A common variant in the 3'UTR of the GRIK4 glutamate receptor gene affects transcript abundance and protects against bipolar disorder. Proc Natl Acad Sci U S A 105:14940-14945.

Pieper AA, Wu X, Han TW, Estill SJ, Dang Q, Wu LC, Reece-Fincanon S, Dudley CA, Richardson JA, Brat DJ, McKnight SL (2005) The neuronal PAS domain protein 3 transcription factor controls FGF-mediated adult hippocampal neurogenesis in mice. Proc Natl Acad Sci U S A 102:14052-14057.

Pinheiro P, Mulle C (2006) Kainate receptors. Cell Tissue Res 326:457-482.

Pinheiro PS, Mulle C (2008) Presynaptic glutamate receptors: physiological functions and mechanisms of action. Nat Rev Neurosci 9:423-436.

Porteous DJ, Thomson P, Brandon NJ, Millar JK (2006) The genetics and biology of DISC1--an emerging role in psychosis and cognition. Biol Psychiatry 60:123-131.

Porter RH, Eastwood SL, Harrison PJ (1997) Distribution of kainate receptor subunit mRNAs in human hippocampus, neocortex and cerebellum, and bilateral reduction of hippocampal GluR6 and KA2 transcripts in schizophrenia. Brain Res 751:217-231.

Prades C, Arnould I, Annilo T, Shulenin S, Chen ZQ, Orosco L, Triunfol M, Devaud C, Maintoux-Larois C, Lafargue C, Lemoine C, Denefle P, Rosier M, Dean M (2002) The human ATP binding cassette gene ABCA13, located on chromosome 7p12.3, encodes a 5058 amino acid protein with an extracellular domain encoded in part by a 4.8-kb conserved exon. Cytogenet Genome Res 98:160-168.

Pramparo T, de Gregori M, Gimelli S, Ciccone R, Frondizi D, Liehr T, Pellacani S, Masi G, Brovedani P, Zuffardi O, Guerrini R (2008) A 7 Mb duplication at 22q13 in a girl with bipolar disorder and hippocampal malformation. Am J Med Genet A 146A:1754-1760.
Purcell S, Neale B, Todd-Brown K, Thomas L, Ferreira MA, Bender D, Maller J, Sklar P, de Bakker PI, Daly MJ, Sham PC (2007) PLINK: a tool set for whole-genome association and population-based linkage analyses. Am J Hum Genet 81:559-575.
Quiroz JA, Gould TD, Manji HK (2004) Molecular effects of lithium. Mol Interv 4:259-272.
Race V, Marie S, Vincent MF, Van den Berghe G (2000) Clinical, biochemical and molecular genetic correlations in adenylosuccinate lyase deficiency. Hum Mol Genet 9:2159-2165.
Ramocki MB, Zoghbi HY (2008) Failure of neuronal homeostasis results in common neuropsychiatric phenotypes. Nature 455:912-918.
Rasband WS (1997-2007) ImageJ,. National Institutes of Health, Bethesda,
Maryland, USA, http://rsb.info.nih.gov/ij/,. In.
Redon R, Ishikawa S, Fitch KR, Feuk L, Perry GH, Andrews TD, Fiegler H, Shapero MH, Carson AR, Chen W, Cho EK, Dallaire S, Freeman JL, Gonzalez JR, Gratacos M, Huang J, Kalaitzopoulos D, Komura D, MacDonald JR, Marshall CR, Mei R, Montgomery L, Nishimura K, Okamura K, Shen F, Somerville MJ, Tchinda J, Valsesia A, Woodwark C, Yang F, Zhang J, Zerjal T, Armengol L, Conrad DF, Estivill X, Tyler-Smith C, Carter NP, Aburatani H, Lee C, Jones KW, Scherer SW, Hurles ME (2006) Global variation in copy number in the human genome. Nature 444:444-454.
Reese MG, Eeckman FH, Kulp D, Haussler D (1997) Improved splice site detection in Genie. J Comput Biol 4:311-323.
Represa A, Tremblay E, Ben-Ari Y (1987) Kainate binding sites in the hippocampal mossy fibers: localization and plasticity. Neuroscience 20:739-748.
Riazuddin S, Khan SN, Ahmed ZM, Ghosh M, Caution K, Nazli S, Kabra M, Zafar AU, Chen K, Naz S, Antonellis A, Pavan WJ, Green ED, Wilcox ER, Friedman PL, Morell RJ, Riazuddin S, Friedman TB (2006) Mutations in TRIOBP, which encodes a putative cytoskeletal-organizing protein, are associated with nonsyndromic recessive deafness. Am J Hum Genet 78:137-143.
Rozen S, Skaletsky H (2000) Primer3 on the WWW for general users and for biologist programmers. Methods Mol Biol 132:365-386.
Rozet JM, Gerber S, Ghazi I, Perrault I, Ducroq D, Souied E, Cabot A, Dufier JL, Munnich A, Kaplan J (1999) Mutations of the retinal specific ATP binding transporter gene (ABCR) in a single family segregating both autosomal recessive retinitis pigmentosa RP19 and Stargardt disease: evidence of clinical heterogeneity at this locus. J Med Genet 36:447-451.
Ruifrok AC, Johnston DA (2001) Quantification of histochemical staining by color deconvolution. Anal Quant Cytol Histol 23:291-299.
Ruiz-Perez VL, Carter SA, Healy E, Todd C, Rees JL, Steijlen PM, Carmichael AJ, Lewis HM, Hohl D, Itin P, Vahlquist A, Gobello T, Mazzanti C, Reggazini R,

Nagy G, Munro CS, Strachan T (1999) ATP2A2 mutations in Darier's disease: variant cutaneous phenotypes are associated with missense mutations, but neuropsychiatric features are independent of mutation class. Hum Mol Genet 8:1621-1630.
Sachs NA, Sawa A, Holmes SE, Ross CA, DeLisi LE, Margolis RL (2005) A frameshift mutation in Disrupted in Schizophrenia 1 in an American family with schizophrenia and schizoaffective disorder. Mol Psychiatry 10:758-764.
Sahay A, Hen R (2007) Adult hippocampal neurogenesis in depression. Nat Neurosci 10:1110-1115.
Sakuntabhai A, Ruiz-Perez V, Carter S, Jacobsen N, Burge S, Monk S, Smith M, Munro CS, O'Donovan M, Craddock N, Kucherlapati R, Rees JL, Owen M, Lathrop GM, Monaco AP, Strachan T, Hovnanian A (1999) Mutations in ATP2A2, encoding a Ca2+ pump, cause Darier disease. Nat Genet 21:271-277.
Sambrook J, Fritsch, Maniatis T (1989) Molecular Cloning: a laboratory manual. Cold Spring Harbor: Cold Spring Harbor Press.
Sanchez MM, Young LJ, Plotsky PM, Insel TR (2000) Distribution of corticosteroid receptors in the rhesus brain: relative absence of glucocorticoid receptors in the hippocampal formation. J Neurosci 20:4657-4668.
Sarrieau A, Dussaillant M, Agid F, Philibert D, Agid Y, Rostene W (1986) Autoradiographic localization of glucocorticosteroid and progesterone binding sites in the human post-mortem brain. J Steroid Biochem 25:717-721.
Scarr E, Beneyto M, Meador-Woodruff JH, Deans B (2005) Cortical glutamatergic markers in schizophrenia. Neuropsychopharmacology 30:1521-1531.
Scharfman HE, Hen R (2007) Neuroscience. Is more neurogenesis always better? Science 315:336-338.
Scherer SW, Cheung J, MacDonald JR, Osborne LR, Nakabayashi K, Herbrick JA, Carson AR, Parker-Katiraee L, Skaug J, Khaja R, Zhang J, Hudek AK, Li M, Haddad M, Duggan GE, Fernandez BA, Kanematsu E, Gentles S, Christopoulos CC, Choufani S, Kwasnicka D, Zheng XH, Lai Z, Nusskern D, Zhang Q, Gu Z, Lu F, Zeesman S, Nowaczyk MJ, Teshima I, Chitayat D, Shuman C, Weksberg R, Zackai EH, Grebe TA, Cox SR, Kirkpatrick SJ, Rahman N, Friedman JM, Heng HH, Pelicci PG, Lo-Coco F, Belloni E, Shaffer LG, Pober B, Morton CC, Gusella JF, Bruns GA, Korf BR, Quade BJ, Ligon AH, Ferguson H, Higgins AW, Leach NT, Herrick SR, Lemyre E, Farra CG, Kim HG, Summers AM, Gripp KW, Roberts W, Szatmari P, Winsor EJ, Grzeschik KH, Teebi A, Minassian BA, Kere J, Armengol L, Pujana MA, Estivill X, Wilson MD, Koop BF, Tosi S, Moore GE, Boright AP, Zlotorynski E, Kerem B, Kroisel PM, Petek E, Oscier DG, Mould SJ, Dohner H, Dohner K, Rommens JM, Vincent JB, Venter JC, Li PW, Mural RJ, Adams MD, Tsui LC (2003) Human chromosome 7: DNA sequence and biology. Science 300:767-772.
Schiffer HH, Heinemann SF (2007) Association of the human kainate receptor GluR7 gene (GRIK3) with recurrent major depressive disorder. Am J Med Genet B Neuropsychiatr Genet 144B:20-26.
Schmidt D, Jiang QX, MacKinnon R (2006) Phospholipids and the origin of cationic gating charges in voltage sensors. Nature 444:775-779.

Schmitt A, May B, Muller B, Jatzko A, Petroianu G, Braus DF, Henn FA (2003) Effects of chronic haloperidol and clozapine treatment on AMPA and kainate receptor binding in rat brain. Pharmacopsychiatry 36:292-296.
Schmitt A, Wilczek K, Blennow K, Maras A, Jatzko A, Petroianu G, Braus DF, Gattaz WF (2004) Altered thalamic membrane phospholipids in schizophrenia: a postmortem study. Biol Psychiatry 56:41-45.
Schwab SG, Wildenauer DB (1999) Chromosome 22 workshop report. Am J Med Genet 88:276-278.
Schwartz PJ, Spazzolini C, Crotti L, Bathen J, Amlie JP, Timothy K, Shkolnikova M, Berul CI, Bitner-Glindzicz M, Toivonen L, Horie M, Schulze-Bahr E, Denjoy I (2006) The Jervell and Lange-Nielsen syndrome: natural history, molecular basis, and clinical outcome. Circulation 113:783-790.
Segal D, Koschnick JR, Slegers LH, Hof PR (2007) Oligodendrocyte pathophysiology: a new view of schizophrenia. Int J Neuropsychopharmacol 10:503-511.
Segurado R, Detera-Wadleigh SD, Levinson DF, Lewis CM, Gill M, Nurnberger JI, Jr., Craddock N, DePaulo JR, Baron M, Gershon ES, Ekholm J, Cichon S, Turecki G, Claes S, Kelsoe JR, Schofield PR, Badenhop RF, Morissette J, Coon H, Blackwood D, McInnes LA, Foroud T, Edenberg HJ, Reich T, Rice JP, Goate A, McInnis MG, McMahon FJ, Badner JA, Goldin LR, Bennett P, Willour VL, Zandi PP, Liu J, Gilliam C, Juo SH, Berrettini WH, Yoshikawa T, Peltonen L, Lonnqvist J, Nothen MM, Schumacher J, Windemuth C, Rietschel M, Propping P, Maier W, Alda M, Grof P, Rouleau GA, Del-Favero J, Van Broeckhoven C, Mendlewicz J, Adolfsson R, Spence MA, Luebbert H, Adams LJ, Donald JA, Mitchell PB, Barden N, Shink E, Byerley W, Muir W, Visscher PM, Macgregor S, Gurling H, Kalsi G, McQuillin A, Escamilla MA, Reus VI, Leon P, Freimer NB, Ewald H, Kruse TA, Mors O, Radhakrishna U, Blouin JL, Antonarakis SE, Akarsu N (2003) Genome scan meta-analysis of schizophrenia and bipolar disorder, part III: Bipolar disorder. Am J Hum Genet 73:49-62.
Selemon LD, Goldman-Rakic PS (1999) The reduced neuropil hypothesis: a circuit based model of schizophrenia. Biol Psychiatry 45:17-25.
Selemon LD, Rajkowska G, Goldman-Rakic PS (1995) Abnormally high neuronal density in the schizophrenic cortex. A morphometric analysis of prefrontal area 9 and occipital area 17. Arch Gen Psychiatry 52:805-818; discussion 819-820.
Serretti A, Mandelli L (2008) The genetics of bipolar disorder: genome 'hot regions,' genes, new potential candidates and future directions. Mol Psychiatry 13:742-771.
Severinsen JE, Als TD, Binderup H, Kruse TA, Wang AG, Vang M, Muir WJ, Blackwood DH, Mors O, Borglum AD (2006a) Association analyses suggest GPR24 as a shared susceptibility gene for bipolar affective disorder and schizophrenia. Am J Med Genet B Neuropsychiatr Genet 141:524-533.
Severinsen JE, Bjarkam CR, Kiaer-Larsen S, Olsen IM, Nielsen MM, Blechingberg J, Nielsen AL, Holm IE, Foldager L, Young BD, Muir WJ, Blackwood DH, Corydon TJ, Mors O, Borglum AD (2006b) Evidence implicating BRD1 with brain development and susceptibility to both schizophrenia and bipolar affective disorder. Mol Psychiatry 11:1126-1138.

Severinsen JE, Bjarkam, C.R., Olsen, I.M., Nielsen, M.M., Blechingberg, J., Nielsen, I.E., Foldager, L., Young, B.D., Muir, W.J., Blackwood, D.H.R., Corydon, T.J., Mors, O., Borglum, A.D. (2006) Evidence implicating *BRD1* with brain develpoment and susceptibilty to both schizophrenia and bipolar affective disorder. submitted.

Shahin H, Walsh T, Sobe T, Abu Sa'ed J, Abu Rayan A, Lynch ED, Lee MK, Avraham KB, King MC, Kanaan M (2006) Mutations in a novel isoform of TRIOBP that encodes a filamentous-actin binding protein are responsible for DFNB28 recessive nonsyndromic hearing loss. Am J Hum Genet 78:144-152.

Sheffield VC, Stone EM, Carmi R (1998) Use of isolated inbred human populations for identification of disease genes. Trends in Genetics 14:391-396.

Shibata H, Aramaki T, Sakai M, Ninomiya H, Tashiro N, Iwata N, Ozaki N, Fukumaki Y (2006) Association study of polymorphisms in the GluR7, KA1 and KA2 kainate receptor genes (GRIK3, GRIK4, GRIK5) with schizophrenia. Psychiatry Res 141:39-51.

Shifman S, Johannesson M, Bronstein M, Chen SX, Collier DA, Craddock NJ, Kendler KS, Li T, O'Donovan M, O'Neill FA, Owen MJ, Walsh D, Weinberger DR, Sun C, Flint J, Darvasi A (2008a) Genome-wide association identifies a common variant in the reelin gene that increases the risk of schizophrenia only in women. PLoS Genet 4:e28.

Shifman S, Bhomra A, Smiley S, Wray NR, James MR, Martin NG, Hettema JM, An SS, Neale MC, van den Oord EJ, Kendler KS, Chen X, Boomsma DI, Middeldorp CM, Hottenga JJ, Slagboom PE, Flint J (2008b) A whole genome association study of neuroticism using DNA pooling. Mol Psychiatry 13:302-312.

Silberberg G, Levit A, Collier D, St Clair D, Munro J, Kerwin RW, Tondo L, Floris G, Breen G, Navon R (2008) Stargazin involvement with bipolar disorder and response to lithium treatment. Pharmacogenet Genomics 18:403-412.

Simon DK, Johns DR (1999) Mitochondrial Disorders: Clinical and Genetic Features. AnnuRev Med 50:111-127.

Simons K, Ikonen E (1997) Functional rafts in cell membranes. Nature 387:569-572.

Simons M, Trotter J (2007) Wrapping it up: the cell biology of myelination. Curr Opin Neurobiol 17:533-540.

Sklar P, Smoller JW, Fan J, Ferreira MAR, Perlis RH, Chambert K, Nimgaonkar VL, McQueen MB, Faraone SV, Kirby A, de Bakker PIW, Ogdie MN, Thase ME, Sachs GS, Todd-Brown K, Gabriel SB, Sougnez C, Gates C, Blumenstiel B, Defelice M, Ardlie KG, Franklin J, Muir WJ, McGhee KA, MacIntyre DJ, McLean A, VanBeck M, McQuillin A, Bass NJ, Robinson M, Lawrence J, Anjorin A, Curtis D, Scolnick EM, Daly MJ, Blackwood DH, Gurling HM, Purcell SM (2008) Whole-genome association study of bipolar disorder. 13:558-569.

Slatter TL, Jones GT, Williams MJ, van Rij AM, McCormick SP (2008) Novel rare mutations and promoter haplotypes in ABCA1 contribute to low-HDL-C levels. Clin Genet 73:179-184.

Smesny S, Rosburg T, Nenadic I, Fenk KP, Kunstmann S, Rzanny R, Volz HP, Sauer H (2007) Metabolic mapping using 2D 31P-MR spectroscopy reveals frontal and thalamic metabolic abnormalities in schizophrenia. Neuroimage 35:729-737.
Smith AL, Weissman MM (1992) Handbook of Affective Disorders, second edition Edition. Edinburgh: Churchill Livingstone.
Snyder SH (1973) Amphetamine Psychosis: A "Model" Schizophrenia Mediated by Catecholamines. Am J Psychiatry %R 101176/appiajp130161 130:61-67.
Sokolov BP (1998) Expression of NMDAR1, GluR1, GluR7, and KA1 glutamate receptor mRNAs is decreased in frontal cortex of "neuroleptic-free" schizophrenics: evidence on reversible up-regulation by typical neuroleptics. J Neurochem 71:2454-2464.
Sokolov BP (2007) Oligodendroglial abnormalities in schizophrenia, mood disorders and substance abuse. Comorbidity, shared traits, or molecular phenocopies? Int J Neuropsychopharmacol 10:547-555.
Song W, Li W, Feng J, Heston LL, Scaringe WA, Sommer SS (2008) Identification of high risk DISC1 structural variants with a 2% attributable risk for schizophrenia. Biochem Biophys Res Commun 367:700-706.
Sooksawate T, Simmonds MA (2001) Effects of membrane cholesterol on the sensitivity of the GABA(A) receptor to GABA in acutely dissociated rat hippocampal neurones. Neuropharmacology 40:178-184.
Squire LR, Zola-Morgan S (1991) The medial temporal lobe memory system. Science 253:1380-1386.
St Clair D, Blackwood D, Muir W, Carothers A, Walker M, Spowart G, Gosden C, Evans HJ (1990) Association within a family of a balanced autosomal translocation with major mental illness. Lancet 336:13-16.
Stanley JA, Williamson PC, Drost DJ, Carr TJ, Rylett RJ, Morrison-Stewart S, Thompson RT (1994) Membrane phospholipid metabolism and schizophrenia: an in vivo 31P-MR spectroscopy study. Schizophr Res 13:209-215.
Stefansson H, Rujescu D, Cichon S, Pietilainen OP, Ingason A, Steinberg S, Fossdal R, Sigurdsson E, Sigmundsson T, Buizer-Voskamp JE, Hansen T, Jakobsen KD, Muglia P, Francks C, Matthews PM, Gylfason A, Halldorsson BV, Gudbjartsson D, Thorgeirsson TE, Sigurdsson A, Jonasdottir A, Bjornsson A, Mattiasdottir S, Blondal T, Haraldsson M, Magnusdottir BB, Giegling I, Moller HJ, Hartmann A, Shianna KV, Ge D, Need AC, Crombie C, Fraser G, Walker N, Lonnqvist J, Suvisaari J, Tuulio-Henriksson A, Paunio T, Toulopoulou T, Bramon E, Di Forti M, Murray R, Ruggeri M, Vassos E, Tosato S, Walshe M, Li T, Vasilescu C, Muhleisen TW, Wang AG, Ullum H, Djurovic S, Melle I, Olesen J, Kiemeney LA, Franke B, Kahn RS, Linszen D, van Os J, Wiersma D, Bruggeman R, Cahn W, Germeys I, de Haan L, Krabbendam L, Sabatti C, Freimer NB, Gulcher JR, Thorsteinsdottir U, Kong A, Andreassen OA, Ophoff RA, Georgi A, Rietschel M, Werge T, Petursson H, Goldstein DB, Nothen MM, Peltonen L, Collier DA, St Clair D, Stefansson K (2008) Large recurrent microdeletions associated with schizophrenia. Nature.
Steward O, Wallace CS (1995) mRNA distribution within dendrites: relationship to afferent innervation. J Neurobiol 26:447-449.

Stratton MR, Rahman N (2008) The emerging landscape of breast cancer susceptibility. Nat Genet 40:17-22.
Strauss KA, Puffenberger EG, Huentelman MJ, Gottlieb S, Dobrin SE, Parod JM, Stephan DA, Morton DH (2006) Recessive symptomatic focal epilepsy and mutant contactin-associated protein-like 2. N Engl J Med 354:1370-1377.
Sudhof TC (2008) Neuroligins and neurexins link synaptic function to cognitive disease. Nature 455:903-911.
Suh H, Consiglio A, Ray J, Sawai T, D'Amour KA, Gage FH (2007) In vivo fate analysis reveals the multipotent and self-renewal capacities of Sox2+ neural stem cells in the adult hippocampus. Cell Stem Cell 1:515-528.
Supek F, Vlahovicek K (2005) Comparison of codon usage measures and their applicability in prediction of microbial gene expressivity. BMC Bioinformatics 6:182.
Swift M, Swift RG (2005) Wolframin mutations and hospitalization for psychiatric illness. Mol Psychiatry 10:799-803.
Swift RG, Polymeropoulos MH, Torres R, Swift M (1998) Predisposition of Wolfram syndrome heterozygotes to psychiatric illness. Mol Psychiatry 3:86-91.
Takahashi R, Yokoji H, Misawa H, Hayashi M, Hu J, Deguchi T (1994) A null mutation in the human CNTF gene is not causally related to neurological diseases. Nat Genet 7:79-84.
Takeda K, Inoue H, Tanizawa Y, Matsuzaki Y, Oba J, Watanabe Y, Shinoda K, Oka Y (2001) WFS1 (Wolfram syndrome 1) gene product: predominant subcellular localization to endoplasmic reticulum in cultured cells and neuronal expression in rat brain. Hum Mol Genet 10:477-484.
Tashiro A, Dunaevsky A, Blazeski R, Mason CA, Yuste R (2003) Bidirectional regulation of hippocampal mossy fiber filopodial motility by kainate receptors: a two-step model of synaptogenesis. Neuron 38:773-784.
Theberge J, Bartha R, Drost DJ, Menon RS, Malla A, Takhar J, Neufeld RW, Rogers J, Pavlosky W, Schaefer B, Densmore M, Al-Semaan Y, Williamson PC (2002) Glutamate and glutamine measured with 4.0 T proton MRS in never-treated patients with schizophrenia and healthy volunteers. Am J Psychiatry 159:1944-1946.
Thompson JD, Gibson TJ, Plewniak F, Jeanmougin F, Higgins DG (1997) The CLUSTAL_X windows interface: flexible strategies for multiple sequence alignment aided by quality analysis tools. Nucleic Acids Res 25:4876-4882.
Tkachev D, Mimmack ML, Huffaker SJ, Ryan M, Bahn S (2007) Further evidence for altered myelin biosynthesis and glutamatergic dysfunction in schizophrenia. Int J Neuropsychopharmacol 10:557-563.
Trask BJ (1991) Fluorescence in situ hybridization: applications in cytogenetics and gene mapping. Trends Genet 7:149-154.
Tucker SJ, Baukrowitz T (2008) How highly charged anionic lipids bind and regulate ion channels. J Gen Physiol 131:431-438.
Uitto J (2005) The gene family of ABC transporters--novel mutations, new phenotypes. Trends Mol Med 11:341-343.

Van Camp G, Smith, R., (2005) The Hereditary Hearing Loss Homepage. In. URL:http://www.webhost.ua.ac.be/hhh/.
van Driel MA, Maugeri A, Klevering BJ, Hoyng CB, Cremers FP (1998) ABCR unites what ophthalmologists divide(s). Ophthalmic Genet 19:117-122.
van Meer G, Voelker DR, Feigenson GW (2008) Membrane lipids: where they are and how they behave. Nat Rev Mol Cell Biol 9:112-124.
Van Vught PW, Van Wijk J, Bradley TE, Plasmans D, Jakobs ME, Veldink JH, de Jong JM, Van den Berg LH, Baas F (2007) Ciliary neurotrophic factor null alleles are not a risk factor for Charcot-Marie-Tooth disease, hereditary neuropathy with pressure palsies and amyotrophic lateral sclerosis. Neuromuscul Disord 17:964-967.
Verkhratsky A, Kirchhoff F (2007) Glutamate-mediated neuronal-glial transmission. J Anat 210:651-660.
Vincent P, Mulle C (2008) Kainate receptors in epilepsy and excitotoxicity. Neuroscience.
Volz HR, Riehemann S, Maurer I, Smesny S, Sommer M, Rzanny R, Holstein W, Czekalla J, Sauer H (2000) Reduced phosphodiesters and high-energy phosphates in the frontal lobe of schizophrenic patients: a (31)P chemical shift spectroscopic-imaging study. Biol Psychiatry 47:954-961.
Vorstman JA, Staal WG, van Daalen E, van Engeland H, Hochstenbach PF, Franke L (2006) Identification of novel autism candidate regions through analysis of reported cytogenetic abnormalities associated with autism. Mol Psychiatry 11:1, 18-28.
Wajid M, Abbasi AA, Ansar M, Pham TL, Yan K, Haque S, Ahmad W, Leal SM (2003) DFNB39, a recessive form of sensorineural hearing impairment, maps to chromosome 7q11.22-q21.12. Eur J Hum Genet 11:812-815.
Walsh T, Casadei S, Coats KH, Swisher E, Stray SM, Higgins J, Roach KC, Mandell J, Lee MK, Ciernikova S, Foretova L, Soucek P, King MC (2006) Spectrum of mutations in BRCA1, BRCA2, CHEK2, and TP53 in families at high risk of breast cancer. Jama 295:1379-1388.
Walsh T, McClellan JM, McCarthy SE, Addington AM, Pierce SB, Cooper GM, Nord AS, Kusenda M, Malhotra D, Bhandari A, Stray SM, Rippey CF, Roccanova P, Makarov V, Lakshmi B, Findling RL, Sikich L, Stromberg T, Merriman B, Gogtay N, Butler P, Eckstrand K, Noory L, Gochman P, Long R, Chen Z, Davis S, Baker C, Eichler EE, Meltzer PS, Nelson SF, Singleton AB, Lee MK, Rapoport JL, King MC, Sebat J (2008) Rare structural variants disrupt multiple genes in neurodevelopmental pathways in schizophrenia. Science 320:539-543.
Walsh TD SH, Morrow J, King M-C, Lynch E, Avraham KB, Kanaan M (2000) DFNB28, a novel locus for prelingual nonsyndromic autosomal recessive hearing loss maps to 22q13 in a large consanguineous Palestinian kindred. In: 50th Annual Meeting of American Society of Human Genetics Philadelphia.
Warburton P, Baird G, Chen W, Morris K, Jacobs BW, Hodgson S, Docherty Z (2000) Support for linkage of autism and specific language impairment to 7q3 from two chromosome rearrangements involving band 7q31. Am J Med Genet 96:228-234.

Weir BS, Anderson AD, Hepler AB (2006) Genetic relatedness analysis: modern data and new challenges. Nat Rev Genet 7:771-780.
Weissman MM, Broadhead WE, Olfson M, Sheehan DV, Hoven C, Conolly P, Fireman BH, Farber L, Blacklow RS, Higgins ES, Leon AC (1998) A diagnostic aid for detecting (DSM-IV) mental disorders in primary care. Gen Hosp Psychiatry 20:1-11.
Wenzel JJ, Piehler A, Kaminski WE (2007) ABC A-subclass proteins: gatekeepers of cellular phospho- and sphingolipid transport. Front Biosci 12:3177-3193.
Werner P, Voigt M, Keinanen K, Wisden W, Seeburg PH (1991) Cloning of a putative high-affinity kainate receptor expressed predominantly in hippocampal CA3 cells. Nature 351:742-744.
WHO (2003) ICD-10 classification of mental and behavioural disorders: clinical descriptions and diagnostic guidelines., Second edition Edition. Geneva: World Health Organization.
Willer CJ, Sanna S, Jackson AU, Scuteri A, Bonnycastle LL, Clarke R, Heath SC, Timpson NJ, Najjar SS, Stringham HM, Strait J, Duren WL, Maschio A, Busonero F, Mulas A, Albai G, Swift AJ, Morken MA, Narisu N, Bennett D, Parish S, Shen H, Galan P, Meneton P, Hercberg S, Zelenika D, Chen WM, Li Y, Scott LJ, Scheet PA, Sundvall J, Watanabe RM, Nagaraja R, Ebrahim S, Lawlor DA, Ben-Shlomo Y, Davey-Smith G, Shuldiner AR, Collins R, Bergman RN, Uda M, Tuomilehto J, Cao A, Collins FS, Lakatta E, Lathrop GM, Boehnke M, Schlessinger D, Mohlke KL, Abecasis GR (2008) Newly identified loci that influence lipid concentrations and risk of coronary artery disease. Nat Genet 40:161-169.
Williams JH, Errington ML, Lynch MA, Bliss TV (1989) Arachidonic acid induces a long-term activity-dependent enhancement of synaptic transmission in the hippocampus. Nature 341:739-742.
Wilson GM, Flibotte S, Chopra V, Melnyk BL, Honer WG, Holt RA (2006) DNA copy-number analysis in bipolar disorder and schizophrenia reveals aberrations in genes involved in glutamate signaling. Hum Mol Genet 15:743-749.
Wisden W, Seeburg PH (1993) A complex mosaic of high-affinity kainate receptors in rat brain. J Neurosci 13:3582-3598.
Wolpert CM, Donnelly SL, Cuccaro ML, Hedges DJ, Poole CP, Wright HH, Gilbert JR, Pericak-Vance MA (2001) De novo partial duplication of chromosome 7p in a male with autistic disorder. Am J Med Genet 105:222-225.
Won JS, Singh I (2006) Sphingolipid signaling and redox regulation. Free Radic Biol Med 40:1875-1888.
Woo TU, Walsh JP, Benes FM (2004) Density of glutamic acid decarboxylase 67 messenger RNA-containing neurons that express the N-methyl-D-aspartate receptor subunit NR2A in the anterior cingulate cortex in schizophrenia and bipolar disorder. Arch Gen Psychiatry 61:649-657.
Woods CG, Valente EM, Bond J, Roberts E (2004) A new method for autozygosity mapping using single nucleotide polymorphisms (SNPs) and EXCLUDEAR. J Med Genet 41:e101-.

Woods CG, Cox J, Springell K, Hampshire DJ, Mohamed MD, McKibbin M, Stern R, Raymond FL, Sandford R, Malik Sharif S, Karbani G, Ahmed M, Bond J, Clayton D, Inglehearn CF (2006) Quantification of homozygosity in consanguineous individuals with autosomal recessive disease. Am J Hum Genet 78:889-896.

Wright AF, Teague PW, Bruford E, Carothers A (1997) Problems in dealing with linkage heterogeneity in autosomal recessive forms of retinitis pigmentosa. In: Genetic mapping of disease genes (Pawlowitzki IH, Edwards JH, Thompson EA, eds), pp 255-272. London.

WTCCC (2007) Genome-wide association study of 14,000 cases of seven common diseases and 3,000 shared controls. Nature 447:661-678.

Xiong L, Labuda M, Li DS, Hudson TJ, Desbiens R, Patry G, Verret S, Langevin P, Mercho S, Seni MH, Scheffer I, Dubeau F, Berkovic SF, Andermann F, Andermann E, Pandolfo M (1999) Mapping of a gene determining familial partial epilepsy with variable foci to chromosome 22q11-q12. Am J Hum Genet 65:1698-1710.

Yao JK, van Kammen DP, Gurklis J (1994) Red blood cell membrane dynamics in schizophrenia. III. Correlation of fatty acid abnormalities with clinical measures. Schizophr Res 13:227-232.

Yao JK, Leonard S, Reddy RD (2000) Membrane phospholipid abnormalities in postmortem brains from schizophrenic patients. Schizophr Res 42:7-17.

Yoon JS, Park HJ, Yoo SY, Namkung W, Jo MJ, Koo SK, Park HY, Lee WS, Kim KH, Lee MG (2008) Heterogeneity in the processing defect of SLC26A4 mutants. J Med Genet 45:411-419.

Zaitseva J, Jenewein S, Jumpertz T, Holland IB, Schmitt L (2005) H662 is the linchpin of ATP hydrolysis in the nucleotide-binding domain of the ABC transporter HlyB. Embo J 24:1901-1910.

Zeng W, Gillis T, Hakky M, Djousse L, Myers RH, MacDonald ME, Gusella JF (2006) Genetic analysis of the GRIK2 modifier effect in Huntington's disease. BMC Neurosci 7:62.

Zhao C, Deng W, Gage FH (2008) Mechanisms and functional implications of adult neurogenesis. Cell 132:645-660.

Zimmer L, Delion-Vancassel S, Durand G, Guilloteau D, Bodard S, Besnard JC, Chalon S (2000) Modification of dopamine neurotransmission in the nucleus accumbens of rats deficient in n-3 polyunsaturated fatty acids. J Lipid Res 41:32-40.

Zollner S, Pritchard JK (2007) Overcoming the winner's curse: estimating penetrance parameters from case-control data. Am J Hum Genet 80:605-615.

APPENDICES

Appendix 1: Clinical description of consanguineous family

The family from a small village in North West Punjab where there is a strong tradition of marriages between cousins was identified by Mohammed Ayub, an experienced psychiatrist who speaks the local language. Clinical information was gathered through multiple interviews with all members of the family and inspection of hospital records of inpatient admissions. The parents gave no history of still births or miscarriages. Physical examination of all members revealed no signs of systemic illness or dysmorphic features. Investigations confirmed normal haematology, liver and renal function. Computed tomography (CT) brain scans of two affected siblings indicated no structural changes and electroencephalography (EEG) showed only minor non-specific alterations in the same two individuals. The diagnosis of schizophrenia was made according to ICD-10 criteria based on direct interviews using the Schedule of Affective Disorders and Schizophrenia, and information from informants and hospital care records. Audiometry confirmed sensori-neural hearing impairment.

Cognitive function was assessed by a clinical psychologist and schools were approached for information about educational performance. The affected siblings had normal physical and cognitive development with normal performance in school until around the age of 8 years when they presented with partial complex seizures sometimes leading to generalized seizures. At approximately the same age these individuals developed tinnitus and sensori-neural hearing loss that became progressively more profound during adolescence leading to severe loss of hearing by the age of twenty. Three siblings had experienced psychotic episodes by the age of twenty-five years and met ICD 10 criteria for schizophrenia. Symptoms included auditory hallucinations and delusions of reference and persecution with no affective component. The psychosis is intermittent with good recovery between the episodes which have responded well to treatment with antipsychotic medication. The oldest sibling, now in late forties, is unaffected. Three of

the siblings who are over thirty years old have all three components of the phenotype. One of the younger siblings has only impaired hearing and one has epilepsy but neither of these siblings who are in their twenties have had symptoms of psychosis although they remain at risk of developing symptoms. The oldest of the affected siblings received inpatient treatment in a psychiatric unit where she responded to antipsychotic medication but later relapsed because of poor compliance. In all of the affected siblings epilepsy has responded to carbamazepine. Between episodes of psychosis the social and occupational functioning of the affected siblings is well preserved.

Table S1 Re-calculated p-values for collective significance of the associated ABCA13 variants.
Statistical analysis based upon the genotypng 'replication' phase data only.

Variant	AA change	Cases (total)	Controls (total)	Total cases P-value	Total cases Odds Ratio	SCZ P-value	SCZ Odds Ratio	BP P-value	BP Odds Ratio	MDD P-value	MDD Odds Ratio
1	T4031A	3 (2072)	0 (2262)	0.109	infinity			**0.012**	infinity		
2	R4728X	10 (2058)	5 (2270)	0.110	2.21(0.81)	0.370	1.51	0.057	3.35	0.600	1.21
3	R4843C	19 (1770)	6 (1025)	0.132	1.84 (0.80)	**0.047**	2.54	0.400	1.38	0.630	1.02
4	S3704R	0 (1606)	0 (939)								
5	H3609P	25 (1607)	8 (939)	0.089	1.84 (0.9)	0.334	1.37	0.050	2.43	0.130	2.62
6	R3604Q	0 (1666)	1 (951)								
7	T4550A	18 (1608)	3 (938)	**0.022**	3.52 (1.19)	0.054	3.29	**0.0097**	5.25	0.63	1.18
7	R4590W	17 (1846)	4 (971)	0.1	2.25 (0.84)	0.38	1.5	0.087	2.75	0.14	2.78
5	H4262R	0 (1717)	0 (980)								
Global significance of all variants by diagnosis:						**5.70E-03**	1.93 (1.24)	**7.42E-05**	2.71 (1.73)	**9.66E-02**	1.67 (0.88)
Population attributable risk by diagnosis:						2.21%		4.00%		0.02%	

	P-value	Odds ratio
Global significance of all variants across all diagnoses:	**2.60E-04**	2.1 (1.45)
Population attributable risk across all diagnoses:	2.61%	

P-values calculated using Fisher's exact test (one-tailed) excluding variant counts from the discovery schizophrenia and control sets.
Brackets denote 95% lower limit confidence interval.
Genomic position based on NCBI build 36.1
SCZ schizophrenia, BP bipolar disorder, MDD major depressive disorder
NBD, nucleotide binding domain; TMD, transmembrane domain clusters; HDR, hydrophobic dipping region

Appendix 3: Figure S1

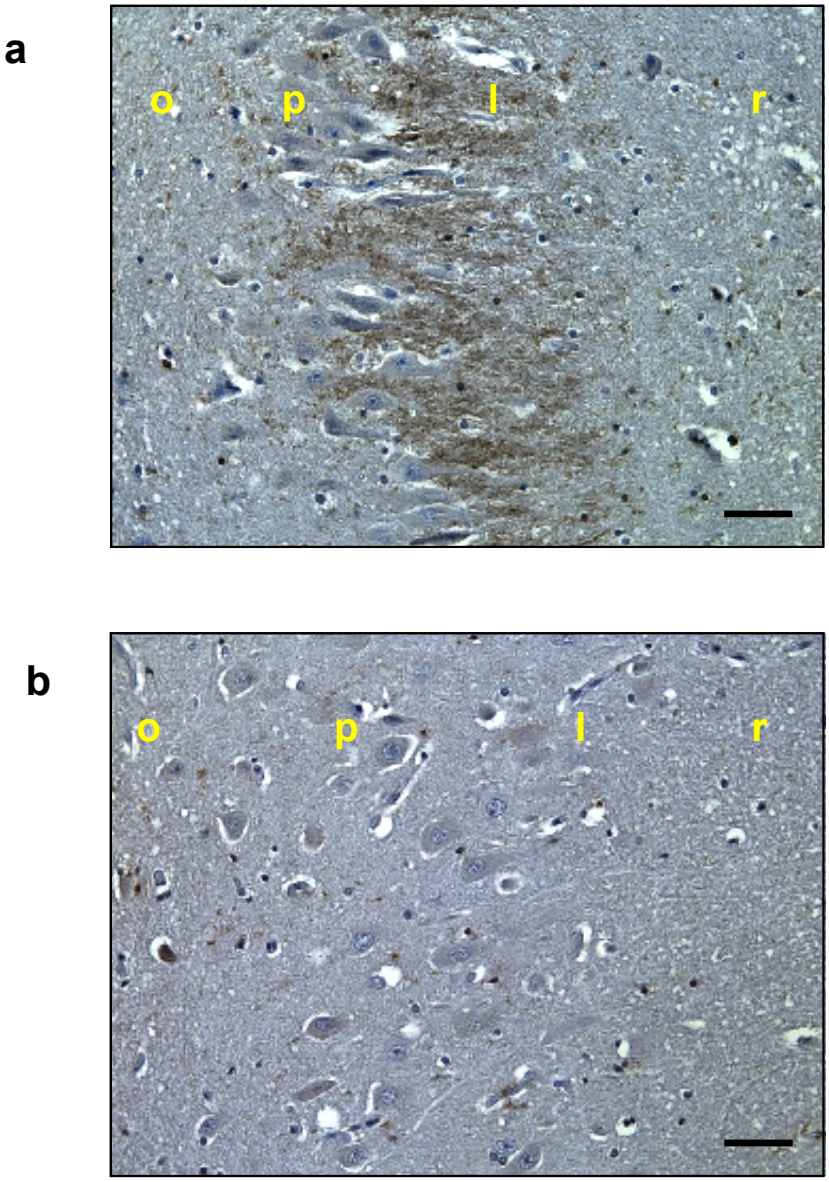

Figure S1 Comparison of KA1 expression in the CA3 field of the hippocampus in a heterozygous indel individual (a) and a homozygous insertion individual (b). The strongest signal was observed in the stratum lucidum of the CA3 region. The black bar represents 50μm. l, stratum lucidum; o, stratum oriens; p, stratum pyramidal; r, stratum radiatum.

Appendix 4: Published Papers

Paper 1: Homozygosity mapping in a family presenting with schizophrenia, epilepsy and hearing impairment.

Paper 2: A common variant in the 3'UTR of the GRIK4 glutamate receptor gene affects transcript abundance and protects against bipolar disorder.